Winter 2012

The use of multibeam and split-beam echo sounders for assessing biomass and distribution of spring-spawning Atlantic cod in the Gulf of Maine

Christopher William Damon Gurshin
University of New Hampshire, Durham

THE USE OF MULTIBEAM AND SPLIT-BEAM ECHO SOUNDERS FOR ASSESSING BIOMASS AND DISTRIBUTION OF SPRING-SPAWNING ATLANTIC COD IN THE GULF OF MAINE

BY

CHRISTOPHER WILLIAM DAMON GURSHIN

B.S., The University of Tampa, 1998

M.S., Auburn University, 2000

DISSERTATION

Submitted to the University of New Hampshire

in Partial Fulfillment of

the Requirements for the Degree of

Doctor of Philosophy

in

Zoology

December, 2012

This dissertation has been examined and approved.

Dissertation Director, Dr. W. Huntting Howell,
Professor of Zoology,
University of New Hampshire

Dr. J. Michael Jech,
Research Fisheries Biologist,
NOAA/NMFS Northeast Fisheries Science Center

Dr. Larry A. Mayer,
Professor of Earth Science and Ocean Engineering,
University of New Hampshire

Dr. Pingguo He,
Associate Professor of Fisheries Oceanography,
University of Massachusetts Dartmouth

Dr. Thomas C. Weber,
Research Assistant Professor in Ocean Engineering,
University of New Hampshire

DEDICATION

I dedicate this dissertation to my family, who gave so much of themselves in supporting and encouraging my endeavors and exploration of the sea. First and foremost, the success of this dissertation would not have been physically and mentally possible without the patience and generosity of my best friend and wife, Denise A. Gurshin, who gave so much of herself for my success. I share this success with her. I thank my three-year old daughter, Alexia L. Gurshin, who not only endured many nights without me but also understood the reason for doing so, which was in her words, "You working on your Ph.D. so you can become a fish doctor, right Daddy?"

I owe my love for learning to my late mother, Carole A. Gurshin, who would have been so proud to see this success. I am eternally grateful to my mother and father, Christopher W.B. Gurshin, for nurturing my curiosity of fish throughout my childhood and through my adolescent years, from bringing home guppies in first grade to almost burning down the house with aquarium pumps a decade later. I thank my father for taking me to the beaches of Rye and Marblehead on countless summer afternoons to peer into the sea through my dive mask. Lastly, the extraordinary support from my father- and mother-in-law, Richard and Janet Marnell, my father, and from my sister, Vanessa Douglas, allowed me to continue this research.

The culmination of the lifetime experiences, hardships and obstacles, triumphs and failures, shared in these relationships have led to all of my success. And so it goes, I share this accomplishment with all of you. Thank you.

ACKNOWLEDGEMENTS

This research would not have been possible without the assistance, guidance, collaboration, and funding support from many people and agencies. I am tremendously grateful for the generosity, wisdom, and guidance that my advisor, Dr. Hunt Howell, has given me through this process. I am also eternally indebted to committee member, Dr. Mike Jech, for not only introducing me to fisheries acoustics but also for his incredible generosity with his time and expertise over the years, and putting his trust in me to conduct this research with NOAA's equipment. I appreciate the assistance and professional guidance provided by my other committee members: Dr. Pingguo He, Dr. Larry Mayer, and Dr. Tom Weber. The support from Dr. Larry Mayer and all of his staff at the Center for Coastal and Ocean Mapping (CCOM), whether it was vessel time, equipment, infrastructure, logistics, or expertise, was instrumental in performing this research. I thank Dr. Tom Weber for his time assisting me with various acoustic problems and holding this research to his high scientific standards.

The collaboration with commercial fishing Captains Carl Bouchard, David Goethel, Charles Felch II, Charles Felch III, and Dennis Robillard was essential to this research. In addition to providing a skillful crew and vessel platform, their experience identified key study areas and secured sufficient number of live Atlantic cod for the study. In addition to collaborations with NOAA, I also thank Massachusetts Division of Marine Fisheries, Dr. Kathryn Ford in particular, for their cooperation and generosity of lending the Kongsberg Maritime EM3002 multibeam echo sounder for this research.

Data were also collected using another EM3002 system, which Kongsberg graciously agreed to allow to be used for parts of this research while on loan to CCOM.

While many valuable contributions by multiple individuals were acknowledged in each chapter, I must acknowledge the quality of the research was undoubtedly enhanced by countless technical discussions with Matt Balge, Paul Geoghegan, Mashkoor Malik, Sean Maxwell, Patrick Nealson, Amy Poe, Laughlin Siceloff, and Drew Trested. The Howell lab, UNH Open Ocean Aquaculture team, and many friends and colleagues had graciously assisted me in the field. I am fortunate to be able to surround myself by such generous, bright, and inspiring colleagues and friends. I thank Normandeau Associates for their flexibility and collective support in pursuing this research while employed full time as a staff scientist. I thank Dr. Jeffrey Cooper, Dr. Richard Freeman, Dr. Andreas Klein, Dr. Young-Mee Lee, and Dr. Richard Rohrer for their miracles, which allowed me to complete this research.

Finally, this research would not have been possible without the financial support of three grants received. First, the Northeast Consortium Project Development Award provided the necessary funding for Chapter I. Chapter II was funded by a Northeast Consortium Collaborative Research Award granted in 2009. The data collected for Chapter III was funded by a two year (2008-2009) New Hampshire Sea Grant.

PREFACE

The structure of each chapter in this dissertation follows the standard format of a manuscript for publication, with exception of the List of References, which were compiled from each manuscript into a single section at the end of the document to reduce redundancy and provide a comprehensive List of References. Chapter 1 was presented at the ICES Symposium on the Ecosystem Approach with Fisheries Acoustics and Complementary Technologies (SEAFACTS) in Bergen, Norway during 16-20 June, 2008 and published in a special issue of the ICES Journal of Marine Science (Gurshin et al. 2009). Preliminary findings from Chapter 2 were presented at the Northeast Consortium Workshop on Reconciling Spatial Scales and Stock Structures for Fisheries Science and Management held in Portsmouth, New Hampshire during 27-28 June 2011. An abbreviated version of Chapter 2 was accepted for publication, with minor revisions, in Fisheries Research on 9 August, 2012. Chapter 3 was prepared as a manuscript to be submitted for publication. Where appropriate, spelling and format was changed from the publication version to conform to American English spelling, University format requirements, and the style of American Fisheries Society publications.

TABLE OF CONTENTS

LIST OF TABLES

LIST OF FIGURES

ABSTRACT

THE USE OF MULTIBEAM AND SPLIT-BEAM ECHO SOUNDERS FOR ASSESSING BIOMASS AND DISTRIBUTION OF SPRING-SPAWNING ATLANTIC COD IN THE GULF OF MAINE

by

Christopher William Damon Gurshin

University of New Hampshire, December, 2012

This research focused on advancing the application of split-beam and multibeam echo sounding to remotely locate and describe spatial distribution, and to provide a relative measure of abundance of the spring-spawning Atlantic cod (*Gadus morhua*) in the western Gulf of Maine. Specifically, the main objectives of this research were 1) to test the feasibility of a multibeam echo sounder to detect changes in volume backscatter proportional to incrementally decreasing quantities of cod held in a submerged cage, and to compare results to a split-beam echo sounder; 2) to describe the spatio-temporal distribution and estimate biomass of spring-spawning cod in the Gulf of Maine cod spawning protection area (GOMCSPA) by repeated acoustic and trawl surveys; and 3) to determine a predictive relation between target strength and length for 38-kHz and 120-kHz split-beam echo sounders and a 300-kHz multibeam echo sounder, and characterize other factors affecting backscattering of sound.

The multibeam echo sounder detected a small and large reduction in volume backscatter proportional to reductions in stocking density of caged cod, while the split-

beam echo sounder only detected a large reduction in stocking density. The spatial information from the multibeam echo sounder helped interpret and explain results from the split-beam echo sounder. Repeated acoustic and trawl surveys showed cod were relatively widespread in the survey area in May, but congregated at higher densities in areas adjacent to two elevated bathymetric features. Most cod converged to a single location in June, and were at a higher concentration than observations in May. This congregation decreased in size and density in July. Survey estimates of cod biomass ranged 184-494 mt in May, 138-617 mt in June, and 39-135 mt in July, depending on the estimation method. Based on echo classification and extrapolation, cod biomass to the GOMCSPA ranged 260-466 mt in May, 196-513 mt in June, and 91-198 mt in July. The biomass being protected by the closure may have represented 4-5% of the GOM cod spawning stock biomass at the time of the study based on these estimates.

The three echo sounders synchronously collected acoustic data of individual free-swimming captive cod, while the movements of most individuals were observed with underwater video. The standard TS-L equations were $\mathrm{TS} = 20 \log_{10}(L) - 66.4$ at 38 kHz, $\mathrm{TS} = 20 \log_{10}(L) - 67.4$ at 120 kHz, and $\langle \mathrm{TS} \rangle = 20 \log_{10}(L) - 71.4$ at 300 kHz. The study demonstrated a significant TS-L relation at 300 kHz from aggregated data collected by a multibeam echo sounder with narrow beams over multiple beam-pointing angles and without split-beam target tracking.

INTRODUCTION

Historical Significance of Atlantic Cod

"Few words concerning cod gill-nets. The schooner Northern Eagle arrived from Ipswich Bay Wednesday. Was gone eight days. Landed 33,000 pounds large cod; stocked $800; crew's share, $63 per capita.... One thing strange, that all the fish are male fish; always before the female fish came first.... I was on board the schooner Northern Eagle Thanksgiving-day. She had 5,000 pounds cod they got the day before. There were but 14 female fish. The male fish are not large, average 15 pounds each; the female fish, 20 pounds each. In two of the female fish the spawn was ripe. A few of the male fish were ripe." — November 25, 1881, S.J. Martin (Martin 1881)

"I will send you last week's report of the cod gill-nets. There were 160,000 pounds of codfish caught in cod gill-nets last week. Fish are scarce. Six boats have taken their nets up in Ipswich Bay and set them off here. The fish off here are most all male fish, good size, averaging 19 pounds each. The trawlers and netters don't agree in Ipswich Bay. The trawlers think the nets scare the fish and stop them from coming in." — December 22, 1881, S.J. Martin (Martin 1881)

"The schooner Sarah C. Wharff took 36,000 pounds of codfish with gill-nets, while fishing only three days in Ipswich Bay...The codfish found, in Ipswich Bay seem to have followed in, or been followed by, a large body of shrimp, their stomachs being full of them. The shrimp are from two to four inches long, of a bright red color, and full of spawn. The codfish taken in Ipswich Bay average seventeen pounds each, about half of them being female fish." — W. A. Wilcox (Wilcox 1886a)

"Ipswich Bay, from October until May, is a favorite resort for codfish, and is one of the most prolific fishing grounds on the coast." — W. A. Wilcox (Wilcox 1886b)

"In Ipswich Bay a fleet of sixty sail has found codfish both abundant and large in size." — W. A. Wilcox (Wilcox 1887)

Like the above quoted passages from letters appearing in Fishery Bulletin, there are many historical accounts of Atlantic cod being plentiful in the Gulf of Maine, particularly in greater Ipswich Bay. A full account of the ecological history of Atlantic cod is given by Rose (2007). Kurlansky (1997) provides another historical account of Atlantic cod feeding the Vikings and the Pilgrims, causing the "Cod Wars" over fishing territory rights between the United Kingdom and Iceland in the 1950's and 1970's, and supporting the economies of many coastal communities over centuries.

Groundfsh, particularly Atlantic cod (*Gadus morhua*), continue to support an important commercial fishery that impacts the economy and culture of New England, and many other coastal communities throughout its North Atlantic range. According to 2010 landings data (NOAA 2012), commercial landings of Atlantic cod in New England were worth about $28 million. Commercial landings of the Gulf of Maine (GOM) cod stock have increased from 3,772 mt in 2010 to 5,356 mt in 2010 (NEFSC 2012). In 2010, total catch (i.e., commercial landings and discards, and recreational landings and discards combined) of GOM Atlantic cod was 11,139 mt (NEFSC 2012).

Life History Summary

A thorough review of the life history of Atlantic cod, particularly in the Gulf of Maine, can be found in Klein-MacPhee (2002) and ICES (2005). Atlantic cod occur in the Northwest Atlantic Ocean, from Greenland to Cape Hatteras. While historically they are known to reach 183 cm and 96 kg, cod are considered rare these days to reach 34 kg and are more commonly 2.5-4 kg in commercial catches (Klein-MacPhee 2002). Pentilla et al. (1989) reported a maximum age of 18 years. Median length at maturity for females and males in the Gulf of Maine is 32 cm and 36 cm, respectively, and the median age at maturity is 2.1 years for females and 2.3 years for males (O'Brien et al. 1999). Fishes, followed by decapods and squids, comprise the majority of the diet for adult Atlantic cod (Klein-MacPhee 2002).

Atlantic cod are known for exhibiting spawning site fidelity by returning to same area to spawn over multiple seasons (Robicahud and Rose 2001; Howell et al. 2008; Windle and Rose 2005). Atlantic cod are known to congregate in Ipswich Bay to spawn during winter (November through January) and another group congregate during April-July (Howell et al. 2008). The larger spring-spawning group is resident to the area and displays spawning site fidelity (Howell et al. 2008). Using data storage tags and acoustic telemetry, Siceloff and Howell (2012) confirmed spawning site fidelity and residency, and found that spawning activity, which peaked in May, was concentrated in a small (~35km^2) area on the southern and western edges of an elevated bathymetric feature in the northwestern corner of Area 133 known as "Whaleback". Microsatellite and single nucleotide polymorphism DNA analyses from cod samples collected from various sites within the Gulf of Maine and Georges Bank have shown that the spring spawning group is part of a genetically-distinct northern spring spawning coastal complex (Wirgin et al. 2007; Kovach et al. 2010). Males are known to produce sounds such as grunts during spawning season (Brawn 1961). Spawning typical takes place during night and when water temperatures are between -1° and 12 °C (Klein-MacPhee 2002). Females are extremely fecund and a 50-cm fish can release 500,000 buoyant eggs.

Fishery Management

Atlantic cod are managed by the New England Fishery Management Council as two stocks: Gulf of Maine, and Georges Bank and South. Regulations in place to reduce fishing mortality include gear restrictions, minimum fish size limits, trip limits, and time/area closures. Seasonal and year-round area closures are designed to reduce fishing mortality by displacing fishing effort away from highly populated areas or important habitats by closing areas to harvesting. Another area management measure currently popular in fisheries management is the concept of EFH, which is defined in the federal rule (CFR, Vol 27, No. 12 § 600.10) as "those waters and substrate necessary to fish for spawning, breeding, feeding, or growth to maturity." A provision to the Magnuson-Stevens Act was finalized in 2002 to require fisheries management plans to identify, describe, assess, conserve and enhance EFH. Quality science-based information on relative abundance and spatial distribution is essential for the success of these management strategies to maintain a sustainable cod fishery.

The GOM Atlantic cod stock is overfished, and overfishing is occurring (NEFSC 2012). Total population biomass of this stock has ranged from 11,885 mt in 1998 to 41,475 mt in 1982 (NEFSC 2012). While Mayo et al. (2009) had estimated the 2007 spawning stock biomass (SSB) to have been 33,877 mt, the most recent assessment estimates 2003-2010 SSB has fluctuated between approximately 8,000 and 14,000 mt, with 2010 SSB estimated at 11,868 mt (NEFSC 2012).

Rationale of the Research

The successful management of cod, as with any species, depends on high quality, science-based information. Among the most fundamentally important metrics is relative abundance, which is typically estimated for Gulf of Maine cod through fishery-independent trawl surveys. These have the advantage of standardized, long time series (typically decades), and also serve to collect biological samples needed to study age and growth, reproduction, genetics, and feeding ecology. While trawl surveys are effective, and should continue, they do have some disadvantages. They are time-consuming, relatively expensive, result in the inevitable death of some fish, can result in habitat damage, are unsuitable over rough/rocky bottom, may miss fish high in the water column, and have some bias associated with the behavior of the fish towards a moving trawl.

Fisheries acoustics can overcome some of the limitations and sampling biases associated with trawl surveys, and acoustic surveys to estimate relative abundance are becoming more common. The advantage of acoustic surveys is that they allow greater spatial coverage per unit time, do not result in unintended mortality, are not limited by bottom type, sample the majority of the water column, do not damage the habitat, and there is no bias associated with gear avoidance. An incomplete understanding of the relationship between acoustic data and the fish populations being surveyed has hampered more widespread use.

While most stock assessments are based on trawl data collected from a stratified-random sampling design, split-beam echo sounder technology is used to provide acoustic indices of abundance in the assessments of some fish stocks. In the US, acoustic survey data are used for stock assessments of commercially important pelagic species such as Atlantic herring (*Clupea harengus*) by the NOAA Northeast Fisheries Science Center (NEFSC) (Jech and Michaels 2006), Pacific hake (*Merluccius productus*) by the NOAA Northwest Fisheries Science Center (Fleischer et al. 2008), and walleye pollock

(*Theragra chalcogramma*) by the NOAA Alaska Fisheries Science Center (Horne and Walline 2005).

Although acoustic surveys on cod and haddock (*Melanogrammus aeglefinus*) have not been widely developed in the US, they have been used for estimating abundance of cod stocks in Canadian Atlantic waters (Rose 2003; McQuinn et al. 2005a, 2005b; Mello and Rose 2005) and in the Barents Sea (Godø and Wespestad 1993; Korsbrekke et al. 2001). Rose (2003) used 38-kHz single-beam and dual-beam echo sounders in 1995-1997, and 38-kHz split-beam echo sounders since 1998, to estimate biomass of Atlantic cod in Smith Sound, Newfoundland during over-wintering months, when dense, size- and age-structured mono-specific aggregations (congregations) are formed prior to spawning. Mello and Rose (2005a, 2005b) used acoustic data to quantify seasonal distribution and aggregation patterns of Atlantic cod in Placentia Bay, Newfoundland. McQuinn et al. (2005) estimated the effects of acoustic and trawl dead zones on density estimates of Atlantic cod and demonstrated the advantages of an integrated acoustic-trawl survey for Atlantic cod in the Gulf of St. Lawrence. Stock assessment models (e.g., virtual population analysis) for the Northeast Arctic cod stock have been based on fishery-independent abundance estimates obtained from bottom-trawl and acoustic surveys (Korsbrekke et al. 2001). Since 1985, Norwegian researchers have used an acoustic index of spawning stock biomass obtained from acoustic surveys of spawning grounds (Korsbrekke et al. 2001).

In a review of the Atlantic stock structure in the Gulf of Maine, Ames (2004) estimated nearly half of the coastal spawning grounds have been abandoned after 50-75 years. Given the commercial importance and status of the Atlantic cod in Gulf of Maine, spatial distribution of spawning populations and their abundance is subject to continuing research for improving assessment estimates of biomass, characterizing EFH and evaluating area closure management.

Scope of the Dissertation

Three chapters comprise this dissertation, with each chapter written as manuscripts formatted for publication, so some redundancy was necessary. In general, the research was aimed at advancing the application of split-beam and multibeam echo sounding to remotely locate cod and describe their spatial distribution, and to provide a relative measure of abundance of the spring-spawning group of Atlantic cod in the western Gulf of Maine. Multibeam echo sounders increase spatial coverage by simultaneously receiving multiple overlapping beams, and their application for fishery research has advanced (Fernandes et al. 2002, Mayer et al. 1999, 2002). Multibeam echo sounders can expand observations of fish by providing larger sample volumes, better spatial resolution of fish distributions, and potentially fewer behavior-related sampling biases than surveys using conventional echo sounders. While there are numerous examples of multibeam echo sounders used to study fish behavior, their application in providing quantitative estimates of fish abundance are difficult to derive without accurate calibration, background-noise reduction, predicted target strength (TS) vs. incidence angle, and advances in processing software (Gerlotto et al. 2000; Cochrane et al. 2003).

During the course of this research, the multibeam echo sounder with split-beam functionality (ME70) developed by Simrad has gained increased usage and its applications continue to develop (Trenkel et al. 2008; Ona et al. 2009; Kang 2011). With regard to developing multi-disciplinary acoustic and trawl surveys using multibeam echo sounders for multi-purpose missions such as bathymetry, habitat mapping, and fish population assessment, one can adapt the ME70 multibeam echo sounder, which is specialized for fisheries research, to provide sufficient quality hydrographic results (Bourguignon et al. 2009; Cutter et al. 2010), or one can adapt the lesser expensive and more commonly used hydrographic-grade multibeam echo sounder capable of logging water column backscatter to study fish. This research makes a contribution of the latter approach.

Chapter I focused on providing a proof of concept of using the EM3002 multibeam echo sounder for detecting fish and providing an acoustic measure proportional to fish density. This study was designed to simultaneously collect acoustic backscatter of known quantities of Atlantic cod in a cage with two split-beam echo sounders (38-kHz and 120-kHz Simrad EK60) that have become standards in acoustic surveys and a 300-kHz multibeam echo sounder (Kongsberg Maritime EM3002).

In Chapter II, the research focused on using well established acoustic survey techniques to investigate the several questions about the spring-spawning Atlantic cod that congregate in Ipswich Bay:

1) Is the size and time of the Gulf of Maine Cod Spawning Protection Area appropriate?
2) What is the biomass of Atlantic cod in this area spawning during this fishing closure?
3) What is the spatial and temporal distribution within this area before, during, and after the fishing closure?
4) How do the survey estimation methods affect results?

Chapter III focused on studying the scattering properties of individual mature Atlantic cod from this spring-spawning group in effort to relate acoustic size (target strength) to physical size (length), and characterize the variability in scattering particularly for a high-frequency multibeam echo sounder with overlapping narrow beams. Two appendices complement the research described in Chapter III.

CHAPTER I

MEASUREMENTS OF ACOUSTIC BACKSCATTER AND DENSITY OF CAPTIVE ATLANTIC COD WITH SYNCHRONIZED 300-KHZ MULTIBEAM AND 120-KHZ SPLIT-BEAM ECHO SOUNDERS

Abstract

Effective management strategies for Atlantic cod (*Gadus morhua*) in the Gulf of Maine require stock assessments based on accurate estimates of its abundance and distribution. If multibeam echo sounders are to provide data for such estimates, the relationship between acoustic backscatter and fish biology must be better understood. Working towards this goal, a series of acoustic measurements was made using a 120-kHz, split-beam echo sounder (Simrad EK60) and a 300-kHz, multibeam echo sounder (Kongsberg EM3002). The transducers from both systems were fixed to a platform over a submerged 98 m^3 cage made of 5 cm stretched-nylon mesh. After standard-sphere calibrations, the cage was stocked with live, mature Atlantic cod, with a mean total length of 80.7 cm (range: 51.5 – 105.0 cm). The echo sounders synchronously collected acoustic data, while the cod were monitored with two underwater video cameras. Cod were incrementally removed from the cage to provide a time-series of acoustic backscatter at four densities (n = 128, 116, 66, and 23). Backscatter measurements of cod are compared between echo sounders and over time, and the factors affecting the acoustically derived

density estimates are discussed. The benefits and limitations of the EM3002 are highlighted.

Introduction

Fishery-acoustic techniques can overcome some of the limitations and sampling biases of traditional trawl surveys and provide important biological information on fish density and biomass, spatial distribution, and behavior. Single-, dual-, and split-beam echo sounders are commonly used for surveying fish populations, but multibeam technology has only recently been adapted for fishery research, following developments in hardware, digital acquisition of acoustic backscatter in the water column, and three-dimensional visualization of acoustic data (Fernandes et al. 2002; Mayer et al. 2002). Potential uses of multibeam technology in fishery research go beyond just seabed mapping and classification (Mayer et al. 1999). Multibeam echo sounders can expand observations of fish by providing larger sample volumes, better spatial resolution of fish distributions, and potentially fewer behavior-related sampling biases than surveys using conventional echo sounders and trawls.

Multibeam echo sounders have been used to investigate a variety of schooling pelagic species, such as Atlantic herring and Atlantic mackerel (Misund 1993), capelin (Hafsteinsson and Misund 1995), sardine and anchovy (Gerlotto et al. 1999; Soria et al. 2003), and clupeids (Gerlotto and Paramo 2003; Paramo et al. 2007). These studies have provided information about three-dimensional spatial distributions (Gerlotto et al. 1999), school morphology and classification (Gerlotto and Paramo 2003), migration and swimming behavior (Hafsteinsson and Misund 1995), and abundance (Misund 1993; Gerlotto et al. 2000), and have also provided some fisheries-relevant behavioral findings on diel migrations, vessel avoidance, and gear performance (Hafsteinsson and Misund 1995; Soria et al. 1996; Gerlotto et al. 1999, 2000). However, accurate and precise estimates of fish biomass, and numerical abundance, are difficult to derive from multibeam echo sounder data without accurate calibration, background-noise reduction, predicted target strength (TS) vs. incidence angle, and advances in processing software (Gerlotto et al. 2000; Cochrane et al. 2003).

Although acoustic technology has been applied successfully to survey pelagic species, there have been fewer applications for demersal species. Acoustic surveys of Atlantic cod (*Gadus morhua*) and haddock have not been widely developed in the United States, but studies in the North Atlantic, off Canada and Europe, have yielded promising results. In conjunction with surveys, TS measurements of Atlantic cod have been made using immobile fish (Nakken and Olsen 1977; Fedovota and Shatoba 1983; Rose and Leggett 1988), caged fish (Foote 1983a; Edwards and Armstrong 1984; Goddard and Welsby 1986; Rose and Porter 1996), and wild fish (Rose and Porter 1996; McQuinn and Winger 2003). Rose and Porter (1996) used 38- and 120-kHz, dual-beam echo sounders for TS measurements of individual Atlantic cod inside a monofilament mesh bag, large enough for the fish to swim in freely. Interpretation of any TS measurement requires consideration of the variation as a result of diel changes in body orientation and depth, and the associated compression and decompression of gas-filled swimbladders (Simmonds and MacLennan 2005). In this study, split-beam and multibeam echo sounders are used to estimate indices of abundance of Atlantic cod of known sizes and numbers in a cage.

Methods

Experimental Setup

The cage (~98 m^3) was made from 5 cm stretched-nylon mesh (Figure 1-1). A floating platform made from high-density polyethylene pipe (10.2 – 25.4 cm diameter) supported the cage. The cage was suspended by eight lines, and the bottom of the net was weighted by a rectangular steel frame. Two underwater video cameras provided upward- and sideward-looking records of the spatial distribution and behavior of cod during the experiments.

A 300-kHz, multibeam echo sounder (Kongsberg EM3002; Seafloor Information System, SIS Ver. 3.4.1) and a 120-kHz, split- beam echo sounder (Simrad EK60) were used to collect acoustic backscatter of live, mature Atlantic cod in the cage. The EM3002 generates 160 beams with nominal beam widths of 1.5° x 1.5°, covering a 130° swath. The beam width of the EK60 transducer (ES120-7G) was 7°. Both transducers were mounted on a rigid pole, with the EM3002 array in the center and the EK60 transducer mounted on one side. The transducers were lowered from a bridge across the center of the cage to a fixed depth of ~1 m, for the duration of the experiment (Figure 1-1). The cage was positioned directly under the transducers and fastened so as to be least affected by currents. The depth of the bottom of the cage varied between 6.5 and 11 m (Table 1-1), because of raising and lowering the cage to remove cod.

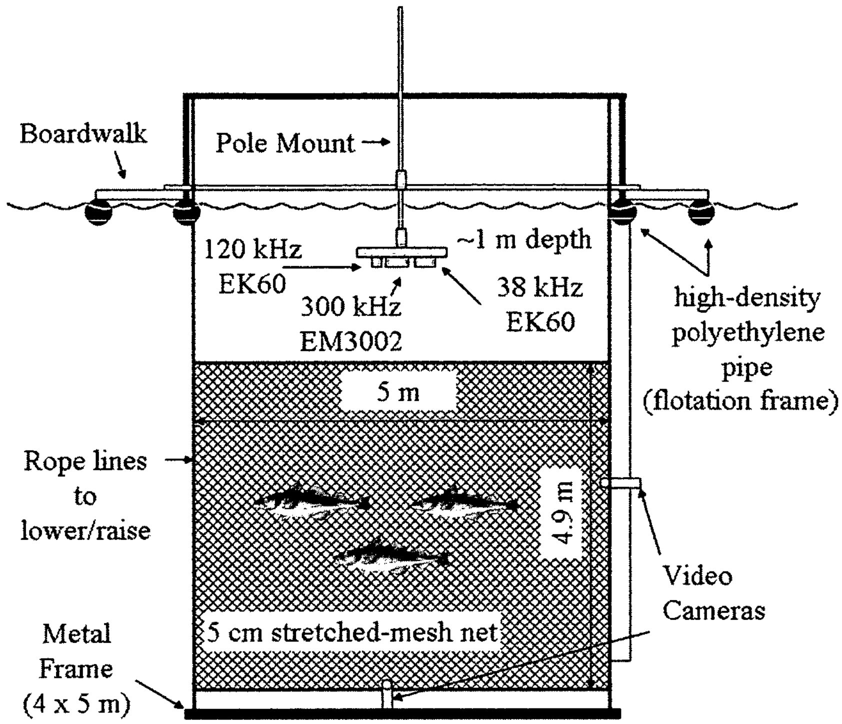

Figure 1.1. The submersible 98-m net cage (5 m long x 4.9 m x 4 m wide) and floating platform with a 120-kHz, split-beam transducer, a 300-kHz, multibeam transducer array, and a 38-kHz, split-beam transducer mounted on a centrally located pole for insonification of caged live Atlantic cod. Data from the 38-kHz EK60 system were not used in this analysis because the source level was unstable using firmware V2.0.0.

The 11-m depth was used to compare backscatter at two depths (8 and 11 m). Sound speed was continuously monitored (Odom Digibar-Pro) at the transducer depth for input to the beamforming calculations, and sound speed profiles of the full water column were taken periodically. The 10-m RV "*Cocheco*" provided power and shelter for the electronics. Transmissions from the EK60 were synchronized to the trigger of the EM3002. Bandwidths and pulse durations were 8 kHz and 199 ms for the EM3002, and 5.6 kHz and 512 ms for the EK60, respectively.

Both systems were calibrated using a standard sphere (Foote et al. 1987). A 38.1-mm-diameter tungsten-carbide sphere was used to calibrate the EM3002, and a 23-mm-diameter copper sphere was used to calibrate the EK60. The cage was lowered so that the top of the cage was ~12 m below the transducers, then in succession; each sphere was attached to a monofilament line and lowered by a fishing rod from the transducer platform to a depth of 8 – 10 m. For the EM3002, calibration of all beams (Foote et al. 2005) was not feasible. Therefore, the calibration gain was estimated and applied during post-processing as the difference between the TS of the sphere measured in the 20 most vertical beams and the theoretical TS (38.1 dB at 300 kHz with an 8 kHz bandwidth; K. Foote, pers. comm.).

Experiments

The acoustic characteristics of the empty cage were measured before stocking it with cod. Visual inspection of the echograms revealed that the top and bottom of the net formed discrete echoes in the EK60 echogram, and all four sides were resolved in the EM3002 images. Therefore, the bottom of the cage was positioned at between 6.5 and 11 m depths for the experiments.

Live Atlantic cod were collected on spawning grounds 10 –15 km off the coast of New Hampshire, USA, and the cage experiments were done nearby at the Open Ocean Aquaculture site (Chambers and Howell 2006), located ~1.6 km south of the Isles of Shoals. The cod were collected at depths between 60 and 80 m, using an otter trawl of 16.5 mm mesh during 13 10 –30-min tows with FV "*Stormy Weather*", on 21, 22, and 25 June 2007. The total length (L_T) of each cod was measured, and those of $L_T > 110$ cm or <50 cm were released. Retained cod were placed for transport in insulated polyethylene containers, each with a volume of 1 m^3. A continuously running deck hose circulated and exchanged the water in the containers during transit to the cage. Moribund or dead cod were not placed in the cage. The initial 195 cod in the cage were subsequently reduced by either mortality or removal to 128, then 116 and 66, and finally 23 fish (with approximate densities of 1.31, 1.18, 0.67, and 0.23 fish m^{-3}, respectively, assuming the fish were homogeneously high distributed throughout the cage volume). The cod were acclimated over 48 – 72 h post-capture, with their rate of descent and ascent restricted to 3 m depth per 30 min. After each stage of the experiment, individual cod were removed from the cage with large dipnets, then measured, counted, and returned to the ocean.

The L_T of cod ranged from 52 to 105 cm in the experiment, and the mean L_T was 80.7 + 10.9 cm (+s.d.). The mean L_T was not significantly different among the four densities (ANOVA, $P < 0.802$, Table 1-1). Some 96 h after stocking the cage, a video camera revealed that 34% of the cod ($n = 67$) had died and settled on the cage bottom. The dead fish were acoustically resolved from the live cod and were not included in the analysis volume. Therefore, the initial population only totaled 128 cod, and not $n = 195$. On subsequent days, the observed 24 h mortalities decreased to 6.9% ($n = 8$), 3.0% ($n = 2$), and 4.4% ($n = 1$). Because the timing and locations of these deaths during the data collections were unknown, no adjustments were made in the analyses to the nominal population sizes (i.e. 128, 116, 66, and 23 cod were used). Gonads from dead cod ($n = 70$) removed from the cage revealed that 37% were female and 63% were male.

Data Analysis

The primary objectives of this study were to compare acoustic- backscatter measurements from the EM3002 and EK60 with known cod abundances. EK60 data were post-processed using Echoview (Myriax Software Pty. Ltd., Hobart, TAS, Australia). Statistical analyses were done using SAS (SAS Institute Inc., Cary, NC, USA) and R (The R Foundation for Statistical Computing, www.r-project.org) software.

EM3002 data were post-processed using Matlab (Math Works, Natick, MA, USA). The raw amplitude (64 dB dynamic range) from the water column measured by the EM3002 was defined as

$$A_{WC} = EL - SL - 10\log_{10}(\Omega_{TX}\Omega_{RX}) + 2\alpha R + 30\log_{10}R + C, \quad (1)$$

where EL is the echo level, SL is the source level, α is the attenuation coefficient, Ω_{TX} and Ω_{RX} are respectively the transmitting and receiving beam widths (radians), R is range (m) from the transducer, and C is the calibration gain (R. Eckhoff, Kongsberg, pers. comm.). The product of Ω_{TX} and Ω_{RX} approximates (Kinsler et al. 2000) the effective solid angle (ψ; MacLennan et al. 2002) in the definition of volume-backscattering strength (S_v, dB) for the EM3002 (Figure 1-2a):

$$S_v = A_{WC} - (X - 20)\log_{10}(R) - 10\mathrm{Log}_{10}(\frac{c\tau}{2}), \quad (2)$$

where $X = 30$ is the range-dependent, time-varied gain applied during collection of A_{WC} ($30\log_{10}R$), c (m s^{-1}) is the sound speed, and τ (s) is the pulse duration. Mean volume-backscattering strength ($\overline{S}_v$), calculated as a temporal average of each voxel, was displayed for visual selection of the spatial domain within the cage encompassing the cod, but not including echoes from the cage (Figure 1-2b – e). To investigate short-term variability (i.e. ping-to-ping), the $\overline{S}_v$ was calculated for each transmission by spatially averaging across selected beams within the cage (Figure 1-3).

To minimize correlation between pings, the $\overline{S}_v$ was calculated by averaging spatially (i.e. from all selected beams within the cage) and temporally (1 min intervals; 60 pings; Figure 1-1-4). This time interval provided temporally independent samples (correlation length ≈ 50 s). The overall $\overline{S}_v$ was computed from an average of the 1 min and spatially averaged $\overline{S}_v$. This mean was used as a relative index of cod abundance. To exclude contributions by background noise and non-cod scatterers, minimum S_v thresholds of -36 and -30 dB (Jech and Michaels 2006) were applied to data from the EM3002 and EK60, respectively. These thresholds reduced background noise by 93.3 and >99.9%, while reducing the $\overline{S}_v$ attributed to cod by 1.3 and 1.3%, respectively. Computations were done in the linear domain and presented in the logarithmic domain.

Results

The swath images from the EM3002 revealed differences in spatial and temporal distributions, and S- v within the cage stocked with 128, 66, and 23 cod (Figure 1-2b – e). During a 1000 ping sequence, ping-to-ping $\overline{S}_v$ for selected EM3002 beams varied over 14 dB for the depth layer of the caged cod (Figure 1-3). Trends in $\overline{S}_v$ were apparent for the four populations (Figure 1-4). The split- and multi- beam echo sounders demonstrated similar trends; except for the large variability in the EK60 data when only 23 cod were present (Figure 1-4d). The $\overline{S}_v$ for each echo sounder for the initial cod population and sequential reductions of 9, 48, and 82% are presented (Table 1-1). The $\overline{S}_v$ from the EM3002 decreased as cod were removed from the cage, except for the 66 cod stage, where they remained densely congregated in the middle (Figure 1-2d and g). With 52%

of the initial population size, $\overline{S}_v$ was highest at both depths on 27 June (Table 1-1). The $\overline{S}_v$ estimated from both echo sounders was highest and lowest for the 66 and 23 cod stages, respectively. The $\overline{S}_v$ estimated from the EK60 data was similar for cage populations of 116 and 66 cod. The $\overline{S}_v$ estimated from the EM3002 and the EK60 data was reduced by 9.9 and 9.4 dB, respectively, when the initial cod population was reduced by 82%. These differences were larger than the observed variability (the range was 6 dB for the EM3002 and 7 dB for the EK60) in the time-series of the 60-ping-averaged $\overline{S}_v$ of the initial 128 cod.

The $\overline{S}_v$ of the cage containing 66 cod was 0.7 dB different when the cage was lowered from 8 to 11 m (Table 1-1 Figure 1-4c). The $\overline{S}_v$ from the 29 central beams of the EM3002 overestimated the 9 and 82% reductions in initial cod abundance as 35% (+26%) and 90% (+8%), respectively. However, data from both the EM3002 and the EK60 showed increases in $\overline{S}_v$ ranging from 17 to 280% rather than the expected 48% decrease owing to the reduction in cod abundance on 27 June.

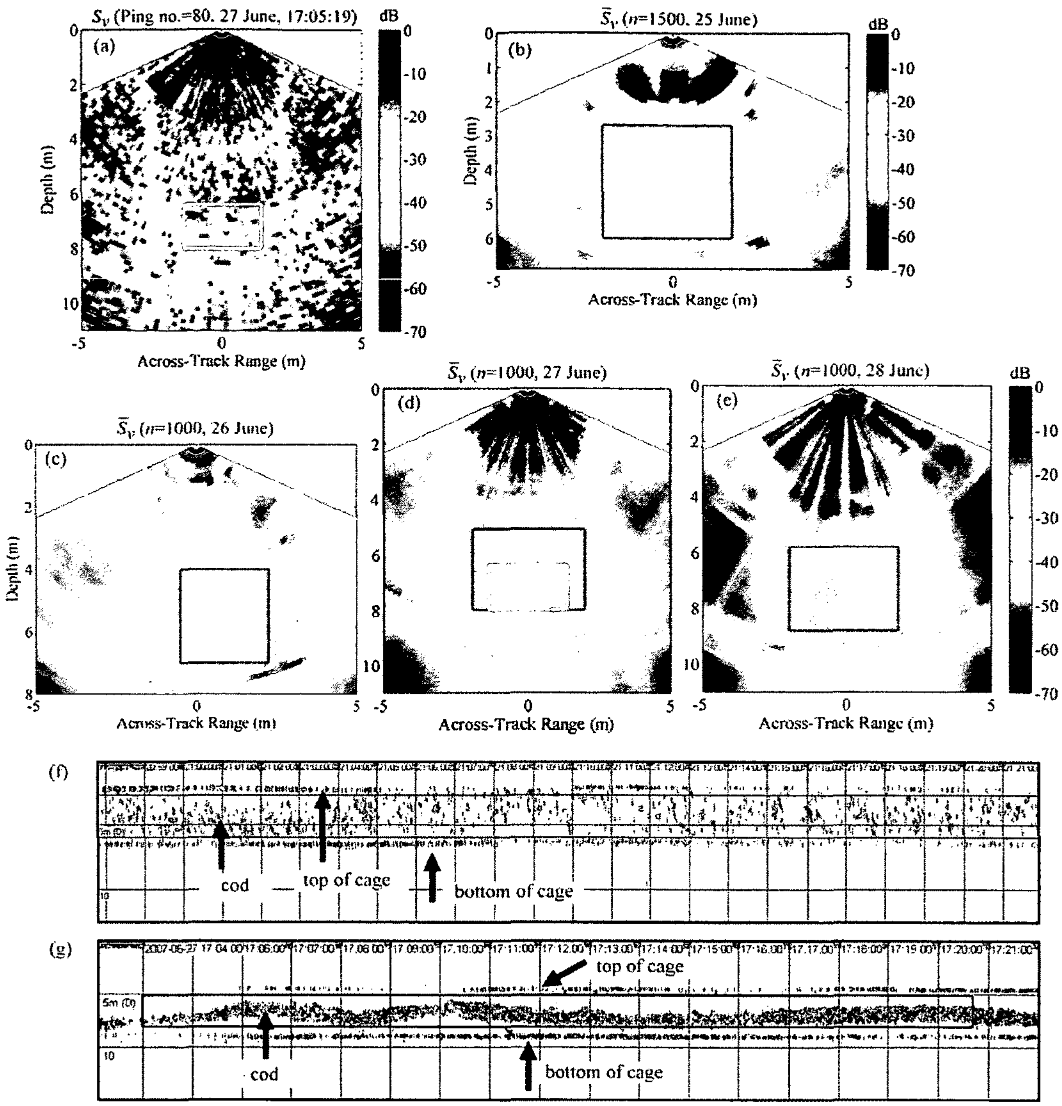

Figure 1-2. (a) Volume-backscattering strength (S_v) of 66 caged Atlantic cod (in white rectangle) from a single ping by the 300-kHz, EM3002 multibeam echo sounder; (b) mean volume-backscattering strength ($\bar{S}_v$) for each voxel averaged over 1500 pings with 128 cod distributed throughout the cage; (c) $\bar{S}_v$ for each voxel averaged over 1000 pings with 116 cod in the cage; (d) $\bar{S}_v$ for each voxel averaged over 1000 pings by the EM3002, where the voxels within the red rectangle were used for analysis of fish density and voxels within the white rectangle for estimation of S_v threshold; (e) $\bar{S}_v$ for each voxel averaged over 1000 pings with 23 cod located towards the lower side of the cage; (f and g) S_v from the 120-kHz, EK60 split-beam echo sounder, with a minimum threshold of S_v)= -30 dB, with 128 cod (f) and 66 cod (g) in the cage.

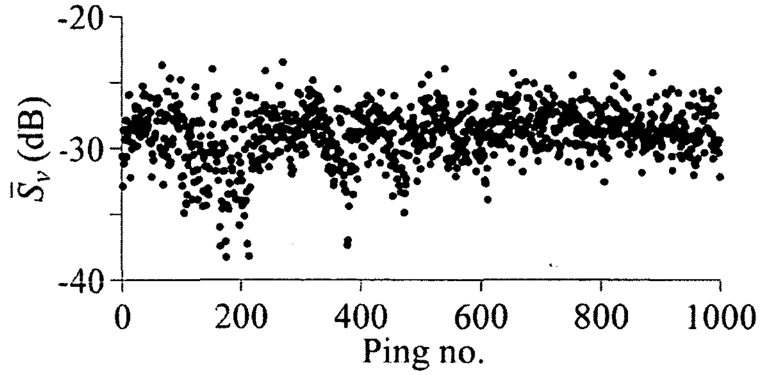

Figure 1-3. Time-series of mean volume-backscattering strength ($\bar{S}_v$) within the cage stocked with 66 Atlantic cod for 1000 pings by the EM3002 multibeam echo sounder.

Table 1-1. Mean volume-backscattering strength ($\bar{S}_v$) inside a 98 m^3 net cage stocked with mature Atlantic cod at four densities for a 300-kHz, EM3002 multibeam echo sounder and 120-kHz, EK60 split-beam echo sounder.

Date (pings)	Cage bottom depth (m)	L_T (cm)	Cage population N	Cage population %	300-kHz EM3002 $\bar{S}_v$ (dB; 95% C.I.)	300-kHz EM3002 %	120-kHz EK60 $\bar{S}_v$ (dB; 95% C.I.)	120-kHz EK60 %	TS[a]	Expected[b] S_v at 120 kHz
25 June (1,500)	6.5	80.7	128	100	−29.8 (−30.3,−29.3)	100	−29.4 (−30.0, −28.8)	100	−26.9	−25.7
26 June (7,140)	7.2	81.1	116	91	−31.7 (−31.9, −31.5)	65	−26.5 (−26.9, −26.2)	195	−26.8	−26.1
27 June (1,680)	8.0	82.1	66	52	−28.4 (−28.7, −28.2)	138	−23.6 (−24.2, −23.1)	380	−26.7	−28.4
(1,800)	11.0	82.1	66	52	−29.1 (−29.4, −28.8)	117	−26.4 (−26.9, −25.8)	200	−26.7	−28.4
28 June (5,940)	8.8	82.9	23	18	−39.7 (−40.3, −39.1)	10	−38.8 (−40.0, −37.8)	11	−26.6	−32.9

Changes in $\bar{S}_v$ relative to the initial population of cod are tabulated for each echo sounder. The expected S_v at 120 kHz, which assumes a random distribution of fish throughout the cage volume, is illustrated for comparison. $\bar{S}_v$ and 95% confidence intervals were computed from 60 ping spatial averages.

[a]$TS = 20\log_{10}(L_T) - 65$ (Rose and Porter 1996) at 120 kHz where L_T = total length (cm).
[b]$S_v = TS + 10\log_{10}(N/V)$ where n = number of cod in the sampled volume V.

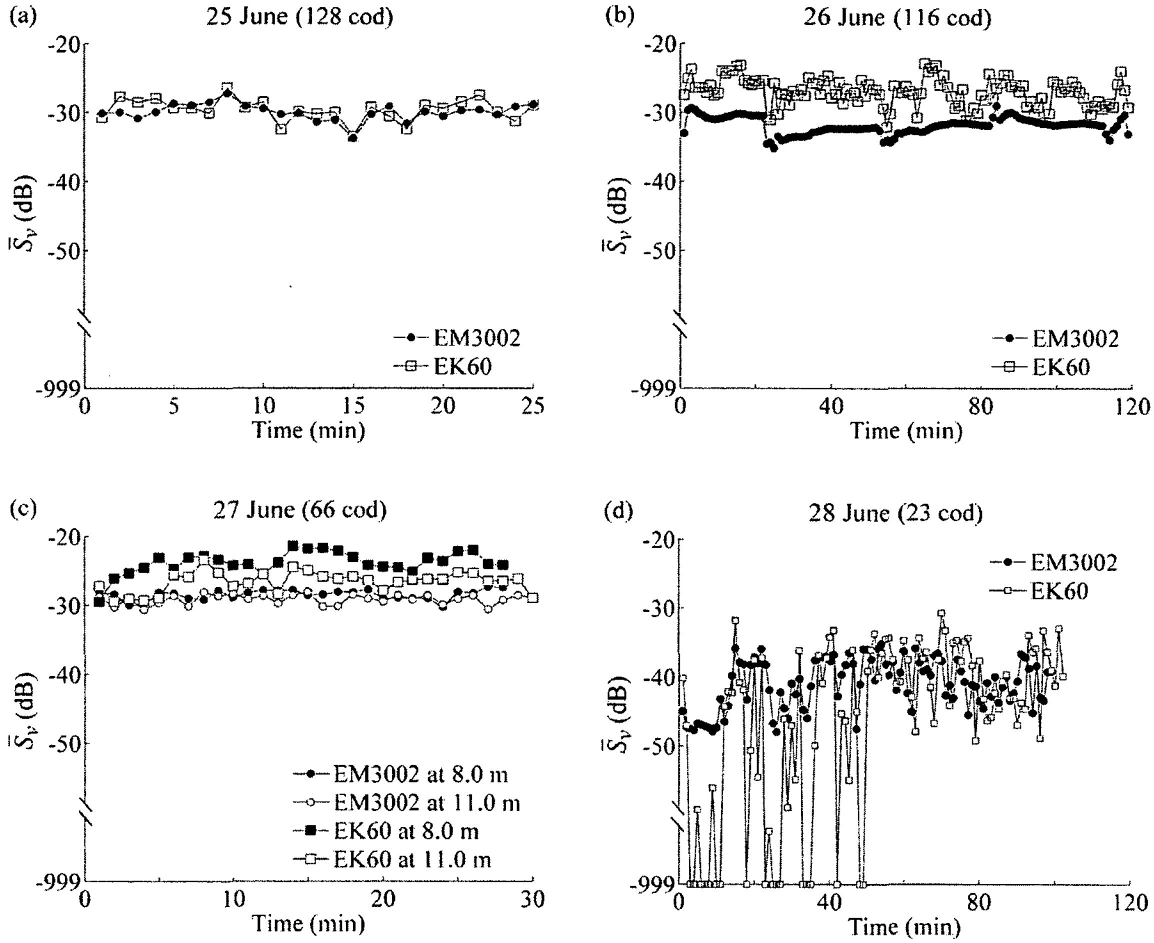

Figure 1-4. Time-series of mean volume-backscattering strength ($\bar{S}_v$) from the 300-kHz, EM3002 multibeam echo sounder and the 120-kHz, EK60 split-beam echo sounder within the cage stocked with (a) 128, (b) 116, (c) 66, and (d) 23 mature Atlantic cod. $\bar{S}_v$ was averaged over 60 ping intervals and selected depth layers inside the cage. Transducers were at a fixed depth and the cage was lowered from 8 to 11 m on 27 June.

Discussion

These results demonstrate the capability of a hydrographic multibeam echo sounder to detect cod in the water column, describe their spatial distribution, and measure large differences in their biomass or density. However, for both the EM3002 and the EK60, the acoustic-density estimates were not proportional to the known fish biomass at intermediate stocking densities. The observed differences between $\overline{S}_v$ and fish abundance may have resulted from side-lobe interference from the cage, or cod behavior, or a combination of both factors. The S_v was expected to decrease proportionally with the number of cod removed from the cage (assuming linearity in echo-integration; Foote, 1983), which requires random and homogeneous distributions of targets within the acoustic beams, and constant fish orientations. The narrow (78) beam of the 120-kHz transducer makes the EK60 more sensitive to non-uniform distributions of cod within the cage compared with the EM3002, because the multibeam array has a much larger insonified volume. Conversely, the EK60 is less sensitive to variability resulting from transducer rotation (yaw) than the EM3002. Measurements from both echo sounders can be affected by the patchiness of the cod and their pitch and roll, even within a controlled environment such as a cage (Figure 1-2). For example, on 27 June, the cod were densely congregated in the center of the cage and were consistently insonified by the most vertical EM3002 beams. Other factors, such as the large fish lengths relative to the beam widths and short measurement ranges relative to the nearfield range for the multibeam array (~7 m), potentially contributed to the observed variability in acoustic-abundance estimates.

Data from the EM3002 and the underwater video cameras described the spatial distribution and behavior of cod in the cage. This information elucidated differences between the expected cod densities and those estimated using the EK60 data at intermediate densities. Those estimated with the EK60 data tended to be biased high when the cod were concentrated near the center of the cage and low when they were distributed non-uniformly to either the sides or the bottom. The $\overline{S}_v$ should theoretically have been proportional to the densities when cod were homogeneously distributed, but the $\overline{S}_v$ of the homogeneously distributed 128 cod measured by the EK60 was 3.7 dB lower than that expected based on the number of fish, cage volume, and predicted TS (Rose and Porter, 1996). The percentage change in cod abundance detected by changes in $\overline{S}_v$ was -35% for the EM3002 and +95% for the EK60 when the number of cod was reduced by 9%. Without additional information, it was difficult to determine whether the $\overline{S}_v$ of the initial population was lower because of changes in tilt-angle, which could have lessened the difference between these two percentages, or whether the spatial distribution on the second day could have accounted for the differences in $\overline{S}_v$ between the echo sounders.

The EM3002 is a hydrographic instrument modified to collect water-column data. Its performance for measuring *Sv* is limited by a 64 dB, dynamic range, split-beam phase detection in the athwartships direction only, and a nearfield range of ~7 m. The newer fisheries multibeam echo sounder, Simrad ME70, has several advantages over hydrographic multibeam echo sounders, such as an adjustable beam width (2.2 – 20°) and split-beams operating at multiple frequencies (Trenkel et al. 2008). Regardless of these and other limitations, a calibrated EM3002 has great potential for improving surveys of cod. To realize the full potential of the EM3002, additional research should include calibration of all beams, single-target detections and TS estimations, and quantification of the effect of different incidence angles and overlapping beams on volume-backscatter measurements. Ultimately, the intent is to use a single EM3002 to collect useful data concurrently for both fisheries and hydrographic surveys.

Acknowledgements

The authors extend their gratitude to many people who contributed to this project. C. Rillahan is thanked for providing the underwater video equipment. Captain B. Smith and his crew are thanked for their help during many hours working offshore. This study would not have been possible without the contributions of T. Ford, D. Gurshin, C. Humbyrd, R. Love, M. Malik, T. Milton, L. Siceloff, and M. Walsh. Without the experience of Captain C. Bouchard and his crew, live cod would not have been available for this study. We thank Kongsberg Maritime for assisting with the use of the EM3002 equipment, and K. Foote for modeling the sphere target strength at 300 kHz. This study was funded by a Northeast Consortium Project Development Award.

CHAPTER II

SYNOPTIC ACOUSTIC AND TRAWL SURVEYS OF SPRING-SPAWNING ATLANTIC COD IN THE GULF OF MAINE COD SPAWNING PROTECTION AREA

Abstract

Repeated acoustic and trawl surveys were performed in the Gulf of Maine cod spawning protection area (GOMCSPA) to: (a) describe their spatial and temporal distribution of the spring-spawning Atlantic cod (*Gadus morhua*); (b) estimate their abundance and biomass; (c) evaluate precision of the survey methods; and (d) compare densities in adjacent areas inside and outside of the area closure. A fishing vessel equipped with 38- and 120-kHz split-beam echo sounders surveyed once monthly from dusk to dawn along ten parallel transects that covered a 80.8 km^2 area during April-July 2011. During each survey, two bottom trawl vessels (one with a small mesh net and one with a large mesh net) each made ten tows in parallel behind the acoustic survey vessel. Cod abundance and biomass was derived from acoustic backscatter by a combination of methods: (1) species apportionment based on trawl catch vs. echo classification; (2) *in situ* vs. predicted target strength (TS); (3) size of elementary distance sampling unit (EDSU) and statistical approach; and (4) with and without dead zone correction.

No Atlantic cod were observed by trawl or acoustics during the survey on 7-8 April 2011. The numbers of individual cod in the combined trawl catch were 609 in May, 317 in June, and 70 in July, and the mean total lengths were 66 cm in May, 73 cm in June, and 71 cm in July. The mean cod density based on echo classification and a 100-m EDSU resulted in a substantially lower coefficient of variation when the variance was estimated by geostatistics compared to any other method used. Based on echo classification, semivariogram modeling revealed that 67-77% of the variance in cod biomass density was explained by a spatial structural component at a range (correlation length) of 2.0-2.4 km. Density maps, produced by ordinary kriging, showed cod were relatively widespread in the survey area in May, but congregated at higher densities in areas adjacent to two elevated bathymetric features. Most cod converged to a single location in June, and were at a higher concentration compared to the highest densities observed in May. This congregation decreased in size and density in July.

The survey estimates of cod biomass were 184-494 mt in May, 138-617 mt in June, and 39-135 mt in July. Based on echo classification, the biomass for the GOMCSPA, extrapolated from these survey estimates, were 260-466 mt in May, 196-513 mt in June, and 91-198 mt in July. While biomass density of Atlantic cod was not significantly different between adjacent areas inside and outside of the GOMCSPA during May and July, mean biomass density based on echo classification was significantly higher inside the GOMCSPA than that outside the GOMCSPA during June. These results provide some evidence that adult Atlantic cod in spawning condition congregated within the GOMCSPA during the seasonal fishing closure, and that the biomass being protected by the closure may have represented 4-5% of the GOM cod spawning stock biomass at the time of the study.

Introduction

Historic population declines of Atlantic cod (*Gadus morhua*) are well documented throughout its range (Myers et al. 1997; Ames, 2004), yet cod continue to support a commercial and recreational fishery in many regions of the North Atlantic Ocean, including the Gulf of Maine (GOM). The recovery of the GOM cod stock, in part, depends on the successful management and conservation of the spawning stock biomass (SSB). Protection of cod from fishing activities during spawning season is one strategy for rebuilding populations and managing a sustainable fishery (Chiappone and Sealey 2000; Guénette et al. 2000; Mangel 2000; Schopka et al. 2010), particularly for highly fecund species with a predictable spawning season and site fidelity (Burton et al. 2005; Nemeth 2005; Evans et al. 2008). The effectiveness of area management measures in rebuilding the GOM cod stock partly depends on high-quality information on the spatial and temporal scale of spawning cod congregations (Chiappone and Sealey 2000) and the movement of individuals (Schopka et al. 2010). Moreover, the establishment of biological reference points necessary for successful fishery management depends on accurate SSB estimates.

While most stock assessments use fishery-independent trawl data collected from a stratified-random sampling design, systematic surveys using split-beam echo sounders provide acoustic indices of abundance and distribution in the assessments of some fish stocks. In the United States, acoustic survey data have been used in stock assessments of commercially important pelagic species such as Atlantic herring (*Clupea harengus*) by the NOAA Northeast Fisheries Science Center (Jech and Michaels 2006), Pacific hake (*Merluccius productus*) by the NOAA Northwest Fisheries Science Center (Fleischer et al. 2008), and walleye pollock (*Theragra chalcogramma*) by the NOAA Alaska Fisheries Science Center (Horne and Walline 2005). Although acoustic surveys on cod and haddock have not been widely developed in the US, they have been used for estimating abundance of cod stocks in Canadian Atlantic waters (Rose 2003; McQuinn et al. 2005; Mello and Rose 2005a, 2005b) and in the Barents Sea (Godø and Wespestad 1993; Korsbrekke et al. 2001). Rose (2003) and Rose et al. (2011) used 38-kHz single- and dual-beam echo sounders in 1995-1997, and 38-kHz split-beam echo sounders since 1998, to estimate biomass of the stock of Atlantic cod in Smith Sound, Newfoundland during over-wintering months, when dense, size- and age-structured mono-specific aggregations are formed prior to spawning. Mello and Rose (2005a, 2005b) used acoustic data to quantify seasonal distribution and aggregation patterns of Atlantic cod in Placentia Bay, Newfoundland. McQuinn et al. (2005) estimated the effects of acoustic and trawl dead zones on density estimates of Atlantic cod and demonstrated the advantages of an integrated acoustic-trawl survey for Atlantic cod in the Gulf of St. Lawrence. Stock assessment models (e.g., virtual population analysis) for the Northeast Arctic cod stock have been based on fishery-independent abundance estimates obtained from bottom-trawl and acoustic surveys (Korsbrekke et al. 2001). Since 1985, Norwegian researchers have used an acoustic index of spawning stock biomass obtained from acoustic surveys of spawning grounds (Korsbrekke et al. 2001). Acoustic surveys can be used to estimate biomass and map distributions of GOM cod that could prove valuable in stock assessment and marine spatial planning (e.g., fishery area closures), particularly in habitat not accessible by bottom trawling.

The GOM cod spawning protection area (GOMCSPA) is an example of an area management measure recently implemented in the Northeast Multispecies Fishery Management Plan (New England Fishery Management Council 2011), which prohibits commercial and recreational fishing, from 1 April through 30 June, in the 0.5° longitude x 0.5° latitude seasonal area closure 133 (New England Fishery Management Council 1998) in the western Gulf of Maine. The spring-spawning GOM Atlantic cod caught in the GOMCSPA, locally referred as the "Whaleback" area, have been shown to be genetically distinct from winter-spawning cod in this area (Wirgin et al. 2007; Kovach et al. 2010) and exhibit a high degree of inter-annual site fidelity and residency (Howell et al. 2008; Siceloff and Howell 2012). However, the relative importance of this area has not been quantified, and the appropriateness of its size and timing has not been assessed. What is the biomass of GOM cod spawning stock that use this area for spawning during the closure? Should the size of the closed area be reduced, expanded, or redefined? These questions are quite fundamental, and this research was designed to investigate such questions.

Specifically, repeated acoustic and trawl surveys were performed in the GOMCSPA to: (a) describe their spatial and temporal distribution of the spring-spawning cod; (b) estimate their abundance and biomass; (c) evaluate precision of the survey methods; and (d) compare densities in adjacent areas inside and outside the GOMCSPA . First, geostatistics were used to describe the spatial autocorrelation and distribution of cod based on densities derived from acoustic backscatter and trawl information. Then, several techniques were used to estimate abundance and biomass of cod within the survey area and the GOMCSPA, and their associated precision is discussed. Lastly, the presence of any boundary effect of the area fishing closure on cod density from adjacent transects inside and outside GOMCSPA was investigated.

Methods

Study Area

The study area was located in the western Gulf of Maine (NAFO Subarea 5Y) of the northwest Atlantic Ocean where cod congregate for spawning in large numbers annually (Howell et al. 2008). A focal area of the major activity was identified by a tracking study of acoustically-tagged cod (Siceloff and Howell 2012), and was selected for repeated acoustic and trawl surveys. The survey area (approximately 80.8 km^2), overlapped the GOMCSPA (114.3 km^2) by approximately 47%, and was located approximately 8 km east of the coast of New Hampshire and Massachusetts, USA approximately 5 km south of the Isles of Shoals (Figure 2-1). The bottom depth of the survey area ranged from approximately 37 m to 93 m, with an average depth of 57 m. A series of humps and ridges, collectively referred as "Whaleback" was at the northern section of the area. Muddy flat bottom extends to the south, occasionally broken by a few large humps that are tens of meters in elevation. The largest of these, locally referred to as the "Southwest Hump", is located in the eastern portion of the GOMCSPA.

Acoustic Sampling

A 14-m fishing vessel ("F/V Lady Victoria") equipped with Simrad 38- and 120-kHz split-beam EK60 echo sounders (Andersen, 2001) surveyed ten parallel transects that were approximately 8.2 km long and spaced 1 km apart (Figure 2-1). Location,

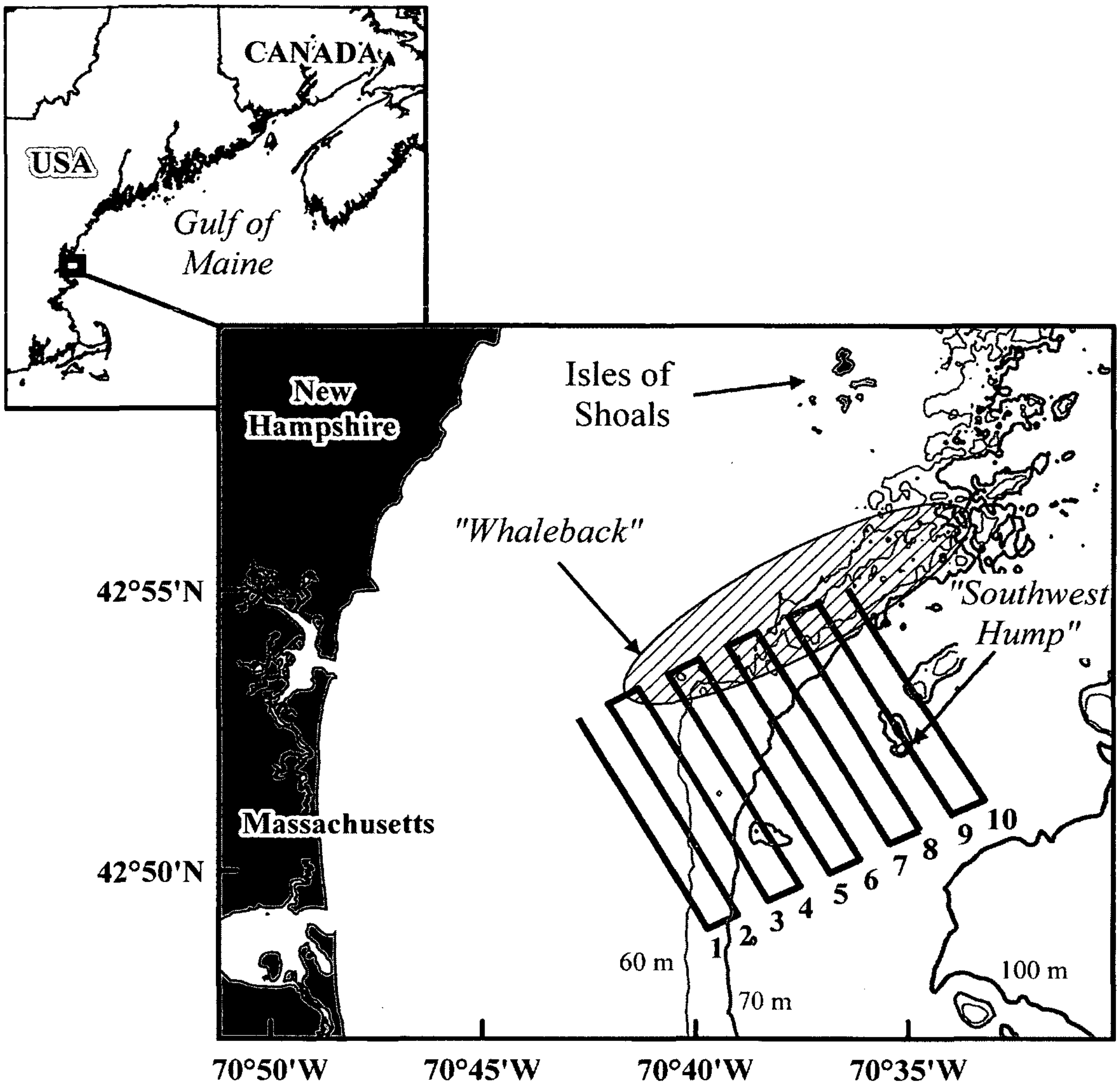

Figure 2-1. Acoustic and trawl surveys were conducted along the 8.2-km parallel transects (solid black lines numbered 1 to 10) with 1-km spacing overlapping the Gulf of Maine cod spawning protection area (grey shaded polygon) off the western Atlantic coasts of New Hampshire and Massachusetts, USA. The series of humps and ridges that comprise "Whaleback" area are highlighted by the cross-hatched ellipse. The 60-m, 70-m, and 100-m isobaths are shown.

orientation, length and spacing of transects were selected based on prior knowledge of cod movements and catches, tow path considerations, desired coverage and resolution, survey vessel speed (~5 knots), and the allowable ship time (~10 h/d). Although multiple survey designs were possible, we chose to use systematic uniform transect spacing, which is optimal for obtaining the most precise abundance estimate (Simmonds and Fryer, 1996). Surveys were performed largely during dusk to dawn on 7-8 April, 28-29 May, 18-19 June and 3-4 July 2011. The split-beam transducers, with nominal 3-dB beam widths of 12° for the 38 kHz (ES38-12) and 7° for the 120 kHz (ES120-7G), were mounted from a pole attached mid ship and 2.5 m below the water surface. Sound transmission was based on a 0.512-ms pulse duration, 2-Hz ping rate, and a power of 1000 W at 38 kHz and 500 W at 120 kHz.

Acoustic backscatter, geo-referenced with the global positioning system (GPSMAP78sc, Garmin International Inc., Olathe, Kansas, USA) at approximately 3 m accuracy, was collected using the Simrad ER60 data acquisition software (v2.2). Prior to each survey, the echo sounders were calibrated by the standard target method using a reference target (38.1-mm tungsten carbide sphere) suspended 10-12 m from each transducer by a monofilament line (Foote et al. 1987). Only the 120-kHz data were used for the abundance estimates for the June and July surveys due to a transducer cable break in the 38-kHz split-beam transducer during the June survey. Cod abundance was estimated from data collected during May at both frequencies. Ambient noise was evaluated using data passively collected by the echo sounders at various vessel speeds following the Simrad operation manual.

At the start and end of each survey, salinity and temperature depth profile measurements were taken at 2 to 3 locations using a Sea-Bird Electronics SBE-25 CTD and used for sound speed estimates during post processing. In an effort to detect spawning sounds produced by male cod (Brawn, 1961; Rowe and Hutchings, 2006), underwater sound was recorded by a calibrated omnidirectional hydrophone (C-55, Cetacean Research Technology, Seattle, Washington, USA) for 1 to 5 minute duration at the start and end of the survey, and in areas of high cod abundances immediately following the survey. Mean sensitivity of the hydrophone was -163.3 dB re 1 V/μPa. These sound recordings were acquired and processed using SpectraPRO332 professional sound analysis software.

Trawl Sampling

The primary purposes of trawling during the acoustic survey were to verify the presence of cod, describe the species and size composition of fish near the sea floor, and correlate acoustic and trawl densities of cod sampled closely in space and time by both gear. Secondarily, areal densities of Atlantic cod estimated from trawl samples provided another measure of cod abundance within the study area, and allowed for an inter-annual comparison to trawl-based cod densities within the study area sampled in previous years without acoustics. During each survey, two bottom trawl vessels (one with a small-mesh net and one with a large-mesh net) each made ten tows parallel to each other behind the acoustic survey vessel for a duration of 10 minutes (time between winch engagements) at approximately 2-2.5 knots. In recognition of size selectivity of trawl mesh sizes, two bottom trawls of different mesh sizes were used to ensure all sizes of adult Atlantic cod were represented in the combined catch. Given the spawning behavior and densities of cod expected during the surveys within the fishing closure, a short tow duration was selected to avoid large catches, spatially distribute the verification sampling effort at sufficient spatial resolution, and reduce post-release mortality (Ross and Hokenson 1997; Davis 2002;). A shrimp net with a stretch mesh of 4.4 cm throughout the body and cod end was towed by the 14-m "*F/V Julie Ann II*" (small-mesh net). A commercial multispecies bottom trawl with a 15.2-cm stretch mesh body and 16.5-cm stretch mesh cod end was towed by the 14-m "*F/V Ellen Diane*" (large-mesh net). Each tow had an approximate 30-m spread between doors and an average estimated swept area of 23,100 m^2.

Trawl samples were processed by first separating out the flatfish, and other demersal fishes without a swimbladder. These were held in 1-m^3 insulated polyethylene containers with a running sea water hose for circulation. Species that were considered acoustic targets with a swimbladder such as cod, haddock (*Melanogrammus aeglefinus)*, silver hake (*Merluccius bilnearis*), hakes (*Urophycis* spp.), and Atlantic herring, and without a swimbladder, such as Atlantic mackerel (*Scomber scombrus*) and spiny dogfish (*Squalus acanthias*), were placed in separate 1-m^3 insulated polyethylene containers with a running sea water hose. Total length (L) of up to 50 individuals of each species within a sample was measured, and the remaining fish counted. Total weights (W) of 111 cod individuals were measured to the nearest 0.1 kg to derive an empirical length-weight (W) relation ($W=aL^b$) using linear regression of the natural log-transformed variables. Estimated parameters were compared to the L-W relation of GOM cod collected over the entire time series of NEFSC spring bottom trawl surveys (Wigley et al. 2003) using one-sample t-tests. The Kolmogorov-Smirnov two-sample test was used to compare total length distributions of cod caught by the two mesh sizes or between monthly catches. When possible, reproductive condition and sex was noted (individuals expelling milt or eggs). All fish were returned to the sea after measurement.

To provide some insight into inter-annual variability of cod density near the GOMCSPA, trawl estimates of fish density (thousands/km^2) from this study were compared to those from previously unpublished data collected by the *"F/V Stormy Weather"*. As part of earlier studies (Gurshin et al. 2009), this vessel made tows with a similar large-mesh bottom trawl, but with a door spread of 64 m (He 2007), within the GOMCSPA during the day of 21, 22, 25 June 2007, 26 June 2008, and 8 May 2009. The trawl estimates during 2007-2009 probably underrepresented cod abundance because efforts were made to avoid dense congregations of cod identified by the vessel's echo sounder.

Echogram Processing and Echo Classification

Raw acoustic backscatter was imported into Echoview software (v4.9, Myriax Pty. Ltd., Hobart, Tasmania) for processing echograms (Figure 2-2). Analyses of acoustic data were based on standard terminology defined by MacLennan et al. (2002) and Simmonds and MacLennan (2005). Acoustic backscatter was attributed to cod by two classification methods: manual classification of echo traces in the echograms (hereafter referred as "echo classification") and apportionment of acoustic backscatter based on catch composition (hereafter referred as "catch apportionment"). Echo classification was the assignment of echoes or regions within the echogram to cod based on target strength of individual echo traces, location in the water column, catch composition of nearby trawl samples, and spatial structure of the appearance of echoes in the echogram. Because cod are known to vertically migrate off the bottom and to be loosely organized during night, acoustic detectability of cod near the bottom and identification of individual echo traces was expected to be higher by surveying at night than at day (McQuinn and Winger 2003; Rose 2003, 2009; McQuinn et al. 2005).

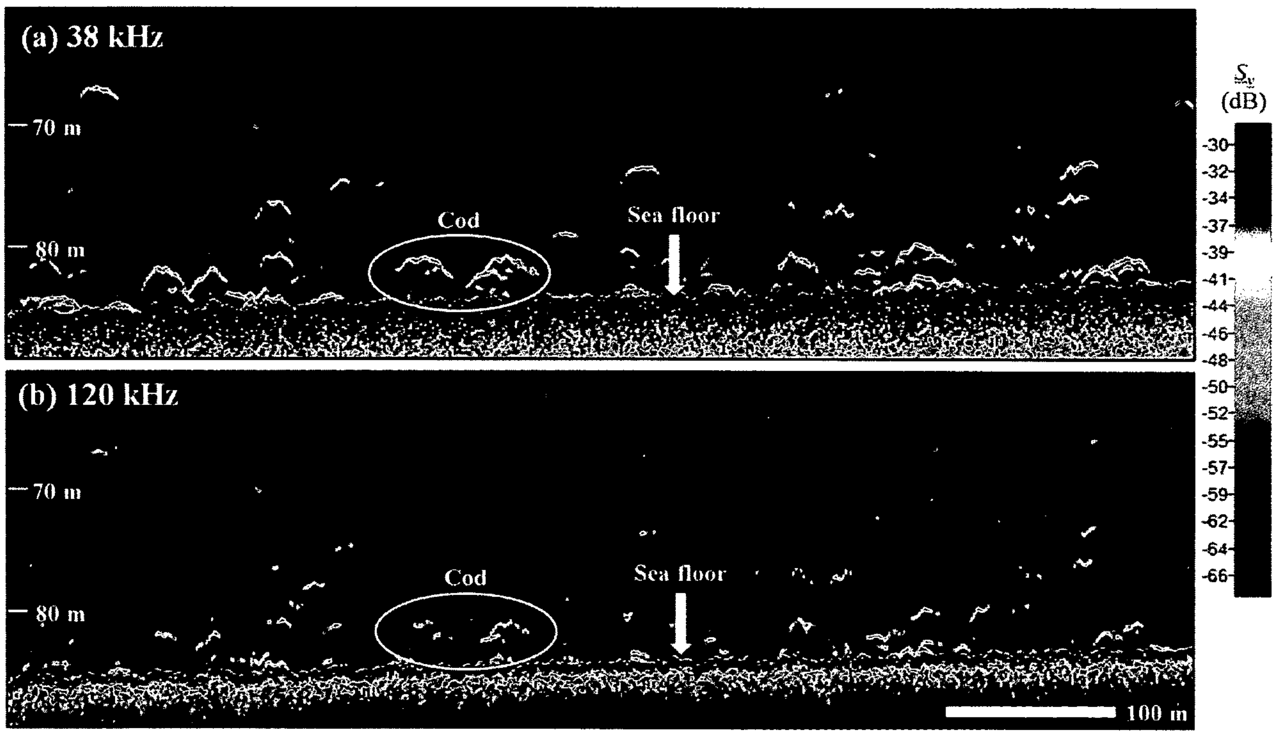

Figure 2-2. Echograms showing the volume backscattering strength (S_v dB re m^{-1}) of individual echoes of Atlantic cod (examples are circled) clustered within 30 m above the sea floor (arrow) that were typical of areas of high abundance in the Gulf of Maine cod spawning protection area during the night of 28-29 May 2011 as observed by (a) 38-kHz and (b) 120-kHz Simrad EK60 split-beam echo sounders and verified by bottom trawl. The vertical scale is depth relative to the surface and the horizontal scale is vessel distance.

For the echo classification method, mean area backscattering coefficient ($s_{a,\,\text{cod}}$) attributed to cod was based on echo integration above a minimum volume backscattering strength (S_v) threshold (-66 decibels referenced to 1 m^{-1} [dB re m^{-1}]) selected to maximize exclusion of backscatter of non-target species and minimize exclusion of cod (sensu Jech and Michaels 2006). For the catch apportionment method, $s_{a,\,\text{WC}}$ was based on echo integration of the acoustic backscatter in the water column below 30 m water depth, above 0.3 m above the sea-floor echo (bottom detection), and above a minimum S_v threshold of -72 dB, which was approximately 2 dB higher than the maximum modeled background noise (De Robertis and Higginbottom 2007). To account for unmeasured cod densities near the sea floor (i.e., acoustic dead zone and partial integration zone), the S_v for Atlantic cod within this dead zone, which was equivalent to approximately 1.1 m height, was estimated by the mean S_v from the 2-m depth layer immediately above it (Kloser, 1996; Ona and Mitson, 1996). The echo classification and catch apportionment methods were based on echo integration along the transects at intervals, referred as elementary distance sampling units (EDSUs), that were appropriate for describing spatial autocorrelation in the data and then accounting for the autocorrelation to estimate the variance (geostatistics), or removing the autocorrelation and then assuming samples were independent and identically distributed (i.i.d.) to estimate the variance (classical statistics).

Target Strength Estimation

Fish density (per area) was estimated from echo integration by dividing s_a by the mean (expected) acoustic backscattering cross-section ($\langle \sigma_{bs} \rangle$) in units of m^2/kg or m^2/fish as defined by MacLennan et al. (2002) and reviewed by Simmonds and MacLennan

(2005). The logarithmic equivalent of σ_{bs}, is the target strength (TS, dB re 1 m^2) and is defined as $10\log_{10}(\sigma_{bs})$ and mean TS is the decibel equivalent of the mean $\langle\sigma_{bs}\rangle$ (i.e., averaged in the linear domain). Target strength was estimated using trawl-based fish lengths or *in situ* measurements.

Trawl-based target strength was predicted from individual length measurements from the combined trawl catch of each paired tow for the species considered acoustically detectable (Table 2-1). This TS-L relation was modeled as TS = $20\log_{10}(L) + b_{20}$ where the slope was assumed to be 20, based on the theory that TS should be proportional to the square of the effective acoustic fish length, and b_{20} is the y-intercept parameter (McClatchie et al. 2003; Simmonds and MacLennan 2005). Target strength in units of dB re 1 m^2/kg was derived from parameters of published TS-L and L-W relations (Table 2-1) and was defined as $m_w \log_{10}(L) + b_w$ where m_w = 20-(10b) and $b_w = b_{20} - 10\log_{10}(a)$ (Simmonds and MacLennan 2005). For cod, TS was predicted by the TS-L relation of Rose and Porter (1996), which was TS = $20\log_{10}(L)$ - 66 at 38 kHz and TS = $20\log_{10}(L)$ - 65 at 120 kHz. These TS-L relations have been applied in subsequent acoustic surveys of cod (Lawson and Rose 2000; Fudge and Rose 2009), but b_{20} = -67.5 has also been used to estimate cod density from acoustic surveys at 38 kHz (Rose 2003) and at 120 kHz (Mello and Rose 2005a, 2005b). A b_{20} of -67.5 was first suggested to scale echo integration at 38 kHz for gadoids (Foote et al. 1986; Foote 1987). For comparison, TS of cod was also predicted using b_{20} = -67.5, and later compared to *in situ* TS estimates, but was not used in abundance estimation.

Table 2-1. Parameters for length-weight (L-W) relation and target strength-length (TS-L) relations in units of weight ($TS_w = m_w \log_{10}(L) + b_w$) for acoustically detectable species caught by a small-mesh (4.4-cm cod end) and large-mesh (16.5-cm cod end) bottom trawl. TS-L parameters used were specific to frequency (f, kHz) when possible.

	$W = aL^b$ (Wigley et al. 2003)		TS-L relation				
Species	a (x10^{-6})	b	f	b_{20}	Source for TS = $20\log_{10} + b_{20}$	b_w	m_w
Acadian redfish	8.2897	3.2036	38	-68.7	Gauthier and Rose 2002	-17.885	-12.036
Atlantic cod	5.515	3.1283	38	-66	Rose and Porter 1996	-13.416	-11.283
	(this study)	(this study)	120	-65		-12.416	-11.283
Atlantic herring	9.3887	2.9794		-71.2	Fässler et al. 2009	-20.926	-9.794
Atlantic mackerel	3.1400	3.3119	120	-88	Clay and Castonguay 1996	-32.969	-13.119
Butterfish	8.4411	3.2930	100	-69.3	based on Japanese butterfish *Psenopsis anomala;* Mukai et al. 1993	-18.564	-12.930
Fourbeard	4.2258	3.0979	38	-66	based on Atlantic cod	-12.259	-10.979
rockling	(red hake)	(red hake)	120	-65		-11.259	-10.979
Haddock	7.4582	3.0766	38	-66	based on Atlantic cod	-14.726	-10.766
			120	-65		-13.726	-10.766
Pollock	6.7877	3.1024	38	-66	based on Atlantic cod	-14.317	-11.024
			120	-65		-13.317	-11.024
Red hake	4.2258	3.0979	38	-66	based on Atlantic cod	-12.259	-10.979
			120	-65		-11.259	-10.979
Silver hake	3.7513	3.1512	38	-68	based on Pacific hake (*M. productus*); Traynor 1996	-13.742	-11.512
Spiny dogfish	1.7955	3.0596	120	-83	Goddard and Welsby 1986*	-25.542	-10.596

* b_{20} was estimated from TS = $22.5\log_{20}(L, \text{cm})$ - 88.6 at 120 kHz and adding a1 dB to compensate for an averaging error in the experiments according to Foote (1986).

Mean *in situ* TS of cod was estimated from single echo detections (SEDs) within echogram regions classified as cod for each transect. Single echo detections were based on a maximum two-way beam compensation of 6 dB, an echo envelope between 0.6 and 1.5 normalized pulse lengths, 6-dB pulse length determination level, and a -50 dB minimum TS threshold. Single echo detections were not used if the Sawada index was greater than 0.1 in 2-m depth layers within each EDSU (Sawada et al. 1993; Rudstam et al. 2009). Mean *in situ* TS in units of kg was calculated by adding $10\log_{10}(N_{kg})$ to the mean *in situ* TS for each transect where N_{kg} is the number of cod per 1 kg of biomass (Clay and Castonguay 1996; e.g., $N_{kg} = 0.5$ if the mean individual weight from the combined trawl catch for a given paired tow is 2 kg).

The mean difference between the predicted TS for each paired tow and mean *in situ* TS of cod from manually-classified echo traces (i.e., track of SEDs) was tested against zero using a Wilcoxon signed-rank test for paired samples (D-test statistic) if the assumption of normality was not met, or a paired t-test (t-test statistic) if normality was met. Only SEDs below 30 m water depth and from transect segments along the tow paths were used to maintain the reasonable assumption of a similar size distribution between the cod caught by trawl and detected by acoustics. Mean *in situ* TS for tows represented by less than three individual fish echoes were considered not representative and as such were excluded. Single echo detections above the trawl zone, but below 30 m water depth, were included to improve sample size. Based on the May survey data, the mean difference of *in situ* TS between 38 kHz and 120 kHz for simultaneous single echo detections classified as cod was tested against zero using a paired t-test.

Geostatistics

Geostatistics is a statistical approach that incorporates both spatial structure and randomness. The theory of geostatistics, which originated from mapping mining deposits by interpolation based on the spatial covariance structure of core samples (Matheron 1965), is described in contemporary text such as Cressie (1993), Journel and Huijbregts (1978), and Schabenberger and Gotway (2005). The application of geostatistics for fish stock assessments based on acoustic survey data is well documented (Petitgas 1993, 2001; Rivoirard et al. 2000; Páramo and Roa 2003; Cubillos et al., 2008), and in particular for acoustic surveys of cod abundance (Lawson and Rose 2000; Rose 2003; Mello and Rose 2005a, 2005b). Geostatistical techniques were used in this study to describe the spatial structure of the data, to map the distribution of cod by spatial interpolation (prediction) using the model parameters that describe the spatial covariance, and to estimate the variance of spatially correlated acoustic estimates of cod density.

A two-stage geostatistical approach was taken to estimate abundance and distribution of Atlantic cod. First, the spatial covariance was described through structural analysis using semivariograms and then the modeled parameters obtained by the structural analysis were used to spatially predict cod densities by ordinary kriging within the survey area (Rivoirard et al. 2000; Mello and Rose 2005b). The structural tool used to describe the spatial autocorrelation in cod density, as a function of distance between any two locations, was the robust empirical semivariogram, which is commonly used for fisheries data to reduce the influence of many zero values and few large values (Páramo and Roa, 2003; Mello and Rose 2005b). The robust semivariance estimate was given by Cressie and Hawkins (1980) as:

$$\bar{\gamma}(h) = \frac{\left\{\frac{1}{|N(h)|}\sum_{N(h)}\left|z_i - z_j\right|^{0.5}\right\}^4}{2[0.457+0.494/|N(h)|]} \qquad (1)$$

where $N(h)$ is the set of all pairwise distances h between locations i and j in a two-dimensional plane, $|N(h)|$ is the number of distinct pairs in $N(h)$, z_i and z_j are the response variables at locations i and j, respectively, and 0.457 and 0.494 are bias correction coefficients. The robust empirical semivariograms were initially fitted with the exponential, spherical, and Gaussian covariance models using weighted least squares (Cressie 1993), and the final model was selected based on the minimization of the weighted sum of squares. To detect the presence of geometric anisotropy, directional semivariograms were computed by restricting the distances considered along axes centered at 0°, 30°, 60°, 90 °, 120°, and 150° with an angle tolerance of ±30° and then fitted with the selected covariance model to estimate the correlation length (range) at each angle. Because anisotropy may be falsely detected at the direction of parallel transects (Rivoirard et al. 2000), anisotropy was assumed not present if the ratio between the maximum range and the range at the direction perpendicular to the direction with the maximum range was less than 2.0 (Cubillos et al. 2008).

Area backscatter attributed to cod by echo classification was integrated over 10-m, 100-m and 500-m EDSUs for each month for evaluating the spatial structure at different scales. For display, s_a was rescaled to the commonly used mean nautical area backscattering coefficient ($s_A = 4\pi(1852)^2 s_a$, m^2/nmi^2; MacLennan et al. 2002). Empirical robust semivariograms were computed using $\log_{10}(s_A+1)$ values for cod based on these three spatial scales. The covariance models used to fit the empirical robust semivariograms were used to describe the variance and range of the three spatial scales

(Rivoirard et al. 2000). Based on this spatial analysis, the EDSU for calculating arithmetic mean cod densities assuming mean s_a values was approximately independent and identically distributed (i.i.d.) was selected, such that the correlation between successive samples was considered small. In contrast, a smaller EDSU was chosen to allow the spatial structure to be adequately described for estimating the variance of cod density using geostatistics and mapping the spatial distribution using kriging methods, and smooth micro-scale variability. The total sill parameter of the fitted semivariogram model represents the maximum level of variability in density among sampling locations, and is often close to the dispersion variance (Petitgas, 1993, 2001; Rivoirard et al., 2000). The total sill consists of the partial sill parameter, which is the amount of variation explained by the spatial structure, and the nugget parameter, which is y-intercept of the fitted semivariogram model and represents either micro-scale variation or measurement error. The geostatistical estimation variance (σ_E^2) of the mean cod density for the survey area was estimated from the fitted semivariogram model and the extensive-elementary variance given the geometry of the survey area, EDSU, and transect length using EVA2 geostatistical software (Petitgas and Lafont 1997). The geostatistical estimator of the coefficient of variation (CV, %) of the mean cod density was calculated as the square root of divided by the arithmetic mean density and then multiplied by 100 (Rivoirard et al. 2000).

The spatial distribution of cod within the survey area was mapped onto a fine-scale grid of points within the survey domain. The grid was created by dividing each dimension of the rectangular spatial extent of the survey area by 500 points (i.e., 500 x 500 nodes), and then clipped by the boundary of the survey domain. Ordinary kriging was used to spatially interpolate cod densities at unsampled locations based on weighting cod densities at sampled locations within a moving local neighborhood of 150 points based on the fitted semivariogram model (Rivoirard et al. 2000; Páramo and Roa 2003). The size of the local neighborhood was selected based on the neighborhood size that resulted in the lowest mean squared error by cross-validation (Isaaks and Srivastava 1989; Páramo and Roa 2003). Geostatistical analyses were performed using the package "geoR" in R statistical computing software (Ribeiro and Diggle 2001; R Development Core Team, Version 2.13.2, 2012).

Abundance and Biomass Estimation

Abundance (Q), as number of individuals, and total biomass (B), expressed as metric tons, was estimated as the product of the area (A) and areal density (D) of cod in units of fish/m^2 or kg /m^2. Abundance and biomass was calculated for the entire survey area from sample density values along transects 1-10 and for the GOMCSPA by two extrapolations, assuming the mean density was representative of the area not sampled. First, Q and B for the survey area sampled by transects 1-10 were extrapolated to the GOMCSPA proportionally based on the ratio of the areas (114.3 km^2:80.8 km^2). Second, assuming there is a boundary effect outside the closure (transects 1-3), Q and B for the GOMCSPA was estimated as the product of the mean density inside the GOMCSPA (transects 4-10) and the area.

Mean cod density in units of fish/m^2 (D_f) and kg/m^2 (D_w) from the large-mesh and small-mesh bottom trawl catch was calculated as:

$$D_f = \frac{1}{N_i}\sum_{i=1}^{N_i} C_{\text{cod},i}/A_{S,i} \qquad (2)$$

$$D_w = \frac{1}{N_i}\sum_{i=1}^{N_i} W_{\text{cod}i}/A_{S,i} \qquad (3)$$

where $C_{\text{cod},i}$ is the number of cod in tow i, $A_{\text{S},i}$ is the swept area (m^2) of tow i, $W_{\text{cod}i}$ is the predicted total weight (kg) of cod in tow i, and N_i is the number of tows. The coefficient of variation (CV, %) of the mean trawl density was calculated as the standard error divided by the mean and multiplied by 100.

The acoustically derived density of cod estimated by the catch apportionment method (McQuinn et al. 2005) was defined as:

$$D = \frac{1}{N_j}\sum_{j=1}^{N_j} s_{a,\text{WC},j} P_{\text{cod},i}/\langle\sigma_{\text{bs}}\rangle_{\text{cod},i} \qquad (4)$$

$$P_{cod,i} = \frac{1}{N_k}\langle\sigma_{\text{bs}}\rangle_{\text{cod},i} W_{\text{cod},i}/\sum_{k=1}^{N_k} W_{k,i}/\langle\sigma_{\text{bs}}\rangle_{k,i} \qquad (5)$$

$$P_{cod,i} = \frac{1}{N_k}\langle\sigma_{\text{bs}}\rangle_{\text{cod},i} C_{\text{cod},i}/\sum_{k=1}^{N_k} C_{k,i}/\langle\sigma_{\text{bs}}\rangle_{k,i} \qquad (6)$$

where mean $s_{a,\text{WC}}$ for EDSU j was apportioned to cod based on the proportion of cod ($P_{cod,i}$, by weight [W] or catch by number [C]) in the combined total catch of tow i assigned to EDSU j corresponding to each transect i, which was weighted by $\langle\sigma_{\text{bs}}\rangle$ in units of m^2/kg or m^2/fish of each species (k), excluding species assumed to have negligible acoustic contributions (Table 2-1). The density of cod at each EDSU was also estimated as the $s_{a,\text{ cod}}$ defined by echo classification divided by $\langle\sigma_{\text{bs}}\rangle$ based on the *in situ* and predicted TS, either by number or weight. When mean cod densities were derived from echo integration using an EDSU that assumed spatial autocorrelation was negligible and the i.i.d. assumption held, the CV was calculated as the standard error divided by the arithmetic mean, and multiplied by 100.

Abundance and biomass were estimated by two statistical approaches, classical statistics and geostatistics, each based on different EDSUs determined by the spatial analysis. Abundance and biomass estimates from trawl densities of cod were made by using classical statistics. To compare acoustically derived estimates using classical statistics or geostatistics, four sets of estimates were made: (1) echo classification and in situ TS, (2) echo classification and predicted TS, (3) catch apportionment and in situ TS, and (4) catch apportionment and predicted TS. The dead zone correction was applied to all acoustically derived estimates of abundance and biomass. In addition, the dead zone correction was not applied to acoustically derived estimates based on classical statistics. In addition, the correlation between trawl densities and acoustic densities derived by echo classification of cod along the segment of each transect coinciding with the tow paths, which were close together in space and time, was examined by major axis (Model II) regression since both x and y variables were expressed in the same units and had equally unknown error (Sokal and Rohlf 1995; Emmrich et al. 2010). Densities (fish/m^2) were $\log_{10}$(density+c) transformed to approximate a bivariate normal distribution and homoscedasticity. A constant of 10^{-6} was chosen for c, which was approximately 50% of the minimum fish density value. Regressions were performed based on acoustically derived densities of cod that were derived from echo integrating over a bottom depth layer of varying heights (Aglen 1996; McQuinn et al. 2005). The different bottom heights evaluated were 1, 2, 2.5, 3, 3.5, 4, 4.5, 5, 6, 8, 10, 12, 15, 20, 25, and 30 m. Each regression was tested against a 1:1 fit (i.e., slope = 1, y-intercept = 0). Major axis regression analysis was performed using the package "smatr" in R statistical computing software (R Development Core Team, Version 2.13.2, 2012; Warton et al. 2012).

Density Comparison Between Adjacent Areas In and Out of the GOMCSPA

The abundance and biomass density of cod in adjacent areas inside and outside of the GOMCSPA was compared based on the four acoustically derived densities. To test the null hypothesis of equal density of cod inside and outside the GOMCSPA for each month, a spatial linear model via PROC MIXED in SAS software (SAS Institute, Inc., Cary, North Carolina) was used for an analysis of variance to assess the fixed effect of the fishing closure on the mean density and estimate the spatially correlated errors by the restricted/residual maximum likelihood function (Littell et al. 1996). The fine-scale cod densities, expressed either in thousands/km^2 or mt/km^2, were transformed by $\log_{10}$(density+1) for shifting the data closer to a normal distribution, which is often done for abundance data (Sokal and Rolf 1995). The spatial covariance parameters specified for each model was based on fitted semivariograms of the log-transformed values for each survey and estimation method. The area unprotected by the fishing closure was represented by transects 1-3 and the adjacent protected area of equal size was represented by transects 5-7. Transect 4 was excluded because it was on the boundary of the GOMCSPA.

Results

Catch statistics

Total catch and mean total length of species caught by small-mesh and large-mesh bottom trawls are presented for each survey in Tables 2-2 and 2-3, respectively. Neither bottom trawl caught cod during the survey in April, so no other results are presented for April. The dominant species in the large-mesh trawl catch was cod, followed by species not considered acoustically detectable, such as American plaice (*Hippoglossoides* *platesoides*), yellowtail flounder (*Limanda ferruginea*), skates (Rajidae), and witch flounder (*Glyptocephalus cynoglossus*). In the small-mesh trawl catch, silver hake, cod, Atlantic herring, and red hake (*Urophycis chuss*) were the most numerically abundant species considered acoustically detectable. In general, cod were the largest fish with a swimbladder caught by both trawls. Spiny dogfish were the longest fish caught, but lacked a swim bladder and were expected to produce weaker acoustic backscatter. The *L-W* relation of cod measured in the May survey resulted in growth parameters *a* and *b* that were not significantly different from those derived from the time-series data of NEFSC spring bottom-trawl surveys (Wigley et al. 2003; Figure 2-3). The monthly spatial distribution of the relative composition of acoustically detectable species by weight and number in the combined trawl catches was derived from the empirical *L-W* relation for cod, and those *L-W* relations in Wigley et al. (2003) for other species (Table 2-1; Figure 2-4). Cod was the most abundant species considered acoustically detectable throughout the survey area based on relative biomass, while silver hake was by relative number during the June and July survey.

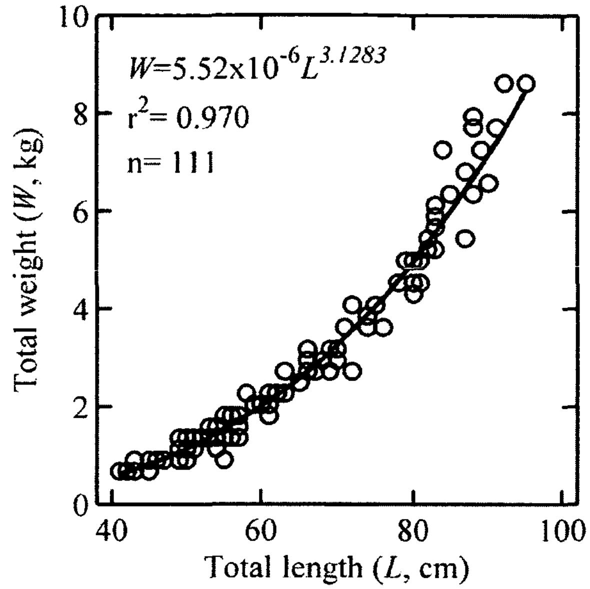

Figure 2-3. Total length (L) and total wet weight (W) relation of Atlantic cod measured during the 28-29 May 2011 survey. Parameter estimates from the regression were not significantly different from parameters $Log_e(a)$ (t value=-1.54, p=0.12) and b (t value=1.42, p=0.14) in the L-W relation reported by Wigley et al. (2003).

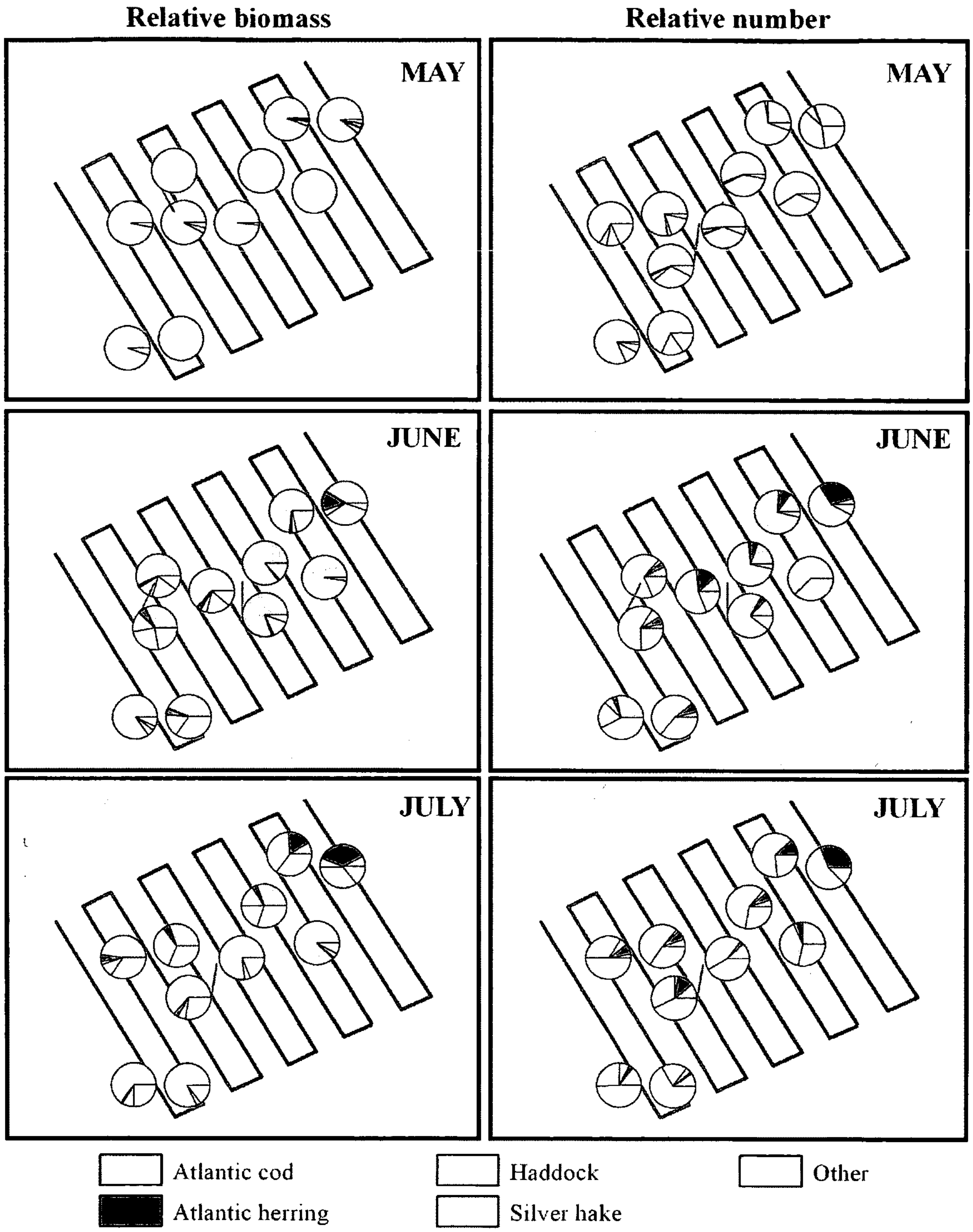

Figure 2-4. Spatial distribution of the relative biomass (left) and number of acoustically detectable species in the combined catch of paired tows with a small-mesh (4.4-cm cod end) and a large-mesh (16.5-cm cod end) bottom trawl along acoustic survey transects (red lines) overlapping the Gulf of Maine cod spawning protection area (shaded) on 28-29 May, 18-19 June and 3-4 July 2011.

Table 2-2. Total catch (by number) of fish caught by ten tows with a small-mesh (4.4-cm cod end) and large-mesh (16.5-cm cod end) bottom trawl on 7-8 April, 28-29 May, 18-19 June and 3-4 July 2011.

	Large mesh trawl				Small mesh trawl			
Species	April	May	June	July	April	May	June	July
Considered acoustically detectable species								
Acadian redfish (*Sebastes fasciatus*)						27	21	33
Alewife (*Alosa pseudoharengus*)					144			
Atlantic cod (*Gadus morhua*)		339	139	36		270	178	34
Atlantic herring (*Clupea harengus*)				2	727	9	164	242
Atlantic mackerel (*Scomber scombrus*)								1
Butterfish (*Peprilus triacanthus*)								1
Fourbeard rockling (*Enchelyopus cimbrius*)						3	5	9
Haddock (*Melanogrammus aeglefinus*)		8		1	1	28	26	24
Pollock (*Pollachius virens*)		1				1	2	1
Red hake (*Urophycis chuss*)					13	68	137	264
Silver hake (*Merluccius bilinearis*)	1		4	2	411	355	958	615
Spiny dogfish (*Squalus acanthias*)			4	6		1	2	21
White hake (*Urophycis tenuis*)					26			
Not considered acoustically detectable species								
American plaice (*Hippoglossoides platesoides*)	5	44	75	62	94	355	358	323
Four-spot flounder (*Paralichthys oblongus*)					2	4	2	3
Goosefish (*Lophius americanus*)		1		3	1	1		
Ocean pout (*Zoarces americanus*)					1			1
Sculpins (*Myoxocephalus* spp.)	2				7	6	9	10
Sea raven (*Hemitripterus americanus*)		1		1	1	2		3
Skates (Rajidae)	61	17	17	31	13	6	8	12
Windowpane (*Scophthalmus aquosus*)					11	1		
Winter flounder (*Pseudopleuronectes americanus*)	3				6	1	1	2
Witch flounder (*Glyptocephalus cynoglossus*)		21	46	55	2	29	38	107
Wrymouth (*Cryptacanthodes maculatus*)								2
Yellowtail flounder (*Limanda ferruginea*)	7	20	83	57	29	116	120	107

Table 2-3. Mean total length (cm) of fish caught by ten tows with a small-mesh (4.4-cm cod end) and large-mesh (16.5-cm cod end) bottom trawl on 7-8 April, 28-29 May, 18-19 June and 3-4 July 2011.

	Large mesh trawl				Small mesh trawl			
Species	April	May	June	July	April	May	June	July
Considered acoustically-detectable species								
Acadian redfish (*Sebastes fasciatus*)						14	15	14
Alewife (*Alosa pseudoharengus*)					12			
Atlantic cod (*Gadus morhua*)		69	79	78		63	70	63
Atlantic herring (*Clupea harengus*)				25	15	18	27	28
Atlantic mackerel (*Scomber scombrus*)								28
Butterfish (*Peprilus triacanthus*)								17
Fourbeard rockling (*Enchelyopus cimbrius*)						19	20	20
Haddock (*Melanogrammus aeglefinus*)		56		61	19	36	41	28
Pollock (*Pollachius virens*)		78				27	52	23
Red hake (*Urophycis chuss*)					17	27	30	30
Silver hake (*Merluccius bilinearis*)	27		38	32	16	16	25	25
Spiny dogfish (*Squalus acanthias*)			86	84		89	85	83
White hake (*Urophycis tenuis*)					17			
Not considered acoustically-detectable species								
American plaice (*Hippoglossoides platesoides*)	28	36	36	33	21	25	25	26
Four-spot flounder (*Paralichthys oblongus*)					23	28	30	29
Goosefish (*Lophius americanus*)		53		40	17	53		
Ocean pout (*Zoarces americanus*)					28			31
Sculpins (*Myoxocephalus* spp.)	29				22	25	25	26
Sea raven (*Hemitripterus americanus*)		42		37	28	31		30
Skates (Rajidae)	44	55	50	48	41	52	56	48
Windowpane (*Scophthalmus aquosus*)					20	16		
Winter flounder (*Pseudopleuronectes americanus*)	33				26	29	26	43
Witch flounder (*Glyptocephalus cynoglossus*)		39	40	37	16	35	34	34
Wrymouth (*Cryptacanthodes maculatus*)								61
Yellowtail flounder (*Limanda ferruginea*)	32	35	34	33	30	32	32	31

The mean total length of cod caught by both bottom trawls in this study was 69 cm (n = 958), and ranged from 15 to 120 cm. The total length distributions of cod caught by the small mesh trawl (mean = 66 cm) and large mesh trawl (mean = 72 cm) were significantly different ($D = 0.250$, $P < 0.001$). The monthly mean total length of cod in the combined trawl catch was 66 cm in May, 73 cm in June and 71 cm in July. The total length distribution of the combined trawl catch of cod significantly differed between May and June ($D = 0.247$, $P < 0.001$) and May and July ($D = 0.184$, $P = 0.011$), but not between June and July ($D = 0.134$, $P = 0.117$; Figure 2-5). The number of individuals observed expelling milt or eggs were 13 males in May, 35 males and 10 females in June, and 16 males and 1 female in July.

<u>*In Situ* Target Strength</u>

The TS distributions of all single echo detections classified as cod are shown for all ten parallel transects from each monthly survey (Figure 2-6). At 38 kHz (May only), predicted TS was significantly lower than *in situ* TS by approximately 2.3 dB when b_{20} was equal to -67.5 (S = -18, P = 0.008, n = 8), but was not significantly lower (-0.8 dB) than *in situ* TS when b_{20} was equal to -66 (S = -5, P = 0.547, n = 8). At 120 kHz, predicted TS was significantly lower than *in situ* TS by approximately 1.8 dB when b_{20} was equal to -67.5 (S = -41.5, P = 0.007, n = 14), but was not significantly higher (0.7 dB) than *in situ* TS when b_{20} was equal -65 (S =-20.5, P = 0.217, n = 14). Among single echo detections classified as cod matched by ping number and depth in both beams, *in situ* TS at 38 kHz was significantly higher than at 120 kHz by an average of 1.1 dB (t = 4.17, $P < 0.001$, n = 551).

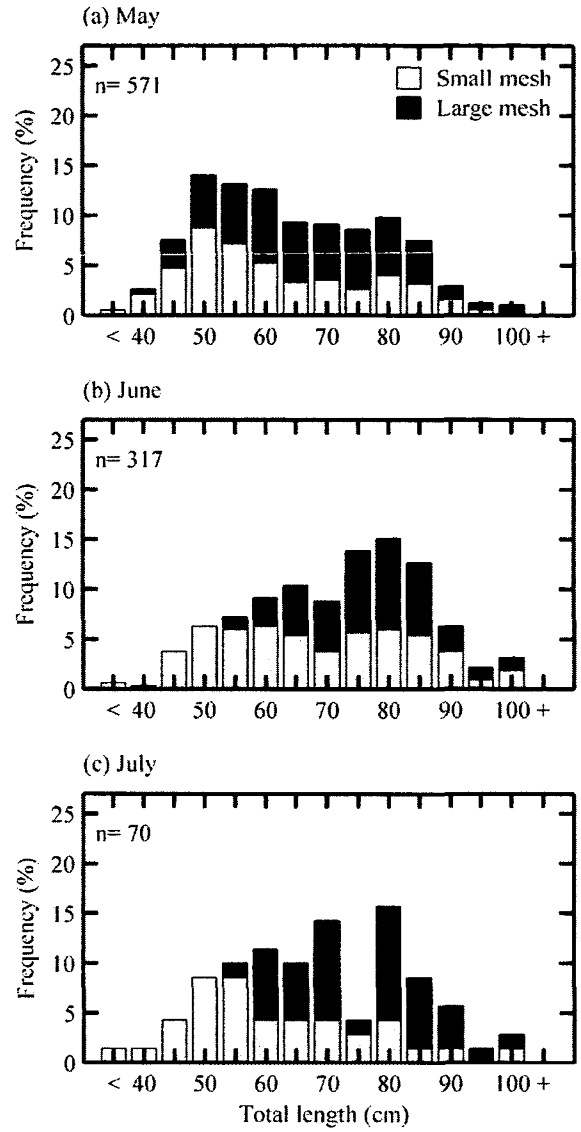

Figure 2-5. Length-frequency distribution of Atlantic cod measured from the combined catch of 10 paired tows made with a small-mesh (4.4-cm cod end) and large-mesh (16.5-cm cod end) bottom trawl during an acoustic survey overlapping the Gulf of Maine cod spawning protection area on (a) 28-29 May, (b) 18-19 June and (c) 3-4 July 2011.

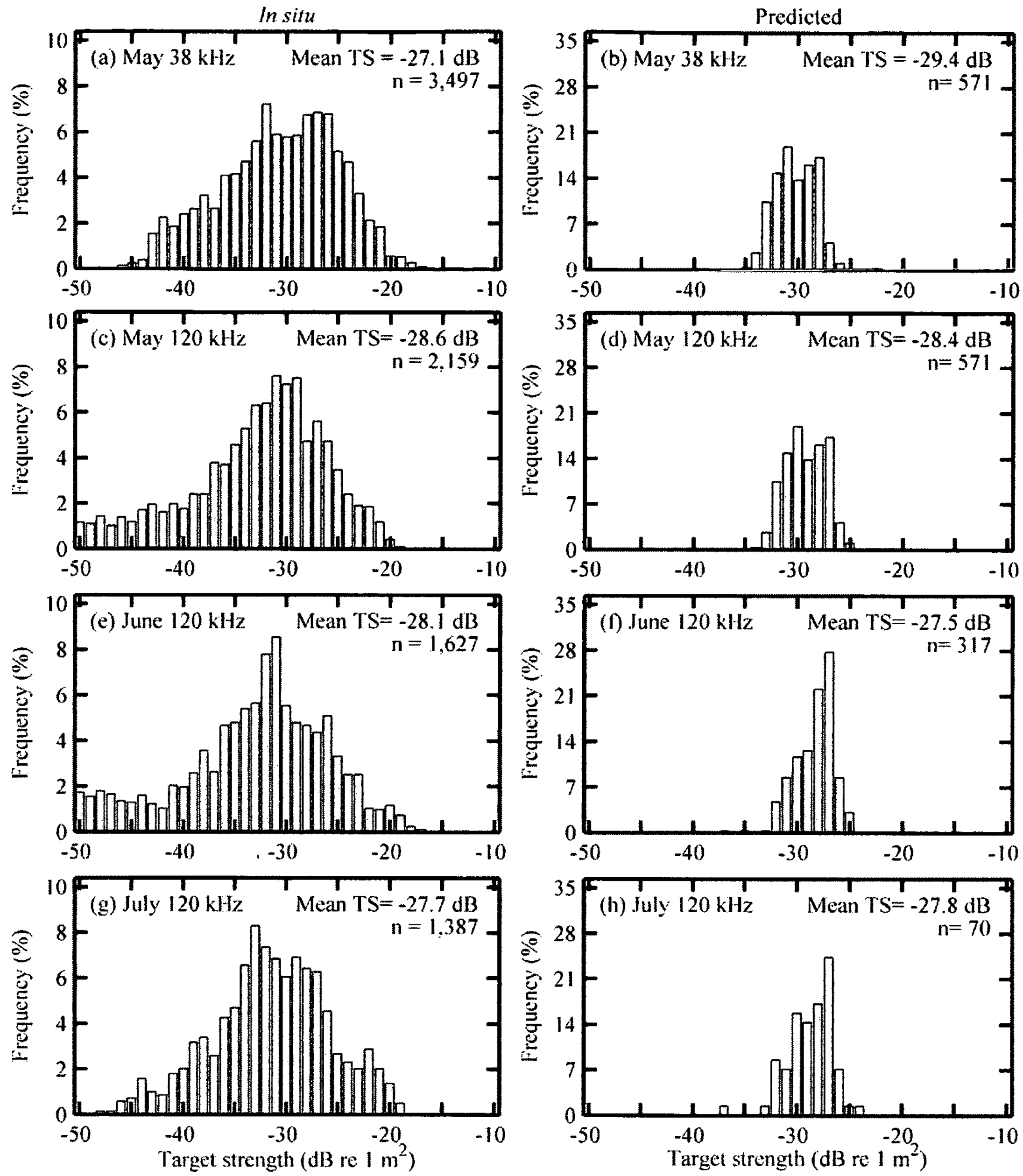

Figure 2-6. Relative frequency distribution of target strength (TS) of spring-spawning Atlantic cod in the Gulf of Maine cod spawning protection area as (left column) measured *in situ* from single echo detections made by 38-kHz and 120-kHz Simrad EK60 split-beam echo sounders and (right column) predicted from total length (L) of the combined trawl catch (Rose and Porter, 1996) on 27-28 May, 16-17 June, and 4-5 July, 2012. Note different scales on y-axis.

Spatial Distribution

Two spatial patterns emerged from fitting the robust empirical semivariograms of $\log_{10}(s_A + 1)$-transformed s_A attributed to cod by echo classification and echo integrated over three different spatial scales (Figure 2-7). Based on a 10-m EDSU, the fitted semivariograms showed the variance at short distances (< 200 m) was explained by a spatial component occurring at a range of approximately 35-43 m and no or negligible nugget effect. When echo integration was averaged over 100 m and 500 m, this fine-scale spatial structure vanished and its associated variance became embedded in the nugget component of the semivariogram, which accounted for approximately 8-39% of the total sill depending on the month and acoustic frequency (Figure 2-7). The nugget component was smallest in June and largest in July. The semivariograms for these two EDSUs revealed a larger spatial component with a range of approximately 3.0 km and 3.3 km in May at 38 kHz, 2.9 km and 3.3 km in May at 120 kHz, 4.9 km and 5.2 km in June at 120 kHz, and 3.7 km and 3.2 km July at 120 kHz, respectively. Based on this spatial analysis, an EDSU of 4.1 km (half-transect distance) was chosen as a convenient unit to remove most of the spatial autocorrelation along transects, making the data more appropriate for abundance estimates and statistical comparisons of density under the i.i.d. assumption of classical statistics. A 100-m EDSU was selected for geostatistical estimation of cod abundance based on the compromise between preserving the spatial structure explaining most of the variation, and improving computational efficiency and reducing variability.

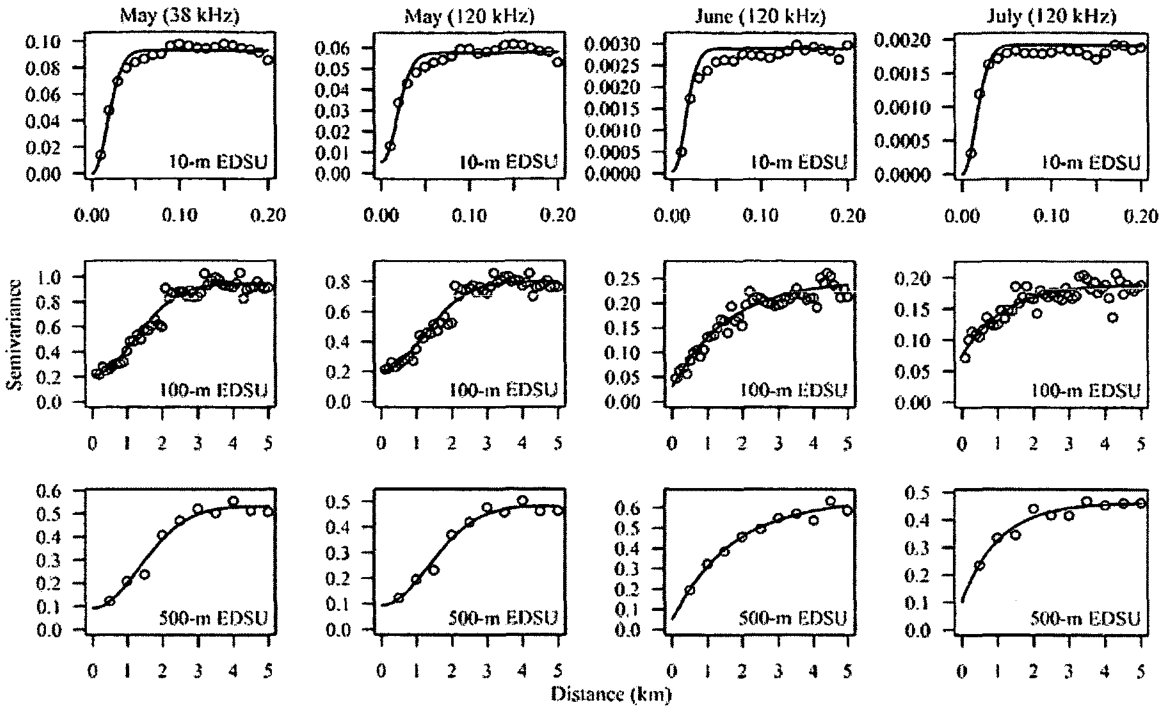

Figure 2-7. Omnidirectional robust empirical (circles) and theoretical (lines) semivariograms of $\log_{10}(s_A+1)$-transformed values of the mean nautical area backscattering coefficient (s_A) attributed to Atlantic cod by echo classification from an acoustic survey of the Gulf of Maine Cod Spawning Protection Area on 28-29 May, 18-19 June, and 3-4 July 2011 based on echo integrating over elementary distance sampling units (EDSU) of 10 m, 100 m, and 500 m.

Based on 100-m EDSUs, nugget and spatial components were present in the semivariograms of the biomass density of cod acoustically derived from 120-kHz area backscatter by all four estimation methods, but varied among the estimation methods and surveys (Figure 2-8). In May, the spatial structural component of the Gaussian semivariogram model for cod biomass density was approximately 70% of the variance (total sill) based on echo classification and 65% based on catch apportionment at a range of approximately 2.4 km. The semivariograms of cod biomass density derived from 38 kHz area backscatter collected in May describe a spatial structure similar to that based on 120-kHz data (Figures 8 and 9). For the June survey, a spherical semivariogram model described a spatial structural component equal to 76-77% of the variance at a range of approximately 2.3-2.4 km based on echo classification, while semivariogram based on the catch apportionment method was best described by an exponential covariance model with a larger spatial structural component equal to 92% of the variance, and a range of approximately 3.7 km based on *in situ* TS and 5.8 km based on predicted TS (Figure 2-8). The spatial structural component and range for the July survey varied among all estimation methods ranging from 65% to 80% of the variance and 1.6 km to 2.4 km (Figure 2-8). Based on abundance density (thousands/km^2) derived by 120-kHz backscatter, the percentage of the variance explained by the spatial structure modeled by the semivariograms was 62-69% in May, 71-90% in June, and 52-69% in July, while the range was estimated as 2.4-2.5 km in May, 1.8-4.7 km in June, and 1.9-2.7 km in July (Figure 2-10). In general, the highest relative amount of spatial structure for cod was observed in June, and the longest range was observed in May or June depending on estimation method. The lowest relative amount of spatial structure was observed in July.

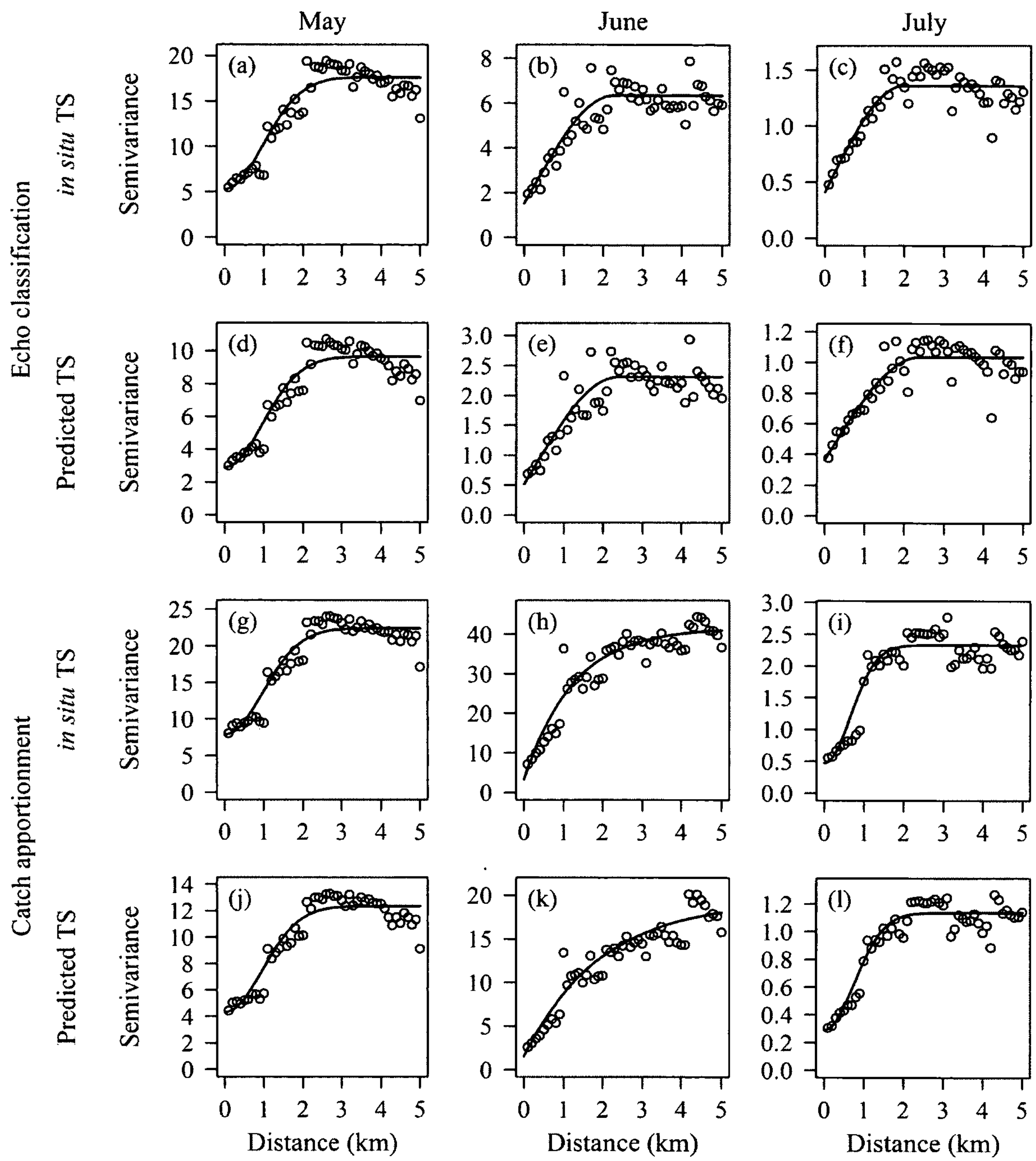

Figure 2-8. Omnidirectional robust empirical semivariograms (open circles) fitted with a Gaussian (a, d, g, i, j, l), spherical (b, c, e, f) and exponential (h, k) semivariogram model for acoustically derived biomass density (mt/km^2) based on attributing area backscatter to Atlantic cod by echo classification or catch apportionment and target strength (TS) of Atlantic cod predicted from the total length of the trawl catch or measured *in situ* during nighttime surveys overlapping the Gulf of Maine cod spawning protection area on 28-29 May, 18-19 June and 3-4 July 2011.

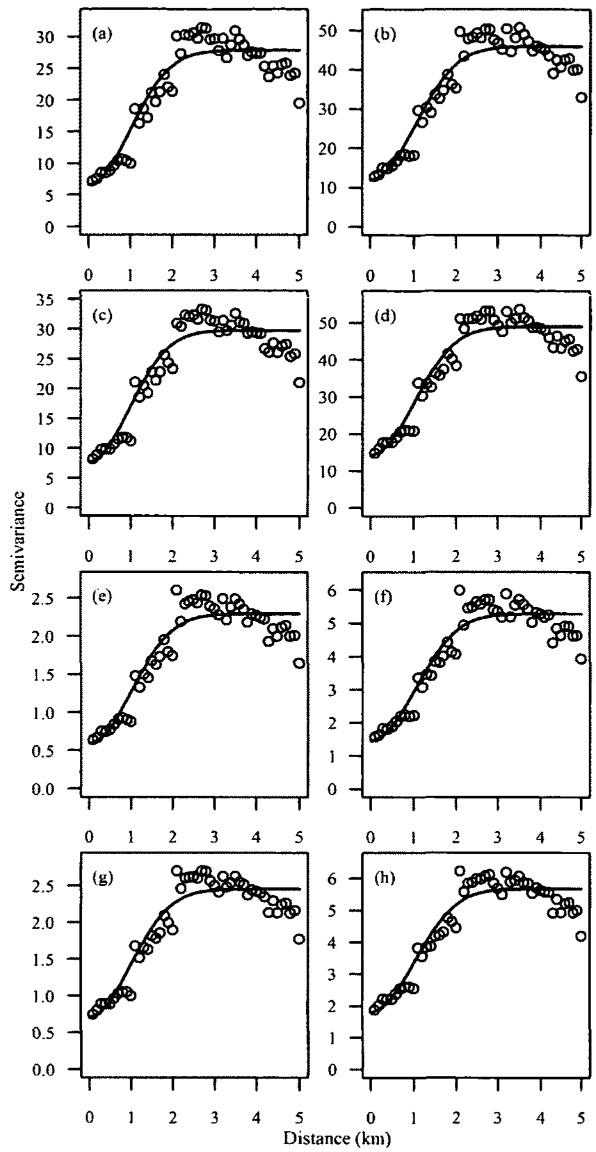

Figure 2-9. Empirical omnidirectional robust semivariograms (open circles) fitted with a Gaussian covariance model (line) for (a-d) biomass density (mt/km^2) and (e-h) fish density ($thousands/km^2$) of Atlantic cod derived from the area backscattering coefficient (s_a) at 38 kHz based on (a and e) echo classification and measured *in situ* target strength (TS), (b and f) echo classification and TS predicted from the total length of the trawl catch, (c and g) catch apportionment and *in situ* TS, and (d and h) catch apportionment and predicted TS during a nighttime survey overlapping the Gulf of Maine cod spawning protection area on 28-29 May 2011.

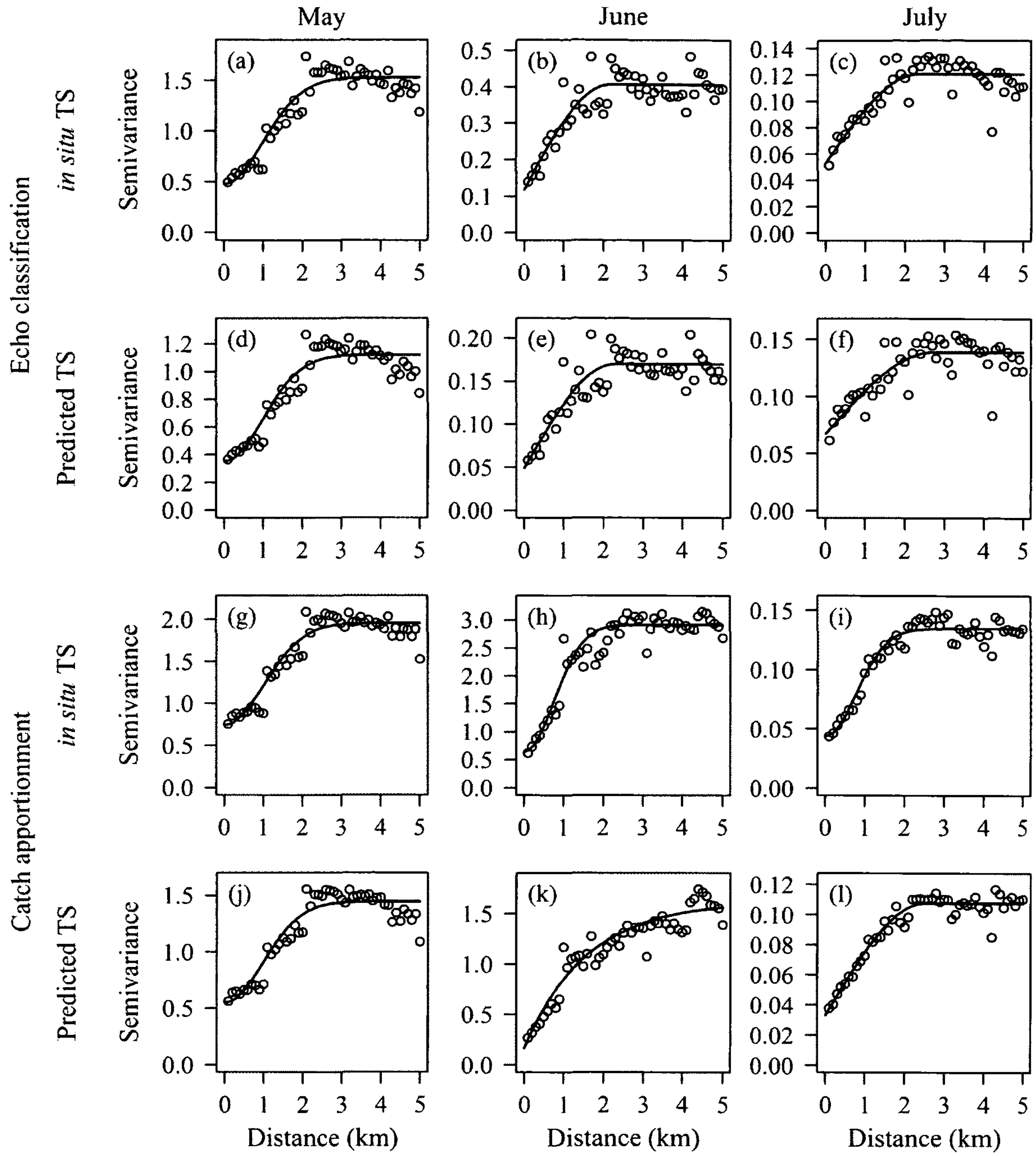

Figure 2-10. Omnidirectional robust empirical semivariograms (open circles) fitted with a Gaussian (a, d, g-j), spherical (b, c, e, f, l) and exponential (k) covariance model for acoustically derived density of individual fish (thousands/km^2) based on attributing area backscatter to Atlantic cod by echo classification or catch apportionment and target strength (TS) of Atlantic cod predicted from the total length of the trawl catch or measured *in situ* during nighttime surveys overlapping the Gulf of Maine cod spawning protection area on 28-29 May, 18-19 June and 3-4 July 2011.

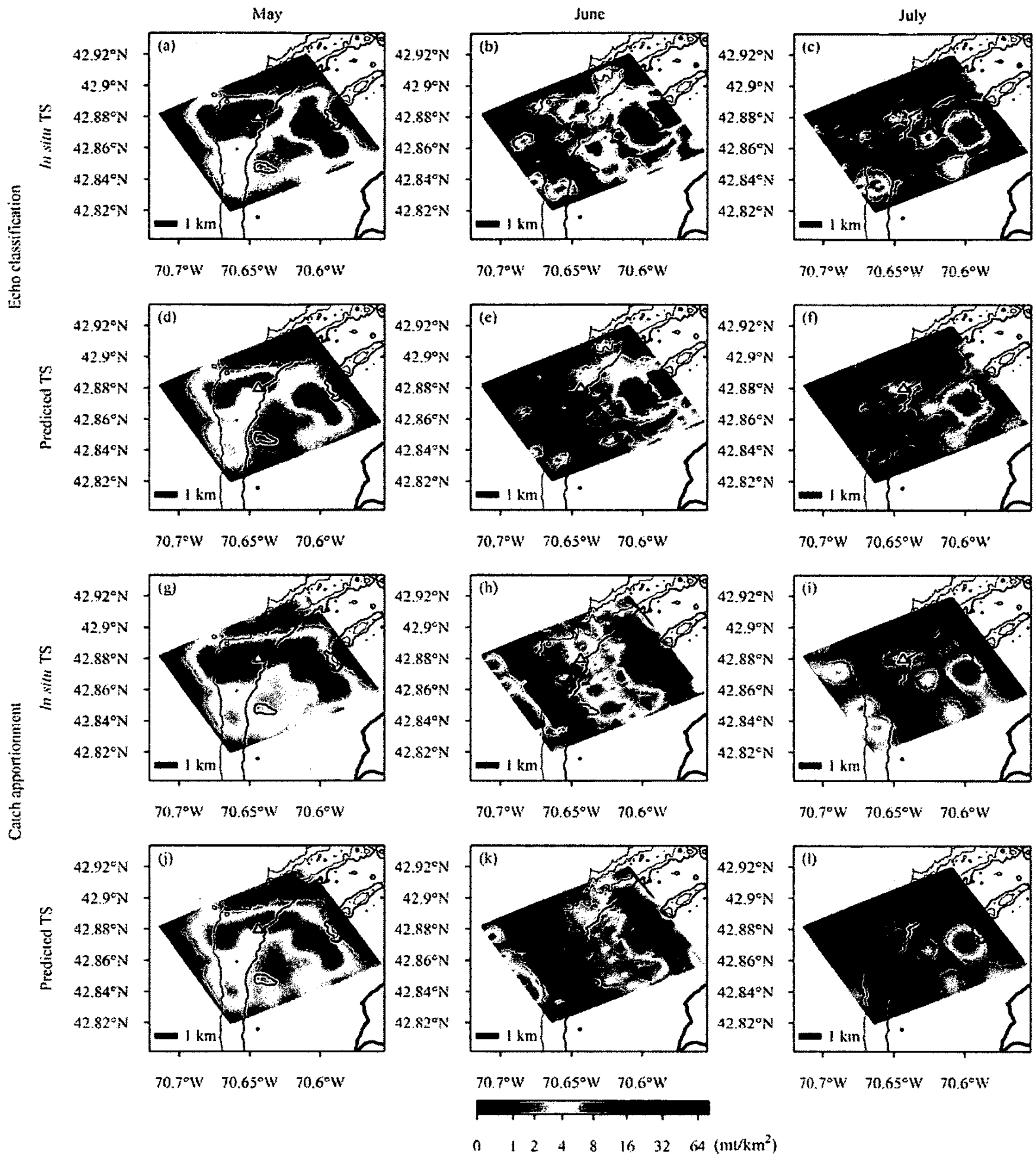

Figure 2-11. Kriged maps of biomass density (mt/km^2) of Atlantic cod on the nights of 28-29 May, 18-19 June and 3-4 July 2011 based on data collected by a 120-kHz split-beam echo sounder every 100 m along ten parallel transects and ten paired tows with a large-mesh and small-mesh bottom trawl. Densities were estimated by four methods: attributing area backscatter to Atlantic cod by echo classification (a-f) or catch apportionment (g-l).and target strength (TS) of Atlantic cod measured *in situ* (a-c and g-i) or predicted from the total length of the trawl catch (d-f and j-l). The Gulf of Maine cod spawning protection area is represented as the grey shaded polygon and the 60 m, 70 m, and 100 m depth contours are shown by the thin, medium, and thick lines. The triangle marks the position of an acoustic recording of cod sounds.

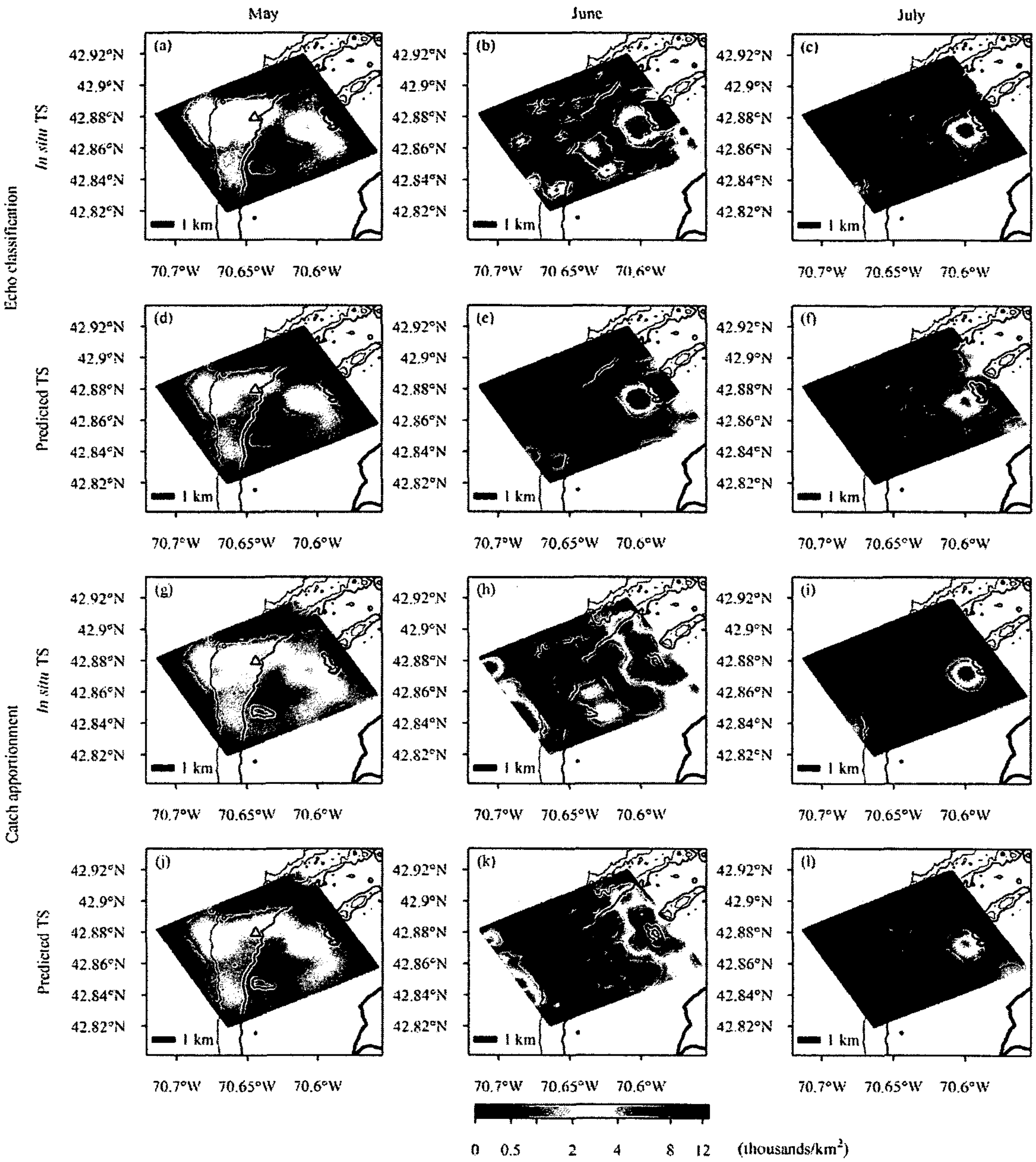

Figure 2-12. Kriged maps of density of individual Atlantic cod (thousands/km^2) on the nights of 28-29 May, 18-19 June and 3-4 July 2011 based on data collected by a 120-kHz split-beam echo sounder every 100 m along ten parallel transects and ten paired tows with a large-mesh and small-mesh bottom trawl. Densities were estimated by four methods: attributing area backscatter to Atlantic cod by echo classification (a-f) or catch apportionment (g-l) and target strength (TS) of Atlantic cod measured *in situ* (a-c and g-i) or predicted from the total length of the trawl catch (d-f and j-l). The Gulf of Maine cod spawning protection area is represented by the grey shaded polygon and the 60 m, 70 m, and 100 m depth contours are shown by the thin, medium, and thick lines. The triangle marks the position of an acoustic recording of cod sounds.

Regardless of the estimation method, two general patterns in the horizontal spatial distribution of cod emerged from the kriged density maps. During May, cod were relatively widespread throughout the survey area, but congregated at a higher density over an area approximately 2-3 km in diameter that was adjacent to two elevated bathymetric features: the southwest side of Whaleback and to the west of Southwest Hump (Figures 11-13). In June, cod appeared to converge mostly to the west side of Southwest Hump at a higher concentration compared to the highest densities observed in May (Figures 11 and 12). This congregation decreased in size and density in July. The maps based on the catch apportioned s_a resulted in a more scattered distribution, with local areas of high density that were associated with the transect design. Underwater sound passively recorded by the hydrophone immediately following the survey in May at a location of high cod abundance contained the acoustic signature of a cod grunt (Figure 2-14). Based on echo integration in 2-m depth layers, cod were vertically distributed mostly within 20 m of the sea floor, but occasionally were observed as much as 34 m off the sea floor (Figure 2-15).

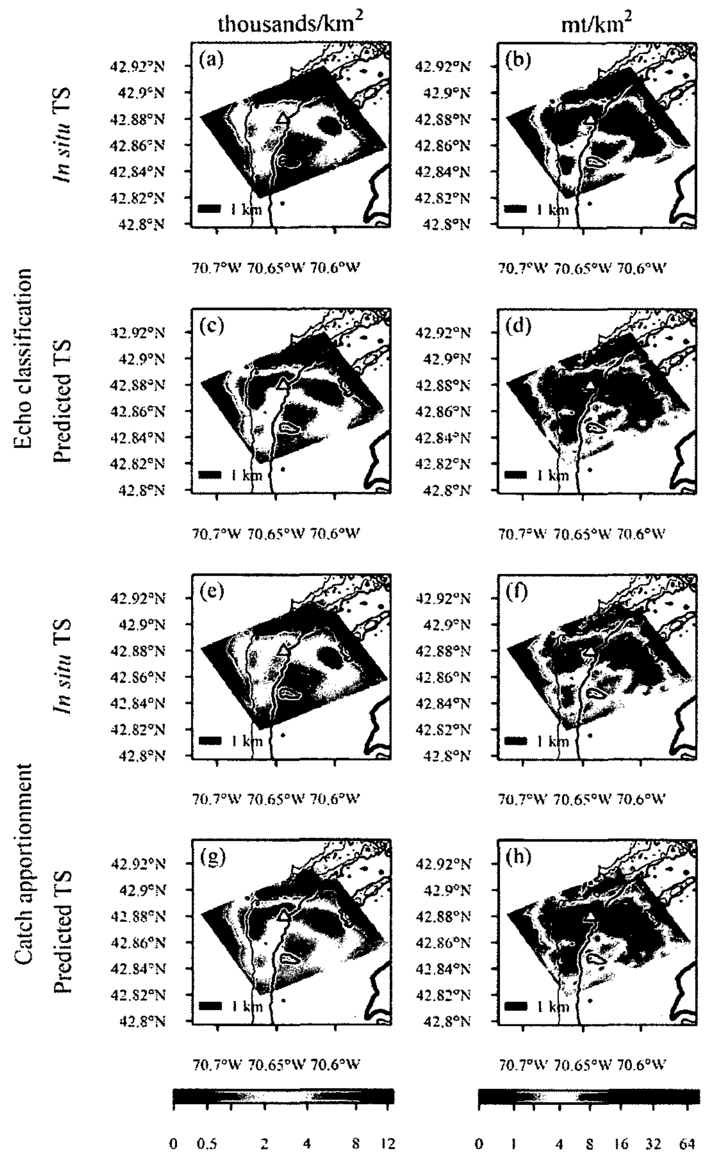

Figure 2-13. Kriged maps of density of Atlantic cod abundance (left, thousands/km^2) and biomass (right, mt/km^2) on the night of 28-29 May 2011 based on data collected by a 38-kHz split-beam echo sounder every 100 m along ten parallel transects and ten paired tows with a large-mesh and small-mesh bottom trawl. Densities were estimated by four methods: attributing area backscatter to Atlantic cod by echo classification (a-d) or catch apportionment (e-h) and target strength (TS) of Atlantic cod measured *in situ* (a-b and e-f) or predicted from the total length of the trawl catch (c-d and g-h). The Gulf of Maine cod spawning protection area is represented by the grey shaded polygon and the 60 m, 70 m, and 100 m depth contours are shown by the thin, medium, and thick lines. The triangle marks the position of an acoustic recording of cod sounds.

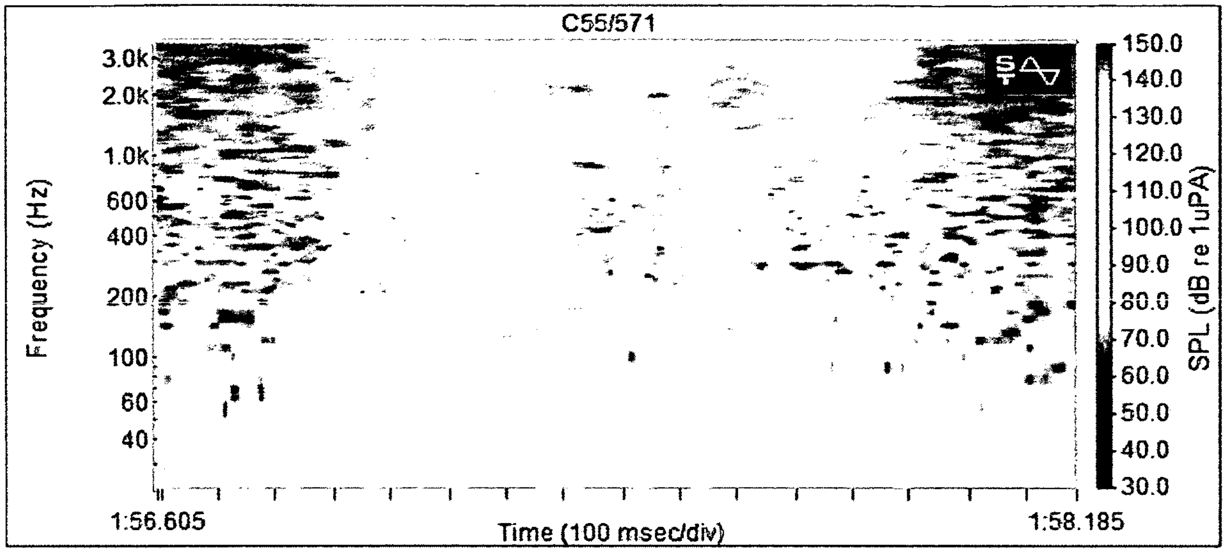

Figure 2-14. Spectrogram of underwater sound recorded immediately following the May survey at a location where Atlantic cod were observed in relative high numbers in the echogram and trawl samples (see Figures 11 and 12). Shown is a signal with a peak frequency of 140 Hz and duration of 100-400 ms characteristic of double cod grunt.

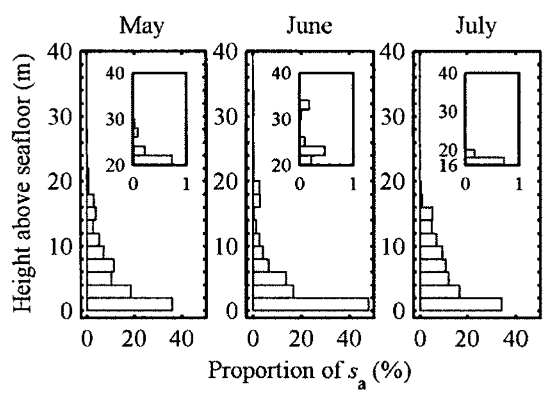

Figure 2-15. Proportion of the area backscattering coefficient (s_a) classified as Atlantic cod in each 2-m depth layer above the sea floor during acoustic surveys overlapping the Gulf of Maine cod spawning protection area on the nights of 28-29 May, 18-19 June, and 3-4 July 2011.

Abundance and Biomass Estimates

Among the fourteen estimation methods, the abundance estimate of cod within the survey area ranged from 63,000 to 127,000 individuals during 28-29 May 2011, 37,000 to 168,000 individuals during 18-19 June 2011, and 13,000 to 42,000 individuals during 3-4 July 2011 (Figure 2-16). Biomass estimates of cod ranged from 184 to 494 mt during May, 138 to 617 mt during June, and 39 to 135 mt during July. The dead zone correction resulted in an increase in abundance or biomass of approximately 19-21% for the May survey, 15-27% for the June survey, and 10-19% for the July survey. In general, the use of *in situ* TS in density estimation resulted in higher estimates of abundance and biomass compared to predicting TS from the length in the trawl catch. Also, apportionment of the area backscatter of all scatterers above the threshold below 30 m depth by the weighted proportion of cod in the trawl catch resulted in higher estimates compared to echo classification, especially in June. While the abundance and biomass estimates were of similar magnitude between the geostatistical approach using a 100-m EDSU and classical statistical approach using a half-transect EDSU, the geostatistical estimate of CV for the mean density based on a 100-m EDSU was lower than the CV for the mean density based on half-transects.

Abundance and biomass estimates based on echo classification and bottom trawl was higher in May than in June, and estimates based on catch apportionment were higher in June than in May. In July, abundance estimates ranged from 10 to 56% of May's estimates and 20 to 97% of June's estimates, while biomass estimates ranged from 13 to 50% of May's estimates and 16 to 66% of June's estimates. The performance of estimating abundance and biomass of cod from acoustically derived densities based on echo classification could be argued as the best measure in this study as it resulted in a lower CV and was shown to be correlated with the trawl-based density within the trawl zone (Figure 2-17). The coefficient of determination (r^2) was slightly higher for the regression based on *in situ* TS than those based on predicted TS.

Based on a proportional extrapolation of the survey estimates for the three surveys, the abundance estimates for the GOMCSPA ranged from 18,000 cod in July based on the small-mesh bottom trawl to 241,000 cod in May based on catch apportioned 38-kHz backscatter and predicted TS with dead zone correction (Table 2-4). Biomass estimates for the GOMCSPA ranged from 260 to 700 mt in May, 196 to 873 mt in June, and 55 to 191 mt in July. Abundance and biomass estimates for the GOMCSPA based on the mean density inside the GOMCSPA (transects or tows 4-10) ranged from 13,000 cod in July to 259,000 cod in May and 31 mt in July to 1,085 mt in June, respectively (Table 2-4). Based on trawl samples collected in the GOMCSPA during 2007-2009, the trawl estimates of cod density from 2011 were of similar magnitude as previous years (Figure 2-18).

Density Inside and Outside the GOMCSPA

The mean of the $\log_{10}$(density+1)-transformed values for cod densities, by weight or number, was not significantly different between the three adjacent transects inside and outside the GOMCSPA, except for the echo-classified estimates during the June survey (Tables 2-5 and 2-6, Figure 2-19 and 2-20). Cod biomass density inside the GOMCSPA was significantly greater than that outside of the GOMCSPA by over five times based on *in situ* TS and over four times based on predicted TS.

Table 2-4. Atlantic cod abundance (number, in thousands) and biomass (metric tons) in the Gulf of Maine cod spawning protection area (114.3 km^2) extrapolated two ways from surveying ten parallel transects covering an area of 80.8 km^2 with a split-beam echo sounder at two frequencies (f) and making ten 10-minute paired tows with a large-mesh and small-mesh bottom trawl during the night of 28-29 May, 18-19 June, and 3-4 July 2011. Acoustically derived densities were based on several methods: mean area backscattering coefficient (s_a) attributed to Atlantic cod by echo classification or catch apportionment, *in situ* or predicted TS, half-transect EDSU (classical statistics) or 100-m EDSU (geostatistics), and with a dead zone correction (DZC).

		Extrapolated survey estimate (transects 1-10) by ratio of areas (114.3:80.8)						Extrapolated as mean density inside GOMCSPA (transects 4-10) x area					
		Abundance			Biomass			Abundance			Biomass		
Estimation method	*f*	May	June	July	May	June	July	May	June	July	May	June	July
Large mesh bottom trawl		180	69	19	699	344	90	179	92	19	728	466	92
Small mesh bottom trawl		153	92	18	432	355	55	152	115	13	450	481	31
Echo classification, half-transect EDSU, *in situ* TS	120	103	79	43	350	311	146	110	98	54	389	408	169
Echo classification, half-transect EDSU, *in situ* TS (DZC)	120	123	99	51	418	390	174	132	124	63	466	513	199
Echo classification, 100-m EDSU, *in situ* TS (DZC)	38	148			518			162			593		
	120	122	99	53	415	388	181	131	123	63	463	510	198
Echo classification, half-transect EDSU, predicted TS (DZC)	120	89	53	51	260	196	129	91	67	69	277	261	167
Echo classification, half-transect EDSU, predicted TS (DZC)	120	106	67	59	309	246	151	108	85	79	331	328	194
Echo classification, 100-m EDSU, predicted TS (DZC)	38	225			662			238			731		
	120	105	67	59	307	244	151	108	85	79	329	326	194
Catch apportionment, half-transect EDSU, *in situ* TS	120	111	204	42	369	750	168	116	229	39	404	934	144
Catch apportionment, half-transect EDSU, *in situ* TS (DZC)	120	133	238	47	441	873	187	140	265	45	484	1085	164
Catch apportionment, 100-m EDSU, *in situ* TS (DZC)	38	157			546			173			629		
	120	149	222	48	497	800	191	163	242	46	566	976	169
Catch apportionment, half-transect EDSU, predicted TS	120	96	148	38	274	494	115	96	172	43	285	631	126
Catch apportionment, half-transect EDSU, predicted TS (DZC)	120	115	171	42	327	571	129	115	198	48	343	728	142
Catch apportionment, 100-m EDSU, predicted TS (DZC)	38	241			700			259			781		
	120	128	160	43	368	526	132	135	181	49	402	662	147

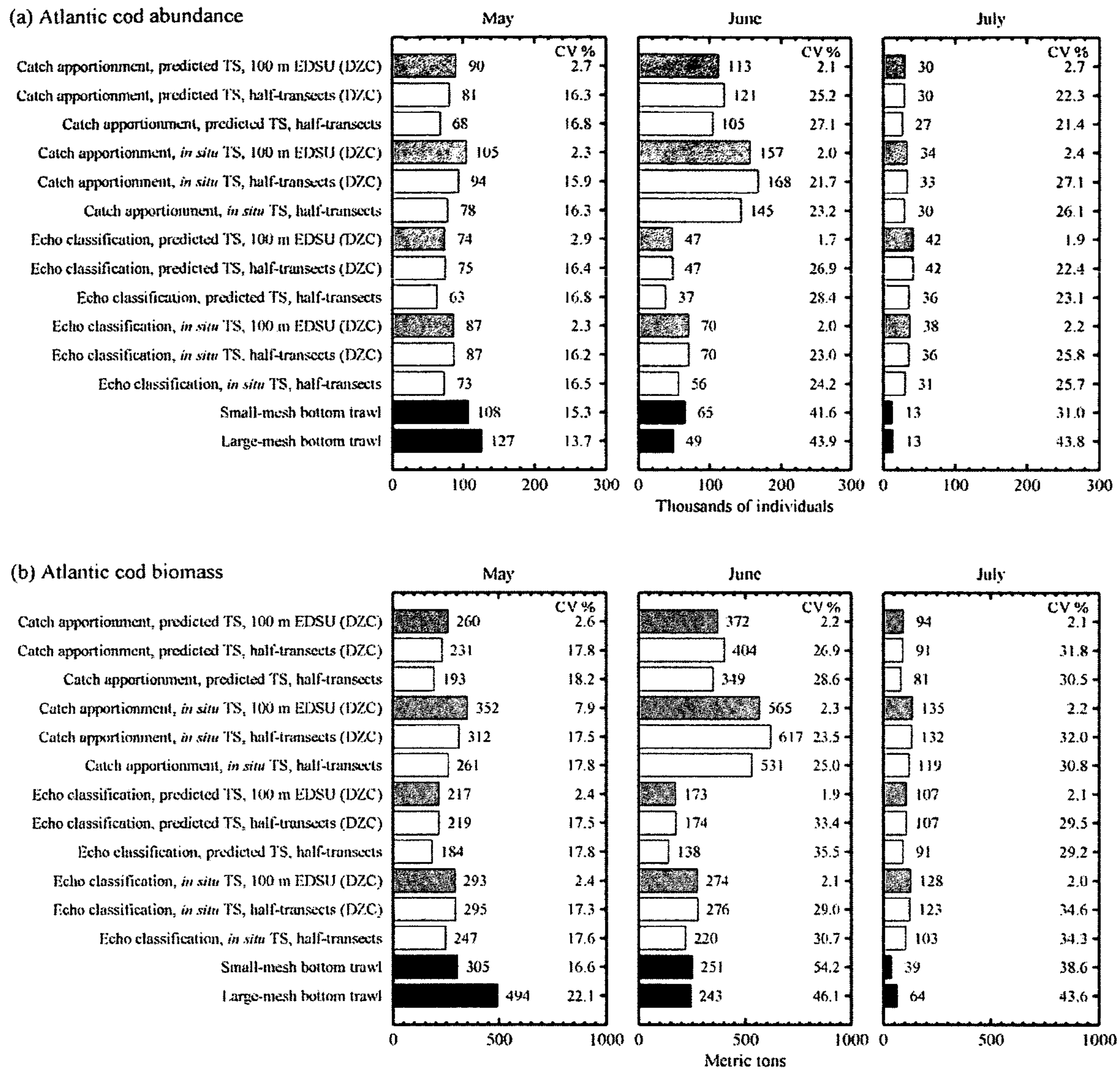

Figure 2-16. Atlantic cod (a) abundance and (b) biomass for a 80.8 km^2 area overlapping the Gulf of Maine cod spawning protection area estimated from surveying ten parallel transects with a 120-kHz split-beam echo sounder and making ten 10-minute paired tows with a large-mesh and small-mesh bottom trawl during 28-29 May, 18-19 June, and 3-4 July 2011. Acoustically derived densities were based on several methods: mean area backscattering coefficient (s_a) attributed to Atlantic cod by echo classification or catch apportionment, *in situ* or predicted TS, half-transect EDSU (classical statistics) or 100-m EDSU (geostatistics), and with and without dead zone correction (DZC).

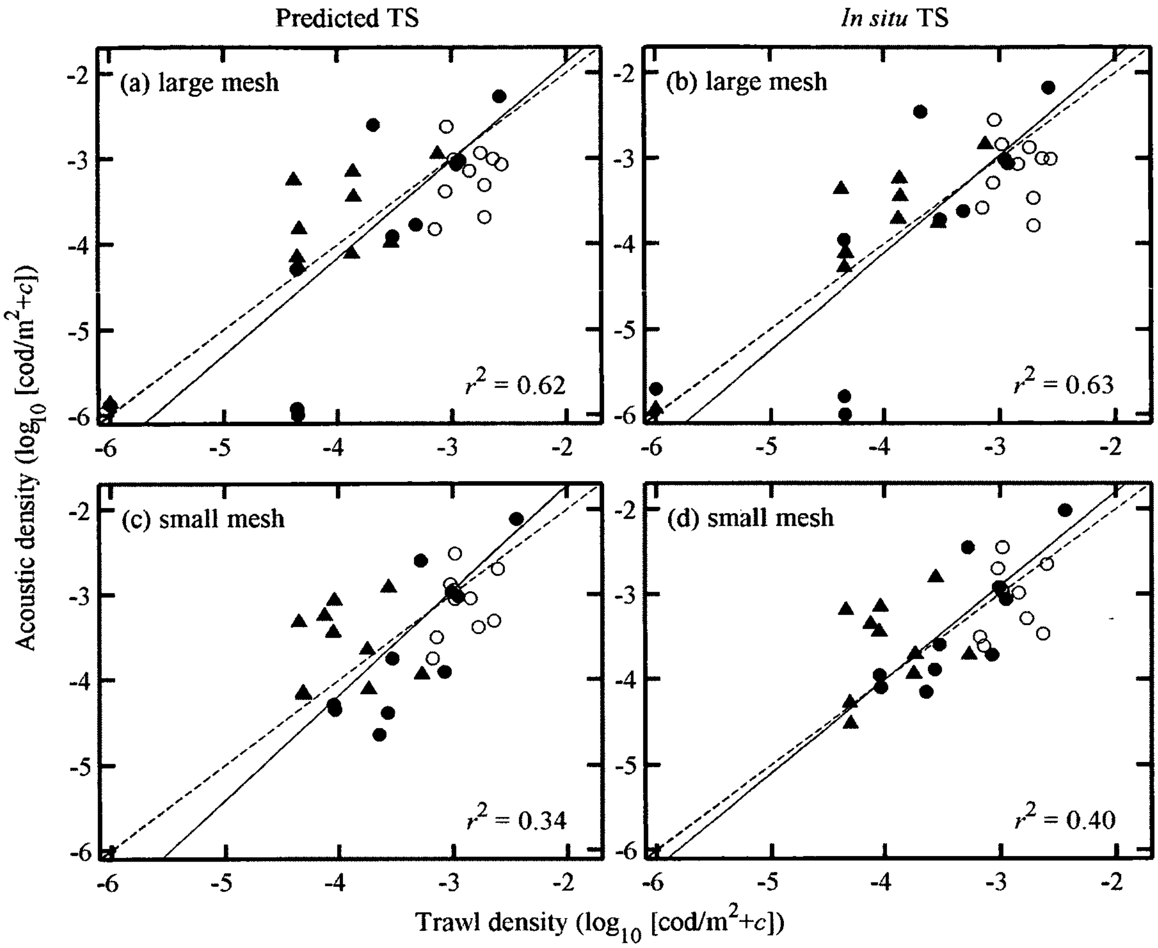

Figure 2-17. Comparisons of $\log_{10}(\text{fish/m}^2+c)$ transformed density of Atlantic cod obtained by a (a and b) large-mesh bottom trawl with a 2.5-m effective trawl zone, (c and d) small-mesh bottom trawl with a 4.5-m effective trawl zone, and 120-kHz echo sounder that sampled within the effective trawl zone along the parallel tow paths on 28-29 May (○), 18-19 June (●) and 3-4 July 2011 (▲). The acoustically derived density was based on the area backscatter from the effective trawl zone, echo classification, an applied dead zone correction, and target strength (TS) either (left) predicted from the mean total length of the combined trawl catch or (right) measured *in situ* along the each corresponding transect. Major axis (Model II) regression was used to fit the data (solid line), test for correlation, and compare to a 1:1 fit (dashed line). Acoustic-based density estimates were significantly correlated with both trawl-based density estimates (P <0.001) and the bottom height was determined by the correlation with the highest coefficient of determination (r^2) which was not significantly different from a 1:1 fit. c = 0.000001.

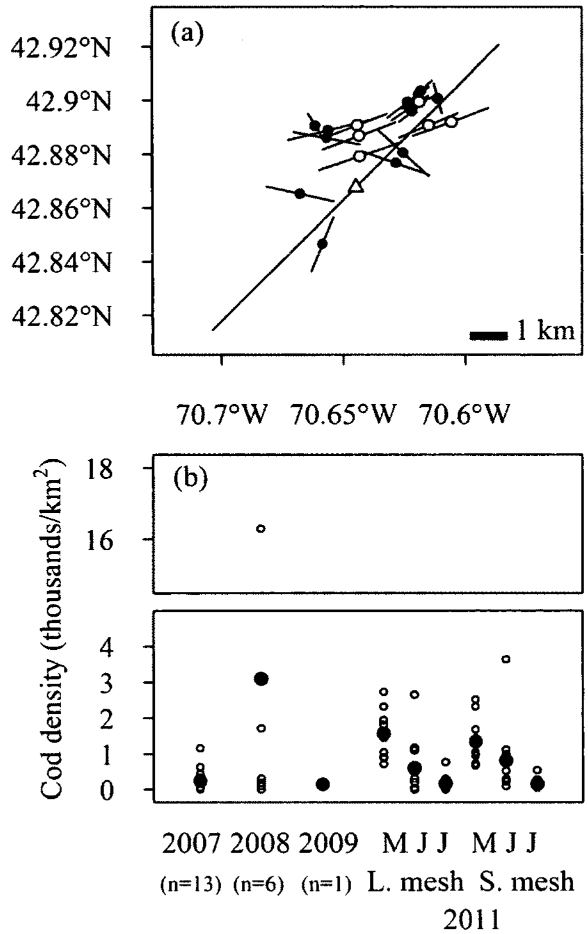

Figure 2-18. (a) Tow paths (lines) of the large-mesh bottom trawl towed by the "*F/V Stormy Weather*" and mid-points during (black circles) 21, 22, and 25 June 2007, (white circles) 26 June 2008, and (triangle) 8 May 2009; (b) Mean (black circle) and samples (open circles) of the Atlantic cod density (thousands/km^2) from a large-mesh bottom trawl towed by the "*F/V Stormy Weather*" during 2007-2009 and tows made with a large-mesh trawl by the "*F/V Ellen Diane*" and a small-mesh bottom trawl by the "*F/V Julie Ann II*" during 28-29 May (M), 18-19 June (J), and 3-4 July (J) 2011.

Table 2-5. Results of the spatial linear model testing the null hypothesis that the $\log_{10}$(density+1)-transformed density (thousands/km^2) of Atlantic cod are equal for adjacent areas inside (transects 1-3) and outside (transects 5-7) the Gulf of Maine cod spawning protection area (GOMCSPA) during each survey with a 38 and 120-kHz split-beam echo sounder based on the method used to estimate backscattering coefficient (s_a) attributed to cod and target strength (TS).

Survey	s_a of cod	TS	Frequency (kHz)	Mean of transformed densities Inside GOMSCSPA	Outside GOMSCSPA	F	P
28-29 May	Echo classification	*In situ*	38	0.086	0.272	3.72	0.054
28-29 May	Echo classification	Predicted	38	0.135	0.327	2.70	0.101
28-29 May	Catch apportionment	*In situ*	38	0.112	0.289	2.94	0.087
28-29 May	Catch apportionment	Predicted	38	0.174	0.353	2.09	0.149
28-29 May	Echo classification	*In situ*	120	0.108	0.190	0.89	0.345
28-29 May	Echo classification	Predicted	120	0.108	0.163	0.47	0.491
28-29 May	Catch apportionment	*In situ*	120	0.137	0.238	1.18	0.279
28-29 May	Catch apportionment	Predicted	120	0.146	0.203	0.42	0.517
18-19 June	Echo classification	*In situ*	120	0.124	-0.036	25.8	0.000
18-19 June	Echo classification	Predicted	120	0.093	0.029	8.17	0.004
18-19 June	Catch apportionment	*In situ*	120	0.142	0.319	2.07	0.151
18-19 June	Catch apportionment	Predicted	120	0.257	0.213	0.23	0.632
3-4 July	Echo classification	*In situ*	120	0.075	0.049	2.17	0.141
3-4 July	Echo classification	Predicted	120	0.075	0.038	3.57	0.060
3-4 July	Catch apportionment	*In situ*	120	0.096	0.126	0.59	0.443
3-4 July	Catch apportionment	Predicted	120	0.106	0.086	0.30	0.585

Table 2-6. Results of the spatial linear model testing the null hypothesis that the $\log_{10}$(density+1)-transformed density (mt/km^2) of Atlantic cod are equal for adjacent areas inside (transects 1-3) and outside (transects 5-7) the Gulf of Maine cod spawning protection area (GOMCSPA) during each survey with a 38 and 120-kHz split-beam echo sounder based on the method used to estimate backscattering coefficient (s_a) attributed to cod and target strength (TS).

				Mean of transformed densities			
Survey	s_a of cod	TS	Frequency (kHz)	Inside GOMSCSPA	Outside GOMSCSPA	*F*	*P*
28-29 May	Echo classification	*In situ*	38	0.179	0.417	2.23	0.136
28-29 May	Echo classification	Predicted	38	0.230	0.439	1.49	0.223
28-29 May	Catch apportionment	*In situ*	38	0.255	0.447	1.28	0.258
28-29 May	Catch apportionment	Predicted	38	0.324	0.477	0.72	0.397
28-29 May	Echo classification	*In situ*	120	0.204	0.296	0.38	0.535
28-29 May	Echo classification	Predicted	120	0.195	0.233	0.09	0.770
28-29 May	Catch apportionment	*In situ*	120	0.290	0.363	0.23	0.629
28-29 May	Catch apportionment	Predicted	120	0.281	0.285	0.00	0.980
18-19 June	Echo classification	*In situ*	120	0.338	0.065	6.17	0.013
18-19 June	Echo classification	Predicted	120	0.261	0.062	6.79	0.009
18-19 June	Catch apportionment	*In situ*	120	0.609	0.295	2.34	0.127
18-19 June	Catch apportionment	Predicted	120	0.451	0.348	0.50	0.481
3-4 July	Echo classification	*In situ*	120	0.114	0.065	0.59	0.444
3-4 July	Echo classification	Predicted	120	0.096	0.041	0.94	0.333
3-4 July	Catch apportionment	*In situ*	120	0.227	0.205	0.04	0.850
3-4 July	Catch apportionment	Predicted	120	0.205	0.156	0.30	0.585

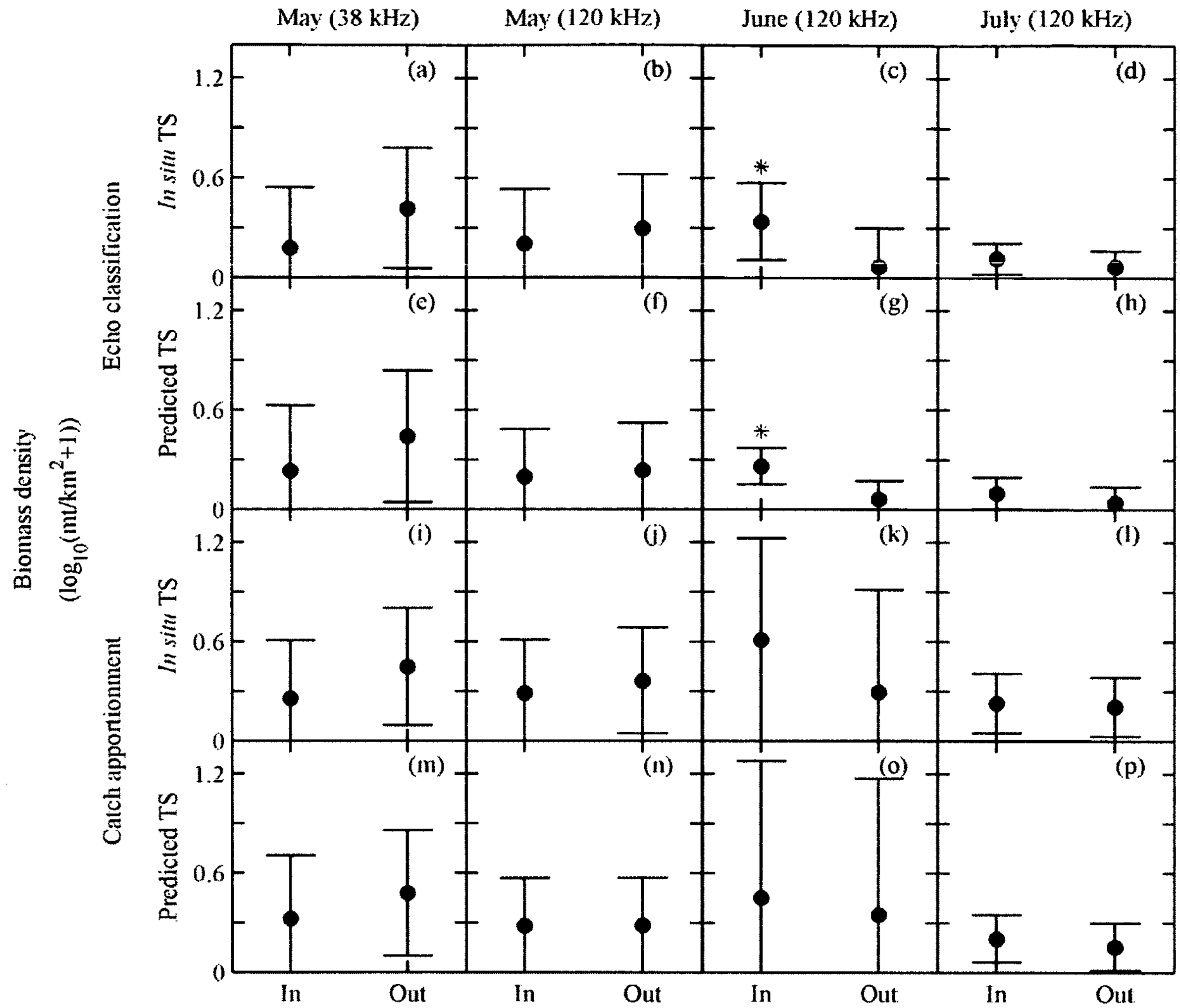

Figure 2-19. Mean (± 95% confidence interval) of the $\log_{10}(\mathrm{mt/km}^2+1)$-transformed density of Atlantic cod from adjacent areas in (transects 5-7) and out (transects 1-3) of the Gulf of Maine cod spawning protection area (GOMCSPA) during each survey (28-29 May, 18-19 June, and 3-4 July 2011) with a 38- and 120-kHz split-beam echo sounder based on the method used to estimate backscattering coefficient (s_a) attributed to cod and target strength (TS). Means marked by an asterisk (*) were significantly different based on a spatial linear model that accounted for spatial autocorrelation ($F = 6.17$, $P = 0.013$ for [c] and $F = 6.79$, $P = 0.009$ for [g]).

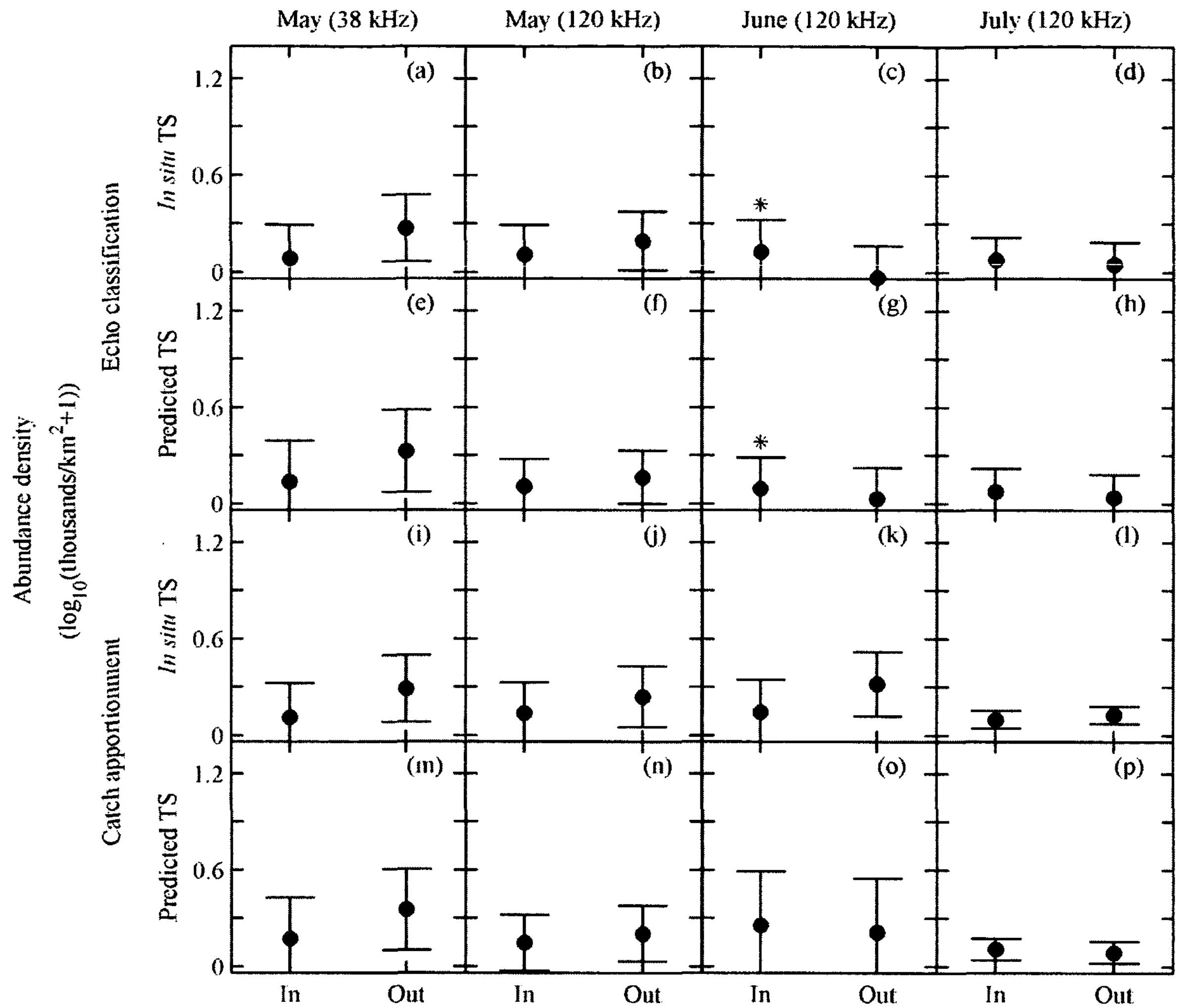

Figure 2-20. Mean (± 95% confidence interval) of the $\log_{10}$(thousands/km^2+1)-transformed density of Atlantic cod from adjacent areas in (transects 5-7) and out (transects 1-3) of the Gulf of Maine cod spawning protection area (GOMCSPA) during each survey (28-29 May, 18-19 June, and 3-4 July 2011) with a 38- and 120-kHz split-beam echo sounder based on the method used to estimate backscattering coefficient (s_a) attributed to cod and target strength (TS). Means marked by an asterisk (*) were significantly different based on a spatial linear model that accounted for spatial autocorrelation (F = 25.8, P < 0.001 for [c] and F = 8.17, P = 0.004 for [g]).

Discussion

This study used several combinations of sampling and analytical techniques to describe the spatial distribution and to estimate abundance and biomass of spring-spawning Atlantic cod inside an area closed to commercial and recreational fishing from 1 April through 30 June. The results clearly indicated that cod congregated inside the closed area during the time of the closure. The abundance and biomass estimates varied among the different methods, but similar spatial patterns did emerge among the techniques. The findings, as well as the uncertainties and potential biases, are discussed in context of results from other studies and the significance relative to fishery management.

One advantage of the continuous nature of acoustic sampling of fish populations is the higher resolution that is provided to describe their spatial distribution, and the use of geostatistics as a method to quantify it. The correlation length (range) of cod densities described by the semivariograms was mostly around 2 to 2.4 km during May and June, and slightly less during July, and can be interpreted as a measure of cluster size. In each survey and estimation method, there was a well-defined sill reflecting the spatial heterogeneity contributing to the variability in cod density within the survey area rather than a pure nugget effect, which would have indicated that spatial structure, if any, could not be quantified by the semivariogram model. The range, sill, and nugget values of the semivariograms demonstrated cod were not randomly distributed, but instead were dispersed over the survey area in several congregations of low to moderate densities that was consistent with conceptual models simulated by Mello and Rose (2005b). The structural analysis revealed micro-scale spatial variation at a range of 35-43 m when densities were calculated at 10-m scale. The high densities observed in the dense congregations within the GOMCSPA were similar to the densities of moderate to dense congregations observed by Mello and Rose (2005b) in Placentia Bay, Newfoundland, during July, but a magnitude less than the dense congregations during April and May.

The spatial distribution described by the kriged maps of the acoustically derived cod densities suggest that the majority of cod in the survey area was concentrated in small areas associated with elevated bathymetric features and shifted as groups between two features between May and June, as shown by acoustic telemetry by Siceloff and Howell (2012) during the 2006 season. The survey was limited to describing the micro- and small-scale spatial patterns of cod, from a single season, and spatial characteristics at large scales within the western Gulf of Maine remain largely not quantified, particularly in coastal areas where spawning and nursery grounds may be present. For example, the cod congregations described by acoustic surveys of Placentia Bay, Newfoundland (Mello and Rose, 2005a, 2005b) were spatially structured with ranges of 9 to 67 km depending on location and month, but the survey also covered an area approximately 132 km x 100 km. Siceloff and Howell (2012) estimated spring-spawning cod in GOMCSPA to be typically active in areas of 41 km^2 (17-57 km^2), which corresponds to a dimension at an approximate scale of 4-8 km, based on 95% activity volume contours of tagged and tracked individuals. Mello and Rose (2005a) argue for the need for small-scale spatial management strategies that take into account seasonal and spatial variation in the availability of various stock components.

Spawning site fidelity and multiyear homing is well documented for many cod populations (Robichaud and Rose 2001; Windle and Rose 2005; Neat, et al. 2006; Espeland et al. 2007; Lindholm et al. 2007; Svedäng et al. 2007; Wright et al. 2007; Howell et al. 2008; Vitale et al. 2008; Siceloff and Howell 2012), but potential explanations for selecting spawning locations vary. Some studies show strong site fidelity and association with hard substrate and vertical relief (Lindholm et al. 2007; Siceloff and Howell 2012). Other spawning locations are closely associated with migratory routes and prevailing currents (Robichaud and Rose 2001; Windle and Rose 2005; Svedäng et al. 2007) or the interaction between egg retention, recruitment, and circulation patterns (Espeland et al. 2007; Runge et al., 2010). Regardless of the reason, the historical spatial complexity of the spawning aggregations formed by GOM cod (Ames 2004; Reich et al. 2009) should be considered in managing this stock. In the eastern North Sea, spatial analyses by Vitale et al. (2008) have shown Atlantic cod to migrate to the same spawning location for over 25 years, which make these spawning aggregations vulnerable to targeted commercial fishery. Results from a tagging study off Iceland demonstrated area closures protect immature Atlantic cod on nursery grounds, but there was no evidence to support the effectiveness of two marine protected reserves studied on protecting migratory adult cod (Schopka et al. 2010).

The synoptic approach of bottom trawling in parallel by two vessels, each with a net of different mesh size, behind the acoustic vessel during the survey served the important role of collecting ground truth data for verifying species identification and size structure, and aiding interpretation of the acoustic data (McClatchie et al. 2000). The small- and large-mesh bottom trawls both verified the presence and relative abundance of cod observed in the echograms corresponding to the transect segments that were trawled. Trawl samples were collected and processed in a way to also provide additional density metrics for comparison with the acoustic estimates. Significant 1:1 correlations between trawl and acoustic estimates of abundance density of cod within the trawl zone supported the validity of acoustically deriving cod density by echo classification. After selecting the bottom height that resulted in the regression with a 1:1 fit and highest r^2, the acoustic estimates of cod density were correlated the best with the large-mesh and small-mesh bottom trawl estimates when echo integration of classified backscatter was restricted to 2.5 m and 4.5 m off the sea floor, respectively, and as such estimated the effective trawl zone.

Rose (2003) found a correlation between trawl and acoustic estimates of cod density that didn't significantly differ from a 1:1 fit when the acoustic measure was restricted to the measured trawl height of 4.5 m for a Campelen 1800 shrimp trawl, which was equivalent to the bottom height for the trawl zone of the small-mesh bottom trawl in this study. If the analysis from this study estimated the effective trawl zone, as done by Aglen (1996) and McQuinn et al. (2005), then these trawl zones were less than the effective trawl zones of 20 m found for trawls of 4-m height by McQuinn et al. (2005) or 30 m for a measured trawl height also of 4 m by Aglen (1996). In a trawl study of mixed species under multiple conditions, Hjellvik et al. (2003) found effective trawl height and the behavioral effects of vertical herding and diving difficult to predict compared to what had been inferred from previous studies (Aglen 1996; Aglen et al. 1999). The results by Hjellvik et al. (2003) showed effective trawl height to generally vary from 10 to 40 m depending on fish length, bottom depth, time of day, season, year, and vertical distribution of the fish. Handegard and Tjøstheim (2009) estimated the typical fishing height for a bottom trawl to be about 20 m, but fish positioned directly in a vessel's path may have low catchability by the trawl or low detection by the echo sounder when strong lateral movements are made. The effective trawl height may typically be greater than the true trawl height (approximately 2.5 m) because fish, particularly gadoids, that are pelagic at night are detected by the echo sounder but dive downward as the trawl approaches and then are herded prior to capture by the trawl (Aglen et al. 1999; Handegard et al. 2003; Handegard and Tjøstheim 2005).

While this diving reaction may have occurred in this study, as cod were observed up to 34 m off the sea floor in the echograms, the bottom height used in the acoustic measure of cod density that produced the best 1:1 fit may have corresponded to a reduced trawl density, if the catchability in this study was reduced by factors such as the short tow duration or if the fish exposed to the acoustics and the trawls differed in space or time. The 10-minute tow durations used in this study were less than the tow duration of 30-60 minutes typically used in groundfish trawl surveys (Walsh 1996). However, shorter tow durations (e.g., 15 minutes) have been reported as being just as efficient as longer tow durations (McQuinn et al. 2005; Walsh 1996). Samples collected by trawls towed at 1-5 minutes were considered representative to estimate fish length and other biological factors in surveys of Atlantic cod in Smith Sound, Newfoundland (Rose 2003). A 10-minute tow duration at 2-2.5 knots (1-1.3 m/s) may not be long enough to exhaust cod swimming ahead of the trawl net before being hauled as endurance for cod at those sustained swimming speeds can range from 2 to 100 minutes depending on water temperature and fish length (He 1991). The swimming endurance at which 50% of cod could endure swimming speeds of 1.0 and 1.3 m/s was experimental shown at 2.6-4.5 °C to be approximately 7-8 minutes and 2 minutes, respectively (Winger et al. 2000). Another explanation of reduced catch or variability between trawl and acoustic estimates, was that cod sampled by the trawl were of less abundance, either because fish moved out of the path of the trawl (Handegard and Tjøstheim 2009), perhaps due to a stronger avoidance response to greater vessel noise of the trawler (Handegard et al. 2003; Handegard and Tjøstheim 2005), or the trawl did not follow the direct path as the vessel (Engås et al. 2000).

As McClatchie et al. (2000) discussed, individual ground truth techniques have their own inadequacies. Mid-water trawls are often used to ground truth data and collect biological samples during acoustic surveys of pelagic species (Jech and Michaels 2006; Páramo and Roa 2003), but would not be optimal for targeting demersal or semidemersal species like Atlantic cod (Rosen et al. 2012). Conversely, the bottom trawl may underrepresent or not catch some pelagic species that may contribute to the area backscatter, which would result in overestimating cod density derived from apportioning the total area backscatter of mixed species assemblages by their relative species composition in the bottom trawl catch. The small-mesh bottom trawl caught small pelagic species such as Atlantic herring, alewife, and Acadian redfish, sometimes in high numbers, while the large-mesh bottom trawl did not. The large-mesh bottom trawl caught a total of 7 silver hake for the study, while the small-mesh bottom trawl caught 2,339 silver hake. In this study, the catch apportionment method often resulted in higher abundance and biomass estimates, particularly in June. This may be partially explained by the high abundance of silver hake in regions not sampled by the trawls, or pelagic species that were underestimated by the small-mesh bottom trawl.

Unlike previous acoustic surveys in Newfoundland waters (Lawson and Rose 2000; Rose 2003), where Atlantic cod are in mono-specific aggregations, the presence of other co-occurring species, especially other gadoids, can complicate species identification of acoustic backscatter collected near the bottom in the western Gulf of Maine (LeFeuvre et al. 2000). In this study, haddock and pollock were caught in few numbers and were generally smaller than most cod in the survey, so misclassification of echoes from these species is probably a low source of error in acoustic estimates of cod densities. Spiny dogfish, another co-occurring species of similar length, was caught during the surveys in June and July. Because spiny dogfish lack a swim bladder, their TS was expected to be approximately 15-20 dB less than that for cod of equivalent size (Foote 1980a; Goddard and Welsby 1986) and as such, their echoes were unlikely misclassified as cod. Apportionment of the acoustic backscatter to cod based on their relative catch composition may be necessary for estimating abundance from acoustic surveys of mixed species assemblages (McQuinn et al. 2005; Simmonds and MacLennan 2005), but the assumption that the samples are representative of the true species composition of the fish assemblage detected by acoustics, and representative of the regions not sampled must hold for reasonable estimates.

The disparity between the catch apportionment and echo classification method was greatest in June, when the assumption that the species composition in the trawl samples was representative of the mixed-species echoes may not be valid. For example, the kriged maps from the June survey illustrate that cod were present at relatively high density in the western edge (transect 1) and the opposite side (transect 9) of the study area based on the catch apportionment method, while cod were present over smaller areas and at lower densities in these areas based on echo classification. The echograms revealed multiple fish schools migrating up toward the surface while transect 1 was sampled, but trawling was performed after these fish made their ascent above the exclusion depth layer (30 m), thereby underestimating the schooling species and overestimating in the apportioned area backscatter of cod. Likewise, a strong scattering layer of presumably silver hake, began their diel vertical migration back toward the sea floor prior to dawn (Bowman and Bowman 1980; Rikhter et al. 2001) during sampling of transect 9. The small-mesh bottom trawl collected large numbers of silver hake on the last two transects.

While acoustics offered the advantage of remotely sensing fish in areas where trawls were unable to be fished, such as the many ridges and humps within the study area, alternative methods are needed to verify species identification of the observed fish echoes. Although only a few locations were monitored by a hydrophone for short durations from the acoustic vessel while adrift, one sound recorded was consistent with the power spectra, peak frequency, and duration of previously published cod grunts (Fudge and Rose 2009; Hawkins 1993). In future acoustic surveys of Atlantic cod, especially in regions of heterogeneous bottom topography unsuited for bottom trawls, a more sophisticated hydrophone deployment system could provide another means of verifying presence of cod, as well as use of sound pressure level or number of grunts as relative indices of abundance for the purpose of verification and interpretation of acoustic data (Van Parijs et al. 2009). Another possible remote sensing method to collect ground truth data would be the use of towed fine-resolution, high-frequency imaging sonar, which are capable of providing high resolution imagery for identifying species or higher taxa, measuring size, and counting individuals with ranges of 30-80 m (Moursund et al. 2003; Boswell et al. 2008;). Underwater video is yet another alternative, but the application for night survey would require artificial illumination that may introduce sampling biases (McClatchie et al. 2000).

Target strength is potentially a substantial source of error in acoustic estimation of abundance or biomass (Simmonds and MacLennan, 2005), which can account for 5-50% of the estimate. Variation in TS has been attributed to many potential physiological (Ona 1990; Horne 2003) and behavioral factors (Foote 1980b; McQuinn and Winger 2003; Rose 2009). For these reasons, when possible, *in situ* measurements may provide the most representative TS for scaling echo integration results to estimates of fish density (Simmonds and MacLennan 2005). In addition, if the combined trawl catch did not represent the true size distribution of the cod, this may also influence predicted TS such that an overestimated size distribution could result in lower abundance or biomass estimates. In this study, *in situ* TS at 120 kHz lead to 12-59% higher estimates of abundance and biomass compared to the use of predicted TS. When cod are pelagic or vertically migrate into the water column at night or to the sea floor near dawn, their tilt angle can change resulting in TS that is lower than often predicted by TS-L equations (McQuinn and Winger 2003; Rose 2009). Cod were observed up to 34 m above the sea floor and approximately 40% were above 4 m above the sea floor. The comparisons between *in situ* and predicted TS from paired acoustic-trawl data in this study detected no significant differences based on the TS-L relations of Rose and Porter (1996). However, *in situ* TS was significantly greater than TS predicted using a b_{20} of -67.5 as used in other acoustic surveys of Atlantic cod (Rose 2003; Mello and Rose 2005a, 2005b). When data were available at both frequencies, *in situ* TS was about 1.1 dB higher at 38 kHz than at 120 kHz, which is the opposite frequency response of Rose and Porter (1996). Pedersen and Korneliussen (2009) found that TS at 38 kHz was about 3-4 dB greater than that at 120 kHz for the northeast Arctic cod stock. Based on these considerations, the estimates using *in situ* TS may provide more accurate estimates of abundance and biomass for the survey area and GOMCSPA.

In this study, estimates with and without dead zone correction were within the range for other acoustic surveys of gadoids. For example, Ona and Mitson (1996) estimated the dead zone correction accounted for 7-19% of total s_A of gadoids. The dead zone correction by Aglen (1996) averaged 12% of the total s_A but was as high as 44%. Mello and Rose (2009) measured the acoustic dead zone independently of the echo sounder depth and found it often to be greater than theoretical dead zone estimates by 0.1-0.9 m, which resulted in negative (6-12%) and positive (9-35%) dead zone corrections to cod densities. Factors that Mello and Rose (2009) attributed to affecting dead zone estimates include gradient of the sea floor, variability of fish density in the dead zone, and wind direction and force. McQuinn et al. (2005) estimated the proportion of cod that were in the acoustic dead zone (~1 m) to be 6-47% in the day and 4-15% at night. Rose (2003) estimated acoustic detectability of cod in Smith Sound to be 86% at night and 73% during the day. The dead zone corrections made in this study increased abundance and biomass estimates, but represented 9-21% of the estimates which were consistent with other studies.

While biological samples from the surveys were not processed for staging maturation and spawning condition, males caught by the trawls were observed to be milting and females appeared gravid or were spilling eggs. The length distribution of the trawl catch indicated that almost all of the fish were at the age at 50% maturity or older (O'Brien et al. 1993; Northeast Fisheries Science Center 2012). In fact, the mean length corresponded to approximately age 5, when fish are fully mature. The latest stock assessment estimated SSB of GOM cod in 2010 to be 11,868 mt (NEFSC 2012). The single-survey biomass estimates of adult cod were 84-494 mt in May and 138-617 mt in June, which represented approximately 1-5% of the SSB estimate of the entire GOM cod stock. Assuming mean cod densities from the survey were representative of the unsampled areas within the GOMCSPA, the biomass of cod within the GOMCSPA estimated from the single surveys was approximately 2-9% of the SSB for GOM cod. The estimates derived from echo classified s_a and *in situ* TS with a dead zone correction were considered the most preferred because of the low CV, spatial coverage, and TS analysis results, and resulted in a biomass estimate for the GOMCSPA approximately equivalent to 4-5% of SSB in May, 3-4% of SSB in June and 1-2% of SSB in July. These acoustic survey estimates represented single realizations or snapshots in time of the cod congregations that may vary within and between days during the seasonal closure. While survey observations of cod covered a time period slightly more than the known residence time of cod in this area as observed by Siceloff and Howell (2012), which averaged 30 days and ranged from 8 to 53 days, it is naïve to expect all of the fish to have arrived and departed the same time. As such, single-survey estimates may underestimate the cumulative abundance and biomass of cod that use GOMCSPA for spawning during the spring because each survey estimates the abundance and biomass of a mixture of cod that differ in arrival, residence time, and departure.

Conclusions

This study located congregations of Atlantic cod in spawning condition associated with elevated bathymetric features within GOMCSPA on 28-29 May, 18-19 June, and 3-4 July, but observed no cod during the 7-8 April survey. Geostatistical analysis revealed cod were spatially organized typically at a scale of 2 km. Maps produced by ordinary kriging illustrated cod during the May survey were present throughout the study area but were concentrated near elevated bathymetric features before converging during the June survey to a single denser congregation adjacent to one of the bathymetric features. Fishery managers should consider redefining the western boundary of the closure because the cod congregations observed during the May survey extended beyond the current western boundary. Approximately 25-50% of the cod remained in this spatial distribution by the July survey, but it remains unknown whether cod naturally dispersed the area following spawning (Howell et al. 2008; Siceloff and Howell 2012), were driven away by fishing activities (Dean et al. 2012), or were caught by fishers. However, temporal shifts in arrival and departure may vary, and if cod remain congregated at relatively high concentrations during July as observed from this study of the 2011 spring spawning season, then further consideration of extending the timing of the closure in the GOCSPA may be warranted.

This study highlighted the effect of estimation and sampling technique on the estimates and variability of cod abundance and biomass. In this study, which surveyed cod at night, echo classification and *in situ* TS was considered to provide the most representative results. Trawls were unable to sample over elevated bathymetric features where cod were sometimes highly abundant and catch apportionment of area backscatter was based on trawl samples that were not necessarily representative of the true mixed-species fish assemblages. The use of acoustics can improve surveys of Atlantic cod by sampling more of the water column, describing fish distributions and behavior at higher spatial resolution, sampling more diverse bottom topography, reducing sampling mortality, and covering more area than bottom trawls. The use of bottom trawls remains important to verify species and size compositions of the fish assemblages surveyed as well as providing information to verify density estimates within the acoustic dead zone. Based on these results, the biomass of spring-spawning Atlantic cod in the GOMCSPA in 2011 represented at least 4-5% of the 2010 SSB estimate of the GOM cod stock. This study hopefully motivates future integrated acoustic-trawl surveys of Atlantic cod in the GOMCSPA and other areas of the western Gulf of Maine, and provides the evidence for fishery managers to consider the use and configuration of seasonal area closures of important spawning grounds to promote the rebuilding of this overfished stock.

Acknowledgements

This study would not have been possible without the experience and generous efforts of Captains D. Goethel, C. Felch II, C. Felch III, and D. Robillard, and all of their crew. The field assistance of M. Balge, J. Bunker, J. Cranney, W. Chaput, G. Ek, A.D. Jain, T. Ford, S. Maxwell, S. Moore, D.H. Yi, and W. Zhang was greatly appreciated. We thank A. H. Hawkins for reviewing the hydrophone recording of the cod grunt and P. Petitgas for providing EVA2. This study was funded by the Northeast Consortium.

CHAPTER III

TARGET STRENGTH MEASUREMENTS OF FREE-SWIMMING CAGED ATLANTIC COD BY A 38- AND 120-KHZ SPLIT-BEAM AND A 300-KHZ MULTIBEAM ECHO SOUNDER

Abstract

Acoustic surveys have been widely used to assess fish stock abundance, yet the uncertainty of these estimates partly depends on how well the acoustic scattering properties of the individuals being surveyed are understood and represented. Abundance of Atlantic cod (*Gadus morhua*), a commercially-important and exploited species throughout most of its range, is traditionally estimated from fishery-independent bottom trawl surveys, such as the Gulf of Maine (GOM) and Georges Bank stocks of the US northwest Atlantic. Acoustic surveys have been used to provide abundance estimates of cod stocks from other regions such as the Canadian Atlantic and the Barents Sea. The spring spawning congregation of GOM cod found in Ipswich Bay, because of it spatial and temporal predictabilities, lends itself to acoustic surveying.

In working toward the goal of developing an acoustic survey of this congregation, target strength (TS) of individual mature GOM cod collected from this spring-spawning congregation was estimated from a series of acoustic measurements made using a 38-kHz and 120-kHz split-beam echosounder (Simrad EK60) and a 300-kHz multibeam echosounder (Kongsberg EM3002). This multibeam echosounder can also be used to

collect high-quality bottom backscatter and bathymetry of the benthic habitat where cod are surveyed. Individual cod, ranging from 59 to 98 cm in total length (*L*), were placed inside a 1.5-m^3 monofilament mesh cage. The cage was then suspended from an anchored vessel at a depth of 8-10 m. The three echo sounders synchronously collected acoustic data of each free-swimming captive cod, while the movements of most individuals were observed with underwater video. The split-beam transducers provided direct measurements of TS after standard sphere calibration, but the TS from the central single beams of the multibeam transducer was statistically estimated from the echo amplitudes after compensating for the beam directivity pattern and on-axis sensitivity loss. The TS-*L* relations at 38 and 120 kHz were compared to those reported in the literature, and to the TS-*L* relation at 300 kHz. Factors affecting the variability are discussed.

Introduction

Target strength (TS) of Atlantic cod (*Gadus morhua*) is important to quantify if acoustically derived abundance indices are to be used in making effective management decisions for sustaining the cod fishery. Declines in Atlantic cod populations have been widely documented throughout its geographic range (Myers et al. 1996, 1997, 2001; Ames, 2004; Rothschild, 2007). In the northwest Atlantic waters of the United States, Atlantic cod are managed as two stocks: Gulf of Maine (GOM) and Georges Bank. Based on the 2011 assessment (NEFSC 2012), the GOM stock was considered overfished and experiencing overfishing. While split-beam echo sounders have been used to survey cod stocks of the Canadian Atlantic (McQuinn et al. 2005; Rose 2003) and Barents Sea

(Korsbrekke et al. 2001), acoustic survey data are not used in stock assessments of GOM cod.

Acoustic surveys have been widely used to assess fish stocks, yet the uncertainty of these estimates partly depends on how well the acoustic scattering properties of the individuals being surveyed are understood and represented. While echo integration is proportional to fish density (Foote, 1983), the acoustic quantity of an individual fish, represented as the backscattering cross-section ($\sigma_{bs,}$ m^2) as defined by MacLennan et al. (2002), has been described as a stochastic process with wide distributions of values often characterized by a Rician or Rayleigh probability density function (PDF) (Clay and Heist 1984; Fässler et al. 2009; Horne 2000; Kieser and Ehrenberg 1990). Target strength, which is the decibel (referenced to 1 m^2) equivalent of σ_{bs} is the quantity more commonly described. Variability in TS of fish have been attributed to swim bladder morphology (Foote 1980a; Francis and Foote 2003; Gorska and Ona 2003; Ona 2003; Gorska et al. 2005), size (Love 1971; McClatchie et al. 1996; McClatchie et al. 2003), physiology (Ona 1990; Hazen and Horne 2003; Horne 2003), behavior (Love 1977; Foote 1980b; McQuinn and Winger 2003), and physical factors (McClatchie et al. 1996; Horne and Clay 1998; Horne 2000; Kloser and Horne 2003). The mean or expected acoustic backscattering cross-section ($\bar{\sigma}_{bs}$) of an individual fish as defined by MacLennan et al. (2002) is used to scale echo integration results to absolute or relative fish densities (Simmonds and MacLennan 2005).

Species-specific TS and length (*L*) relations are commonly used to predict TS based on the length of fish representatively sampled from the population by a capture or visual technique (McClatchie et al. 2000; Simmonds and MacLennan 2005). The TS-*L* relation has been quantified from measurements of wild fish (*in situ*), experimentation of captive fish (*ex situ*), and acoustic scattering models for a variety of species and conditions as described in detail by Foote (1991), McClatchie et al. (1996), and Simmonds and MacLennan (2005). In an early study, Nakken and Olsen (1977) used a tethering apparatus to suspend and angle individual dead or stunned fish of 17 species, including Atlantic cod, in the center of a 38-kHz and 120-kHz single beam transducer to quantify the relation between TS and length, tilt and roll angle. The maximum dorsal-aspect TS-*L* relation determined from that study for Atlantic cod was TS=24.5 $\log_{10}(L)$-66.6 at 38 kHz and TS=24.6 $\log_{10}(L)$-67.6 at 120 kHz.

While TS measurements of immobile anesthetized or dead fish in controlled experiments are useful for describing directivity patterns of cod TS, TS-*L* relations based on these measurements have limited direct application of scaling echo integration to fish density estimates because the swim bladder volume may be different than live fish and TS variation is greater in free-swimming live fish (Nakken and Olsen 1977; Foote 1980a). The TS-*L* relation of live free-swimming cod, and three other species, was described by Goddard and Welsby (1986), who measured peak echo amplitude of individual fish held captive in a small cage at three frequencies (10, 30, and 100 kHz).

The application of multibeam echo sounders in fisheries research has been well established (Misund and Aglen 1992; Gerlotto et al. 1999; Mayer et al. 1999), including recent advancements toward providing quantitative acoustic estimates of fish abundance and biomass (Gerlotto et al. 2000; Cochrane 2003; Trenkel et al. 2008; Cutter et al. 2009). The advantages of having larger sampling volumes, better spatial resolution, and less behavioral biases compared to single beam echo sounders make multibeam echo sounders attractive for surveying fish populations, yet additional uncertainties can be introduced that make accurate acoustic estimation more difficult. One step toward quantitative acoustic backscatter from a multibeam echo sounder comes from successful calibration as described by Foote et al. (2005), Melvin et al. (2003), and Ona et al. (2007). The development of multibeam echo sounder systems like the Simrad ME70 or MS70 which have user-configurable, simultaneous, multiple split beams at multiple frequencies has greatly advanced the utility of multibeam echo sounder for quantitative fisheries research (Trenkel et al., 2008). However, the multibeam echo sounders that are in more widespread use in hydrographic surveys for mapping bottom habitat and bathymetry consist of multiple overlapping single beams operating at one frequency. Those that can store backscatter from the water column (e.g., Kongsberg EM3002, Reson 7125, Reson Seabat 6012, Simrad SA950, Simrad SM2000) have been used in fisheries research (Misund and Coetzee 2000; Gerlotto and Paramo 2003; Melvin et al. 2003; Gurshin et al., 2009; Weber et al. 2009). Quantification of acoustic backscatter of fish from multibeam echo sounders must consider beam-specific effects of incidence angle and body orientation (Cutter and Demer 2007).

Acoustic surveys could provide additional information on GOM cod biomass and distribution, particularly in regions where cod congregate for spawning and aren't suitable for bottom trawling (Chapter II). While acoustic scattering of Atlantic cod from split-beam echo sounders can provide direct measurements representative of the target strength to derive fish density estimates, the use of multibeam echo sounders consisting of multiple single beams that are commonly used in hydrographic surveys may also provide important information on the distribution and abundance of Atlantic cod associated with habitat features. However, to provide information of sufficient quality for science-based decision making, the scattering characteristics, specifically the TS-*L* relation, should be quantified. In this study, the TS-*L* relation of adult Atlantic cod and the variability in scattering are described from measurements obtained by two split-beam echo sounders and a multibeam echo sounder.

Methods

Fish Cage Experiment

Atlantic cod (n=221) were captured from 3 tows (30 to 60 min in duration) by a commercial bottom trawler, *"F/V Stormy Weather"*, from known spawning areas (Howell et al. 2008) in greater Ipswich Bay, western Gulf of Maine. The catch was brought up slower than normal fishing practices, but dead, moribund, or inflated individuals were counted, measured, and released. A subset of live individuals were placed in 1-m^3 polyurethane tote with running seawater for immediate transport to a submersible net cage previously described by Gurshin et al. (2009). A group of live individuals were later transported to a smaller holding cage and lowered to the sea floor at a mean bottom depth of 14-18 m in Gosport Harbor at the Isles of Shoals (Figure 3-1). Acoustic backscatter measurements of individual free-swimming cod held captive in a 1.5-m^2 monofilament cage were made on 18-20, 22, and 25-27 May 2009 (Figure 3-2). A summary of the individual cod and data included in analyses are described in Table 3-1.

Acoustic Instrumentation

Acoustic backscatter measurements of Atlantic cod were collected simultaneously by two Simrad EK60 split-beam echo sounders and a Kongsberg EM3002 multibeam echo sounder. The nominal 3-dB beam widths of the transducers were 12° for 38-kHz split-beam transducer, 7° for the 120-kHz split-beam transducer, and 1.5° for each of the 160 receive beams of the 300-kHz multibeam transducer. The EM3002 receive beams were configured to a cover 130° swath with equiangular beam spacing. Transmission of a 0.256-ms pulse from the EK60 was synchronized to the trigger of the EM3002, which transmitted a 0.200-ms pulse every half second (2 Hz). The transducers were mounted to a plate and center-aligned with the multibeam transducer between the two split-beam transducers (Figure 3-3). An Odom Digibar-Pro was used to continuously monitor sound speed at the transducer depth (0.3-1 m depending on surface conditions) and to periodically take sound speed profiles for input to the beam-forming calculations made by the EM3002.

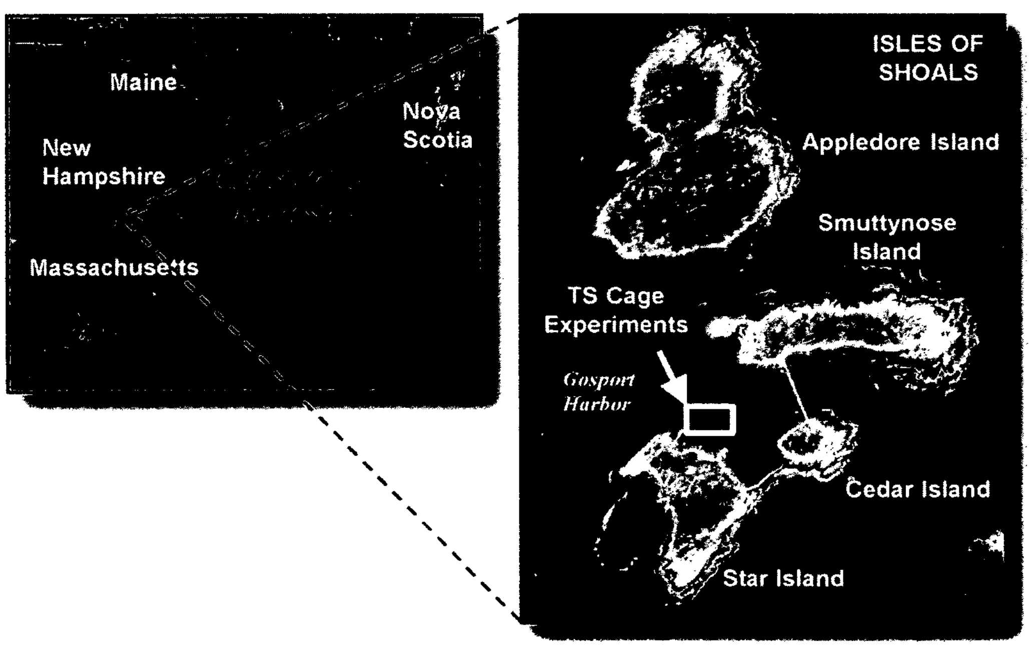

Figure 3-1. Atlantic cod caught off the coast of New Hampshire and Massachusetts, USA, in the western Gulf of Maine (left) and insonified individually inside a monofilament cage for measuring target strength by synchronized split-beam and multibeam echo sounders from an anchored vessel in the protected Gosport Harbor at the Isles of Shoals (right).

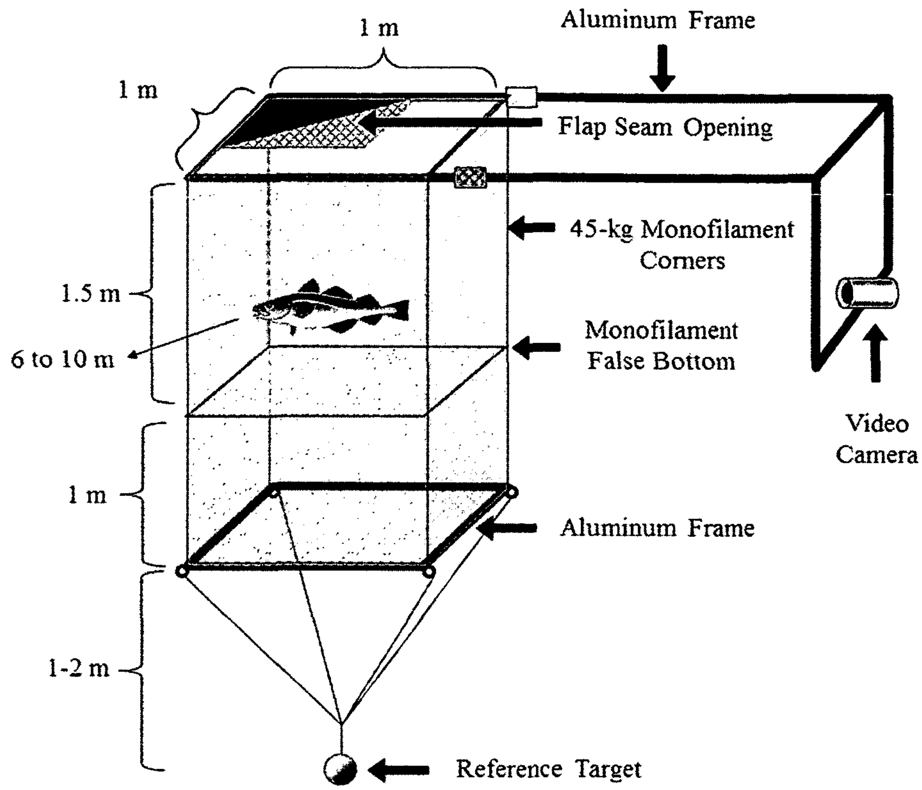

Figure 3-2. Monofilament cage used to hold individual Atlantic cod during acoustic backscatter measurements made by a 38-kHz and 120-kHz split-beam and a 300-kHz multibeam echo sounder.

Table 3-1. Fish identification number (ID), total length (L), mean depth, underwater video recording status (Y = yes and N = no), number of single echo detections by the 38-kHz and 120-kHz split-beam echo sounders (Simrad EK60), ping-maximum and total single echo detections from all selected beams of the 300-kHz multibeam echo sounder (Kongsberg Maritime EM3002), and the minimum (Min) and maximum (Max) beam pointing angles from acoustic backscatter measurements made on individual free-swimming Atlantic cod held in a monofilament cage during 18-27 May 2009.

ID	Day of May	L (cm)	Mean Depth (m)	Video recorded	38-kHz EK60	120-kHz EK60	Ping-maximum detections 300-kHz EM3002	Total single echo detections 300-kHz EM3002	300-kHz EM3002 selected beams	Beam pointing angle (°) Min.	Max.
1	18	74	9.1	Y	121		102	254	85-94	-10.8	-3.6
4	18	82	8.5	Y	103		198	401	83-91	-8.4	-2.0
7	19	72	8.0	N	18	33	150	353	66-74	5.2	11.6
8	19	87	6.5	N	101	52	259	761	78-88	-6.0	2.0
9	20	76	6.7	N	569		44	127	85-88	-6.0	-3.6
11	20	80	5.8	N	696	185	555	1291	73-74	5.2	6.8
12	22	84	7.9	Y	316	9	308	1173	88-92	-9.2	-6.0
15	22	83	8.1	Y	356	3	129	298	80-84	-2.8	0.4
17	25	67	8.7	Y	2192	985	654	1561	81-88	-6.0	-0.4
18	25	75	8.3	Y	1495	214	2478	6894	81-86	-4.4	-0.4
19	25	69	5.3	Y	473	28	134	337	84-89	-6.8	-2.8
20	25	74	5.0	Y	494	177	839	2779	86-97	-13.2	-4.4
21	26	69	8.3	Y	575	901	1552	4027	78-85	-3.6	2.0
22	26	59	9.3	Y	381	483	995	2811	84-91	-8.4	-2.8
24	27	79	8.2	Y	632	547	895	2832	72-79	1.2	6.8
25	27	98	8.1	Y	124	82	397	1388	69-74	5.2	9.2
26	27	63	8.1	Y	478	951	547	1536	79-82	-1.2	1.2
27	27	69	8.1	Y	287	438	111	294	78-79	1.2	2.0

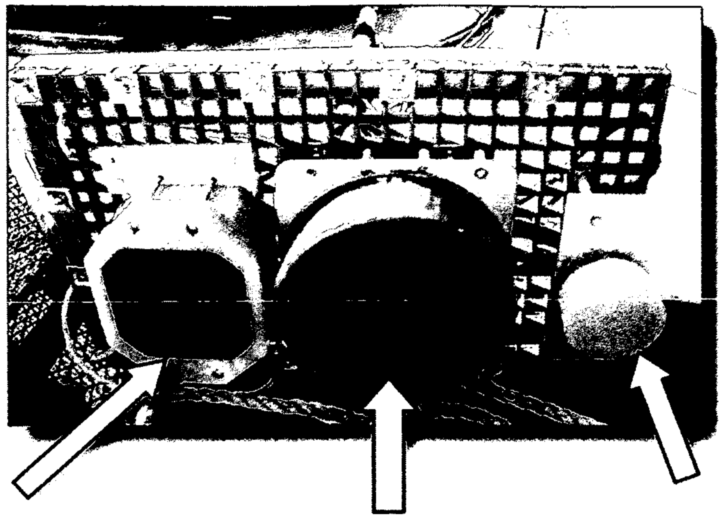

Figure 3-3. Photograph of the transducers mounted to plate and suspended from an anchored vessel (*R/V Meriel B*) to collect acoustic backscatter measurements on free-swimming captive Atlantic cod.

Calibration

The split-beam echo sounders were calibrated by the standard target method using a 38.1-mm tungsten carbide sphere suspended 10-12 m from each transducer by a monofilament line (Foote et al. 1987). For the EM3002, two sets of calibration data were collected. At time of the fish cage experiment, the reference target was suspended by monofilament line and moved every 1-2 min throughout the central beams for describing the scattering statistics of a reference target. Before the fish cage experiment, the EM3002 was installed in an indoor freshwater tank facility (12 m wide x 18 m long x 6 m deep) previously used for calibration of multibeam echo sounders (Foote et al. 2005). Several series of measurements were made to describe and quantify the acoustic backscattering characteristics of the EM3002 such as the transmitting and receiving beam pattern (Figures 3-4 and 3-5) and beam-specific "on-axis" sensitivity by comparison between estimated and theoretical TS of the reference target. The product of the relative transmit and receive beam pattern, after centering the data, did not produce a flat response and the deviation estimated the relative calibration offset for each beam (Figure 3-6).

The relative beam-specific offset created by the product of transmit and receive beam pattern was adjusted to fit one of the five beams with absolute offset for the reference target. Then, these five sets of beam-specific calibration offset (C_b) were averaged for applying to the measured echo strength (Figure 3-6). The theoretical TS of a 38.1-mm tungsten carbide sphere under environmental conditions of the freshwater tank and in the field was coincidentally estimated to be -38.1 dB, based on continuous wave theory and for a 200-ms pulse at 300 kHz (MacLennan 1981) and was collaborated independently by Foote (pers. comm.; See Appendix B). Appendix C details the calibration process for the EM3002.

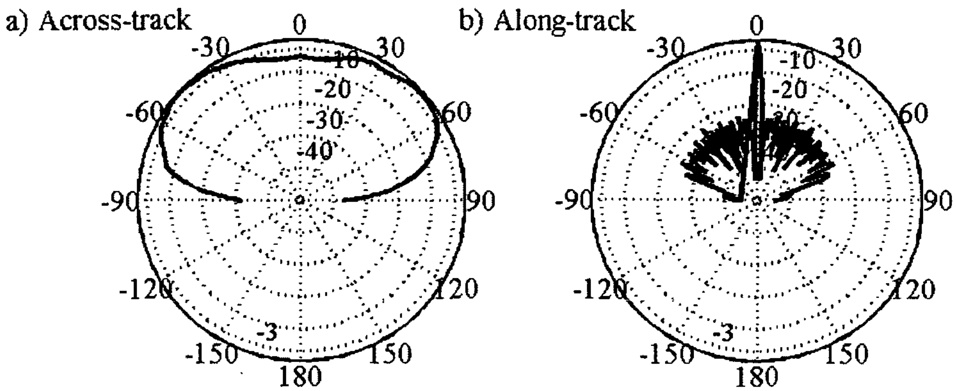

Figure 3-4. Normalized transmit beam pattern of the E3002 multibeam transducer in the (a) across-track and (b) along-track equatorial plane measured by receiving 30 pulse transmissions from a standard transducer (U.S. Naval Undersea Warfare Center/Underwater Sound Reference Division Model 27, S/N 218) at 0.5° intervals as the transducer mechanically rotated from -90° to 90° at a range of 8.5 m inside a freshwater tank facility.

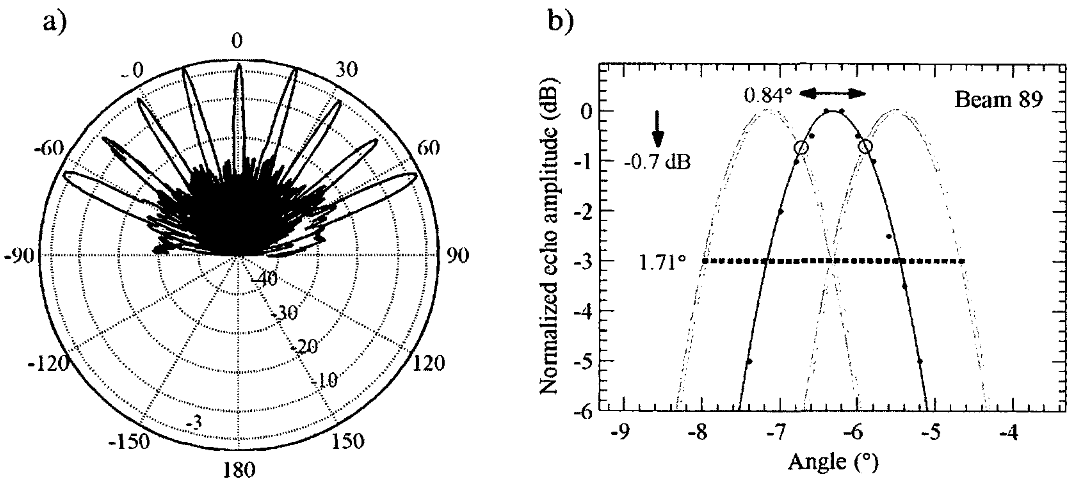

Figure 3-5. (a) Polar plot of the across-track receive beam pattern for beams 1, 20, 40, 60, 80, 100, 120,140, and 160 of the 160 receive beams for the 300-kHz EM3002 multibeam echo sounder;(b) The fitted (solid black line) and measured (dots) across-track beam pattern of receive beam 89 of the EM3002 multibeam echo sounder, 3-dB beam width (dashed line), sensitivity loss off axis (down arrow) down to the intersection (open circles) of adjacent beams 90 and 88 (shaded grey lines), and beam width between overlapping beams (double arrow). Note beams numbered from positive to negative angles.

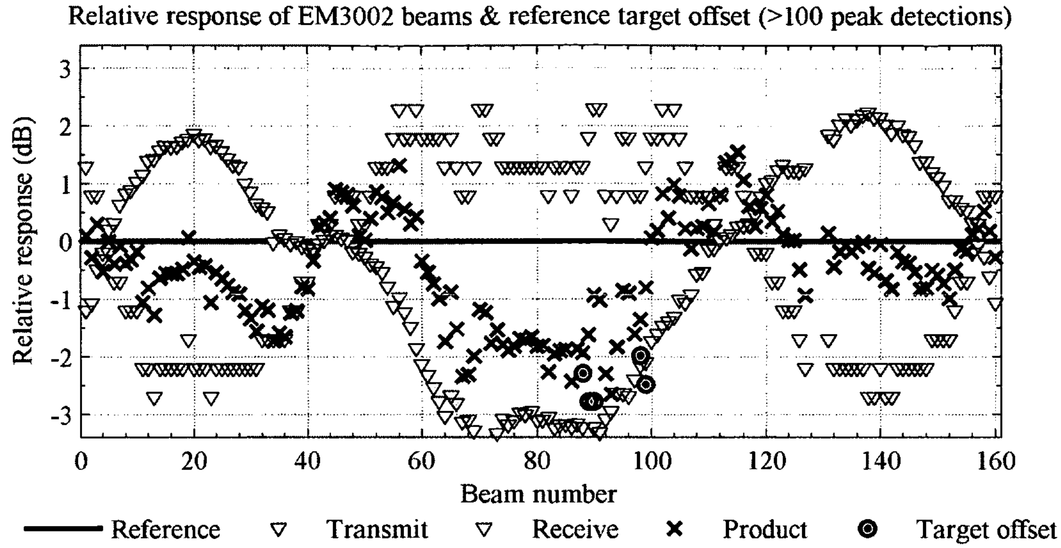

Figure 3-6. The product between the complementary, centered relative transmit and receive beam responses at the major response axis of each receive beam of the 300-kHz EM3002 multibeam echo sounder; and the offset between the theoretical and estimated target strength of a reference target (38.1-mm tungsten carbide sphere) for five reference beams with greater than 100 ping-maximum single echo detections.

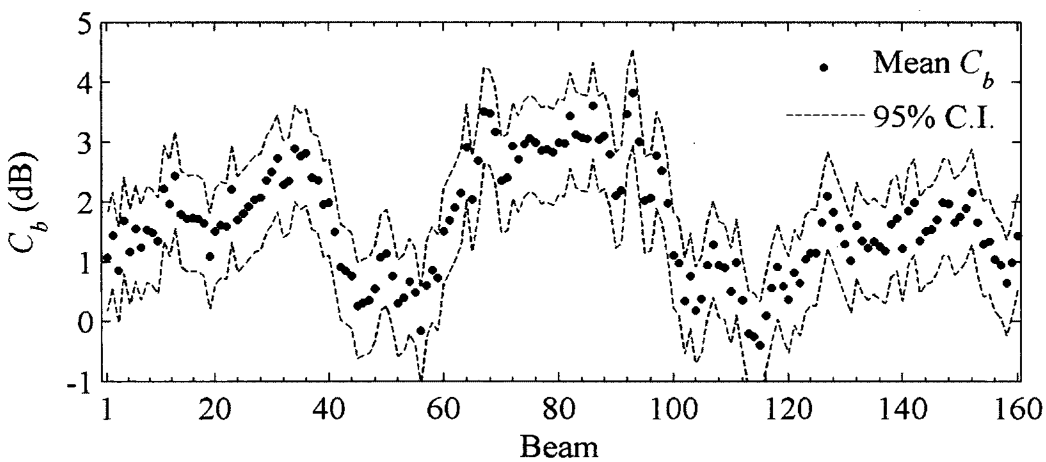

Figure 3-7. The mean and 95% confidence interval of the beam-specific calibration offset (C_b) derived from adjusting the absolute difference between theoretical and estimated target strength of a reference target detected in five reference beams of the 300-kHz Konsgberg EM3002 mutlibeam echo sounder by the relative transmit-receive major axial response of individual beams obtained from laboratory measurements of the beam patterns.

Underwater Video Observations

An underwater video camera was attached 2 m from the side of the cage and 1 m from the top of the cage (Figure 3-2). Video was time stamped and recorded by a digital video recorder during TS measurements of most individuals (Table 3-1). Any changes in the position, body orientation, and swimming activity for individuals were recorded qualitatively, along with the timestamp, to classify segments of the time series of TS measurements, when video was available. The two categorical classifications defined were "calm" and "active." The calm category was applied to fish that maintained near horizontal position (±15-20°) and didn't display fast tail-beating or erratic swimming in the cage. The active category was used when the fish changed its body orientation or swam erratically. Common examples of the active category included swimming or maintaining position with a head-down or head-up position, swimming up and down, changing vertical position, and temporary entanglement in the monofilament mesh wall of the cage.

Analysis of Split-beam Data

Echo strength (ES) and angular position data collected by the EK60 were imported into Echoview software (v4.9, Myriax Pty. Ltd., Hobart, Tasmania) for processing echograms (Figure 3-8). Echo strength is the echo amplitude values in dB with an applied range-dependent, time-varied gain (TVG) of $40\log_{10}(R)$, where R is the range (m) and correction for absorption loss. The angular position data was used in the Simrad LOBE model to estimate TS of single echo detections (SED) by compensating the ES for the sensitivity loss of the target being off the major response axis (MRA) of the sound beam. The SED criteria used were a maximum two-way beam compensation of 6 dB, an echo envelope between 0.6 and 1.5 normalized pulse lengths, 6-dB pulse length determination level, and a -50 dB minimum TS threshold.

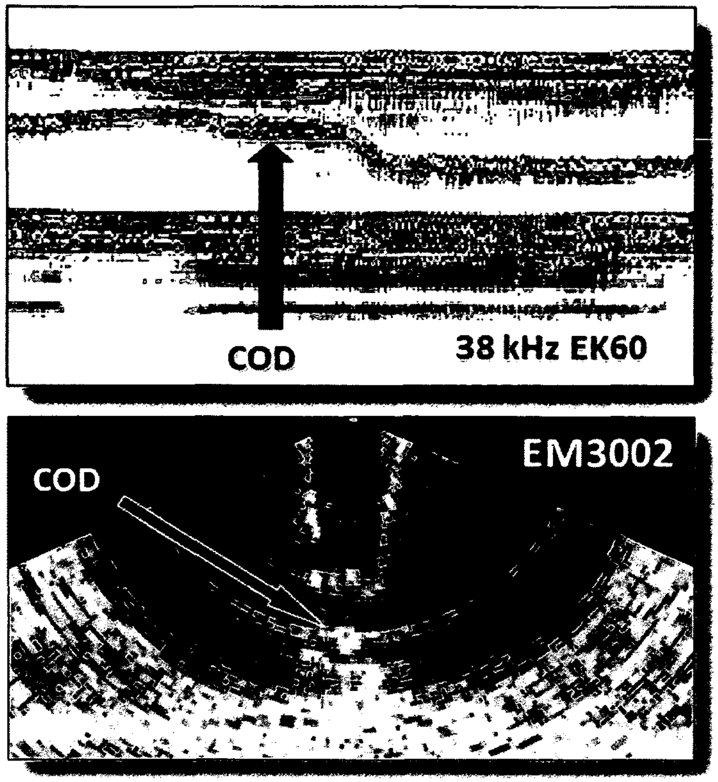

Figure 3-8. Top: example of an echogram from data collected by a 38-kHz split-beam echo sounder (Simrad EK60) illustrating the echo trace from an Atlantic cod swimming inside a cage. The x-axis of the echogram is time over consecutive transmissions (pings) and the y-axis is depth. Bottom: an image of the swath from a single ping by the 300-kHz Konsgberg EM3002 mutlibeam echo sounder which also shows the location of the cod above the bottom cage echo and below the top cage echo.

Analysis of Multibeam Data

The EM3002 data were imported and processed into Matlab (Math Works, Natick, MA, USA). The raw amplitude (A_{WC}, originally stored in units of 0.5 dB) from the water column datagram previously defined by Gurshin et al. (2009) was converted to ES as

$$ES(b, R) = A_{WC}(b, R) + 10\log_{10}(\Omega_{TX}\Omega_{RX}) - (X\text{-}40)\log_{10}R + C_b, \qquad (1)$$

where b is the beam number, Ω_{TX} and Ω_{RX} are, respectively, the along-track transmitting and receiving beam widths (in radians), X is the TVG function applied during data acquisition (30 in this study), and C_b is the beam-specific calibration offset between measured and theoretical TS of a reference target. A similar set of SED criteria (equivalent to single beam method 1 in Echoview; see Appendix D) were applied to the EM3002 data separately for each beam selected and within the range gate where the individual cod was located. Because only one individual cod was insonified in a known region of the water column, the beam with the maximum ES for each ping was retained as the ping-maximum and was expected to be within 1 dB of the MRA in the across-track direction among the overlapping beams detecting the cod, assuming each beam had equal sensitivity after applying C_b.

In addition to presenting the mean echo strength of Atlantic cod insonified by the EM3002 multibeam echo sounder, two measures were used to estimate TS. The EM3002 is unable to directly measure TS because it lacks sufficient angular information to determine position of targets within each beam for compensating the sensitivity loss of a target off the MRA (i.e., beam directivity pattern). As a result, the ES must be compensated for the so-called beam pattern by statistical approximation to estimate TS. To compensate ping-maximum ES for targets located off the MRA in the along-track direction, thereby having weaker echo amplitude, the 95-th percentile of the ping-maximum echo strength distribution provided closer approximation of the expected TS than the mean ES. Figure 3-9 provides a three-dimensional visualization of theoretical overlapping narrow beams based on the across-track beam pattern. The cross-sectional area within 1 dB of the MRA for the portion of the center beam not overlapped by adjacent beams represented approximately 5% of the area (volume) down to -20 dB (just above the side lobes). The 95th percentile statistic of the echo strength distribution then would be within 1 dB or less of the MRA, assuming the fish were randomly distributed throughout this portion of the beam over many detections.

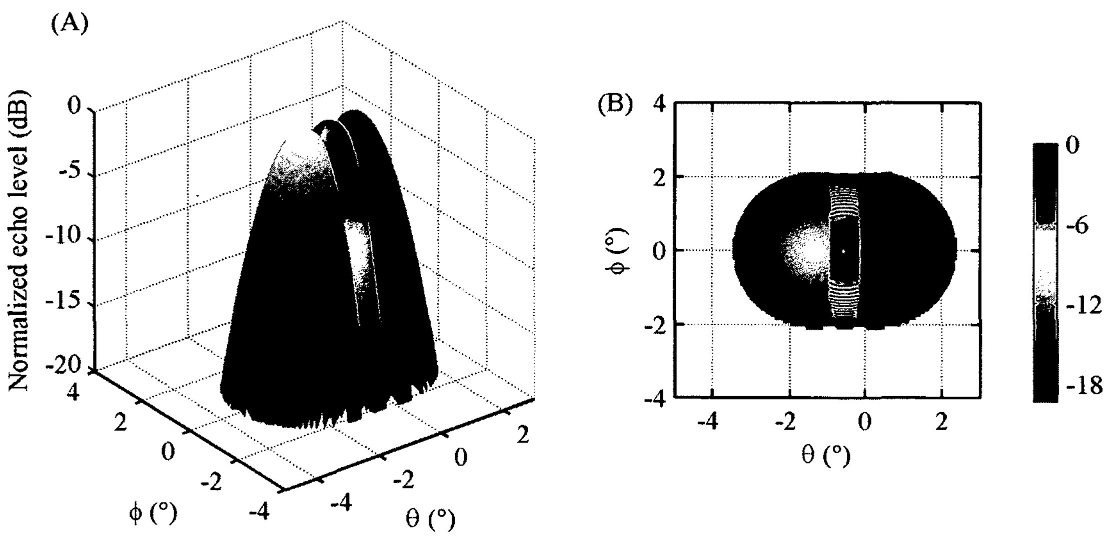

Figure 3-9. (A) Three-dimensional visualization of the overlap between a theoretical beam and two adjacent beams and (B) 1-dB contours of the cross-section of the portion that is not overlapped.

Several indirect, statistical approaches to estimating TS from single beam echo sounders have been described (Peterson et al. 1976; Ehrenberg et al. 1981; Clay 1983; Clay and Castonguay 1996; Hedgepeth et al. 1999). The method used here was a smoothing deconvolution-like technique. Following the statistical principles described by Clay (1983), Peterson et al. (1976), and Stepnowski and Moszyński (2000), the single-beam integral equation defines the probability density function (PDF) of observed echoes (w_e) with amplitude e as the product of two random variables: the PDF of the backscattering process of the fish (w_f) and the PDF of observing the amplitude b for a fish in the transducer beam (w_b). The equation given by Peterson et al. (1976) and Clay (1983) is

$$w_e(e) = \int_0^1 w_b(b) w_f(e/b)\, db/b \qquad (1)$$

As Stepnowski and Moszyński (2000) and Moszynski and Hedgepeth (2000) state, in the decibel domain equation 1 becomes the convolution:

$$w_E(\mathrm{ES}) = \int_0^1 w_{\mathrm{B}}(\mathrm{B}) w_{\mathrm{TS}}(\mathrm{ES} - \mathrm{B}) dB \qquad (2)$$

where ES (dB) is the echo strength of the fish, B (dB) is the sensitivity factor of the echo in the beam given the beam directivity pattern of the transducer and assuming a random angular position of the fish, and TS is the target strength of the fish. The observed ES distribution of all SEDs in each beam combined or separately was discretized into 1-dB bins and then a kernel smoothing density function was applied (via "ksdensity" function in Matlab) to remove sample variability and artifacts and smooth the left tail if the threshold resulted in unobserved data. Then, the smoothed PDF was then re-binned and scaled to integrate to 1.

In determining w_{B}, transmit and receive beam directivity pattern of the EM3002 was modeled assuming radial symmetry of the across-track beam pattern measurements made during calibration ($\mathrm{B}(\theta) = \mathrm{B}(\theta,\phi)$). Compensating echo amplitudes for the beam directivity pattern also requires knowledge about the distribution of the fish within the transducer beam. Here, over many detections, a fish was assumed to be randomly distributed throughout the beam and the probability of the random angular location of a fish within the beam ($P_f(\theta)$) was assumed to equal $\sin(\theta)$ (Hedgepeth 1994; Hedgepeth et al. 1999). Following Peterson et al. (1976) and Clay and Medwin (1977), this can also be expressed as the probability of a fish being within an incremental gated volume ($P(\Delta V)$):

$$P(\Delta V) = \sin(\theta)\, d\theta \qquad (3)$$

The assumption of random angular location of fish within the beam has become a routine assumption in applying indirect TS estimation techniques (Peterson et al. 1976, Clay and Medwin 1977; Hedgepeth et al. 1999; Moszynski and Hedgepeth 2000; Stepnowski and Moszyński 2000). In this study, where individual cod were constrained to a cage centered under the transducers, they may be randomly distributed throughout the main lobe as a result of its movements as well as the transducer motion from wave action. Given equation 3, w_b then was assumed to be expressed as

$$w_b(b) = \left(\frac{1}{\Delta b}\right) \int_{\Delta\theta} \sin(\theta)\, d\theta \qquad (4)$$

where $\Delta\theta$ represents the angular interval corresponding to b which is bounded by $\pm\Delta b/2$ (Peterson et al. 1976; Clay and Medwin 1977).

For simplification, the beam directivity pattern of an individual ideal EM3002 beam was approximated by the beam directivity pattern of a piston transducer with an equivalent 3-dB beam width. The directional response for a piston transducer, D, as a function of θ was calculated as

$$D(\theta) = 2J_1[(ka)\sin(\theta)]/[(ka)\sin(\theta)] \qquad (5)$$

where k is the acoustic wave number, a is the effective radius of a circular transducer, and J_1 is the Bessel function of the first kind order 1. Here, the 3-dB beam widths (θ_{3dB}) of EM3002 beams were estimated from beam pattern measurements (Appendix C) and used to derive a:

$$a = 1.6/[(k)\sin(\theta_{3dB}/2)] \qquad (6)$$

following Stetter-Parker et al. (1999). There is discrepancy in relating the amplitude response variable from the two-way beam directivity pattern, *b*, to the one-way directional response variable *D* in the literature, where in some works, *b* is equal to D^2 (Peterson et al. 1976; Clay and Medwin 1977; Stanton and Clay 1986; Hedgepeth 1994), while in others, b^2 is equal to D^2 (Clay 1983; Moszynski and Hedgepeth 2000; Stepnowski and Moszyński 2000). Assuming $b(\theta)$ is equal to $D(\theta)^2$ and after substituting *u* for $(ka)\sin\theta$, equation 4 is changed to a summation following Peterson et al. (1976) and Clay and Medwin (1977) in the form:

$$w_b(b) = (\frac{1}{ka}) \sum_n \left[u_n(\Delta u_n/\Delta b)/\sqrt{1 - u_n^2(ka)^2}\right] \qquad (4)$$

where *n* represents the intercepts of the Δb. This function was then log-transformed by providing values of $w_B(B)$ where $B = 10\log_{10}(b)$ and *b* included transmission and reception.

Since the across-track transmit beam pattern and the along-track receive beam patterns of the EM3002 were considered relatively flat responses at the scale of an individual transmit or receive beam, w_B calculated assuming the two-way beam directivity pattern of an ideal piston transducer was then reduced to a function of a one-way beam directivity pattern to avoid over compensating for *b*. Beam-pattern compensation using w_B as weighting factors only considered the upper main lobe and assumed the contribution of the side lobes was negligible, which Clay and Castonguay (1996) had shown to be a reasonable assumption. In this study, the -50 dB threshold used in single echo detection likely removed most of side-lobe contribution since side lobes were approximately 20 dB from the MRA and the TS of cod was expected to be between

-25 and -35 dB. To determine the w_{TS} from equation 2, the Matlab "deconv" function was used to deconvolve w_B out of w_E. Negative values were converted to zero.

This procedure was evaluated two ways. First, a backscattering PDF of a target was simulated based on a Rayleigh PDF of known σ_{bs} (e.g., = TS of the reference target). The Rayleigh distribution was selected for simulation because, at 300 kHz, the ratio of L to acoustic wavelength (λ) for Atlantic cod was much greater than 25, when echo amplitudes closely follow a Rayleigh distribution (Ehrenberg et al. 1981). The w_B was used to convolve the simulated w_{TS} which, in turn, was converted back using the described procedure. Figure 3-10 illustrates this process. A second validation came from using the observed echo strengths of the reference target from individual beams and estimating the expected TS ($\langle TS \rangle$) of the reference target using this smoothing-deconvolution technique. The estimated w_{TS} was scaled to integrate to 1, and then the $\langle TS \rangle$ was estimated as the weighted average of the discretized PDF (i.e., $\langle TS \rangle = \Sigma TS_{bin}\, w_{TS}$). An example PDF is shown in Figure 3-10. The average deviation between the $\langle TS \rangle$ and reference TS was 0.5 dB and was not significantly different from zero (paired t-test, t = 1.75, df = 12, P = 0.104). The best agreement was made in this validation when the beam-pattern compensation was restricted to the upper 10 dB.

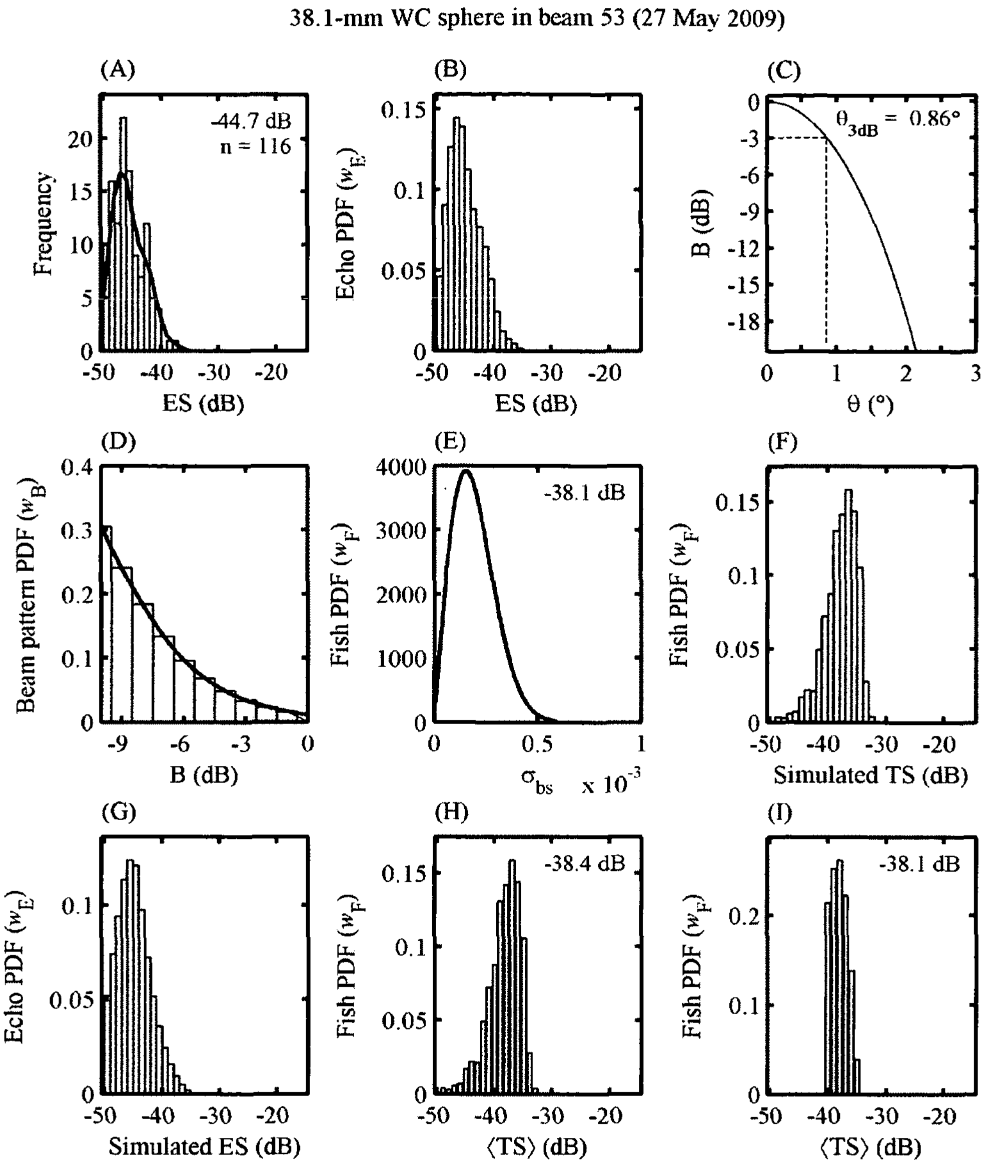

Figure 3-10. (A) Probability density function (PDF, line) fitted to the histogram with smoothing; (B) histogram of the discretized smoothed echo PDF; (C) beam directivity pattern (B) as a function of angle (θ) off the major response axis; (D) beam pattern PDF of the upper 10-dB of the main lobe modeled for a 1.66° 3-dB beam width assuming symmetry; (E) simulated Rayleigh PDF for a fish or target with an acoustic backscattering cross-section (σ_{bs}) equivalent to a target strength of -38.1 dB; (F) scaled PDF of the TS of the simulated σ_{bs}; (G) simulated echo PDF by convolution of the simulated TS PDF and the PDF of the beam pattern; (H) PDF after deconvolution back to the original PDF of the target shown in F; (I) estimated PDF of the expected TS for the reference target.

Statistical Analysis

Ordinary least squares linear regression was used to fit the relation between target strength and total length by TS = $m \log_{10}(L) + b$ for each echo sounder and frequency. The slope from the regression was statistically compared to the standard value of 20 by a one-sample t-test based on the mean and standard error estimate of the slope coefficient from the regression (McClatchie et al. 2003). The common practice of using 20 $\log_{10}(L)$ to predict target strength originates from σ_{bs} being proportional to the square of the effective scattering length (Love 1971; Foote 1987; Simmonds and MacLennan 2005). As a result, the y-intercept parameter b when the slope = 20, referred as b_{20} (McQuinn and Winger 2003; Simmonds and MacLennan 2005), was calculated for the standard equation at each frequency when $20\log_{10}$ dependence was assumed (i.e, TS = $20\log_{10}(L) + b_{20}$). The best-fit regressions for each frequency were compared by analysis of covariance. When the slope was fixed to 20, the b_{20} parameters were compared among frequencies by multiple pair-wise t-tests.

Results

Indirect Target Strength

As examples, Figures 3-11 to 3-15 illustrates the estimated PDF of the expected TS at 300 kHz from the observed echo PDF of five fish of different size and behaviors. Table 3-2 presents the echo statistics of each cod for the echo sounder frequencies used in measurements. The ⟨TS⟩ from the smoothing deconvolution technique was on average about 1 dB less than the 95th percentile of the ping-maximum ES (Paired t-test, t = -3.24, df = 16, P =0.005).

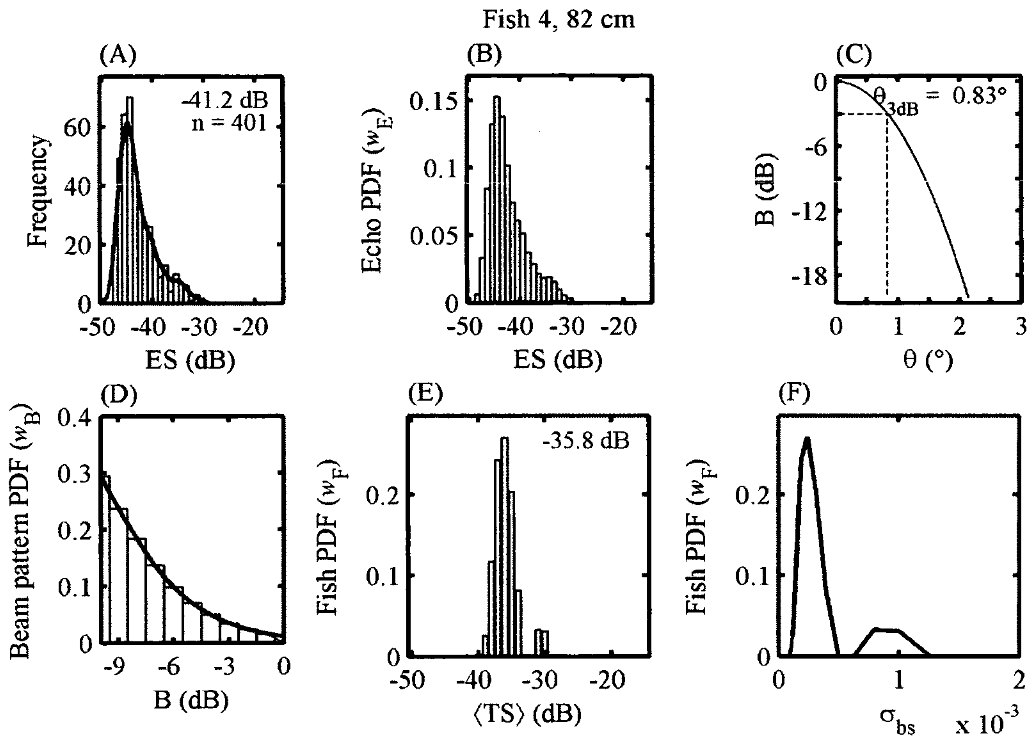

Figure 3-11. (A) Probability density function (PDF, line) fitted to the histogram of the echo strength (ES, mean is inset value) for 82-cm Atlantic cod (ID 4); (B) histogram of the discretized smoothed echo PDF; (C) beam pattern sensitivity (B) as a function of angle (θ) off the major response axis; (D) beam pattern PDF of the upper 10-dB of the main lobe modeled for a 1.66° 3-dB beam width assuming symmetry; (E) deconvolved fish PDF with an expected TS of -35.8 dB; (F) fish PDF expressed as backscattering cross-section (σ_{bs}).

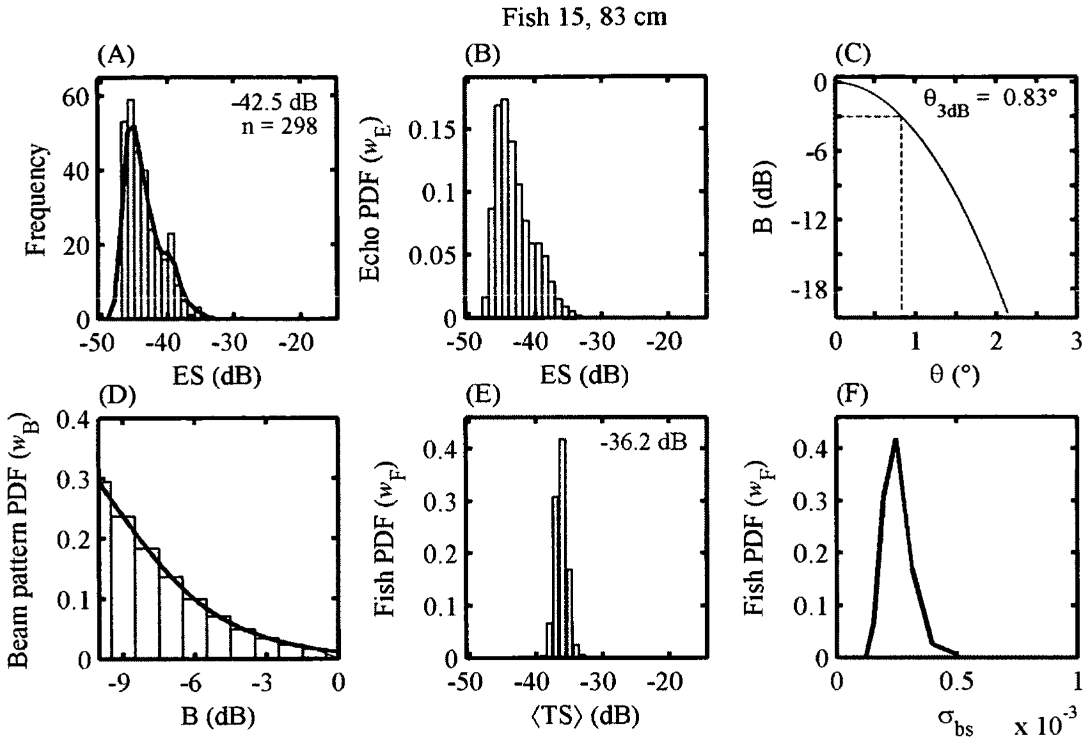

Figure 3-12. (A) Probability density function (PDF, line) fitted to the histogram of the echo strength (ES, mean is inset value) for 83-cm Atlantic cod (ID 15); (B) histogram of the discretized smoothed echo PDF; (C) beam pattern sensitivity (B) as a function of angle (θ) off the major response axis; (D) beam pattern PDF of the upper 10-dB of the main lobe modeled for a 1.66° 3-dB beam width assuming symmetry; (E) deconvolved fish PDF with an expected TS of -36.2 dB; (F) fish PDF expressed as backscattering cross-section (σ_{bs}).

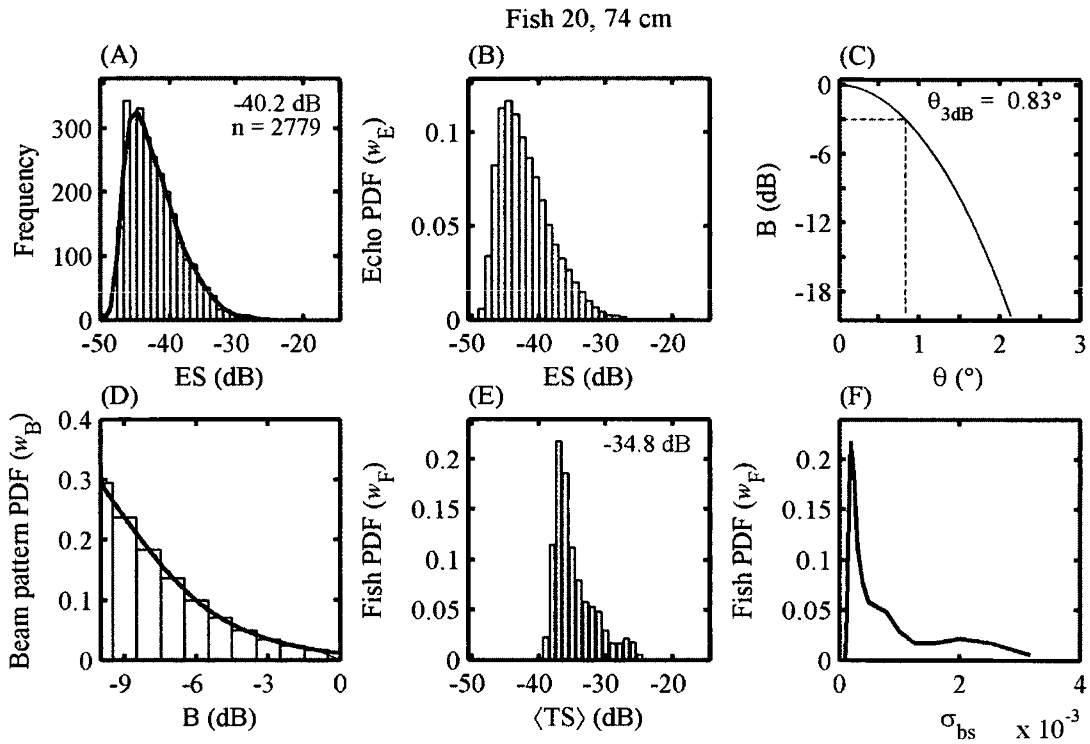

Figure 3-13. (A) Probability density function (PDF, line) fitted to the histogram of the echo strength (ES, mean is inset value) for 74-cm Atlantic cod (ID 20); (B) histogram of the discretized smoothed echo PDF; (C) beam pattern sensitivity (B) as a function of angle (θ) off the major response axis; (D) beam pattern PDF of the upper 10-dB of the main lobe modeled for a 1.66° 3-dB beam width assuming symmetry; (E) deconvolved fish PDF with an expected TS of -34.8 dB; (F) fish PDF expressed as backscattering cross-section (σ_{bs}).

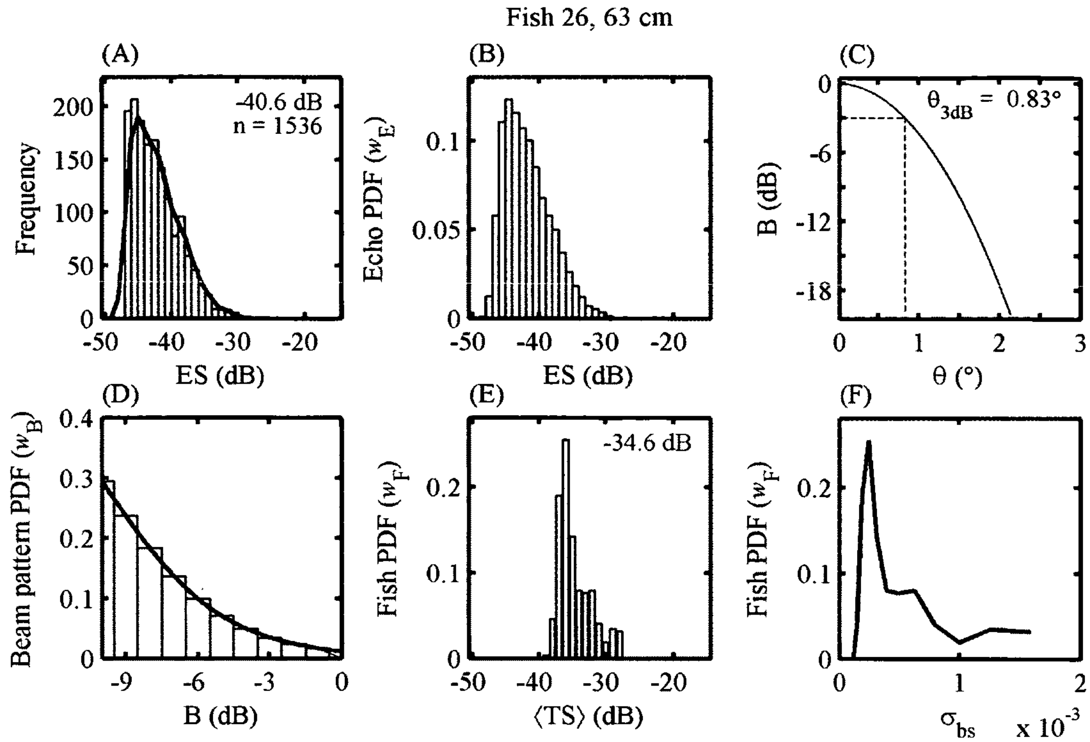

Figure 3-14. (A) Probability density function (PDF, line) fitted to the histogram of the echo strength (ES, mean is inset value) for 63-cm Atlantic cod (ID 26); (B) histogram of the discretized smoothed echo PDF; (C) beam pattern sensitivity (B) as a function of angle (θ) off the major response axis; (D) beam pattern PDF of the upper 10-dB of the main lobe modeled for a 1.66° 3-dB beam width assuming symmetry; (E) deconvolved fish PDF with an expected TS of -34.6 dB; (F) fish PDF expressed as backscattering cross-section (σ_{bs}).

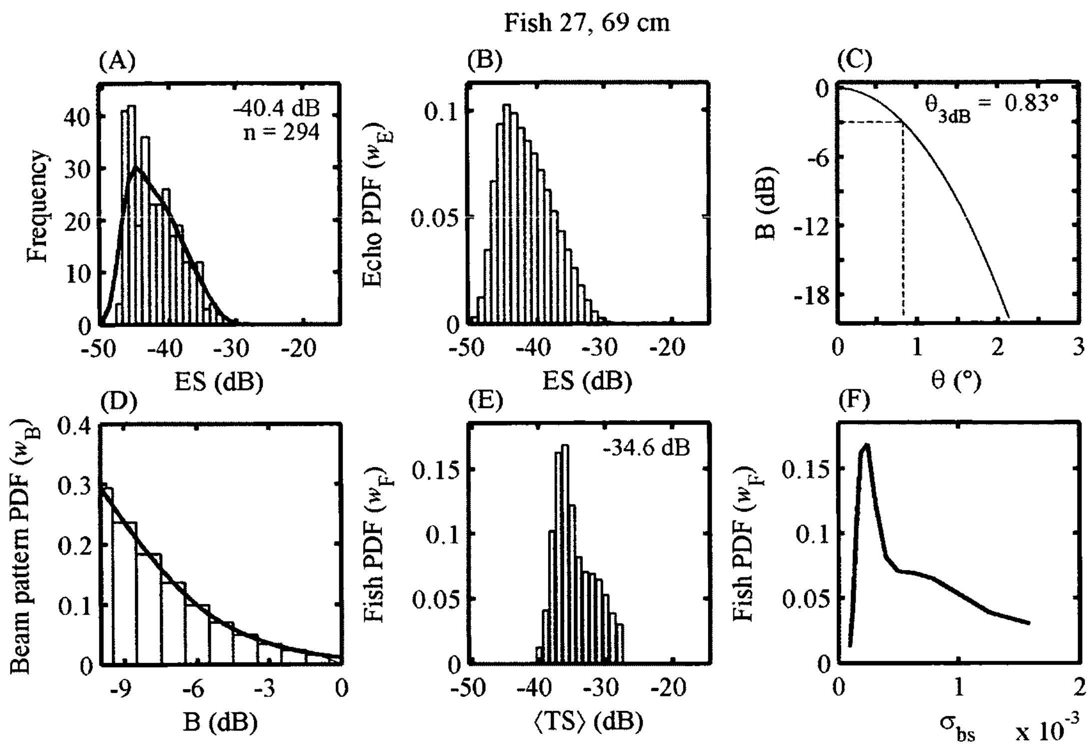

Figure 3-15. (A) Probability density function (PDF, line) fitted to the histogram of the echo strength (ES, mean is inset value) for 69-cm Atlantic cod (ID 27); (B) histogram of the discretized smoothed echo PDF; (C) beam pattern sensitivity (B) as a function of angle (θ) off the major response axis; (D) beam pattern PDF of the upper 10-dB of the main lobe modeled for a 1.66° 3-dB beam width assuming symmetry; (E) deconvolved fish PDF with an expected TS of -34.6 dB; (F) fish PDF expressed as backscattering cross-section (σ_{bs}).

Table 3-2. Fish identification number (ID) of free-swimming captive Atlantic cod, total length (L), number (n) of single echo detections (SED) and target strength (TS) measured by the 38-kHz and 120-kHz split-beam echo sounders (Simrad EK60); and ping-maximum, total SEDs, expected TS (⟨TS⟩), echo strength (ES), and 95th percentile of the ES distribution from all selected beams of the 300 kHz multibeam echo sounder (Kongsberg Maritime EM3002) during 18-27 May 2009.

		38 kHz		120 kHz		300 kHz				
								Ping-maximum SED		
ID	L (cm)	n	TS (dB)	n	TS (dB)	n	⟨TS⟩ (dB)	$ES_{95\%}$ (dB)	ES (dB)	n
1	74	121	-26.4			254	-34.8	-35.7	-40.2	102
4	82	103	-26.2			401	-35.8	-34.9	-40.9	200
7	72	18	-32.0	33	-31.2	353	-35.1	-34.5	-39.9	150
8	87	101	-25.5	52	-29.0	761	-34.2	-33.1	-38.3	261
9	76	569	-26.8			127	-33.2	-30.8	-36.6	44
11	80	696	-28.1	185	-29.3	1291	-32.6	-31.4	-35.4	546
12	84	316	-26.6	9	-25.9	1173	-33.2	-29.0	-35.5	293
15	83	356	-28.0	3	-31.8	298	-36.2	-37.8	-41.8	119
17	67	2192	-32.5	985	-30.5	1561	-35.1	-35.1	-40.4	659
18	75	1495	-30.0	214	-27.8	6894	-33.2	-32.4	-37.5	2477
19	69	473	-29.5	28	-29.0	337	-35.1	-34.9	-40.1	135
20	74	494	-31.0	177	-31.6	2779	-34.8	-33.1	-38.6	847
21	69	575	-28.6	901	-29.9	4027	-34.4	-34.0	-39.2	1557
22	59	381	-31.4	483	-32.1	2811	-34.4	-33.8	-38.9	971
24	79	632	-30.6	547	-30.1	2832	-33.5	-31.7	-36.7	904
25	98	124	-30.2	82	-25.5	1388	-31.0	-27.7	-32.8	377
26	63	478	-33.1	951	-32.9	1536	-34.6	-34.3	-39.2	560
27	69	287	-30.5	438	-32.2	294	-34.6	-34.5	-38.5	115

Target strength-length relations

Table 3-3 presents the regression statistics for the best fitted models between TS and L at 38 and 120 kHz, which were improved when statistical outliers were removed. Mean TS at length for fish ID 25 was considered an outlier for the 38-kHz TS-L relation because the 95% confidence intervals for the residual did contain zero. Likewise at 120 kHz, fish IDs 2, 5, 12, 15 were removed based on the same outlier diagnostics and TS-L relation was refitted. The best-fit and standard (slope = 20) TS-L relations are presented for both frequencies (Figures 3-16 and 3-17). The regression slope from the best-fit model was not significantly different from 20 at 38 kHz ($t = 2.08$, $P = 0.052$) and 120 kHz ($t = 1.22$, $P = 0.180$). The b_{20} parameter estimate of -66.4 was not significantly different than -66 reported by Rose and Porter (1996) at 38 kHz ($t = -0.97$, $P = 0.241$), but the b_{20} estimate of -67.4 at 120 kHz was significantly lower than their value of -65 ($t = -6.56$, $P < 0.001$).

The 95-th percentile of ES distribution and ⟨TS⟩ at 300 kHz significantly increased with L based on linear regressions of the aggregate of single echo detections from multiple selected beams of the EM3002 multibeam echo sounder, but the relation between mean ES and L was not significant (Table 3-3). After removing the two data points corresponding to outlying observations (IDs 4 and 15), mean ES became significantly correlated with L and the best-fit models based on the other two metrics were improved (Figure 3-18; Table 3-3). The ⟨TS⟩ from the estimated PDF from the beam-aggregate of all single echo detections significantly increased as L increased (Figure 3-18; Table 3-3).

The y-intercept and slope parameters of the TS-$\log_{10}(L)$ regression at 38 kHz and 120 kHz, and $\langle$TS$\rangle$-$\log_{10}(L)$ regression at 300 kHz were significantly different for the best-fit regressions (Table 3-4). The slope parameter for the TS-$\log_{10}L$ relation at 300 kHz was significantly lower than the slopes of the regressions based on the 38 kHz and 120 kHz, but the slopes were not significantly different between regressions based on 38 kHz and 120 kHz (Table 3-5). The b_{20} estimates were significantly different among the regressions for the relation between length and TS at 38 kHz, TS at 120 kHz, and $\langle$TS$\rangle$ at 300 kHz, $ES_{95\%}$ at 300 kHz, and ES at 300 kHz (Table 3-6). The b_{20} estimates were not significantly different between the two split-beam frequencies, but were significantly higher than the b_{20} estimates of the three metrics at 300 kHz (Figure 3-19). The b_{20} estimates at 38 kHz and 120 kHz were approximately 5 dB and 4 dB higher than the b_{20} for $\langle$TS$\rangle$ at 300 kHz, respectively.

Table 3-3. Results for linear regression between estimated target strength and total length of free-swimming caged Atlantic cod insonified by 38-kHz and 120-kHz split-beam echo sounders (Simrad EK60) and a 300-kHz multibeam echo sounder (Kongsberg EM3002).

Echo sounder frequency	Regression	Equation	n	F	P	r^2
38 kHz	Best fit	$TS = 27.5\log_{10}(L) - 80.7$	19	7.996	0.012	0.32
	(without outliers 5 and 7)	$TS = 24.0\log_{10}(L) - 74.1$	17	7.112	0.018	0.32
	(without outliers 5,7 and 25)	$TS = 38.0\log_{10}(L) - 100.1$	16	19.335	0.001	0.58
	Slope =20	$TS = 20\log_{10}(L) - 66.4$				
120 kHz	Best fit	$TS = 22.1\log_{10}(L) - 71.3$	17	4.794	0.045	0.24
	(without outliers 5, 12, 15)	$TS = 27.7\log_{10}(L) - 81.8$	13	19.137	0.001	0.64
	Slope =20	$TS = 20\log_{10}(L) - 67.4$				
300 kHz	Best fit, mean echo strength (ES) Pooled selected beams	Not significant	18	3.142	0.095	0.16
	(without outlier 15)	$ES = 20.6\log_{10}(L) - 79.1$	17	5.38	0.035	0.26
	(without outliers 4 and 15)	$ES = 24.5\log_{10}(L) - 86.2$	16	10.024	0.007	0.42
	Slope =20	$ES = 20\log_{10}(L) - 77.8$				
	Best fit, 95-th percentile echo strength ($ES_{95\%}$) Pooled selected beams	$ES_{95\%} = 22.9\log_{10}(L) - 76.2$	18	5.275	0.036	0.25
	(without outlier 15)	$ES_{95\%} = 28.5\log_{10}(L) - 86.3$	17	13.11	0.003	0.47
	(without outliers 4 and 15)	$ES_{95\%} = 31.5\log_{10}(L) - 91.7$	16	18.921	0.007	0.57
	Slope =20	$ES_{95\%} = 20\log_{10}(L) - 70.3$				
	Best fit, expected TS ($\langle TS \rangle$) Pooled selected beams	Not significant	18	3.976	0.064	0.20
	(without outlier 15)	$\langle TS \rangle = 12.9\log_{10}(L) - 52.3$	17	7.970	0.013	0.35
	(without outliers 4 and 15)	$\langle TS \rangle = 12.9\log_{10}(L) - 52.3$	16	16.500	0.001	0.54
	Slope =20	$\langle TS \rangle = 20\log_{10}(L) - 71.4$				

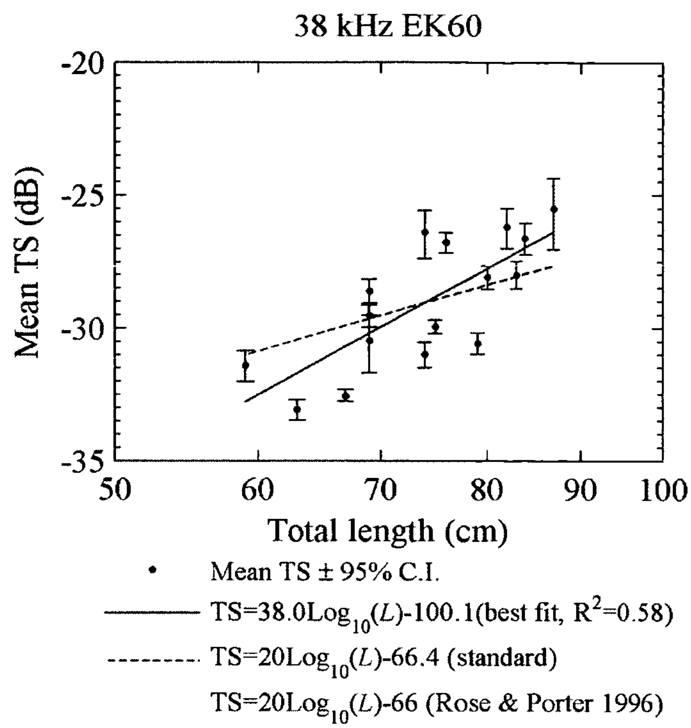

Figure 3-16. Relation between target strength (TS) and total length (*L*) of free-swimming caged Atlantic cod based on measurements from a 38-kHz split-beam echo sounder (Simrad EK60) and predicted by Rose and Porter (1996).

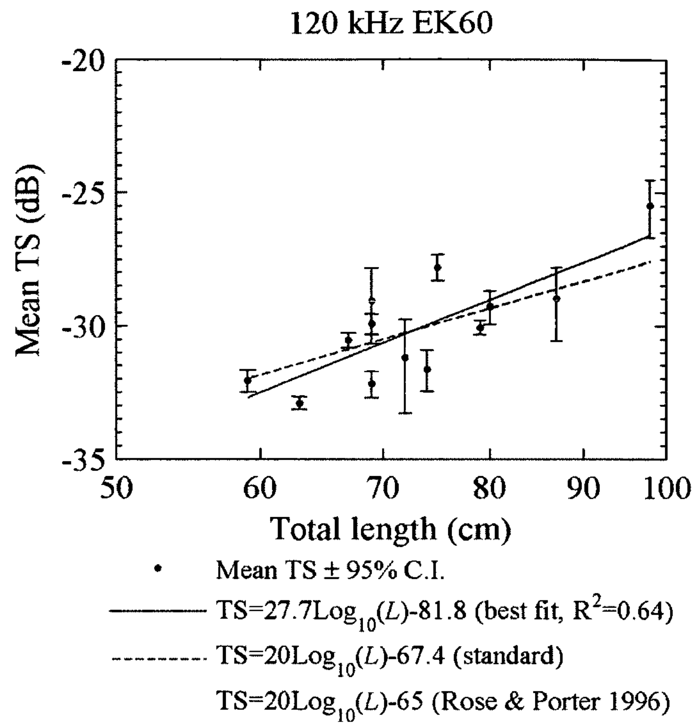

Figure 3-17. Relation between target strength (TS) and total length (L) of free-swimming caged Atlantic cod based on measurements from a 38-kHz split-beam echo sounder (Simrad EK60) and predicted by Rose and Porter (1996).

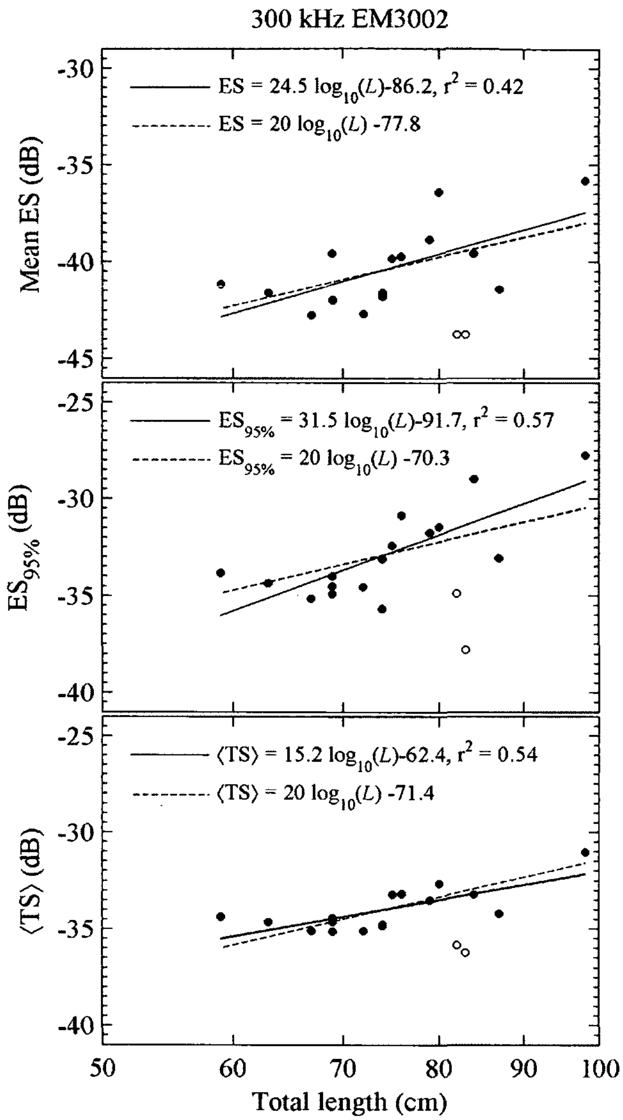

Figure 3-18. Linear relation between total length and three echo statistics of free-swimming captive Atlantic cod insonified by selected beams 66-97, ranging in beam pointing angles from -13.2° to 11.6°, of a 300-kHz multibeam echo sounder (Kongsberg Maritime EM3002): mean and 90th percentile echo strength (ES and $ES_{95\%}$) from ping-maximum single echo detections (top and center), and expected target strength (⟨TS⟩) after deconvolving the beam pattern probability density function (PDF) out of the PDF of all single echo detections (bottom).

Table 3-4. Results from an analysis of covariance (ANCOVA) for testing differences in the relation between estimated target strength (TS) and $\log_{10}$-transformed total length (L) for Atlantic cod among 38-kHz, and 120-kHz split-beam and 300-kHz multibeam echo sounders.

Source	Degrees of freedom	Sum of squares	Mean square	F	P
Model	5	340.37	68.07	37.45	<.0001
Error	41	74.53	1.82		
Corrected Total	46	414.90			
Source	**Degrees of freedom**	**Type III Sum of Squares**	**Mean square**	**F**	**P**
Echo sounder frequency	2	12.75	6.37	3.51	0.039
$\log_{10}(L)$	1	77.58	77.58	42.68	<.0001
Interaction (slope)	2	16.05	8.03	4.42	0.018

Table 3-5. Results from an analysis of covariance (ANCOVA) for testing differences in the relation between estimated target strength and $\log_{10}$-transformed total length for Atlantic cod among 38-kHz, and 120-kHz split-beam and 300-kHz multibeam echo sounders.

Parameter	Echo sounder comparison (frequency)	Difference estimate	Standard Error	t	P
Slope	38 vs. 120	10.3	9.9	1.04	0.306
	38 vs. 300	27.6	9.6	2.88	0.006
	120 vs. 300	17.3	9.1	1.91	0.063
b	38 vs. 120	-18.3	18.5	-0.99	0.330
(y-intercept)	38 vs. 300	-46.3	17.9	-2.58	0.013
	120 vs. 300	-28.0	17.0	-1.65	0.106

Table 3-6. Results from an analysis of variance (ANOVA) on the b_{20}-parameter in TS-L relation of TS = 20 $\log_{10}(L)$ + b_{20} for Atlantic cod among 38-kHz, and 120-kHz split-beam and 300-kHz multibeam echo sounders.

Source	Degrees of freedom	Sum of squares	Mean square	F	P
Model	4	1254.9	313.7	147.9	<.0001
Error	72	152.8	2.1		
Corrected Total	76	1407.7			

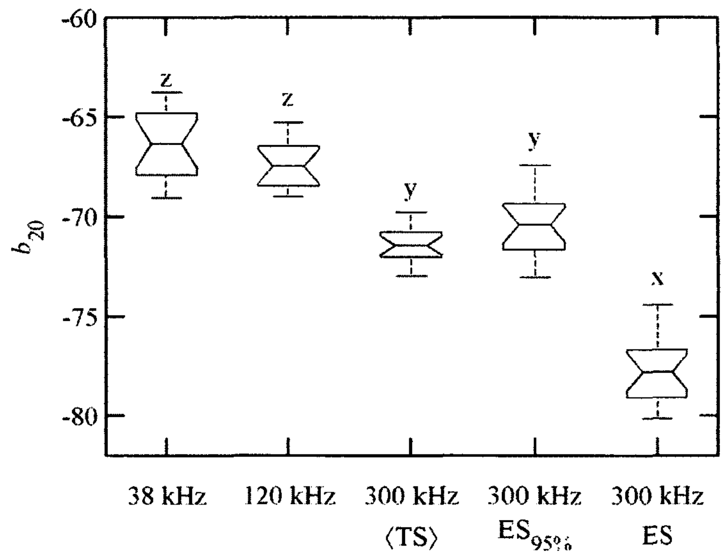

Figure 3-19 Box plot of the b_{20} estimates from linear regressions (= 20 $\log_{10}[L]$ + b_{20}) for the relating total length (L) to target strength (TS) of Atlantic cod at 38-kHz and 120-kHz (Simrad EK60 split-beam echo sounder); and expected TS (⟨TS⟩), 95th percentile of the echo strength distribution ($ES_{95\%}$), and echo strength (ES) at 300-kHz (Kongsberg Maritime EM3002 multibeam echo sounder). Unique lowercase letters (x, y, and z) indicate means were significantly different at 95% confidence level based on ANOVA and Tukey's honestly significant difference multiple pair-wise comparison tests. (Note: box plot notches that do not overlap indicate significant differences in medians).

Variability in Target Strength

Fish IDs 4 and 15, which were statistical outlying observations in the regression analysis, showed sporadic detections with some oscillations in TS or ES (Figures 3-20 and 3-21). Fish ID 4 had no detections in the 120-kHz beam while most of the detections of fish ID 15 were located on one side of the EM3002 beams. Periods of detections of fish ID 20 by the EM3002, which ranged in 10-15 dB ES, appeared to correlate with periods when the fish was observed in the video to be relatively calm and the gaps in the time series when fewer detections were made appeared to correlate well with periods when the fish was observed to be actively swimming around the cage or changing orientation (Figure 3-22). Fish ID 21, for example, did not remain still for long during the measurements, and perhaps can explain the multiple segments of increasing or decreasing trends with large local variation in TS as observed by the 38-kHz beam (Figure 3-23). Split-beam detections for fish ID 20 and 21 indicated the fish detections were distributed throughout the main lobes of many EM3002 beams. With exception of the start and end of the time series, fish ID 27 was active throughout the measurements and both the 38-kHz and 120-kHz beams detected segments of increasing or decreasing trend in TS, while the detections by the EM3002 were substantially less in number (Figure 3-24).

The distribution of TS or ES was compared between calm and active behaviors for those fish that exhibited both behavioral modes with sufficient number of SEDs. For two examples shown in Figure 3-25, the median TS was significantly higher during periods of activity than during periods of low activity and relatively horizontal orientation for fish ID 20 based on detections at 38 kHz only and for fish ID 21at 38 kHz and

120 kHz, but not the narrower 300-kHz beams. The median ES of fish ID 27 was significantly higher during periods of calm behavior than during periods of active behavior from measurements made by the 300-Hz multibeam echo sounder, but not different for the split-beam echo sounders.

Figure 3-26 shows the distribution of the 60-s range values for each cod, which describes the variation among measurements of individuals over time. Figure 3-27 shows variation in echo statistics of approximately 2-5 dB over observed angles, but for fish ID 20 there was a slight increasing trend in $ES_{95\%}$ with increasing beam angle but the opposite was true for fish ID 21. The signal-to-noise ratio metric used to describe γ ranged from 1.3 to 5.7 at 38 kHz, 2.2 to 7.6 at 120 kHz and 1.9 to 6.5 at 300 kHz (Figure 3-28). These values indicate variation in contribution of the swimbladder and body to the backscatter. For example, the signal-to-noise ratio for fish ID 27 at 38 kHz was 1.2 and was most represented by detections when the fish was exhibited extreme orientations and active swimming (Figures 3-24 and 2-28). At 120 kHz, the signal-to-noise ratio for the backscattering of fish ID 27 was 4.4 which was represented by data collected during that same period as the 38 kHz, but included more detections when the fish calm. At 300 kHz, the signal-to-noise ratio was 5.5 and was predominantly represented by data when fish ID 27 was relative calm.

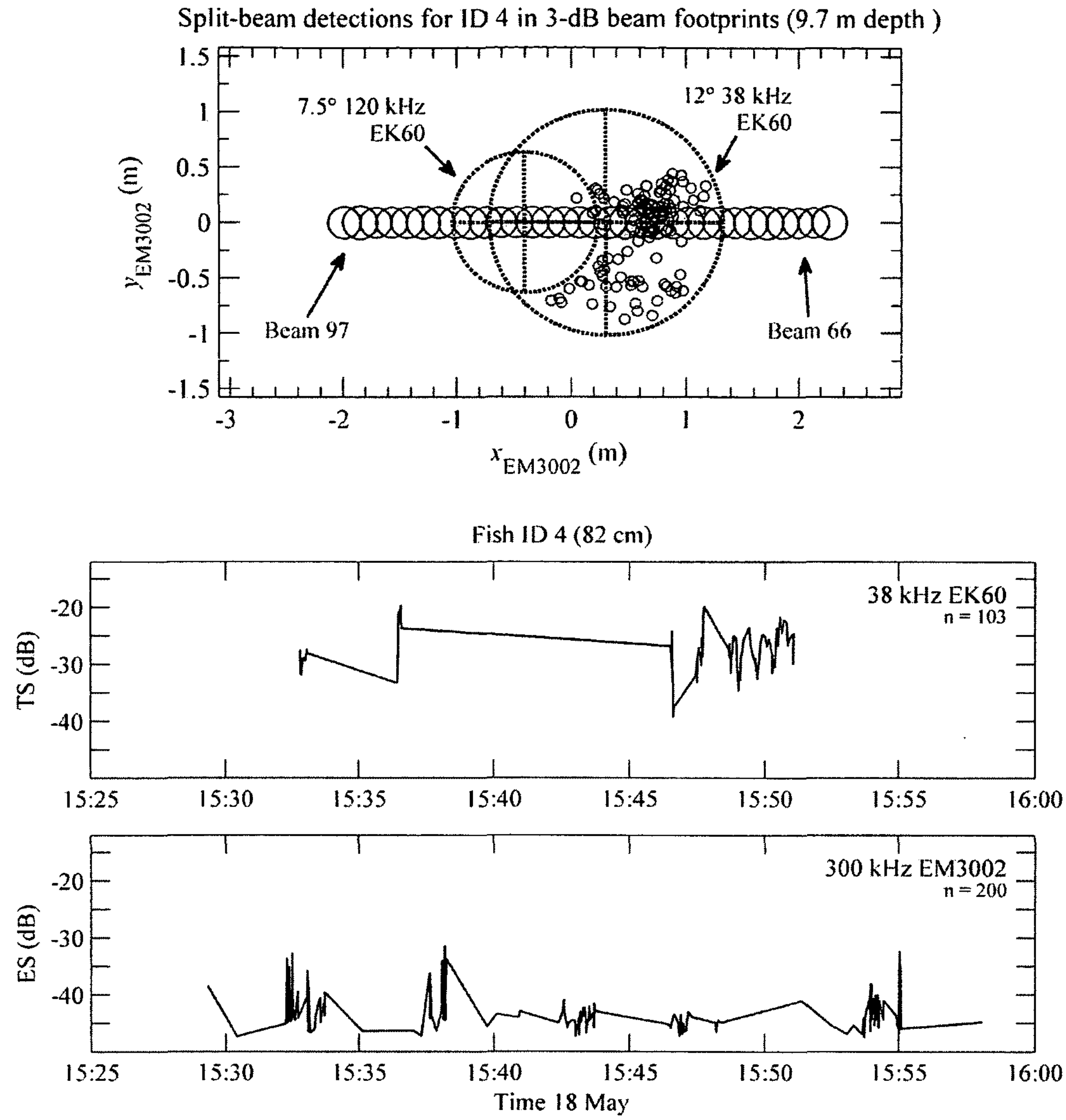

Figure 3-20. Top: split-beam detections of fish ID 4 mapped in the Cartesian coordinate system of selected beams (shaded) from the 300-kHz EM3002 beams multibeam echo sounder; bottom three: time series of acoustic backscatter measurements. Grey shaded bars represent segments when the fish showed relatively calm swimming behavior and near horizontal body orientation.

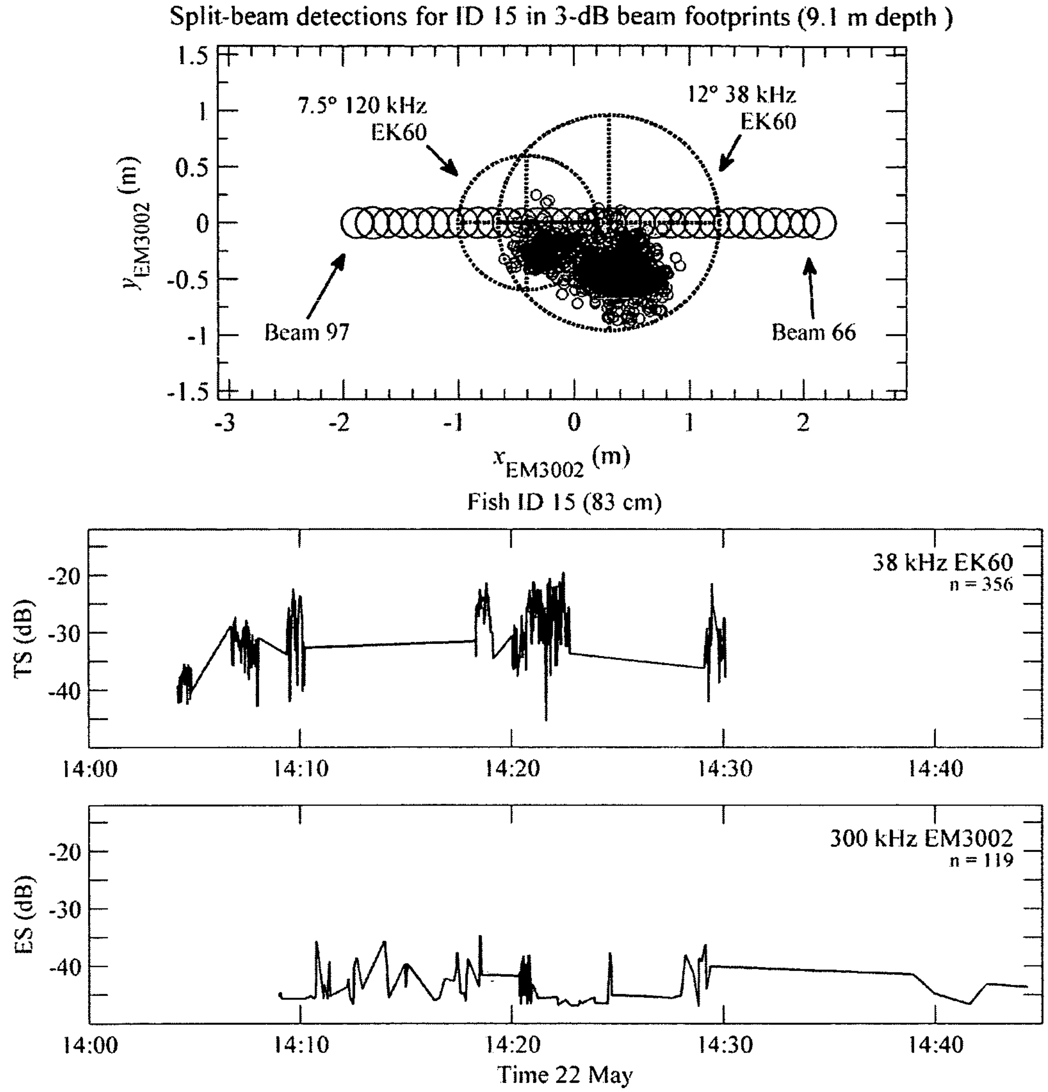

Figure 3-21. Top: split-beam detections of fish ID 15 mapped in the Cartesian coordinate system of selected beams (shaded) from the 300-kHz EM3002 beams multibeam echo sounder; bottom three: time series of acoustic backscatter measurements. Grey shaded bars represent segments when the fish showed relatively calm swimming behavior and near horizontal body orientation.

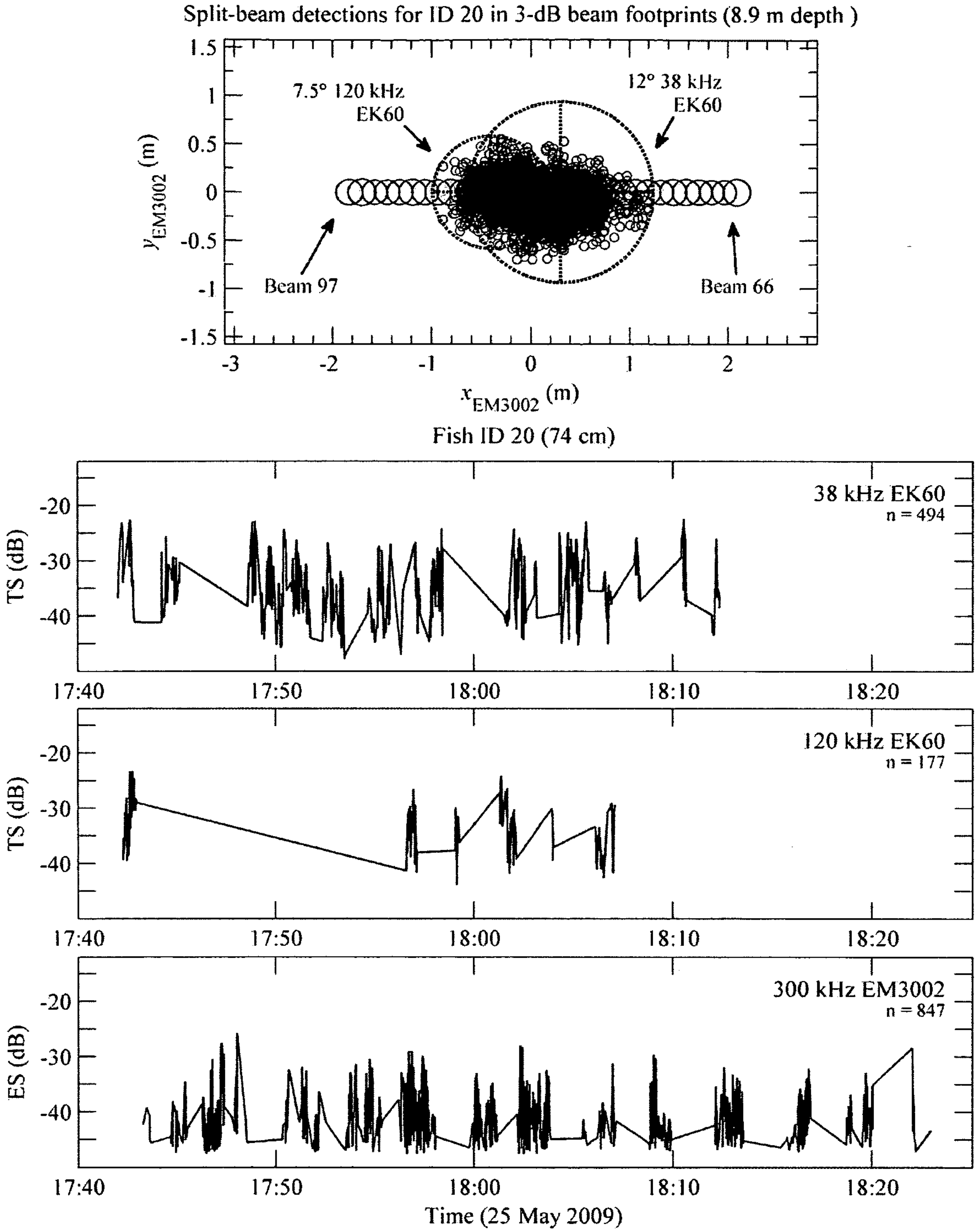

Figure 3-22. Top: split-beam detections of fish ID 20 mapped in the Cartesian coordinate system of selected beams (shaded) from the 300-kHz EM3002 beams multibeam echo sounder; bottom three: time series of acoustic backscatter measurements. Grey shaded bars represent segments when the fish showed relatively calm swimming behavior and near horizontal body orientation.

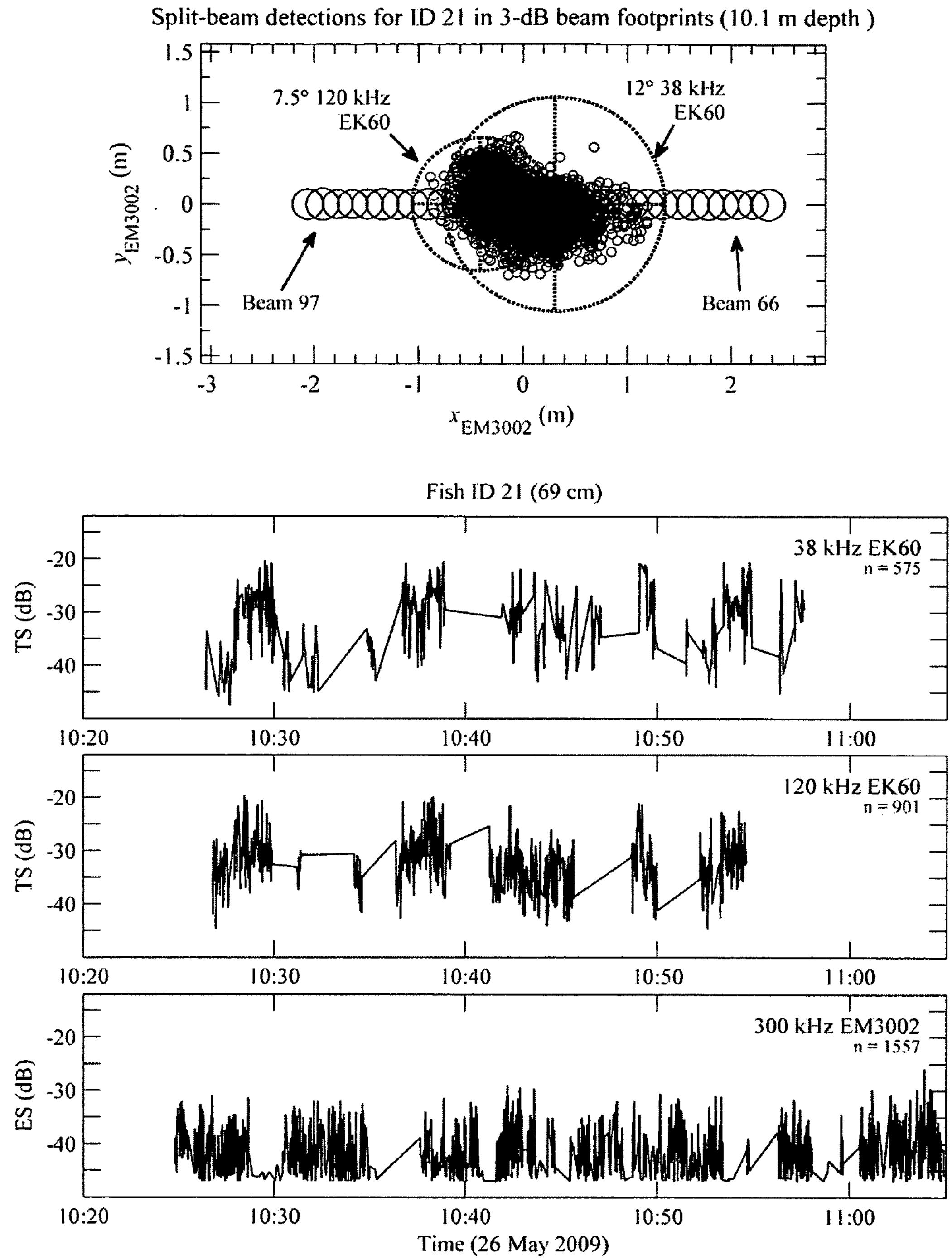

Figure 3-23. Top: split-beam detections of fish ID 21 mapped in the Cartesian coordinate system of selected beams (shaded) from the 300-kHz EM3002 beams multibeam echo sounder; bottom three: time series of acoustic backscatter measurements. Grey shaded bars represent segments when the fish showed relatively calm swimming behavior and near horizontal body orientation.

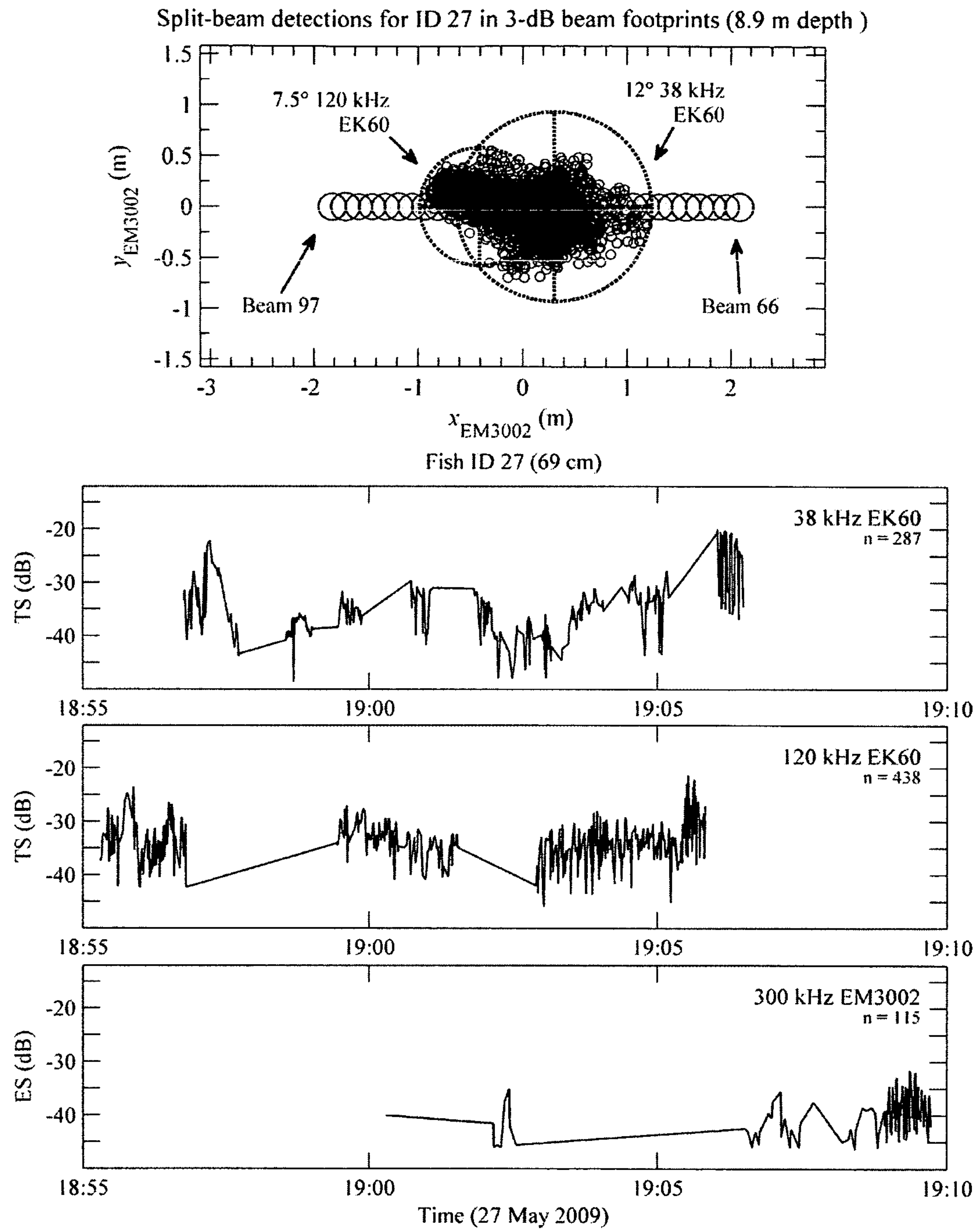

Figure 3-24. Top: split-beam detections of fish ID 4 mapped in the Cartesian coordinate system of selected beams (shaded) from the 300-kHz EM3002 beams multibeam echo sounder; bottom: Time series of acoustic backscatter measurements. Grey shaded bars represent segments when the fish showed relatively calm swimming behavior and near horizontal body orientation.

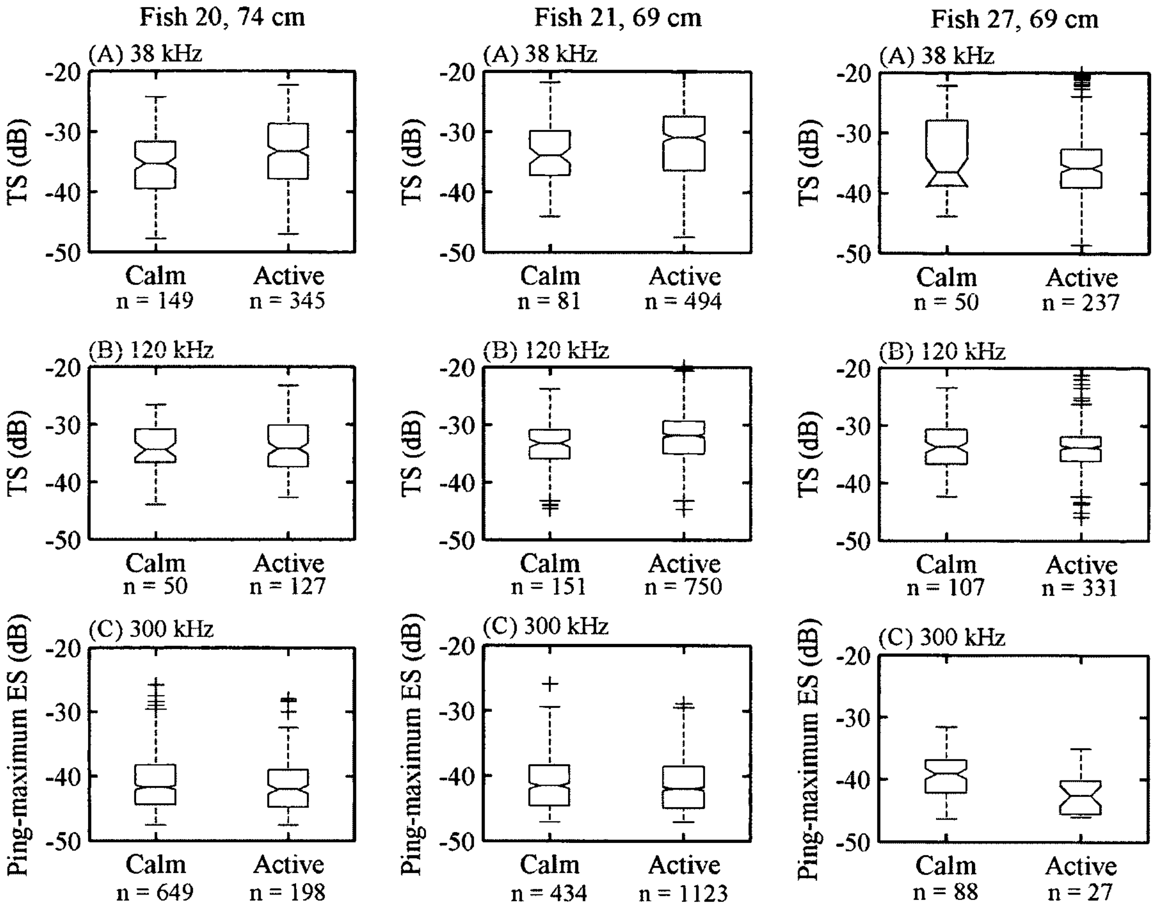

Figure 3-25. Box plot comparing echo statistics between segments of the time series that three fish displayed either calm or active behavior inside the cage. Notches that don't overlap indicate the medians are significantly different at 95% confidence level.

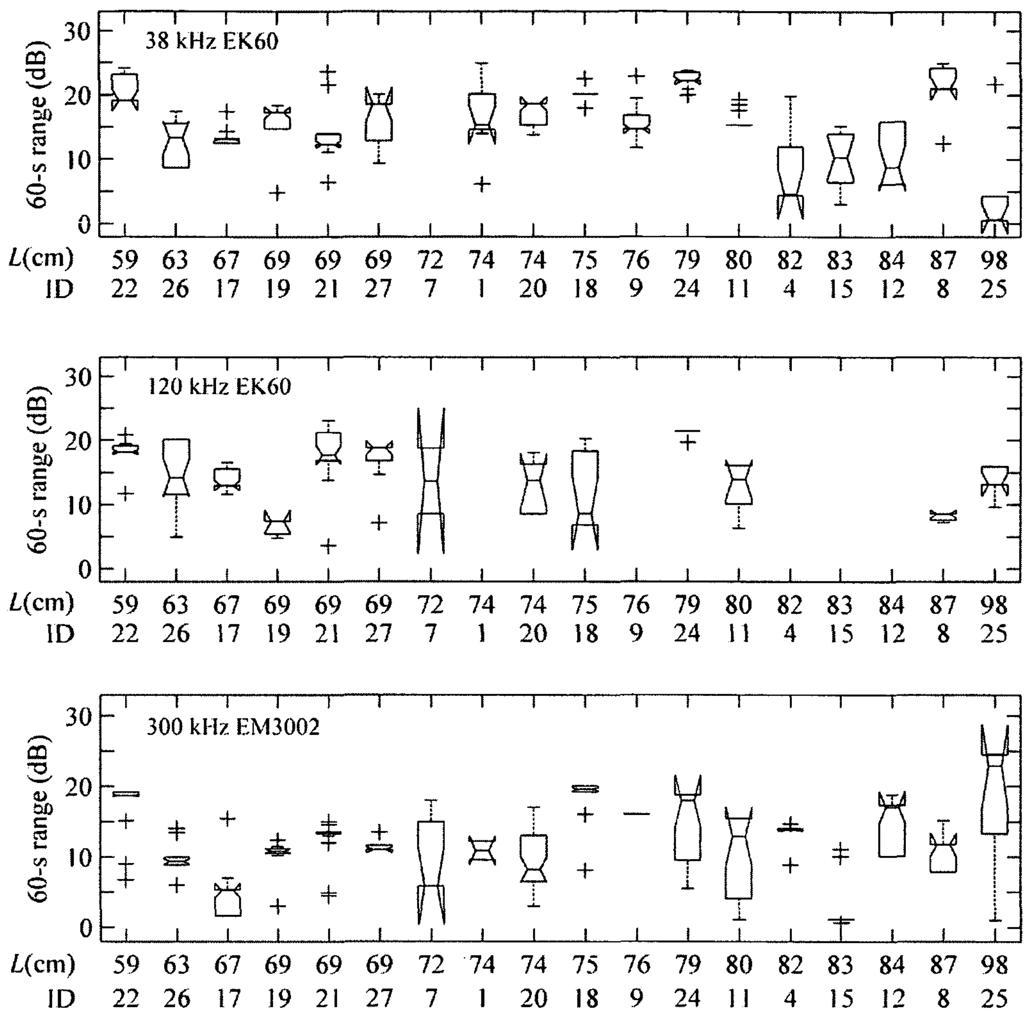

Figure 3-26. Box plot comparing the 60-second range in target or echo strength for each individual Atlantic cod. Notches that don't overlap indicate the medians are significantly different at 95% confidence level.

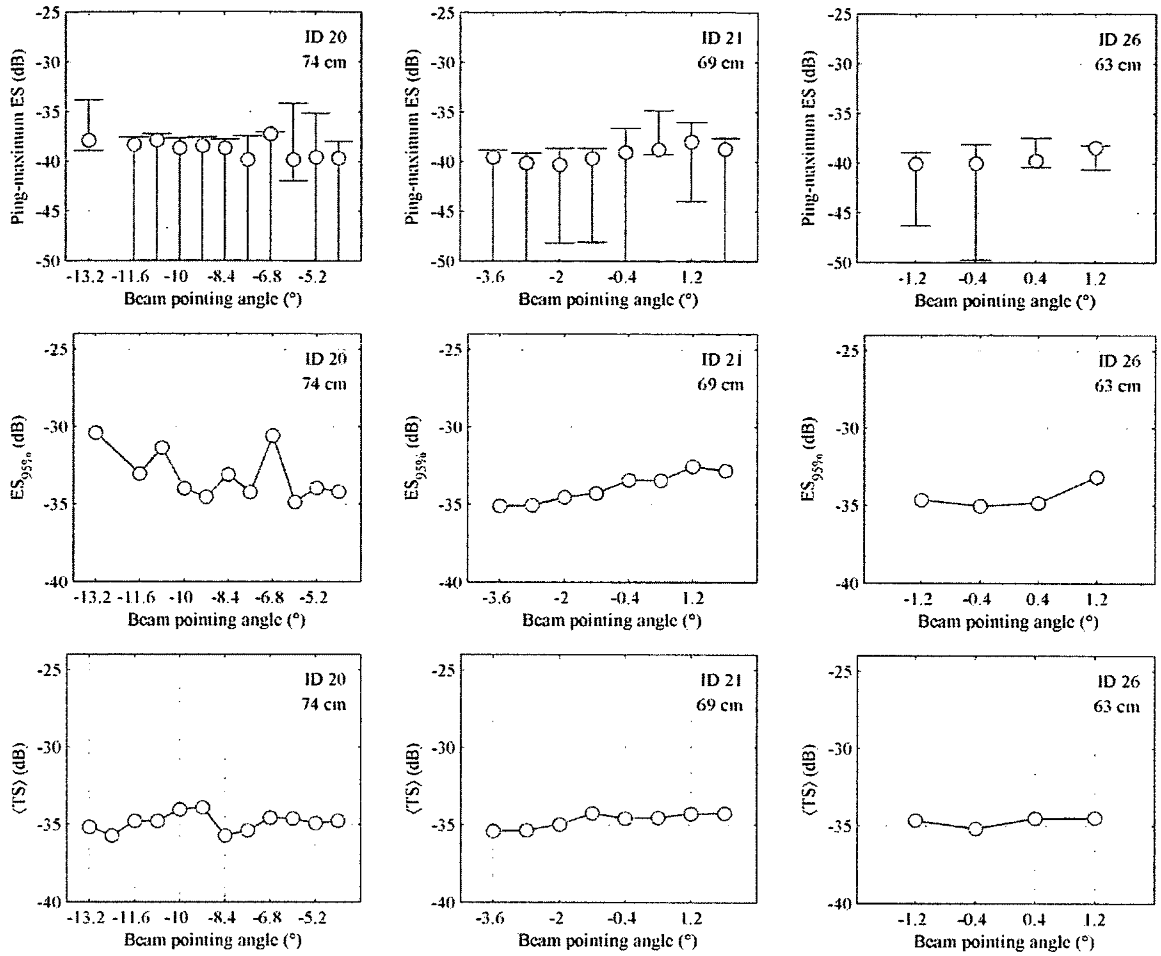

Figure 3-27. Echo strength (ES) of ping-maximum single echo detections, 95th percentile of the ES distribution, and expected target strength (⟨TS⟩) of three individual cod as a function of beam pointing angle of the 300-kHz EM3002 multibeam echo sounder.

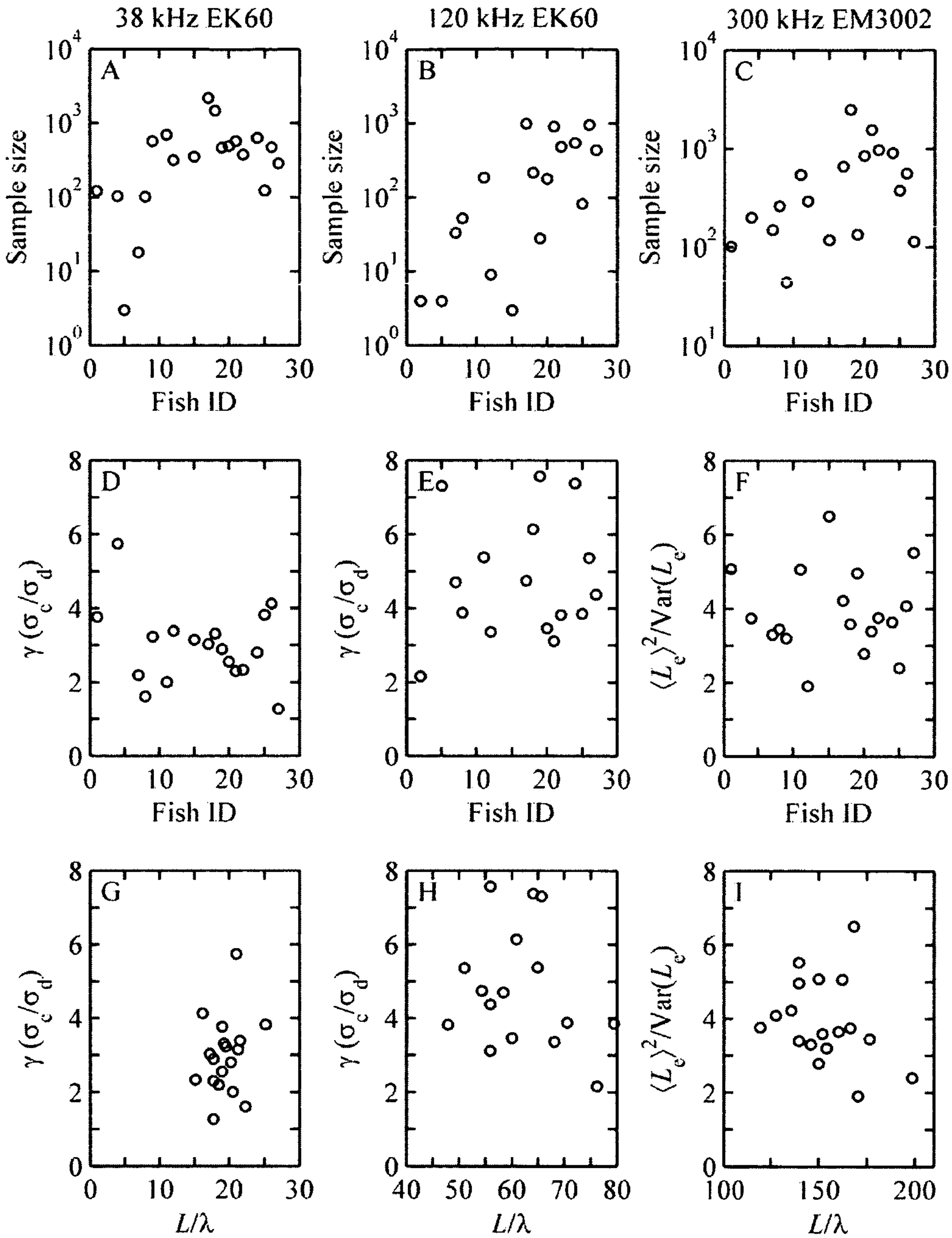

Figure 3-28. Sample size and the signal-to-noise metric proportional to the Rician γ parameter defined as the concentrated scattering component over the distributed (random) scattering component of the backscattering cross-section as described by Clay and Heist (1984) for each fish ID and total length normalized by the acoustic wavelength (λ) for the 38 kHz and 120 kHz split-beam echo sounder and 300 kHz multibeam echo sounder.

Discussion

A simple approximation technique extending from single-beam echo sounder applications enabled TS of Atlantic cod to be estimated from a high-frequency multibeam echo sounder typically used for bathymetry, and a relation between length and TS was established. Results for the split-beam echo sounder measurements support the assumption of $20\log_{10}$ dependence and the use of TS-L equations previously described for Canadian Atlantic cod at 38 kHz, but not necessarily at 120 kHz (Rose and Porter 1996). The b_{20} parameter estimate of -67.4 determined in this study for 120 kHz was significantly lower than -65 (Rose and Porter 1996), but was not significantly different from the 38 kHz estimate of -66.4. However, the *in situ* TS of paired detections during the nighttime surveys described in Chapter 2 was approximately 1 dB higher at 38 kHz than at 120 kHz. The b_{20} estimates from this study indicated TS at 300 kHz was approximately 5 or 4 dB lower than the TS at 38 and 120 kHz, respectively, which was similar to the difference in TS of adult cod between 38 kHz and 200 kHz observed by Pedersen and Korneliussen (2009). Based on Love's (1977) equation, the TS for a 75 cm cod would be about 1 dB lower at 300 kHz compared to the predicted TS at 38 kHz. The results at 300 kHz can be informative for acoustic estimation of fish abundance using a 300 kHz multibeam echo sounder or aid in multi-frequency echo classification.

Results provide insight in several factors potentially influencing TS and accounting for the observed variability among fish and within a fish's time series. For example, the $\langle TS \rangle$ for fish ID 4 and 15 at 300 kHz was about 3-4 dB less than predicted by the regression model, but could be partially explained by a combination of factors that include low sample size, false assumption of a uniformly random distribution of fish within the beam, effect of multiple incidence angles, and partial insonification of the swimbladder. The split-beam detections for ID 15 for example were clearly biased in location within the 38 kHz and 120 kHz beam, and if these were representative of all detections by the 300 kHz beams then a reduced TS could be a result from not fully compensating the off-axis echoes for the sensitivity loss from the beam pattern. Changes in incidence angle of sound may result from changes in body movement, changes in transducer attitude, beam pointing angle in the case of the EM3002 beams, or combination of these factors.

Changes in incidence angle can cause TS to vary 10-20 dB (Love 1977; Foote 1980b; McQuinn and Winger 2003). Scattering by a multibeam echo sounder can be greatly affected by different beam pointing angles and body orientation, particularly by yaw (Cutter and Demer 2007). While incidence angles could have contributed to the observed variability or range in values for a fish and potentially reduce their ⟨TS⟩, that effect might be constant over the angles included if the behavior and body orientations were random (Cutter and Demer 2007). This might be the case here for some fish detected by the EM3002 over multiple beam pointing angles, which did not show a strong evidence of an angular trend in echo statistics. The TS estimates for fish ID 21 showed a slight 1-2 dB increase from beam angles -3.6° to 1.2° and also were significantly higher in the median value during periods of active swimming or tilted orientations compared to the periods of relatively calm behavior at 38 kHz and 120 kHz but not at 300 kHz. This might be explained if the individual closer to its maximum TS response when it was swimming or tilted compared to when it was calm. Nakken and Olsen (1977) observed maximum dorsal-aspect TS for cod was achieved when the head was tilted down approximately 5° from horizontal and the swimbladder axis has been reported to be tilted up by 5-17° based on x-ray images (Clay and Horne 1994). So, if the fish was calm and perfectly horizontal one would expect to have a stronger echo at -3.6° beam angle compared to near nadir but the opposite was observed for fish ID 21.

Another explanation in the observed variability is the contribution of scattering of the swimbladder and body to the TS measurements. The swimbladder can account for 90% of the echo energy at 38 and 120 kHz and may represent a 10-15 dB difference in TS for a fish of equal size (Foote 1980a). Clay and Heist (1993) modeled scattering of fish with signal-to-noise ratio fitting parameter, γ, which tends to zero when fish become active and the random or distributed (incoherent) scattering component of the body contributes more to the backscattering cross-section than the concentrated (coherent) scattering component from scattering off the swim bladder. The metric used in this study as measure of this ratio varied from approximately 2 to 8 indicating fish of similar L/λ differed in the scattering contributions of the swimbladder and body. The swimbladder volume of an Atlantic cod is approximately 5% of its body volume (Harden Jones and Scholes 1985), and its length is about 22% and 25% of its total and standard length, respectively (Clay and Horne 1994). This corresponds to a mean swimbladder length of 17 cm (range = 13 – 22 cm) in this study. Based on mean sampling depths, the mean diameter of the beam footprint (based on 3-dB beam widths) was 161 cm at 38 kHz, 99 cm at 120 kHz, and 20 cm at 300 kHz. The mean ratio between swimbladder length and beam diameter of these measurements by the 300 kHz multibeam echo sounder was 0.9 or 90%. With these relative sizes, it is easily conceivable that the swimbladder was at times partially or completely out of the portion of the main lobe of greatest sensitivity as defined by the 3-dB beam width, and perhaps contributed to the variability, particularly for the multibeam echo sounder. This highlights consideration of the relative size of the swimbladder to the beam width, particularly for researchers using narrow sideward-looking beams to monitor large fish, such as salmonids, in shallow water river systems.

In conclusion, this study determined a TS-*L* relation of mature Atlantic cod from the Gulf of Maine at two commonly used split-beam frequencies, which agreed with the TS-*L* relation of cod at 38 kHz described for Canadian stocks, but was lower TS response at 120 kHz compared to the TS-*L* relation described by Rose and Porter (1996). Secondly, the study demonstrated a significant TS-*L* relation at 300 kHz from beam-aggregated data collected by a multibeam echo sounder with narrow beams over multiple beam-incidence angles and without split-beam target tracking.

Acknowledgements

These measurements would not have been possible without the field assistance of P. Geoghegan, M. Mattson, and the entire crew of the UNH Open Ocean Aquaculture team. Live fish were successfully caught and transported in good condition thanks to the experience and skills of Captain C. Bouchard and his crew on the F/V *"Stormy Weather"*. Special acknowledgement goes to Mashkook Malik who shares ownership of the multibeam calibration data collected in the freshwater tank facility and who provided insightful technical recommendations along the way. This study was funded by New Hampshire Sea Grant.

CONCLUSIONS

Experimental results from Chapter I demonstrate that Atlantic cod can be remotely sensed in the water column by a multibeam echo sounder designed for hydrography. In addition, the multibeam echo sounder was able to detect relative changes in abundance of caged cod and was also less susceptible to bias related to spatial distribution compared to the split-beam echo sounder. The application of a multibeam echo sounder to survey cod in the wild is promising because the repeated acoustic and trawl surveys performed in Chapter II showed cod congregated during spawning and were detected 30 m or more off the bottom during the night when spawning is known to occur.

However, the time series of measurements collected on free-swimming cod held individually inside a monofilament cage demonstrated target strength could vary 10-20 dB for the same fish. Factors such as beam incidence angle, swimming activity, body orientation (pitch, roll, and yaw), size, acoustic frequency, beam width and the performance of indirect target strength methods removing the effects of beam pattern directivity individually and collectively contribute to the determination of the magnitude and variation in acoustic backscatter collected by a multibeam echo sounder. Some of these problems can be resolved by the split-beam, multi-frequency, and user-defined modes suitable for fisheries research featured in the Simrad ME70 multibeam echosounder (Trenkel et al. 2008).

Despite the complexities, a significant relation between target strength and length was established and detection of changes in abundance was possible for the EM3002 multibeam echo sounder. The estimated target strength at 300 kHz was approximately 4-5 dB lower than the 38 and 120 kHz. The weaknesses or difficulties that remain can be mitigated by complementing a survey with a co-located split-beam echo sounder for mapping targets within the beams and providing more precise quantitative acoustic estimates of fish size and density. The advantage of including a multibeam echo sounder to a split-beam echo sounder survey should not be overlooked as results here support the value of the additional spatial information.

The results from the repeated acoustic and trawl surveys within the Gulf of Maine Cod Spawning Protection Area (GOMCSPA) were timely and informative to fishery managers. This study located congregations of Atlantic cod in spawning condition associated with elevated bathymetric features within GOMCSPA on 28-29 May, 18-19 June, and 3-4 July, but observed no cod during the 7-8 April survey. Furthermore, the continued presence of a congregation of cod in July warrants consideration of extending the time frame of the seasonal fishing area closure. Geostatistics revealed cod were spatially organized typically at a scale of 2 km. Maps produced by ordinary kriging illustrated cod during the May survey were present throughout most of the study area but were concentrated near elevated bathymetric features before converging during the June survey to a single dense congregation adjacent to one of the bathymetric features.

This study highlighted the effect of estimation and sampling technique on the survey estimates and variability of cod abundance and biomass. In this study, which surveyed cod at night, echo classification and *in situ* TS was considered to provide the most representative results with the lowest variability. Based on these results, the biomass of spring-spawning Atlantic cod in the GOMCSPA observed in 2011 represented at least 4-5% of the 2010 SSB estimate of the GOM cod stock.

This study hopefully motivates future integrated acoustic-trawl surveys of Atlantic cod in the GOMCSPA and other areas of the western Gulf of Maine, and provides the evidence for fishery managers to consider the use and configuration of seasonal area closures of important spawning grounds to promote the rebuilding of this overfished stock. Acoustic surveys that also use multibeam echo sounders could provide additional information on distribution within the water column, shoal morphology, relative abundance, sea floor type, and bathymetry of many potential coastal spawning grounds where Atlantic cod congregate, making them easier to survey.

Given the current status of the GOM cod stock and their economic importance, this research should pave the way for funding opportunities in experimental and applied research. Advancements in acoustic survey methods for estimating cod stock abundance should focus on (1) developing remote sampling methods (e.g., dual-frequency identification sonar [DIDSON] or underwater video) to verify species and size of cod where habitat is unsuitable for trawling or when disrupting their spawning behavior needs to be minimized (Dean et al. 2012); (2) testing the feasibility of a mobile survey using a multibeam echo sounder and a co-located split-beam echo sounder; and (3) mining the ME70 multibeam and EK60 split-beam echo sounder data collected during NEFSC bottom-trawl surveys that haven't been analyzed. Current information from this research could be used to develop and conduct acoustic assessment surveys of cod stocks on known current and historical spawning grounds (Ames 2004; Armstrong et al. 2012). In the short term, the provision of funding to repeat a split-beam echo sounder survey of the GOMCSPA with expansion of the survey to include surrounding areas and the Massachusetts Bay Spring Cod Conservation Zone would expand our current understanding of the GOM cod stock and provide new information in validating recent stock assessment estimates.

APPENDIX A

INSTITUTIONAL ANIMAL CARE AND USE COMMITTEE (IACUC)

DOCUMENTATION

University *of* New Hampshire

Research Conduct and Compliance Services, Office of Sponsored Research
Service Building, 51 College Road, Durham, NH 03824-3585
Fax: 603-862-3564

02-May-2008

Howell, William
Zoology, Spaulding Life Science Center
Durham, NH 03824

IACUC #: 080405
Project: Development of multi-beam sonar as a fisheries tool for stock assessment and the identification of essential habitat of Atlantic cod
Category: B
Approval Date: 25-Apr-2008

The Institutional Animal Care and Use Committee (IACUC) reviewed and approved the protocol submitted for this study under Category B on Page 5 of the Application for Review of Vertebrate Animal Use in Research or Instruction - *the study involves either no pain or potentially involves momentary, slight pain, discomfort or stress.*

Approval is granted for a period of three years from the approval date above. Continued approval throughout the three year period is contingent upon completion of annual reports on the use of animals. At the end of the three year approval period you may submit a new application and request for extension to continue this project. Requests for extension must be filed prior to the expiration of the original approval.

Please Note:
1. All cage, pen, or other animal identification records must include your IACUC # listed above.
2. Use of animals in research and instruction is approved contingent upon participation in the UNH Occupational Health Program for persons handling animals. Participation is mandatory for all principal investigators and their affiliated personnel, employees of the University and students alike. A Medical History Questionnaire accompanies this approval; please copy and distribute to all listed project staff who have not completed this form already. Completed questionnaires should be sent to Dr. Gladi Porsche, UNH Health Services.

If you have any questions, please contact either Roger Wells at 862-2726 or Julie Simpson at 862-2003.

For the IACUC,
Jessica Bolker
Jessica A. Bolker, Ph.D.
Chair

cc: File

Figure A-1. Image of the IACUC letter for research conducted for Chapters I and III.

University *of* New Hampshire

Research Integrity Services, Office of Sponsored Research
Service Building, 51 College Road, Durham, NH 03824-3585
Fax: 603-862-3564

26-Jul-2010

Howell, William H
Biological Sciences, Rudman Hall
Durham, NH 03824

IACUC #: 100606
Project: Synoptic Acoustic and Trawl Surveys to Characterize Biomass and Distribution of the Spring Spawning Aggregations of Atlantic Cod in Ipswich Bay
Category: D
Approval Date: 14-Jul-2010

The Institutional Animal Care and Use Committee (IACUC) reviewed and approved the protocol submitted for this study under Category D on Page 5 of the Application for Review of Vertebrate Animal Use in Research or Instruction - *Animal use activities that involve accompanying pain or distress to the animals for which appropriate anesthetic, analgesic, tranquilizing drugs or other methods for relieving pain or distress are used.*

Approval is granted for a period of three years from the approval date above. Continued approval throughout the three year period is contingent upon completion of annual reports on the use of animals. At the end of the three year approval period you may submit a new application and request for extension to continue this project. Requests for extension must be filed prior to the expiration of the original approval.

Please Note:

1. All cage, pen, or other animal identification records must include your IACUC # listed above.
2. Use of animals in research and instruction is approved contingent upon participation in the UNH Occupational Health Program for persons handling animals. Participation is mandatory for all principal investigators and their affiliated personnel, employees of the University and students alike. A Medical History Questionnaire accompanies this approval; please copy and distribute to all listed project staff who have not completed this form already. Completed questionnaires should be sent to Dr. Gladi Porsche, UNH Health Services.

If you have any questions, please contact either Dean Elder at 862-4629 or Julie Simpson at 862-2003.

For the IACUC,

Jessica Bolker

Jessica A. Bolker, Ph.D.
Chair

cc: File

Figure A-2. Image of the IUCAC letter for research conducted for Chapter II.

APPENDIX B

TARGET STRENGTH ESTIMATION OF A STANDARD SPHERE

Calibration of echo sounder systems is important in providing system-independent measures of acoustic backscatter to estimate abundance or describe behavior of fish populations. Solid metal spheres have been used as standard targets for calibrating target strength (TS) measurements (Foote 1983b; Foote et al. 1987). The target strength of copper (Cu) and tungsten carbide (WC) spheres at frequencies (e.g, 38 and 120 kHz) commonly used for fishery acoustic surveys in fisheries acoustic research have been published (Foote 1990; Foote and MacLennan 1984; Simmonds and MacLennan 2005). However, the target strength of Cu and WC spheres at high frequencies of shallow-water multibeam echo sounders (e.g., 300-kHz EM3002) are not widely available as a reference. The reference target strength of a 38.1-mm WC and 60-mm Cu sphere at 300 kHz was estimated by computational methods described by MacLennan (1981). The equations given by MacLennan (1981) were corrected for errors that appeared in the original versions by Faran (1951) and Hickling (1962).

The TS computations for a sphere of known material density (ρ_1) were made in Matlab software following these stepwise equations for a continuous incident acoustic wave at a carrier frequency f (in Hz) at a sound speed, c (in m/s), and with an acoustic wavelength λ ($=c/f$):

$$q = ka \qquad (1),$$

where k is the acoustic wave number ($=2\pi/\lambda$) and a is the radius of the metal sphere,

$$q_1 = qc/c_1 \qquad (2),$$

where c_1 is the longitudinal sound speed of the sphere intrinsic to the metal composition,

$$q_2 = qc/c_2 \qquad (3),$$

where c_2 is the transverse sound speed of the sphere intrinsic to the metal composition,

$$A_2 = (n^2 + n - 2)j_n(q_2) + q_n^2 j_n''(q_2) \qquad (4),$$

for the nth scattered partial wave and the $j_n(x)$ is the spherical Bessel function of the first kind which is equivalent to $J_{n+0.5}(x)\sqrt{\pi/2x}$ where $J_n(x)$ is the Bessel function of the first kind (note that the prime symbol denotes differentiation of the function with respect to the argument),

$$A_1 = 2n(n+1)[q_1 j_n'(q_1) - j_n(q_1)] \qquad (5),$$

$$\alpha = 2(\rho_1/\rho)(c_2/c)^2 \qquad (6),$$

$$\beta = (\rho_1/\rho)(c_1/c)^2 - \alpha \qquad (7),$$

$$B_2 = A_2 q_n^2 [\beta j_n(q_1) - \alpha j_n''(q_1)] - A_1 \alpha [j_n(q_2) - q_2 j_n'(q_1)] \qquad (8),$$

$$B_1 = q[A_2 q_1 j_n'(q_1) - A_1 j_n''(q_2)] \qquad (9),$$

and $$\eta_n = \tan^{-1}\left\{-\frac{[B_2 j_n'(q) - B_1 j_n(q)]}{[B_2 y_n'(q) - B_1 y_n(q)]}\right\} \qquad (10),$$

where $y_n(x)$ is the spherical Bessel function of the second kind which is equivalent to $Y_{n+0.5}(x)\sqrt{\pi/2x}$ where $Y_n(x)$ is the Bessel function of the second kind.

In the far field, $kr \gg 1$, the form function, $F_\infty(q)$, is:

$$F_\infty(q) = -(2/q)\sum_{n=0}^{\infty} -1^n(2n-1)\sin\eta_n \exp(i\eta_n) \qquad (11),$$

where i is the imaginary number ($i^2 = -1$). The acoustic scattering cross-section, σ, is then defined as 4π times the backscattered intensity in the far field, when normalized to r = 1 m, divided by the incident wave intensity. For the sphere this becomes

$$\sigma = \pi a^2 |F_\infty(q)|^2 \quad (12),$$

and the target strength (TS) in dB is defined as:

$$\mathrm{TS} = 10\log_{10}(\sigma/4\pi) \quad (13).$$

The accuracy of the Matlab algorithm for estimating the form function and TS was verified by comparing these functions to MacLennan (1981) and MacLennan and Dunn (1984), based on the same physical parameters (Figures B-1 and B-2). The TS estimates for the 38.1-mm WC sphere were similar to those in the literature (Figure B-3). In fact, the TS estimate at 38 kHz matched identically to the reference TS (-42.4 dB) at 38 kHz given by Simmonds and MacLennan (2005), under the assumption of a continuous wave (Figure B-4). The TS estimate for 38.1-mm WC sphere at 300 kHz, which is the center frequency of the EM3002 multibeam echo sounder, was ironically -38.1 dB, which also matches an estimate given by Foote (pers. comm.; Figure B-5).

However, a more realistic estimate of the TS of a reference target should be based on transmission of a pulse from an echo sounder, which here is assumed to be an ideal receiver and transmitter where response function inside the bandwidth of the pulse is constant (=1) and zero outside. The σ for a pulse, with a center frequency of f_0, bandwidth (BW), and pulse duration (τ), was estimated as sum of scattered components of the incident pulse spectrum:

$$\sigma = \pi a^2 \left[\sum_{q_{f_0-BW/2}}^{q_{f_0+BW/2}} |F_\infty(q) g(q)|^2 \,\mathrm{d}q\right] \Big/ \left[\sum_{q_{f_0-BW/2}}^{q_{f_0+BW/2}} |g(q)|^2 \,\mathrm{d}q\right] \quad (14),$$

where $g(q)$ is defined as

$$g(q) = \sin[(q - q_{f_0})\tau/2]/\pi(q - q_{f_0}) \quad (15).$$

Based on parameters in Table 3.2 of Simmonds and MacLennan (2005), the TS of a 38.1-mm WC sphere at 38 kHz estimated by the Matlab algorithm was -42.27 dB, which was in agreement with the reported reference TS of -42.3 dB. Therefore, based on the EM3002 frequency and bandwidth, and experimental conditions in the freshwater tank facility and in the sea, the reference TS to be used for calibration is reported in Table B-1.

The 60-mm Cu sphere produced a stronger echo, but its TS varied greatly on sound speed and salinity at 300 kHz. The TS for the 60-mm sphere at 38 kHz, assuming a continuous acoustic wave, was estimated to be -33.5 dB, which was similar to the published reference TS (Figure B-6). However, the TS estimate for the 60-mm Cu sphere was -33.6 dB based on a pulse with center frequency of 38 kHz and 3 kHz bandwidth. The TS estimate at 300 kHz under the same continuous wave assumptions was estimated to be -34.8 dB (Figure B-7), but was estimated for a pulse to be -31.4 dB under experimental sea conditions and -31.3 dB under freshwater conditions (Table B-2).

Table B-1. Theoretical calculations of reference target strength of 38.1-mm tungsten sphere at 300 kHz and 8 kHz bandwidth under two calibration conditions.

Parameter	Symbol (units)	Calibration Environment: Anchored at sea	Calibration Environment: Freshwater tank facility	Source
Longitudinal sound speed	c_1(m/s)	6853	6853	MacLennan and Dunn (1984); Simmonds and MacLennan (2005)
Transversal sound speed	c_2(m/s)	4171	4171	MacLennan and Dunn (1984); Simmonds and MacLennan (2005)
Sound speed of water	c (m/s)	1074	1481	Measured
Target material density	ρ_1(kg/m^3)	14900	14900	MacLennan and Dunn (1984); Simmonds and MacLennan (2005)
Water (medium) density	ρ(kg/m^3)	1032	1000	Measured
Pulse duration	τ (ms)	0.200	0.200	
Frequency (center)	f(kHz)	300	300	
Nominal receive bandwidth	BWrx (kHz)	8	8	
Target strength estimate	TS (dB re 1 m^2)	-38.13	-38.13	
Reference target strength	TS_{ref} (dB re 1 m^2)	-38.1	-38.1	

Table B-2. Theoretical calculations of reference target strength of 60-mm copper at 300 kHz and 8 kHz bandwidth under two calibration conditions.

Parameter	Symbol (units)	Calibration Environment: Anchored at sea	Calibration Environment: Freshwater tank facility	Source
Longitudinal sound speed	c_1(m/s)	4760	4760	MacLennan and Dunn (1984); Simmonds and MacLennan (2005)
Transversal sound speed	c_2(m/s)	2288	2288	MacLennan and Dunn (1984); Simmonds and MacLennan (2005)
Sound speed of water	c (m/s)	1074	1481	Measured
Target material density	ρ_1(kg/m^3)	8945	8945	MacLennan and Dunn (1984); Simmonds and MacLennan (2005)
Water (medium) density	ρ(kg/m^3)	1032	1000	Measured
Pulse duration	τ (ms)	0.200	0.200	
Frequency (center)	f (kHz)	300	300	
Nominal receive bandwidth	BWrx (kHz)	8	8	
Target strength estimate*	TS (dB re 1 m^2)	-31.40	-31.25	

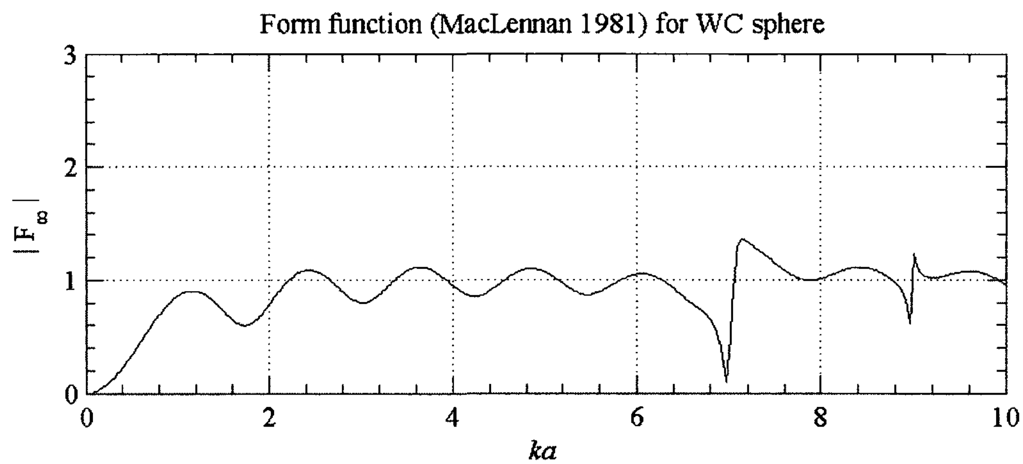

Figure B-1. Matlab algorithm* duplicating Figure 3 of MacLennan (1981) that describes the form function (F_∞) as a function of *ka* where *k* is the acoustic wave number and *a* is the radius of a tungsten carbide (WC) sphere, assuming a continuous acoustic wave, longitudinal and transverse sound speed for WC =6,655 and 3,984 m/s, respectively, density of WC =14,860 kg/m^3, water sound speed of 1490 m/s, and water density of 1030 kg/m^3. * TheoTS_MacLennan1981WC.m

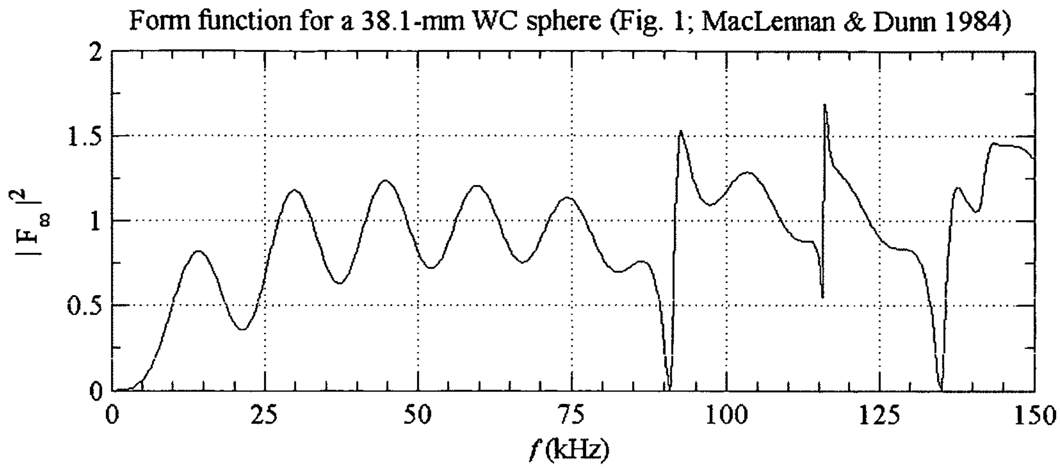

Figure B-2 Matlab algorithm* duplicating Figure 1 of MacLennan and Dunn (1984) that describes the form function ($F\infty$) of a 38.1-mm tungsten carbide (WC) sphere as a function of acoustic frequency (f), assuming a continuous acoustic wave, longitudinal and transverse sound speed for WC =6,864 and 4,161 m/s, respectively, density of WC =14,900 kg/m^3, water sound speed of 1470 m/s, and water density of 1000 kg/m^3. *MacLennanDunnFig1.m

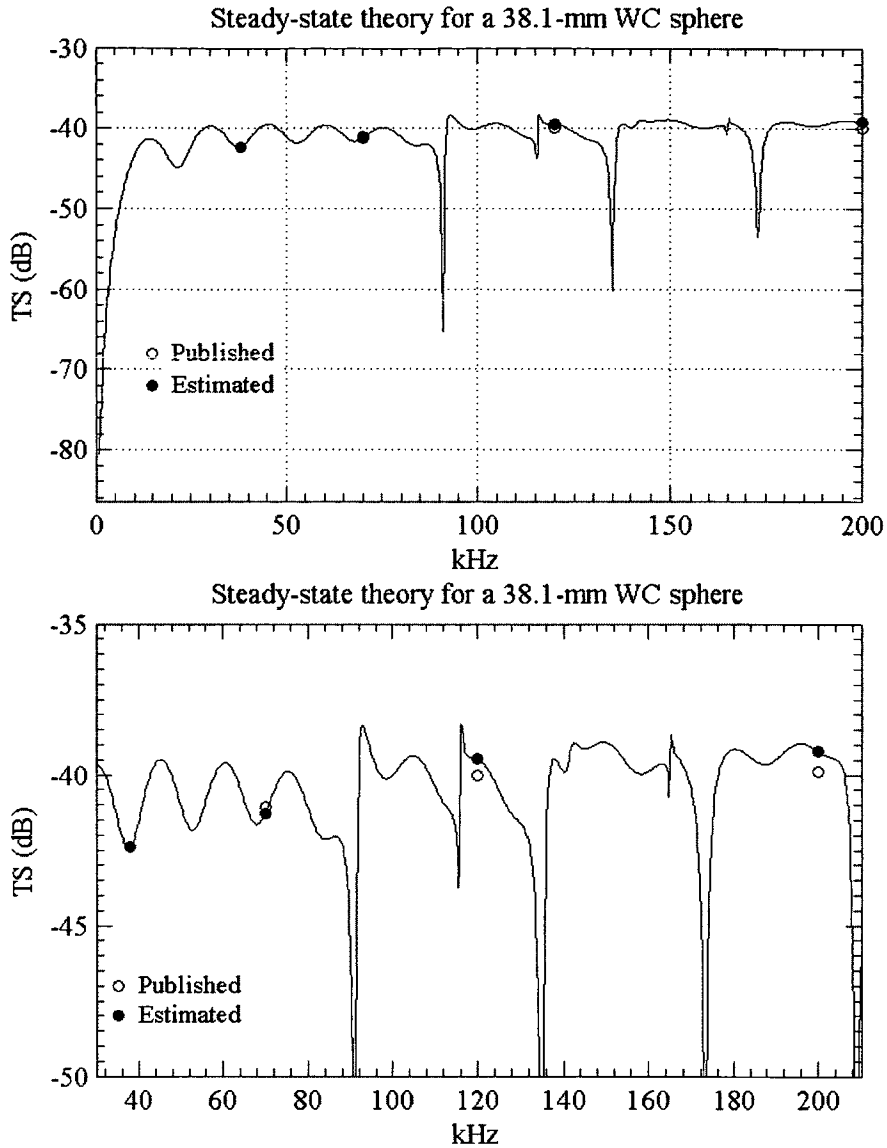

Figure B-3 Matlab algorithm* estimating the target strength (TS) of a 38.1-mm tungsten carbide (WC) sphere at 38, 70, 120, and 200 kHz compared to published reference TS values (Simmonds and MacLennan, 2005), assuming a continuous acoustic wave, longitudinal and transverse sound speed for WC =6,853 and 4,171 m/s, respectively, density of WC =14,900 kg/m^3, water sound speed of 1490 m/s, and water density of 1030 kg/m^3. Note: published TS is based on continuous wave at 38 kHz and pulse at 70, 120, and 200 kHz.
*TheoTSv5_SM2005_WC.m

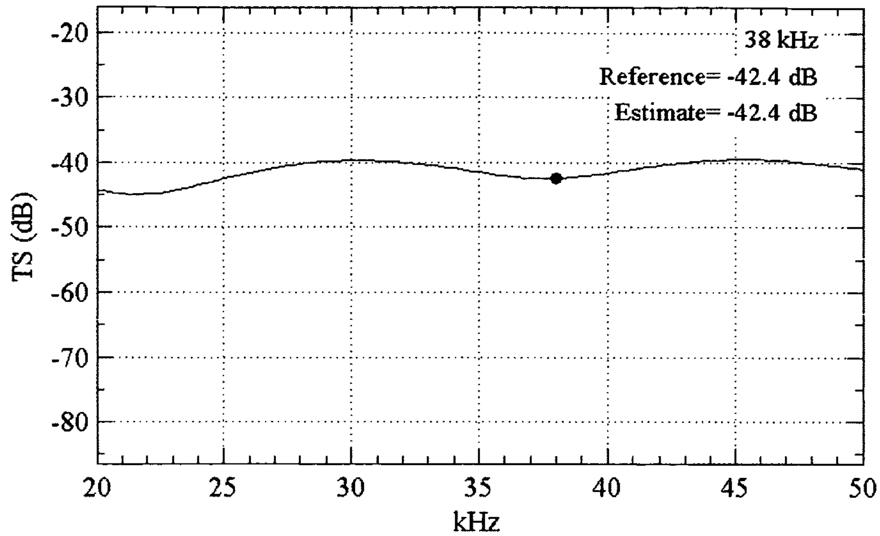

Figure B-4 Matlab algorithm* estimating the target strength (TS) of a 38.1-mm tungsten carbide (WC) sphere at 38 kHz matches the published reference TS value (Simmonds and MacLennan, 2005), assuming a continuous acoustic wave, longitudinal and transverse sound speed for WC =6,853 and 4,171 m/s, respectively, density of WC =14,900 kg/m^3, water sound speed of 1490 m/s, and water density of 1030 kg/m^3. *TheoTSv5_SM2005_WC.m

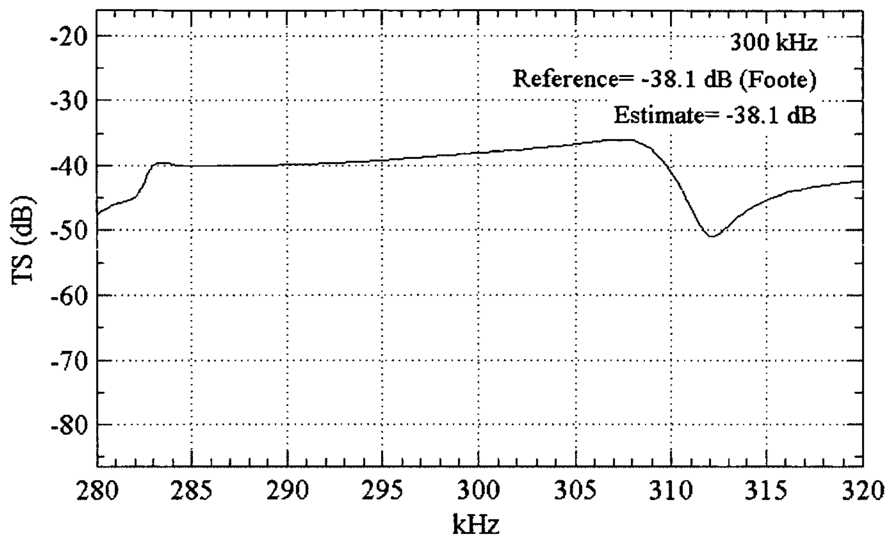

Figure B-5 Matlab algorithm* estimating the target strength (TS) of a 38.1-mm tungsten carbide (WC) sphere at 300 kHz matches the reference TS (K. Foote, pers. comm.) assuming a continuous acoustic wave, longitudinal and transverse sound speed for WC =6,853 and 4,171 m/s, respectively, density of WC =14,900 kg/m^3, water sound speed of 1490 m/s, and water density of 1030 kg/m^3. Note: reference TS was estimated by Foote based on 0.150 ms pulse, 8 kHz bandwidth, 300.15 center frequency, freshwater at 20 °C and seawater (33 ppt) at 9 °C. Sound speed variation of ±10 m/s may result in 0.1 dB difference.
*TheoTSv5_SM2005_WC.m

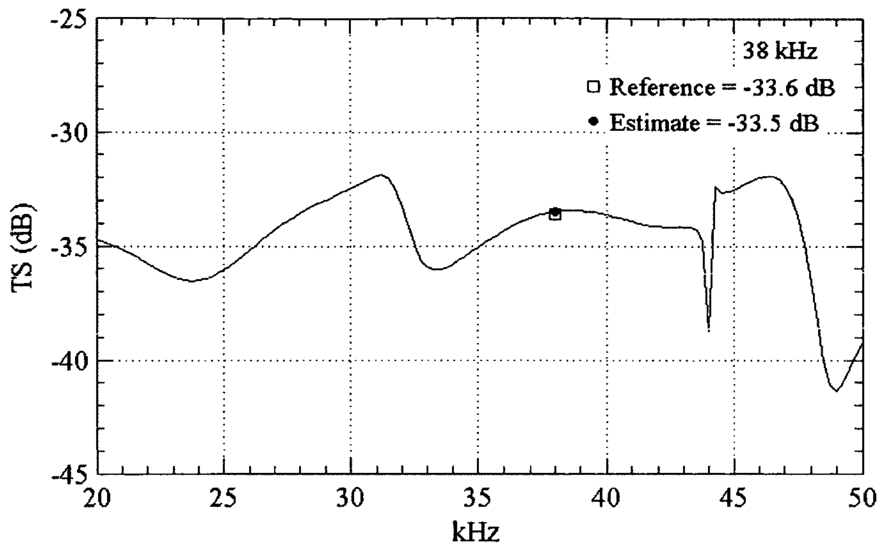

Figure B-6 Matlab algorithm* estimating the target strength (TS) of a 60-mm copper (Cu) sphere at 38 kHz is in close agreement with the published reference TS value (Simmonds and MacLennan, 2005), assuming a continuous acoustic wave, longitudinal and transverse sound speed for Cu =4,760 and 2,288 m/s, respectively, density of WC =8,945 kg/m^3, water sound speed of 1490 m/s, and water density of 1030 kg/m^3. *TheoTSv5_SM2005_Cu.m

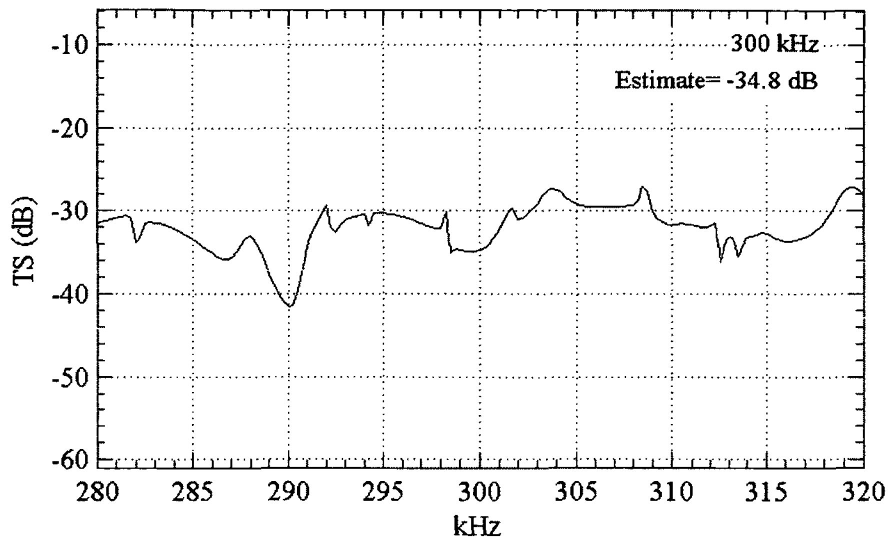

Figure B-7 Matlab algorithm* estimating the target strength (TS) of a 60-mm copper (Cu) sphere at 300 kHz, assuming a continuous acoustic wave, longitudinal and transverse sound speed for Cu =4,760 and 2,288 m/s, respectively, density of WC =8,945 kg/m^3, water sound speed of 1490 m/s, and water density of 1030 kg/m^3. *TheoTSv5_SM2005_Cu.m

APPENDIX C

CALIBRATION OF THE KONGSBERG EM3002 MULTIBEAM ECHO SOUNDER

Introduction

The Kongsberg EM3002 multibeam echo sounder was calibrated from a combination of measurements taken in the field and in the laboratory. The purpose of these measurements were (1) to describe the beam pattern of individual beams, (2) to describe the relative response in echo strength among all beams, (3) to assess the effect of near field conditions on echo strength by measuring the echo strength of a reference target as a function of range, and (4) to calibrate the on-axis echo strength of each beam to correct for system and beam-specific sensitivity differences.

Laboratory Setup

Acoustic measurements made with the EM3002 multibeam echo sounder were obtained under controlled conditions within an indoor freshwater tank facility (12 m wide x 18 m long x 6 m deep) at the Jere A. Chase Ocean Engineering Laboratory at the University of New Hampshire (Figure C-1), which was previously used for calibration of other multibeam echo sounders (Foote et al. 2005; Lanzoni and Weber 2010). The general instrumentation specific to this facility and protocols for multibeam calibrations are described elsewhere (Foote et al. 2005; Lanzoni and Weber 2010). Figure C-2 provides the schematic of the instrumentation configuration for measurements of transmitting and receiving beam patterns.

Figure C-1. (A) The transducer of the Kongsberg EM3002 multibeam echo sounder was mounted to a plate affixed to a rotating pole and aimed horizontally; (B) The transducer-mounting pole and instrumentation was positioned on carriage that can be moved along and across the freshwater tank of the Jere A. Chase Ocean Engineering Laboratory at the University of New Hampshire.

Transmit Beam Pattern

A 0.200-ms pulse at 300 kHz was transmitted from the EM3002 and received by a standard transducer (U.S. Naval Undersea Warfare Center/Underwater Sound Reference Division Model E27, S/N 218) for 30 pings as the EM3002 was mechanically rotated from -90° to 90° by 0.5° intervals. The standard transducer was aligned vertically (~ 3 m water depth) to the major response axis (MRA) of the EM3002 at a range of 8.5 m. The root-mean-square voltage measurements received by the standard transducer were then used to plot the normalized across-track transmit beam pattern of the EM3002. The along-track transmit beam pattern of the EM3002 was described from measurements collected from 0° to 90 ° by 1° intervals after the EM3002 transducer was rotated 90° while the standard transducer was aligned with the MRA of one of the central beams. Figure C-3 shows the across-track and along-track normalized beam patterns of the EM3002 multibeam echo sounder. Figure C-4 shows the along-track transmit pattern in more detail. The 3-dB beam width was estimated from a quadratic fit of the transmit beam pattern measurements of the main lobe down to -18 dB in the along-track equatorial plane (Figure C-5).

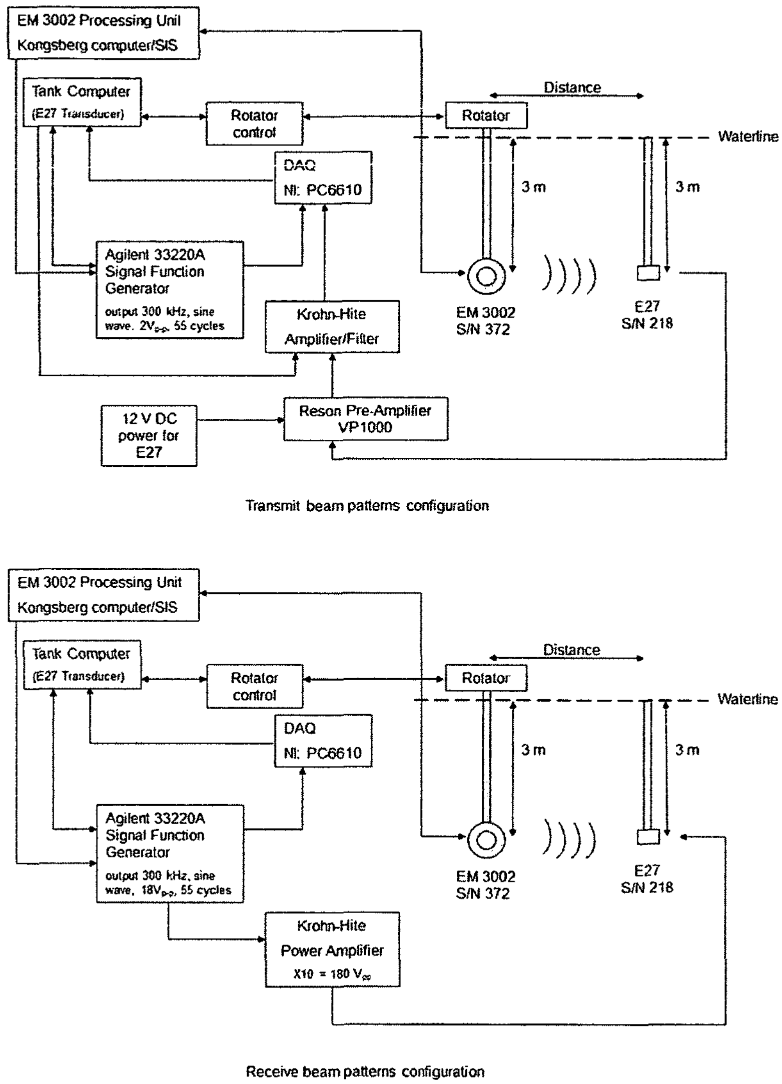

Figure C-2. Schematic diagram of instrumentation used to collect measurements of the transmit (top) and receive (bottom) beam patterns of the Kongsberg EM3002 multibeam echo sounder in the freshwater tank facility at Jere A. Chase Ocean Engineering Laboratory at the University of New Hampshire during June 2008.

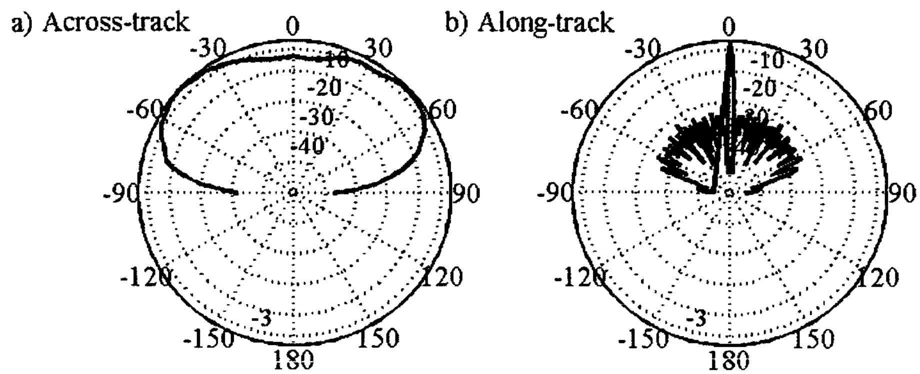

Figure C-3. Polar plots of the normalized transmit beam pattern of the EM3002 multibeam transducer in the (a) across-track and (b) along-track equatorial plane measured by receiving 30 pulse transmissions from a standard transducer (U.S. Naval Undersea Warfare Center/Underwater Sound Reference Division Model E27, S/N 218) as the transducer mechanically rotated from -90° to 90° at a range of 8.5 m inside a freshwater tank facility.

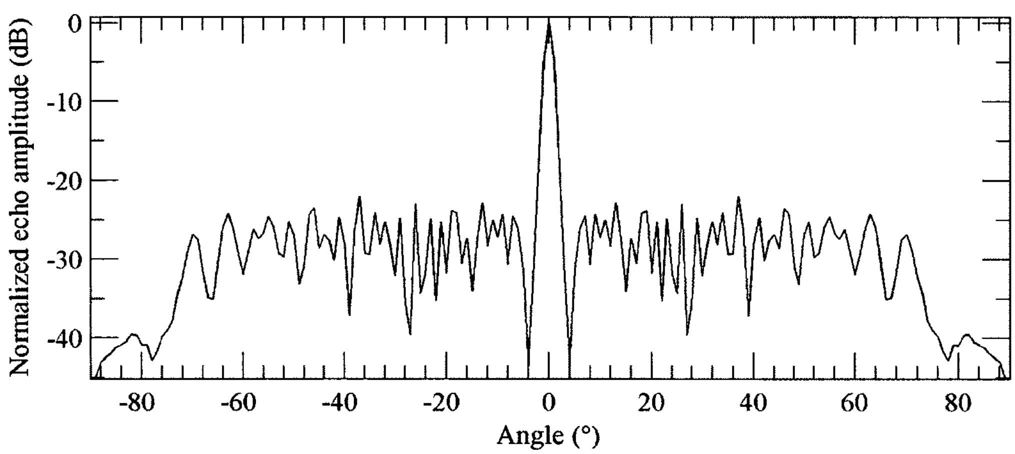

Figure C-4. Two-dimensional plot of the normalized transmit pattern from the EM3002 multibeam transducer in the along-track equatorial plane measured by receiving 30 pulse transmissions from a standard transducer (U.S. Naval Undersea Warfare Center/Underwater Sound Reference Division Model 27, S/N 218) at 0.5° intervals as the transducer mechanically rotated from -90° to 90° at a range of 8.5 m inside a freshwater tank facility.

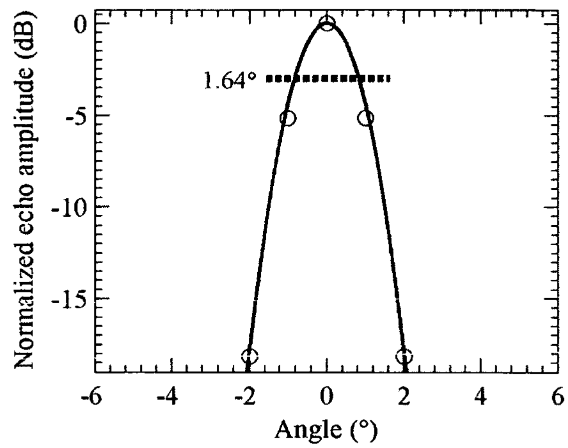

Figure C-5. Fitted (solid line) and measured (circles) along-track transmit beam pattern of the EM3002 multibeam echo sounder and 3-dB beam width (dashed line).

Receive Beam Pattern

The EM3002 has 160 receive beams, each with a nominal 1.5° beam width, were configured to cover a swathe of 130° (-65° to 65°) with equiangular spacing. As before, the EM3002 transducer was mounted 3 m below the water surface in the laboratory tank. The standard transducer was positioned at a range of 5 m and vertically aligned to the MRA of one of the center beams. The EM3002 received the 1-second pulse of 180 $V_{peak\text{-}to\text{-}peak}$ at 300 kHz transmitted from the standard transducer at half the range. The standard transducer transmitted 40 pulses for each 1° interval as the transducer was automatically rotated from -90° to 90° This series of measurements was repeated four more times, with each time starting with an angle shifted by 0.2°. From five measurement series of 180° rotations, the EM3002 received the pulse transmitted by the standard transducer at angles from 90° to 90.8° by 0.2°.

In order to associate the echo amplitude of each rotated angle for any individual EM3002 beam, careful exploratory analysis was performed to determine the starting ping of a step-wise pattern in amplitude (Figure C-6). For each angle, the 21-ping centered median amplitude was used rather than the mean because it was less sensitive to outlying anomalies (Figure C-7). When the receive beam pattern was normalized to the peak beam amplitude, the beam pattern showed less sensitivity in outer beams compared to the central beams (Figure C-8). The 3-dB beam width of each across-track receive beams of the EM3002 multibeam echo sounder was estimated from fitting a quadratic polynomial to the beam pattern measurements for the main lobe down to -6 dB (Figure C-9). Several beams (127-131, 141) were lacking sufficient data for reasonable estimates, but a general trend emerged showing beam widths of the most outer beams being approximately twice that of the center (Figure C-10). The beam widths of the central beams were approximately 0.1° to 0.2° greater than the nominal beam width of 1.5°.

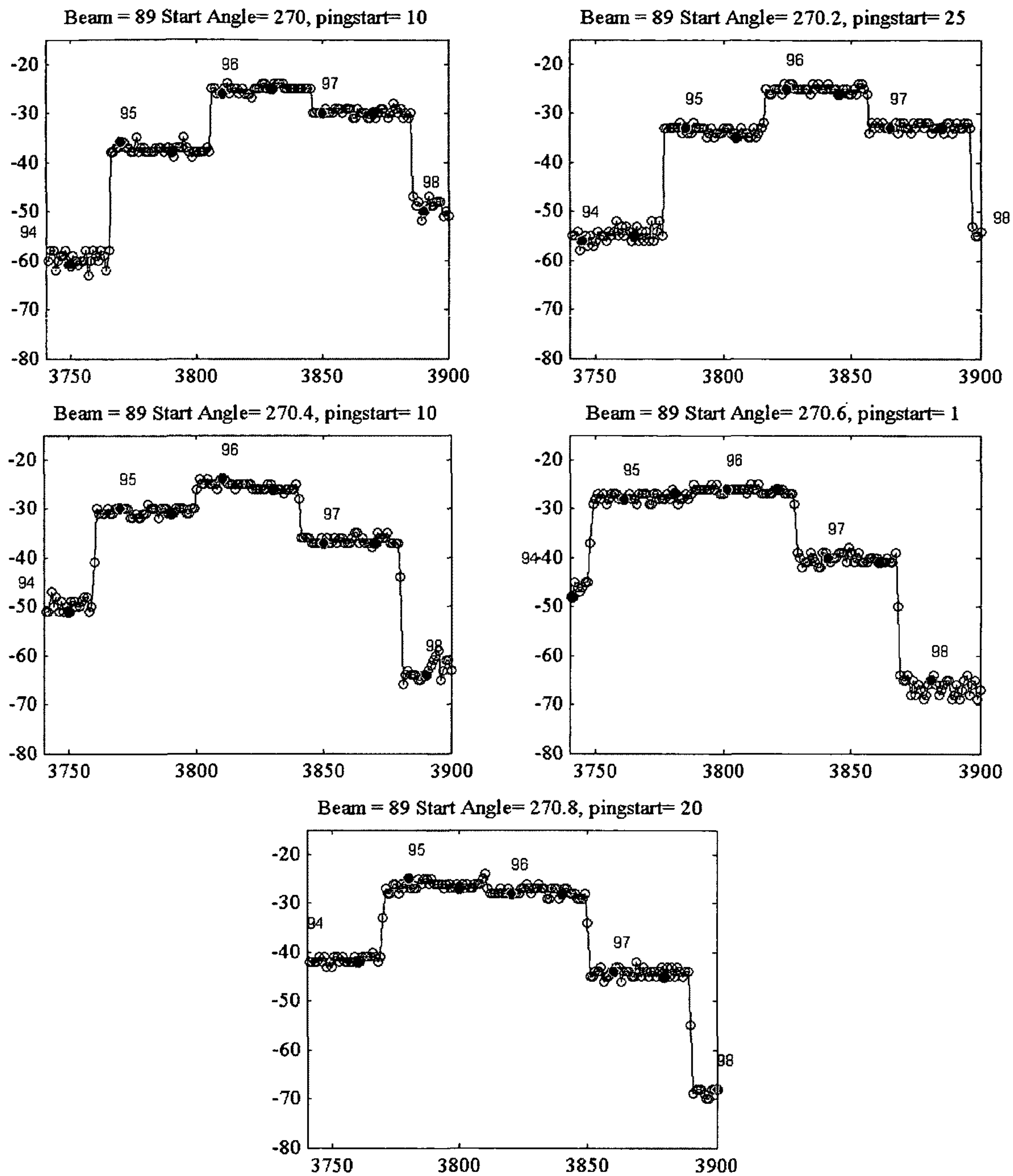

Figure C-6. The step-wise pattern in raw amplitude for the main lobe of EM3002 beam 89 from receiving 40 pulses at each degree interval for five 180° rotations each with a start angle differing by 0.2° A 21-ping interval selected for analysis was extracted for each angle step as identified by the interval start (green) and end (red).

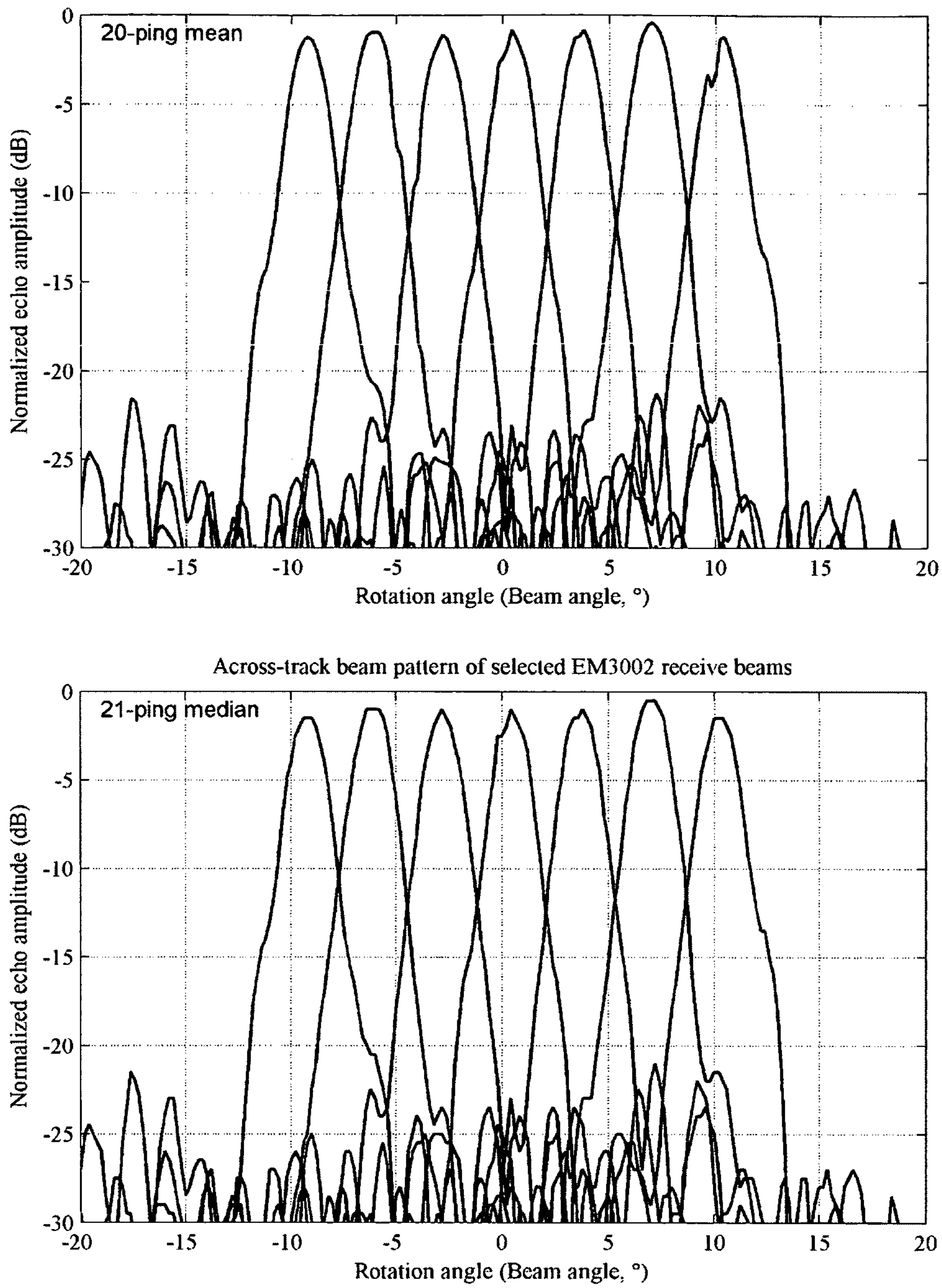

Figure C-7. Examples of the across-track receive beam pattern for beams 68, 72, 76, 80, 84, 88, and 92 of the 300-kHz EM3002 multibeam echo sounder when a centered 21-ping mean (top) and median (bottom) amplitude is calculated from the 40 pings at each 0.2° angle interval.

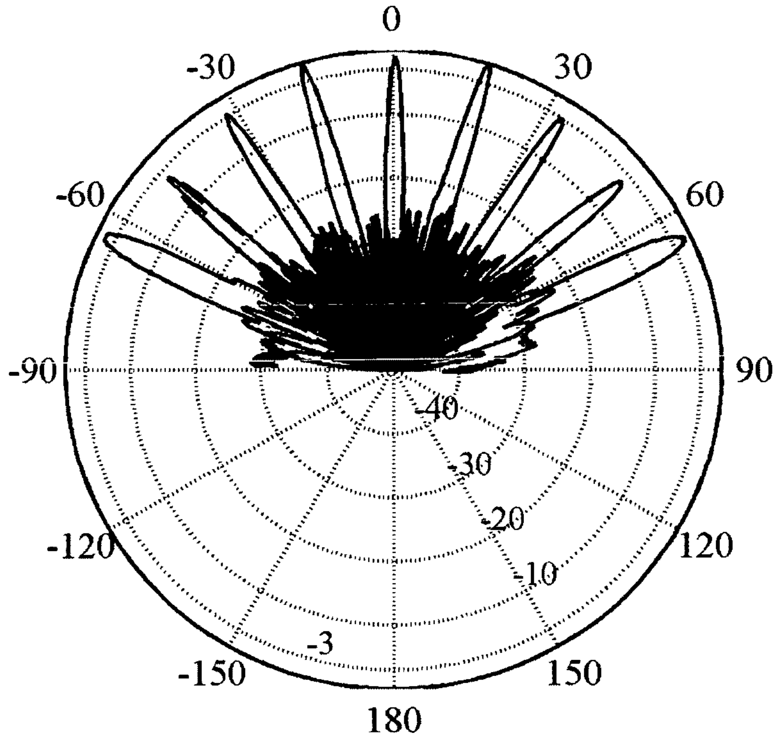

Figure C-8. Polar plot of the across-track receive beam pattern for beams 1, 20, 40, 60, of the 300-kHz EM3002 multibeam echo sounder when a centered 21-ping mean (top) and median (bottom) amplitude is calculated from the 40 pings at each 0.2° angle interval.

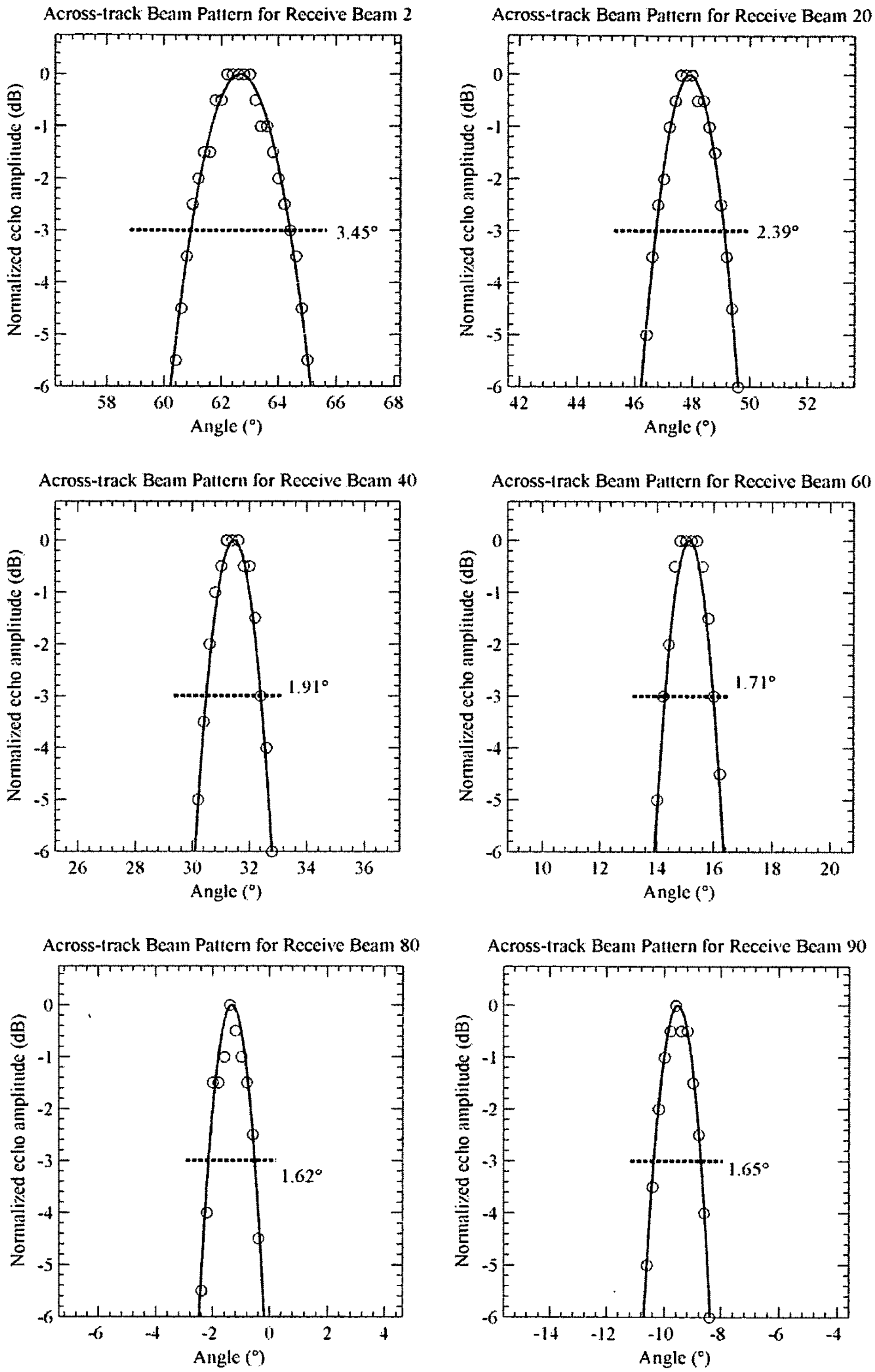

Figure C-9. Examples of estimating the 3-dB beam widths (dashed line) from fitting a quadratic polynomial (solid line) to the measured (circles) beam patterns for the main lobe of selected receive beams of the EM3002 multibeam echo sounder in the across-track equatorial plane.

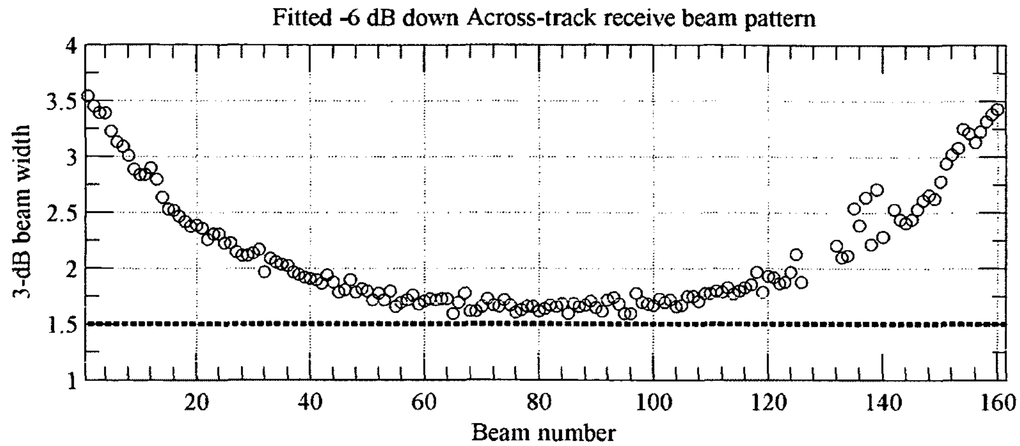

Figure C-10. Estimated 3-dB beam widths of individual receive beams of the 300-kHz EM3002 multibeam echo sounder in the across-track equatorial plane relative to the nominal beam width (thick dashed line).

In contrast to single beam echo sounders, fish and other targets can be detected in multiple overlapping beams of a multibeam echo sounder. The beam that has the fish closest to its MRA will produce the strongest echo, assuming each beam is calibrated accurately. As a result, the beam width and off-axis sensitivity corresponding to an individual beam's detectability of receiving the peak echo among overlapping beams may be of special interest. For example, the maximum echo strength of a fish can be obtained among single echo detections from overlapping beams for an individual ping. An individual beam may have a maximum off-axis sensitivity loss before a target with a stronger echo is detected in an adjacent beam. This off-axis sensitivity loss can be estimated by determining the beam width corresponding to the points where the beam patterns of adjacent beams intersect (Figure C-11).

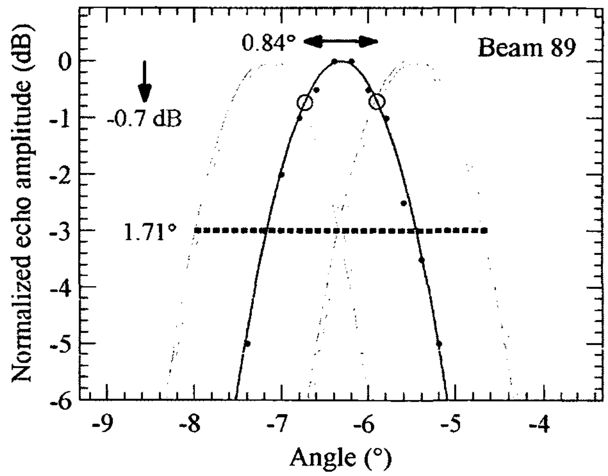

Figure C-11. The fitted (solid black line) and measured (dots) across-track beam pattern of receive beam 89 of the EM3002 multibeam echo sounder, 3-dB beam width (dashed line), sensitivity loss off axis (down arrow) down to the intersection (open circles) of adjacent beams 90 and 88 (shaded grey lines), and beam width between overlapping beams (double arrow). Note beams numbered from positive to negative angles.

Near Field Effects on Echo Strength

At large distances from the transducer, sound is projected as if the transducer is a point source projecting planar wave fronts. This region is considered the far field or Fraunhofer zone. In the far field, the acoustic intensity decreases inversely proportional to the square of the range from the transducer as a result of spherical spreading of the beams. At close ranges to the transducer, this scattering region is called the near field or Fresnel zone. In the near field, the acoustic propagation can be complicated owing to the sum on individual contributions of the transducer elements. The boundary between the near field and far field ($R_{NN\text{-}FF}$) of a transducer can be approximated to be at a range of $2a^2/\lambda$ where a is the effective radius of a piston transducer and λ is the acoustic wavelength. For the EM3002 operating at 300 kHz under sound speed conditions of 1490 m/s, the acoustic wavelength is approximately 0.5 cm. If the sonar head dimension (333 mm) is assumed, the $R_{NN\text{-}FF}$ would be 21 m. For multibeam echo sounders calibrated by Foote et al. (2005), the $R_{NN\text{-}FF}$ was estimated as one half of the square of the maximum transducer dimension divided by the wavelength. Based on this definition, the $R_{NN\text{-}FF}$

was theoretically 11 m. However, Nilsen (2007) of Kongsberg Maritime reports the nearfield extends to approximately 7 m. Echo strength measurements of two reference targets at several distances within the tank show the echo strength to increase with range but then become relatively stable between 5 and 6.5 m (Figure C-12).

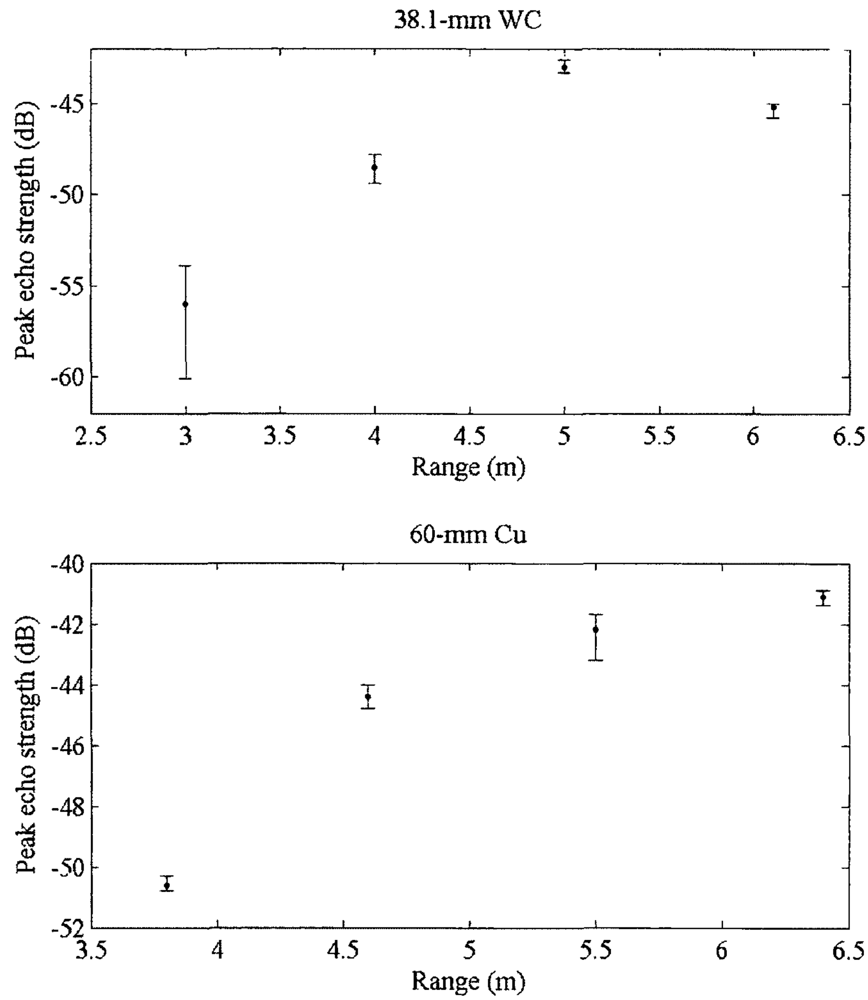

Figure C-12. Peak echo strength (mean ± s.d.) of a 38.1-mm tungsten carbide (WC, top) and 60-mm copper (Cu, top) sphere as a function of range from near field measurements with a 300 kHz multibeam echo sounder (Kongsberg EM3002) transmitting at a pulse duration (τ) of 200 μs and receiving over a 8 kHz bandwidth in a freshwater tank facility. Note: 40log$R$ echo amplitudes were not adjusted for any calibration offsets (raw).

At-Sea Calibration By The Standard Target Method

On two separate occasions (23 and 27 May 2009), a 38.1-mm tungsten carbide sphere was secured to a monofilament line and lowered by a rod and reel from the anchored research vessel "*R/V Meriel B*" to a depth between 8 and 11 m at the site of the fish cage experiments. A time series of data were collected while moving the reference target through the multiple beams of the 300-kHz EM3002 multibeam echo sounder, but concentrating data collection between beams 50 and 110 covering approximately the center 48° of the 130° swathe. Single echo detections from each beam and ping were extracted within the 8 to 11 m range gate. Then, for each ping, the single echo detection from the beam with the highest echo strength among all beams with SEDs for that ping was retained (Figure C-13). These values are the so-called ping-maximum peak echo strengths because the values represent the peak echo strength of the single echo pulse that is the maximum value among overlapping beams for an individual ping.

Figure C-14 shows the maximum of these ping-maximum echo strengths as an approximation of the target strength for each beam, assuming the maximum was virtually on the MRA. The ping-maximum single echo detections can be considered randomly distributed throughout the beam's main lobe within a few dBs of the MRA because the reference target was held and moved haphazardly through multiple beams from the vessel, which also was moving in all directions in response to heave, roll, and pitch from surface waves. The more single echo detections are made randomly located within the beam, the higher the probability of a detection being close to or within error of the MRA. Beams with as few as one ping-maximum single echo detection is unlikely to represent an estimate of TS of the reference target (Figure C-14A), but with sample sizes greater than 30 this assumption becomes more reasonable (Figure C-14B) and most robust when sample sizes were greater than 100 (Figure C-14C). The difference between the measured and theoretical TS of the reference target was used for determining the calibration offset for each beam with sufficient data. Because individual EM3002 beams lack the ability to correct for off-axis sensitivity loss like split- or dual-beams, the maximum echo strength from many (n > 100) randomly distributed ping-maximum single echo detections was considered essentially on axis and was used as an estimate of TS.

Beam-specific Calibration Offset

Calibration is important to remove system-dependence of the acoustic measurements collected by an echo sounder for providing quantitative estimates of fish density or fish size (Foote et al. 1987; Foote et al. 2005; Jech et al. 2005; Ona et al. 2009). A beam-specific calibration offset (C_b) was measured for beams with greater than 100 ping-maximum echo detections of the reference target (Figure C-13) by the difference between the theoretical and maximum observed echo strength of the reference target. To derive C_b for the other beams, the C_b can be adjusted by the remaining difference after taking the product of the relative transmit and receive beam response at each MRA, which in theory should complement each other for a flat response.
Figure C-15 shows the normalized major axial responses for each receive beam obtained from all individual across-track beam patterns and normalized across-track transmit beam pattern response at angles corresponding to each MRA of the receive beams. The product of these two relative responses, when centered at zero, does not produce a flat response (Figure C-15).

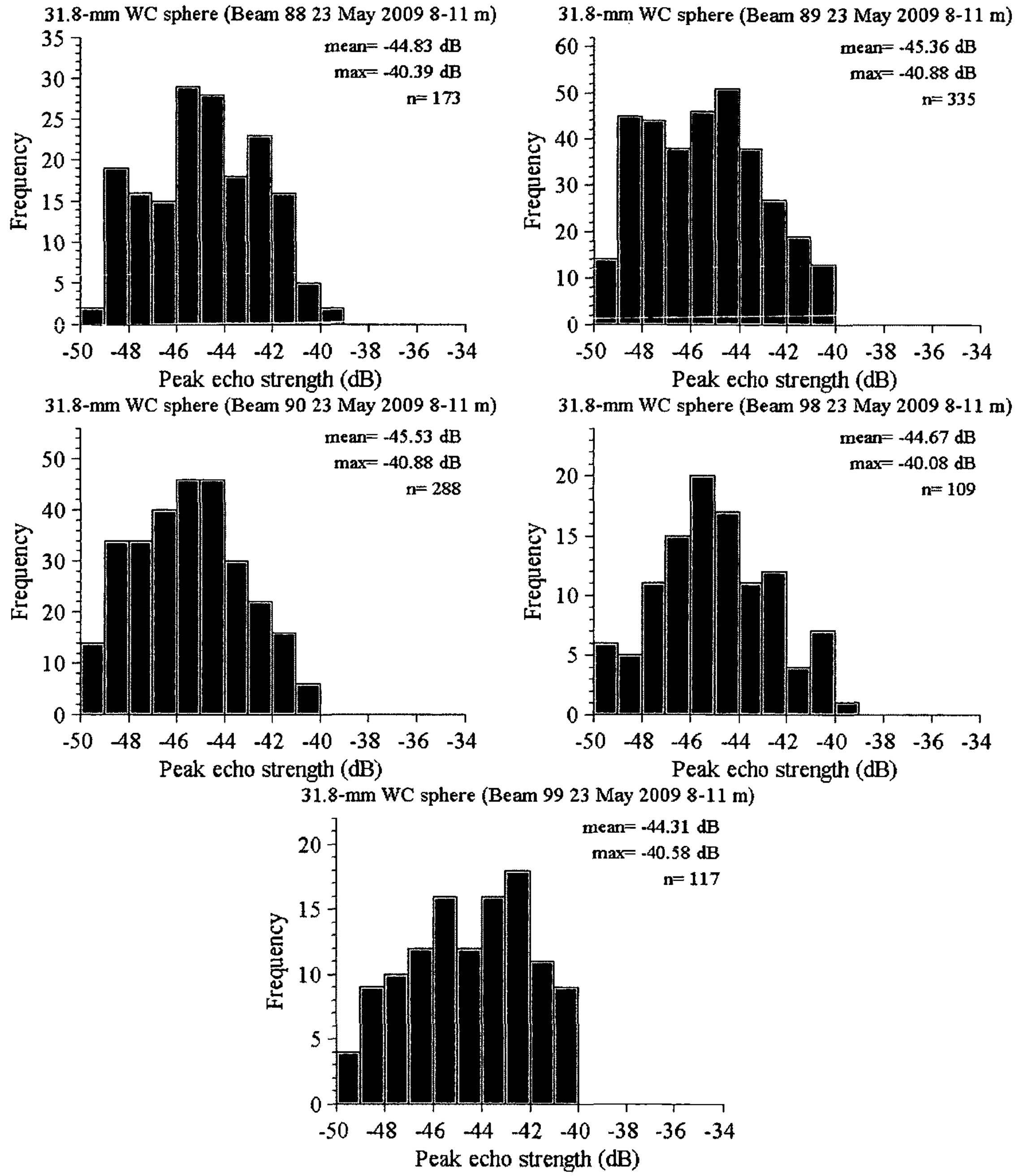

Figure C-13. Frequency distribution of the ping-maximum echo strength from single echo detections of a 38.1-mm tungsten carbide sphere for beams with a sample size greater than 100; the maximum value from these distributions was compared to the reference target strength for determining a beam-specific calibration offset.

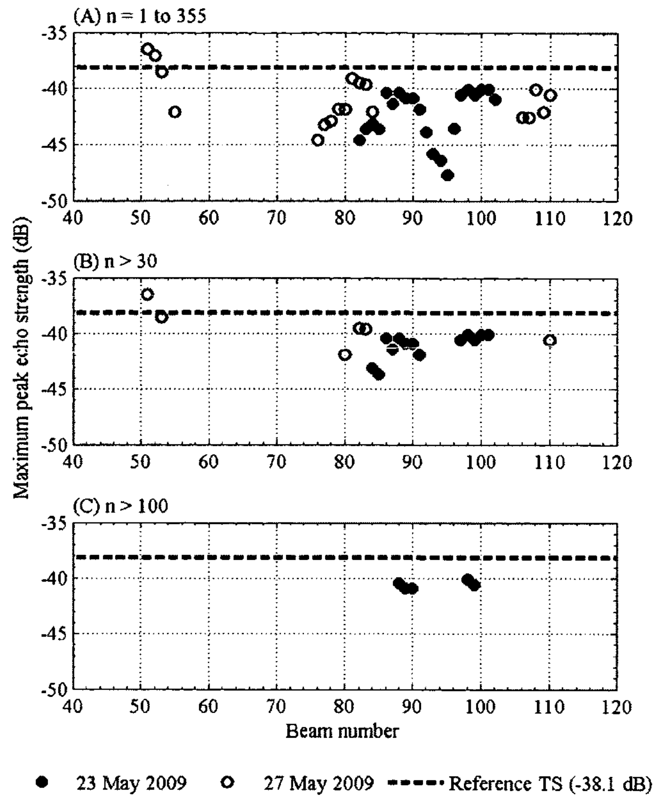

Figure C-14. Maximum echo strength among ping-maximum single echo detections of a 38.1-mm tungsten carbide sphere observed at sea on 23 and 27 May 2009 for (A) all beams with n > 1, (B) beams with n > 30 and (C) beams with n > 100. The maximum value from these distributions was compared to the reference target strength (dashed line) for determining a beam-specific calibration offset.

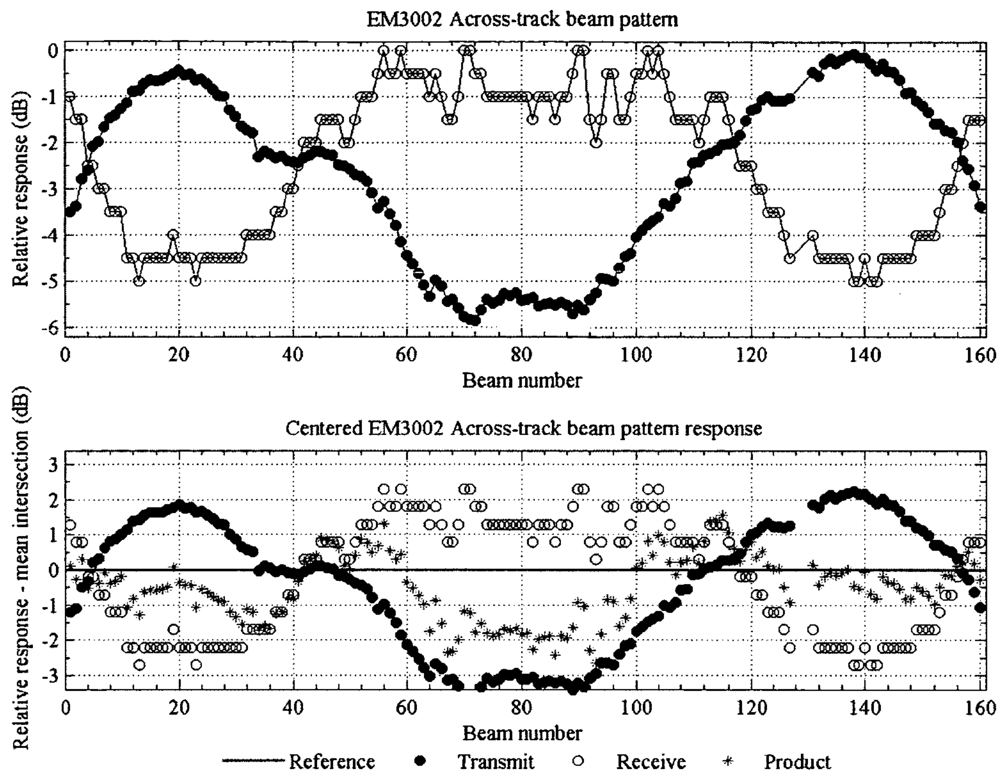

Figure C-15. TOP: Major response axes (MRAs) from each across-track receive beam patterns of the EM3002 multibeam echo sounder normalized to the maximum response and the normalized across-track transmit beam pattern response at angles corresponding to the MRAs of the receive beams. BOTTOM: Product of the relative transmit and receive major axial response when data were centered by subtracting the mean value where both patterns intersected (reflection point).

Figure C-16 shows the offsets between the theoretical and maximum observed echo strength are in similar magnitude as the product of the relative transmit and receive beam responses, but C_b only from beams 88, 89, 90, 98, and 99 were used to derive C_b of all beams. The C_b for all beams were estimated based on each beam calibrated by reference target separately as

$$C_b(i,j) = C_b(j) + [C_{\mathrm{TXRX}}(j) - C_{\mathrm{TXRX}}(i)]\,,$$

where $C_b(i, j)$ is the beam-specific calibration offset for beam i of beams 1-160 based on C_b for reference beam j of the calibrated beams 88, 89, 90, 98, and 99, and $C_{\mathrm{TXRX}}(j)$ and $C_{\mathrm{TXRX}}(i)$ are the products of the relative transmit and receive beam responses at the MRAs of beams i and j, respectively, that are shown in Figure C-16. The five estimates of C_b for all beams developed from each of the five beams calibrated by the standard target method was then averaged, in linear units, and the converted to decibels (Figure C-14). This mean C_b was then applied to the echo strength of the respective EM3002 beams.

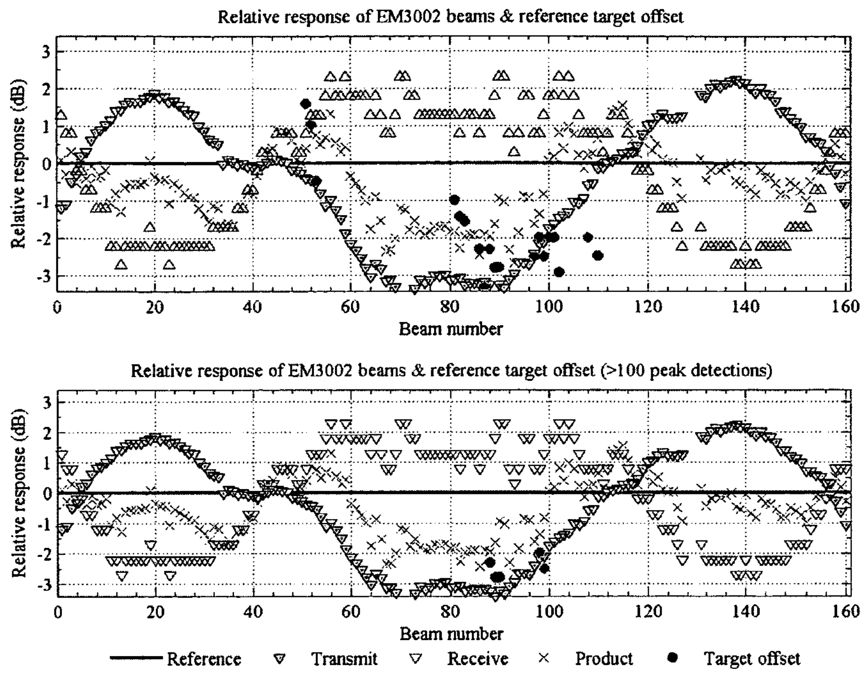

Figure C-16. The product between the complementary relative transmit and receive beam responses at the major response axis of each receive beam of the 300-kHz EM3002 multibeam echo sounder; and the offset between the theoretical and estimated target strength of a reference target (38.1-mm tungsten carbide sphere) for beams with all available data (top) and for five beams with greater than 100 ping-maximum single echo detections.

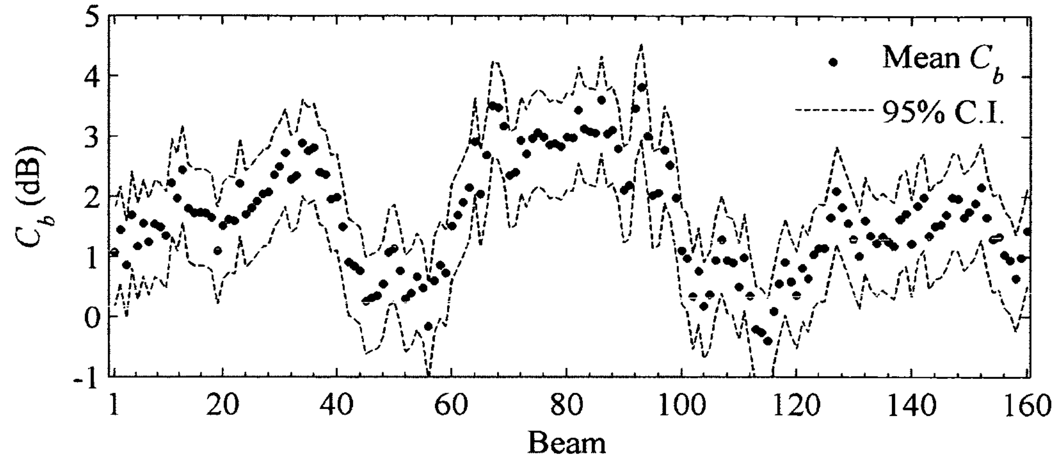

Figure C-17. The mean and 95% confidence interval of the beam-specific calibration offset (C_b) derived from adjusting the absolute difference between theoretical and estimated target strength of a reference target detected in five reference beams of the 300 kHz Konsgberg EM3002 mutlibeam echo sounder by the relative transmit-receive major axial response of individual beams obtained from laboratory measurements of the beam patterns.

APPENDIX D

SINGLE BEAM DETECTION ALGORITHM

The single target detection algorithm (sed.m) is based on Echoview single beam method 1 which is also implemented by Simrad in the EK500 echo sounder (Soule et al. 1995, 1996; Ona et al. 1999). This algorithm runs using echo strength (ES) data with an applied $40\text{Log}_{10}\text{R}$ TVG on a ping by ping basis for a single beam. Herein, ES is equivalent to TS uncompensated for beam pattern.

The first step was to remove all data in analysis region which may be indexed by zeros. Phase I was to determine all peak ES values that may indicate single target and retain peak values if the following peak selection criteria are met. Peak selection criteria were considered in sequential order as follows:

1. The ES value must be a local maximum by being greater than the previous and proceeding sample.
2. The ES value must also be greater than the chosen minimum echo strength threshold (ES_{thr})
3. The pulse length (L_p) of the target must be between the set limits of minimum and maximum normalized pulse length ($L_{np,min}$ and $L_{np,max}$)

The pulse length was determined as the distance (m) between the first and last samples within the pulse envelope. The pulse envelope consisted all samples surrounding the peak value which was above both (peak ES – PLDL) and a chosen threshold. Pulse length determination level (PLDL) defined the dB level down the peak value of the detected pulse to be considered part of the pulse envelope and included in determination of the L_p during single target detection. The threshold chosen is the threshold selected by the user if it is less than or equal to (peak ES – PLDL). If the chosen threshold is greater than (peak ES –PLDL), the lowest value among (ES_{thr} – PLDL), (ES_{thr}–PLDL/2), and ES_{thr} was chosen for the applied minimum ES threshold.

Phase II of this algorithm sequentially screening each pulse from low to high depth ranges for overlapping pulses. If a pulse overlapped an earlier pulse, the pulse with the lower ES was rejected.

LIST OF REFERENCES

Aglen, A. 1996. Impact of fish distribution and species composition on the relationship between acoustic and swept-area estimates of fish density. ICES Journal of Marine Science 53:501-505.

Aglen, A., A. Engås, I. Huse, K. Michalsen, and B. K. Stensholt. 1999. How vertical fish distribution may affect survey results. ICES Journal of Marine Science 56:345-360.

Ames, E. P. 2004. Atlantic cod structure in the Gulf of Maine. Fisheries 29:10-28.

Andersen, L. N. 2001. The new Simrad EK60 scientific echo sounder system. Journal of the Acoustical Society of America 109: 2336.

Armstrong, M. P., M. J. Dean, W. S. Hoffman, D. R. Zemeckis, T. A. Nies, D. E. Pierce, P. J. Diodati, and D. J. McKiernan. 2012. The Application of small scale fishery closures to protect Atlantic cod spawning aggregrations in the inshore Gulf of Maine. Fisheries Research. In Press.

Boswell, K. M., M. P. Wilson, and J. H. Cowan, Jr. 2008. A semiautomated approach to estimating fish size, abundance, and behavior from the dual-frequency identification sonar (DIDSON) data. North American Journal of Fisheries Management 28:799-807.

Bourguignon, S., L. Berger, C. Scalabrin, R. Fablet, and V. Mazauric. 2009. Methodological developments for improved bottom detection with the ME70 multibeam echosounder. ICES Journal of Marine Science 66: 1015-1022.

Bowman, R. E., and E. W. Bowman. 1980. Diurnal variation in the feeding intensity and catchability of silver hake (*Merluccius bilinearis*). Canadian Journal of Fisheries and Aquatic Sciences 37:1565-1572.

Brawn, V. M. 1961. Sound production by the cod (Gadus callarias L.). Behaviour 18:239-255.

Burton, M. L., K. J. Brennan, R. C. Muñoz, and J. Parker, Richard O. 2005. Preliminary evidence of increased spawning aggregations of mutton snapper (*Lutjanus analis*) at Riley's Hump two years after establishment of the Tortugas South Ecological Reserve. Fishery Bulletin 103:404-410.

Chambers, M. D. and W.H. Howell. 2006. Preliminary information on cod and haddock production in submerged cages off the coast of New Hampshire, USA. ICES Journal of Marine Science 63: 385–392.

Chiappone, M., and K. M. S. Sealey. 2000. Marine reserve design criteria and measures of success: lessons learned from the Exuma Cays Land and Sea Park, Bahamas. Bulletin of Marine Science 66:391-705.

Clay, A., and M. Castonguay. 1996. In situ target strengths of Atlantic cod (*Morhua gadus*) and Atlantic mackerel (*Scomber scombrus*) in the Northwest Atlantic. Canadian Journal of Fisheries and Aquatic Sciences 53:87-98.

Clay, C. S. 1983. Deconvolution of the fish scattering PDF from the echo PDF for a single transducer sonar. Journal of the Acoustical Society of America 73:1989-1994.

Clay, C. S., and B. G. Heist. 1984. Acoustic scattering by fish — Acoustic models and a two-parameter fit. Journal of the Acoustical Society of America 75 1077-1083.

Clay, C. S., and J. K. Horne. 1994. Acoustic models of fish: The Atlantic cod (*Gadus morhua*). Journal of the Acoustical Society of America 96:1661-1668.

Clay, C. S., and H. Medwin. 1977. Acoustical Oceanography. John Wiley and Sons, Inc., New York.

Cochrane, N. A., Y. Li., and G.D. Melvin. 2003. Quantification of a multibeam sonar for fisheries assessment. Journal of the Acoustical Society of America 114:745-758.

Cressie, N., and D. M. Hawkins. 1980. Robust estimation of the variogram: I. Journal of the International Association for Mathematical Geology 12:115-125.

Cressie, N. A. C. 1993. Statistics of Spatial Data, Revised Edition. Wiley, New York.

Cubillos, L. A., J. Paramo, P. Ruiz, S. Núñez, and A. Sepúlveda. 2008. The spatial structure of the oceanic spawning of jack mackerel (*Trachurus murpyhi*) off central Chile (1998-2001). Fisheries Research 90:261-270.

Cutter, G.R., Jr., L. Berger, and D.A. Demer. 2010. A comparison of bathymetry mapped with the Simrad ME70 multibeam echosounder operated in bathymetric and fisheries modes. ICES Journal of Marine Science 67:1301-1309.

Cutter, G. R., Jr., and D. A. Demer. 2007. Accounting for scattering directivity and fish behaviour in multibeam-echosounder surveys. ICES Journal of Marine Science 64: 1664-1674.

Cutter, G. R., J. S. Renfree, M. J. Cox, A. S. Brierley, and D. A. Demer. 2009. Modelling three-dimensional directivity of sound scattering by Antarctic krill: progress towards biomass estimation using multibeam sonar. ICES Journal of Marine Science 66: 1245-1251.

Davis, M. W. 2002. Key principles for understanding fish bycatch discard mortality. Canadian Journal of Fisheries and Aquatic Sciences 59: 1834-1843.

De Robertis, A., and I. Higginbottom. 2007. A post-processing technique to estimate the signal-to-noise ratio and remove echosounder background noise. ICES Journal of Marine Science 64:1282-1291.

Dean, M. J., W. S. Hoffman, and M. P. Armstrong. 2012. Disruption of an Atlantic cod spawning aggregation resulting from the opening of a directed gill-net fishery. North American Journal of Fisheries Management 32:124-134.

Edwards, J. L. and Armstrong, E. 1984. Target strength experiments on caged fish. Scottish Fisheries Bulletin 48:12–20.

Ehrenberg, J. E., T. J. Carlson, J. J. Traynor, and N. J. Williamson. 1981. Indirect measurements of the mean acoustic backscattering cross section of fish. Journal of Acoustical Society of America 69:955-962.

Emmrich, M., I. P. Helland, S. Busch, S. Schiller, and T. Mehner. 2010. Hydroacoustic estimates of fish densities in comparison with stratified pelagic trawl sampling in two deep, coregonid-dominated lakes. Fisheries Research 105:178-186.

Engås, A., O. R. Godø, and T. Jørgensen. 2000. A comparison between vessel and trawl tracks as observed by the ITI trawl instrumentation. Fisheries Research 45:297-301.

Espeland, S. H., A. F. Gundersen, E. M. Olsen, H. Knutsen, J. Gjøsæter, and N. C. Stenseth. 2007. Home range and elevated egg densities within an inshore spawning ground of coastal cod. ICES Journal of Marine Science 64:920-928.

Evans, R. D., G. R. Russ, and J. P. Kritzer. 2008. Batch fecundity of *Lutjanus carponotatus* (Lutjanidae) and implications of no-take marine reserves on the Great Barrier Reef, Australia. Coral Reefs 27:179-189.

Fässler, S. M. M., A. S. Brierley, and P. G. Fernandes. 2009. A Bayesian approach to estimating target strength. ICES Journal of Marine Science 66:1197-1204.

Fedovota, T. A. and O. E. Shatoba. 1983. Acoustic backscattering cross-section of cod averaged by sizes and inclination of fish. FAO Fisheries Report 300: 63–68.

Fernandes, P. G., F. Gerlotto, D. V. Holliday, O. Nakken, and E. J. Simmonds. 2002. Acoustic applications in fisheries science: the ICES contribution. ICES Marine Science Symposia 215: 483–492.

Fleischer, G. W., K. D. Cooke, P. H. Ressler, R. E. Thomas, S. K. de Blois, and L. C. Hufnagle. 2008. The 2005 integrated acoustic and trawl survey of Pacific hake, *Merluccius productus*, in U.S. and Canadian waters off the Pacific Coast. NOAA Technical Memorandum NFMS-NWFSC-94:41.

Faran, J. J., Jr. 1951. Sound scattering by solid cylinders and spheres. Journal of the Acoustical Society of America 23:405-418.

Foote, K. G. 1980a. Importance of the swimbladder in acoustic scattering by fish: a comparison of gadoid and mackerel target strengths. Journal of the Acoustical Society of America 67:2064-2089.

Foote, K. G. 1980b. Effect of fish behaviour on echo energy: the need for measurements of orientation distributions. Journal du Conseil International pour l'Exploration de la Mer 39:193-201.

Foote, K. G. 1983a. Linearity of fisheries acoustics, with addition theorems. The Journal of the Acoustical Society of America 73:1932–1940.

Foote, K. G. 1983b. Maintaining precision calibrations with optimal copper spheres. Journal of the Acoustical Society of America 73:1054-1063.

Foote, K. G. 1986. A critique of Goddard and Welsby's paper "The acoustic target strength of live fish". Journal du Conseil International pour l'Exploration de la Mer 42:212-220.

Foote, K. G. 1987. Fish target strengths for use in echo integrator surveys. Journal of the Acoustical Society of America 82:981-987.

Foote, K. G. 1990. Spheres for calibrating an eleven-frequency acoustic measurement system. Journal du Conseil International pour l'Exploration de la Mer 46:284-286.

Foote, K. G. 1991. Summary of methods for determining fish target strengths at ultrasonic frequencies. ICES Journal of Marine Science 48:211-217.

Foote, K. G., A. Aglen, and O. Nakken. 1986. Measurement of fish target strength with a split-beam echo sounder. Journal of the Acoustical Society of America 80:612-621.

Foote, K. G., D. Chu, T. Hammar, K. C. Baldwin, L. A. Mayer, L. C. Hufnagle, Jr., and J. M. Jech. 2005. Protocols for calibrating multibeam sonar. Journal of the Acoustical Society of America 117:2013-2027.

Foote, K. G., H. P. Knudsen, G. Vestnes, D. N. MacLennan, and E. J. Simmonds. 1987. Calibration of acoustic instruments for fish-density estimation: a practical guide. ICES Cooperative Research Report 44:57.

Foote, K. G. and D. N. MacLennan. 1984. Comparison of copper and tungsten carbide calibration spheres. Journal of the Acoustical Society of America 75:612-616.

Francis, D. T. I., and K. G. Foote. 2003. Depth-dependent target strengths of gadoids by the boundary-element method. Journal of the Acoustical Society of America 114:3136-3146.

Fudge, S. A., and G. A. Rose. 2009. Passive- and active-acoustic properties of a spawning Atlantic cod (*Gadus morhua*) aggregation. ICES Journal of Marine Science 66:1259-1263.

Gauthier, S., and G. A. Rose. 2002. In situ target strength studies on Atlantic redfish (*Sebastes* spp.). ICES Journal of Marine Science 59:805-815.

Gerlotto, F., S. Georgakarakos, and P. K. Eriksen. 2000. The application of multibeam sonar technology for quantitative estimates of fish density in shallow water acoustic surveys. Aquatic Living Resources 13:385–393.

Gerlotto, F. and J. Paramo. 2003. The three-dimensional morphology and internal structure of clupeid schools as observed using vertical scanning multibeam sonar. Aquatic Living Resources 16:113–122.

Gerlotto, F., M. Soria, and P. Fréon. 1999. From two dimensions to three: the use of multibeam sonar for a new approach in fisheries acoustics. Canadian Journal of Fisheries and Aquatic Sciences 56:6-12.

Goddard, G. C. and V. G. Welsby. 1986. The acoustic target strength of live fish. Journal du Conseil International pour l'Exploration de la Mer 42: 197–211.

Godø, O. R., and V. G. Wespestad. 1993. Monitoring changes in abundance of gadoids with varying availability to trawl and acoustic surveys. ICES Journal of Marine Science 50:39-51.

Gorska, N., and E. Ona. 2003. Modelling the acoustic effect of swimbladder compression in herring. ICES Journal of Marine Science 60:548-554.

Gorska, N., E. Ona, and R. Korneliussen. 2005. Acoustic backscattering by Atlantic mackerel as being representative of fish that lack a swimbladder. Backscattering by individual fish. ICES Journal of Marine Science 62:984-995.

Guénette, S., T. J. Pitcher, and C. J. Walters. 2000. The potential of marine reserves for the management of northern cod in Newfoundland. Bulletin of Marine Science 66:831-852.

Gurshin, C. W. D., J. M. Jech, W. H. Howell, T. C. Weber, and L. A. Mayer. 2009. Measurements of acoustic backscatter and density of captive Atlantic cod with synchronized 300-kHz multibeam and 120-kHz split-beam echosounders. ICES Journal of Marine Science 66:1303-1309.

Hafsteinsson, M. T., and O.A. Misund. 1995. Recording the migration behaviour of fish schools by multi-beam sonar during conventional acoustic surveys. ICES Journal of Marine Science, 52: 915–924.

Handegard, N. O., K. Michalsen, and D. Tjøstheim. 2003. Avoidance behaviour in cod (*Gadus morhua*) to a bottom-trawling vessel. Aquatic Living Resources 16:265-270.

Handegard, N. O., and D. Tjøstheim. 2005. When fish meet a trawling vessel: examining the behaviour of gadoids using a free-floating buoy and acoustic split-beam tracking. Canadian Journal of Fisheries and Aquatic Sciences 2005:2409-2422.

Handegard, N. O., and D. Tjøstheim. 2009. The sampling volume of trawl and acoustics: estimating availability probabilities from observations of tracked individual fish. Canadian Journal of Fisheries and Aquatic Sciences 66:425-438.

Harden Jones, F. R., and P. Scholes. 1985. Gas secretion and resorption in the swimbladder of the cod *Gadus morhua*. Journal of Comparative and Physiology B 155:319-331.

Hawkins, A. D. 1993. Underwater sound and fish behaviour. Pages 129-169 *in* T. J. Pitcher, editor. Behaviour of Teleost Fishes. 2nd Ed. Chapman and Hall, London.

Hazen, E. L., and J. K. Horne. 2003. A method for evaluating the effects of biological factors on fish target strength. ICES Journal of Marine Science 60:555-562.

Hedgepeth, J.B. 1994. Stock assessment with hydroacoustic estimates of abundance via tuning and smoothed EM estimation. Doctoral dissertation. University of Washington, Seattle, WA

Hedgepeth, J. B., V. F. Gallucci, F. O'Sullivan, and R. E. Thorne. 1999. An expectation maximization and smoothing approach for indirect acoustic estimation of fish size and density. ICES Journal of Marine Science 56:36-50.

He, P. 1991. Swimming endurance of the Atlantic cod, L., at low temperatures. Fisheries Research *Gadus morhua* 12:65-73.

He, P. 2007. Selectivity of large mesh trawl codends in the Gulf of Maine I. Comparison of square and diamond mesh. Fisheries Research 83:44-59.

Hickling, R. 1962. Analysis of echoes from a solid elastic sphere in water. Journal of the Acoustical Society of America 34:1582-1592.

Hjellvik, V., K. Michalsen, A. Aglen, and O. Nakken. 2003. An attempt at estimating the effective fishing height of the bottom trawl using acoustic survey recordings. ICES Journal of Marine Science 60: 967-979.

Horne, J. K. 2000. Acoustic approaches to remote species identification: a review. Fisheries Oceanography 9:356-371.

Horne, J. K. 2003. The influence of ontogeny, physiology, and behaviour on the target strength of walleye pollock (*Theragra chalcogramma*). ICES Journal of Marine Science 60:1063-1074.

Horne, J. K., and C. S. Clay. 1998. Sonar systems and aquatic organisms: matching equipment and model parameters. Canadian Journal of Fisheries and Aquatic Sciences 55:1296-1306.

Horne, J. K., and P. D. Walline. 2005. Spatial and temporal variance of walleye pollock (*Theragra chalcogramma*) in the eastern Bering Sea. Canadian Journal of Fisheries and Aquatic Sciences 62:2822-2831.

Howell, W. H., M. Morin, N. Rennels, and D. Goethel. 2008. Residency of adult Atlantic cod (*Gadus morhua*) in the western Gulf of Maine. Fisheries Research 91:123-132.

ICES. 2005. Spawning and life history information for North Atlantic cod stocks. ICES Cooperative Research Report No. 274. 152 pp.

Isaaks, E. H., and R. M. Srivastava. 1989. Applied Geostatistics. Oxford University Press, New York.

Jech, J. M., K. G. Foote, D. Chu, and L. C. Hufnagle, Jr. 2005. Comparing two 38-kHz scientific echosounders. ICES Journal of Marine Science 62:1168-1179.

Jech, J. M. and W.L. Michaels. 2006. A multifrequency method to classify and evaluate fisheries acoustics data. Canadian Journal of Fisheries and Aquatic Sciences 63:2225–2235.

Journel, A. G., and C. J. Huijbregts. 1978. Mining Geostatistics. Academic Press, New York.

Kang, Myounghee. 2011. Analysis of the ME70 multibeam echosounder data in Echoview – current capability and future directions. Journal of Marine Science and Technology 19:312-321

Kieser, R., and J. E. Ehrenberg. 1990. An unbiased, stochastic echo-counting model. Rapports et Proces-Verbaux des Reunions, Conseil International pour L'Exploration scientifique de la Mer Medeterranee. Monaco 189:65-72.

Kinsler, L. E., Frey, A. R., Coppens, A. B., and Sanders, J. V. 2000. Fundamentals of Acoustics. John Wiley and Sons, Inc., Hoboken, New Jersey, 548 pp.

Klein-MacPhee, G. 2002. Cods. Family Gadidae Pages 223-261. *In* B.B. Collette and G. Klein-MacPhee, Editors. Bigelow and Schroeder's Fishes of the Gulf of Maine. Third Edition. Smithsonian Institution Press, Washington, D.C. 748 pp.

Kloser, R. J. 1996. Improved precision of acoustic surveys of benthopelagic fish by means of a deep-towed transducer. ICES Journal of Marine Science 53:407-413.

Kloser, R. J., and J. K. Horne. 2003. Characterizing uncertainty in target strength measurements of a deepwater fish: orange roughy (*Hoplostethus atlanticus*). ICES Journal of Marine Science 60:516-523.

Korsbrekke, K., S. Mehl, O. Nakken, and M. Pennington. 2001. A survey-based assessment of the Northeast Arctic cod stock. ICES Journal of Marine Science 58:763-769.

Kovach, A. I., T. S. Breton, D. L. Berlinsky, L. Maceda, and I. Wirgin. 2010. Fine-scale spatial and temporal genetic structure of Atlantic cod off the Atlantic coast of the USA. Marine Ecology Progress Series 410:177-195.

Kurlansky, M.K. Cod: A Biography of the Fish that Changed the World. Walker and Company, New York. 294 pp.

Lanzoni, J. C., and T. C. Weber. 2010. High-resolution calibration of a multibeam echo sounder. OCEANS 2010, Seattle, WA, 20-23 September 2010: 7.

Lawson, G. L., and G. A. Rose. 2000. Small-scale spatial and temporal patterns in spawning of Atlantic cod (*Gadus morhua*) in coastal Newfoundland waters. Canadian Journal of Fisheries and Aquatic Sciences 57:1011-1024.

LeFeuvre, P., G. A. Rose, Gosine, R., R. Hale, W. Pearson, and R. Khan. 2000. Acoustic species identification in the Northwest Atlantic using digital image processing. Fisheries Research 47:137-147.

Lindholm, J. A., J. Peter, and A. Knight. 2007. Site fidelity and movement of adult Atlantic cod *Gadus morhua* at deep boulder reefs in the western Gulf of Maine, USA. Marine Ecology Progress Series 342:239-247.

Littell, R. C., G. A. Milliken, W. W. Stroup, and R. D. Wolfinger. 1996. SAS System for Mixed Models. SAS Institute, Inc., Cary, North Carolina.

Love, R. H. 1971. Dorsal-aspect target strength of an individual fish. Journal of the Acoustical Society of America 49: 816-823.

Love, R. H. 1977. Target strength of an individual fish at any aspect. Journal of the Acoustical Society of America 62:1397-1403.

MacLennan, D. N. 1981. The theory of solid spheres as sonar calibration targets. Scottish Fisheries Report 22:1-17.

MacLennan, D. N., and J. R. Dunn. 1984. Estimation of sound velocities from resonance measurements on tungsten carbide calibration spheres. Journal of Sound Vibration 97:321-331.

MacLennan, D. N., P. G. Fernandes, and J. Dalen. 2002. A consistent approach to definitions and symbols in fisheries acoustics. ICES Journal of Marine Science 59:365-369.

Mangel, M. 2000. Trade-offs between fish habitat and fishing mortality and the role of reserves. Bulletin of Marine Science 66:663-674.

Martin, S.J. 1881. Cod gill-nets in Ipswich Bay, Massachusetts. Fishery Bulletin 1:343-345

Matheron, G. 1965. Les Variables Régionalisée et leur Estmation. Masson, Paris.

Mayer, L., Clarke, J. H., and Dijkstra, S. 1999. Multibeam sonar: potential applications for fisheries research. Journal of Shellfish Research 17:1463-1467.

Mayer, L., Li, Y., and Melvin, G. 2002. 3D visualization for pelagic fisheries research and assessment. ICES Journal of Marine Science 59:216-225.

Mayo R.K., G. Shepherd, L. O'Brien, L.A. Col, and M. Traver. 2009. The 2008 assessment of the Gulf of Maine Atlantic cod (*Gadus morhua*) stock. US Department Commerce, Northeast Fish Science Center Reference Document 09-03; 128 p. Available from: National Marine Fisheries Service, 166 Water Street, Woods Hole, MA 02543-1026, or online at http://www.nefsc.noaa.gov/nefsc/publications/

McClatchie, S., J. Alsop, and R. F. Coombs. 1996. A re-evaluation of relationships between fish size, acoustic frequency, and target strength. ICES Journal of Marine Science 53:780-791.

McClatchie, S., G. J. Macaulay, and R. F. Coombs. 2003. A requiem for the use of 20log10Length for acoustic target strength with special reference to deep-sea fishes. ICES Journal of Marine Science 60:419-428.

McClatchie, S., R. E. Thorne, P. Grimes, and S. Hanchet. 2000. Ground truth and target identification for fisheries acoustics. Fisheries Research 47:173-191.

McQuinn, I. H. and P.D. Winger. 2003. Tilt angle and target strength: target tracking of Atlantic cod (*Gadus morhua*) during trawling. ICES Journal of Marine Science 60: 575-583.

McQuinn, I. H., S. Yvan, T. W. F. Stroud, J.-L. Beaulieu, and S. J. Walsh. 2005. An adaptive, integrated "acoustic-trawl" survey design for Atlantic cod (*Gahus morhua*) with estimation of acoustic and trawl dead zones. ICES Journal of Marine Science 62:93-106.

Mello, L. G. S., and G. Rose. 2005a. Seasonal variation in abundance and stock composition of Atlantic cod (*Gadus morhua*) in Placentia Bay, Newfoundland, in relation to fisheries. Fisheries Research 74:142-156.

Mello, L. G. S., and G. A. Rose. 2005b. Using geostatistics to quantify seasonal distribution and aggregation patterns of fishes: an example of Atlantic cod (*Gadus morhua*). Canadian Journal of Fisheries and Aquatic Sciences 62:659-670.

Mello, L. G. S., and G. A. Rose. 2009. The acoustic dead zone: theoretical vs. empirical estimates, and its effect on density measurements of semi-demersal fish. ICES Journal of Marine Science 66:1364-1369.

Melvin, G. D., N. A. Cochrane, and Y. Li. 2003. Extraction and comparison of acoustic backscatter from a calibrated multi- and single-beam sonar. ICES Journal of Marine Science 60:669-677.

Misund, O. A. 1993. Abundance estimation of fish schools based on a relationship between school area and school biomass. Aquatic Living Resources 6:235–241.

Misund, O. A., and A. Aglen. 1992. Swimming behaviour of fish schools in the North Sea during acoustic surveying and pelagic trawl sampling. ICES Journal of Marine Science 49:325-334.

Misund, O. A., and J. Coetzee. 2000. Recording fish schools by multi-beam sonar: potential for validating and supplementing echo integration recordings of schooling fish. Fisheries Research 47:149-159.

Moszynski, M., and J. B. Hedgepeth. 2000. Using single-beam side-lobe observations offish echoes for fish target strength and abundance estimation in shallow water. Aquatic Living Resources 13:379-383.

Moursund, R. A., T. J. Carlson, and R. D. Peters. 2003. A fisheries application of a dual-frequency identification sonar acoustic camera. ICES Journal of Marine Science 60:678-683.

Mukai, T., N. Sano, K. Iida, and S. Sasaki. 1993. Studies on dorsal aspect target strength of ten species of fish collected in the East China Sea. Nippon Suisan Gakkaishi 59:1515-1525.

Myers, R. A., J. A. Hutchings, and N. J. Barrowman. 1996. Hypotheses for the decline of cod in the North Atlantic. Marine Ecology Progress Series 138:293-308.

Myers, R. A., J. A. Hutchings, and N. Barrowman. 1997. Why do fish stocks collapse? the example of cod in Atantic Canada. Ecological Applications 7:91-106.

Myers, R. A., B. R. MacKenzie, K. G. Bowen, and N. J. Barrowman. 2001. What is the carrying capacity for fish in the ocean? A meta-analysis of population dynamics of North Atlantic cod. Canadian Journal of Fisheries and Aquatic Sciences 58:1464-1476

Nakken, O. and Olsen, K. 1977. Target strength measurements of fish. Rapports et Procès-Verbaux des Réunions, Conseil International pour L'Exploration scientifique de la Mer Medeterranee. Monaco, 170:52-69.

Neat, F. C., P. J. Wright, A. F. Zuur, I. M. Gibb, F. M. Gibb, D. Tulett, D. A. Righton, and R. J. Turner. 2006. Residency and depth movements of a coastal group of Atlantic cod (*Gadus morhua* L.). Marine Biology 148:643-654.

Nemeth, R. S. 2005. Population characteristics of a recovering US Virgin Islands red hind spawning aggregation following protection. Marine Ecology Progress Series 286:81-97.

New England Fishery Management Council. 1998. Framework Adjustment 25 to the Northeast Multispecies Fishery Management Plan. http://www.nefmc.org/nemulti/frame/FW25 Finaldoc.pdf.

New England Fishery Management Council. 2011. Framework Adjustment 45 to the Northeast Multispecies Fishery Management Plan. http://www.nefmc.org/nemulti/frame/fw45/110120_Final_FW_45_Resubmit.pdf. pp. 44-46.

Nilsen, K. E. 2007. Signal processing in EM3002. Forum for EM Multibeam Experience (FEMME), Kongsberg Maritime's Users Conference, Amsterdam, Netherlands, 19-23 March 2007.

NOAA (National Oceanic and Atmospheric Administration). 2012. Commercial Fisheries Statistics. Available: www.st.nmfs.noaa.gov/st1/commercial/index.html (November 2012).

Northeast Fisheries Science Center (NEFSC). 2012. 53rd Northeast Regional Stock Assessment Workshop (53rd SAW) Assessment Report. US Department of Commerce, Northeast Fisheries Science Center Reference Document 12-05; 559 p. Available from: National Marine Fisheries Service, 166 Water Street, Woods Hole, Massachusetts 02543-1026, or online at http://www.nefsc.noaa.gov/nefsc/publications/

O'Brien, L., J. Burnett, and R. K. Mayo. 1993. Maturation of Nineteen Species of Finfish off the Northeast Coast of the United States, 1985-1990. NOAA Technical Report NMFS 113. U.S. Department of Commerce, NOAA, National Marine Fisheries Service, Woods Hole, Massachusetts.

Ona, E. 1990. Physiological factors causing natural variations in acoustic target strength of fish. Journal of the Marine Biological Association of the United Kingdom 70:107-127.

Ona, E. 2003. An expanded target strength relationship for herring. ICES Journal of Marine Science 60:493-499.

Ona, E., L. N. Andersen, H. P. Knudsen, and S. Berg. 2007. Calibrating multibeam, wideband sonar with reference targets. OCEANS 2007 June 2007: 1-5.

Ona, E., and M. Barange. 1999. Single-target recognition. ICES Cooperative Research Report 235:28-43.

Ona, E., V. Mazauric, and L. N. Andersen. 2009. Calibration methods for two scientific multibeam systems. ICES Journal of Marine Science 66:3126-1334.

Ona, E., and R. B. Mitson. 1996. Acoustic sampling and signal processing near the seabed: the deadzone revisited. ICES Journal of Marine Science 53:677-690.

Paramo, J., S. Bertrand, H. Villalobos, and F. Gerlotto. 2007. A three-dimensional approach to school typology using vertical scanning multibeam sonar. Fisheries Research 84: 171–179.

Páramo, J., and R. Roa. 2003. Acoustic-geostatistical assessment and habitat-abundance relations of small pelagic fish from the Colombian Caribbean. Fisheries Research 60:309-319.

Parker-Stetter, S. L., L. G. Rudstam, P. J. Sullivan, and D. M. Warner. 2009. Standard operating procedures for fisheries acoustic surveys in the Great Lakes. Great Lakes Fishery Commission Special Publication 09-01.

Pedersen, G., and R. J. Korneliussen. 2009. The relative frequency response derived from individually separated targets of northeast Arctic cod (*Gadus morhua*), saithe (*Pollachius virens*), and Norway pout (*Trisopterus esmarkii*). ICES Journal of Marine Science 66:1149-1154.

Pentilla, J.A. G.A. Nelson, and J.M. Burnett, III. 1989, Guidelines for estimating lengths at age for 18 northwest Atlantic finfish and shellfish species. NOAA Technical Memorandum. NMFS-F/NEC-66. 39 pp.

Peterson, M. L., C. C. Clay, and S. B. Brandt. 1976. Acoustic estimates of fish density and scattering function. Journal of the Acoustical Society of America 60:618-622.

Petitgas, P. 1993. Geostatistics for fish stock assessments: a review and an acoustic application. ICES Journal of Marine Science 50:285-298.

Petitgas, P. 2001. Geostatistics in fisheries survey design and stock assessment: models, variances and applications. Fish and Fisheries 2:231-249.

Petitgas, P., and T. Lafont. 1997. EVA2: Estimation variance. Version 2: a geostatistical software on Windows 95 for the precision of fish stock assessment surveys. ICES CM-1997/Y:22.

R Development Core Team. 2012. R: A language and environment for statistical computing. R Foundation for Statistical Computing, Vienna, Austria URL http://www.R-project.org/.

Reich, D. A., and J. T. DeAlteris. 2009. A simulation study of the effects of spatially complex population structure for Gulf of Maine Atlantic cod. North American Journal of Fisheries Management 29:116-126.

Ribeiro, P. J., Jr., and P. J. Diggle. 2001. geoR: A package for geostatistical analysis. R-News 1.

Rikhter, V. A., I. K. Sigaev, V. A. Vinogradov, and V. I. Isakov. 2001. Silver hake of Scotian Shelf: fishery, environmental conditions, distribution, and biology and abundance dynamics. Journal of Northwest Atlantic Fishery Science 25:51-92.

Rivoirard, J., J. Simmonds, K. G. Foote, P. Fernandes, and N. Bez. 2000. Geostatistics for Estimating Fish Abundance. Blackwell Science, Malden, MA.

Robichaud, D., and G. A. Rose. 2001. Multiyear homing of Atlantic cod to a spawning ground. Canadian Journal of Fisheries and Aquatic Sciences 58:2325-2329.

Rose, G. A. 2003. Monitoring coastal northern cod: towards an optimal survey of Smith Sound, Newfoundland. ICES Journal of Marine Science 60:453-462.

Rose, G.A. 2007. Cod: The Ecological History of the North Atlantic Fisheries. Breakwater Books Ltd. St. John's, Newfoundland, Canada. 591 pp.

Rose, G. A. 2009. Variations in the target strength of Atlantic cod during vertical migration. ICES Journal of Marine Science 66:1205-2011.

Rose, G. A. and Leggett, W. C. 1988. Hydroacoustic signal classification of fish schools by species. Canadian Journal of Fisheries and Aquatic Sciences 45:597-604.

Rose, G. A., R. J. Nelson, and L. G. S. Mello. 2011. Isolation or metapopulation: whence and whither the Smith Sound cod? Canadian Journal of Fisheries and Aquatic Sciences 68:152-169.

Rose, G. A. and Porter, D. R. 1996. Target-strength studies on Atlantic cod (*Gadus morhua*) in Newfoundland waters. ICES Journal of Marine Science 53:259–265.

Rosen, S., A. Engås, A. Fernö, and T. Jörgensen. 2012. The reactions of shoaling adult cod to a pelagic trawl: implications for commercial fishing. ICES Journal of Marine Science 69:303-312.

Ross, M., and S. R. Hokenson. 1997. Short-term mortality of discarded finfish bycatch in the Gulf of Maine fishery for northern shrimp *Pandalus borealis*. North American Journal of Fisheries Management 17:902-909.

Rothschild, B. J. 2007. Coherence of Atlantic cod stock dynamics in the Northwest Atlantic Ocean. Transactions of the American Fisheries Society 136:858-874.

Rowe, S., and J. A. Hutchings. 2006. Sound production by Atlantic cod during spawning. Transactions of the American Fisheries Society 135:529-538.

Rudstam, L. G., S. L. Parker-Stetter, P. J. Sullivan, and D. M. Warner. 2009. Towards a standard operating procedure for fishery acoustic surveys in the Laurentian Great Lakes, North America. ICES Journal of Marine Science 66:1391-1397.

Runge, J.A., A.I. Kovach, J.H. Churchill, L.A. Kerr, J.R. Morrison, R.C. Beardsley, D.L. Berlinsky, C.S. Chen, S.X. Cadrin, C.S. Davis, K.H. Ford, J.H. Grabowski, W.H. Howell, R.B. Ji, R.J. Jones, A.J. Pershing, N.R. Record, A.C. Thomas, G.D. Sherwood, S.M.L. Tallack, and D.W. Townsend. 2010. Understanding climate impacts on recruitment and spatial dynamics of Atlantic cod in the Gulf of Maine integration of observations and modeling. Progress in Oceanography 87:251–263.

Sawada, K., M. Furusawa, and N. J. Williamson. 1993. Conditions for the precise measurement of fish target strength in situ. Journal of the Marine Acoustical Society of Japan 20:73-79.

Schabenberger, O., and C. A. Gotway. 2005. Statistical Methods for Spatial Data Analysis. Chapman and Hall, New York.

Schopka, S. A., J. Solmundsson, S. A. Ragnarsson, and V. Thorsteinsson. 2010. Using tagging experiments to evaluate the potential of closed areas in protecting migratory Atlantic cod (*Gadus morhua*). ICES Journal of Marine Science 67:1024-1035.

Simmonds, E. J., and R.J. Fryer. 1996. Which are better, random or systematic acoustic surveys? A simulation using North Sea herring as an example. ICES Journal of Marine Science 53:39-50.

Simmonds, J. and D. MacLennan. 2005. Fisheries Acoustics: Theory and Practice. Blackwell Science, Oxford, UK, 437 pp.

Siceloff, L., and W. H. Howell. 2012. Fine-scale temporal and spatial distributions of Atlantic cod (*Gadus morhua*) on a western Gulf of Maine spawning ground. Fisheries Research. In Press.

Sokal, R. R., and F. J. Rohlf. 1995. Biometry. W. H. Freeman and Company, New York.

Soria, M., T. Bahri, and F. Gerlotto. 2003. Effect of external factors (environment and survey vessel) on fish school characteristics observed by echosounder and multibeam sonar in the Mediterranean Sea. Aquatic Living Resources 16:145–157.

Soria, M., P. Fréon, and F. Gerlotto. 1996. Analysis of vessel influence on spatial behaviour of fish schools using a multi-beam sonar and consequences for biomass estimates by echo-sounder. ICES Journal of Marine Science 53:453–458.

Soule, M., M. Barange, and I. Hampton. 1995. Evidence of bias in estimates of target strength obtained with a split-beam echo-sounder. ICES Journal of Marine Science 52:139-144.

Soule, M., I. Hampton, and M. Barange. 1996. Potential improvements to current methods of recognizing single targets with a split-beam echo-sounder. ICES Journal of Marine Science 53:237-243.

Stanton, T. K., and C. S. Clay. 1986. Sonar echo statistics as a remote-sensing tool: volume and seafloor. IEEE Journal of Oceanic Engineering 2:79-96.

Stepnowski, A., and M. Moszyński. 2000. Inverse problem solution techniques as applied to indirect *in situ* estimation of fish target strength. Journal of Acoustical Society of America 107:2554-2562.

Svedäng, H., D. Righton, and P. Jonsson. 2007. Migratory behaviour of Atlantic cod Gadus morhua: natal homing is the prime stock-separating mechanism. Marine Ecology Progress Series 345:1-12.

Traynor, J. J. 1996. Target-strength measurements of walleye pollock (*Theragra chalcogramma*) and Pacific whiting (*Merluccius productus*). ICES Journal of Marine Science 53:253-258.

Trenkel, V. M., V. Mazauric, and L. Berger. 2008. The new fisheries multibeam echosounder ME70: description and expected contribution to fisheries research. ICES Journal of Marine Science, 65:645–655.

Van Parijs, S. M., C. W. Clark, R. S. Sousa-Lima, S. E. Parks, S. Rankin, D. Risch, and I. C. Van Opzeeland. 2009. Management and research applications of real-time and archival passive acoustic sensors over varying temporal and spatial scales. Marine Ecology Progress Series 395:21-36.

Vitale, F., P. Börjesson, H. Svedäng, and M. Casini. 2008. The spatial distribution of cod (*Gadus morhua* L.) spawning grounds in the Kattegat, eastern North Sea. Fisheries Research 90:36-44.

Walsh, S. 1996. Efficiency of bottom sampling trawls in deriving survey abundance indices. NAFO Scientific Council Studies 28:9-24.

Warton, D. L., R. A. Duursma, D. S. Falster, and S. Taskinen. 2012. smatr 3 - an R packaga for estimation and inference about allometric lines. Methods in Ecology and Evolution 3:257-259.

Weber, T. C., H. Peña, and J. M. Jech. 2009. Consecutive acoustic observations of an Atlantic herring school in the Northwest Atlantic. ICES Journal of Marine Science 66:1270-1277.

Wigley, S. E., H. M. McBride, and N. J. McHugh. 2003. Length-weight relationships for 74 fish species collected during NEFSC research vessel bottom trawl surveys, 1992-99. NOAA Technical Memorandum NMFS-NE-171:26.

Wilcox, W.A. 1886a. New England Fisheries in March, 1886. Fishery Bulletin 6:94-95

Wilcox, W.A. 1886b. New England Fisheries in April, 1886. Fishery Bulletin 6:106-108

Wilcox, W.A. 1887. 24.-The fisheries of Gloucester, Mass., in March, 1887, with notes on those of other localities. Fishery Bulletin 7:70-71.

Windle, M. J. S., and G. A. Rose. 2005. Migration route familiarity and homing of transplanted Atlantic cod (*Gadus morhua*). Fisheries Research 75:193-199.

Winger, P. D., P. He, and S. J. Walsh. 2000. Factors affecting the swimming endurance and catchability of Atlantic cod (*Gadus morhua*). Canadian Journal of Fisheries and Aquatic Sciences 57:1200-1207.

Wirgin, I., A. I. Kovach, L. Maceda, N. K. Roy, J. Waldman, and D. L. Berlinsky. 2007. Stock identification of Atlantic cod in U.S. waters using microsatellite and single nucleotide polymorphism DNA analyses. Transactions of American Fisheries Society 136:375-391.

Wright, P. J., E. Galley, I. M. Gibb, and F. C. Neat. 2007. Fidelity of adult cod to spawning grounds in Scottish waters. Fisheries Research 77:148-158.